Dissertations | Theses and Dissertations

2012

Molecular Mechanisms Regulating Chemokine Receptor CXCR4 Signaling and Trafficking

Rohit Malik

Loyola University Chicago

Recommended Citation

LOYOLA UNIVERSITY CHICAGO

MOLECULAR MECHANISMS REGULATING CHEMOKINE

RECEPTOR CXCR4 SIGNALING AND TRAFFICKING

A DISSERTATION SUBMITTED TO

THE FACULTY OF THE GRADUATE SCHOOL

IN CANDIDACY FOR THE DEGREE OF

DOCTOR OF PHILOSOPHY

PROGRAM IN MOLECULAR BIOLOGY

BY

ROHIT MALIK

CHICAGO, ILLINOIS

MAY 2012

ACKNOWLEDGEMENTS

I want to thank my advisor Dr. Adriano Marchese, who has been very helpful and supportive in the completion of my dissertation work. His boundless dedication and enthusiasm has inspired me to pursue a career in research. This thesis would not have been possible without him. I look forward to his mentorship throughout the development of my career as a scientist.

I am indebted by my brilliant supportive committee members, Drs. Neil Clipstone, Tarun Patel, Ajay Rana and Edward Campbell, for their excellent suggestions that helped to shape this dissertation. I appreciate the time and effort the members of my thesis committee put in to advise me over the years.

I am also thankful to the American Heart Association for awarding me a pre-doctoral fellowship for two years.

I will be forever grateful to my present and past lab mates in the Marchese Lab, especially Deepali and Adriana who were more like family members than coworkers. I also thank Program in Molecular Biology and the Department of Molecular Pharmacology at Loyola University, Chicago for accepting me as a graduate student.

I want to thank my parents Lt Col. Pitam Singh and Rita Malik, my brother Sandeep Malik, whose love and support has made this possible. They allowed me to dream big and gave me the freedom to follow those dreams. I also want to thank my in-laws

This thesis is a testament to the love and support of my family through all aspects of my life

TABLE OF CONTENT

LIST OF TABLES

LIST OF FIGURES

LIST OF ABBREVIATIONS

7TMR	7 transmembrane receptor
β2AR	Beta 2 adrenergic receptor
μg	Microgram
μl	Microliter
μM	Micromolar
AC	Adenylyl Cyclase
AMSH	Associated molecule with the SH3 domain of STAM
ANOVA	Analysis of Variance
AP2	Adaptor protein 2
APS	Ammonium persulfate
ARF	ADP-ribosylation factor 6
ATP	Adenosine-5'-triphosphate
BSA	Bovine serum albumin
Ca2+	Calcium
cAMP	Cyclic Adenosine monophosphate
CAR	Carbachol
CAV	Caveolin
CC	Coiled coil

CCP	Clathrin-coated pits
CCV	Clathrin-coated vesicles
CDC26	Cell surface protease dipeptidase 26
CFP	Cyan fluorescent protein
CSD	Caveolin scaffolding domain
CXCR4	C-X-C Chemokine receptor 4
CXCL12	Chemokine ligand 12
C-tail	Carboxyl-terminal tail
DAG	Diacyl glycerol
DAPI	4',6-diamidino-2-phenylindole
DMEM	Dulbecco's modified Eagle's medium
DMSO	Dimethyl Sulfoxide
DOR	Delta opioid receptor
DTT	DL-Dithiothreitol
DUB	Deubiquitinase
EBP50	Ezrin–radixin–moesin (ERM)-binding phosphoprotein-50
ECL	Enhanced chemiluminescence
EDTA	Ethylenediaminetetraacetic acid
EE	Early endosome
EEA1	Early endosome antigen
e.g.	Exempli gratia
EGF	Epidermal growth factor

EGFR	Epidermal growth factor receptor
EL	Extracellular loop
ENaC	Epithelial sodium channels
EPC	Endothelial progenitor cells
EPS15	Epidermal growth factor receptor substrate 15
ERK	Extracellular signal regulated kinase
ESCRT	Endosbmal sorting complex required for transport
FALS	Familial amyotrophic lateral sclerosis
FBS	Fetal bovine serum
FPR	N-formyl peptide receptor
FRET	Fluorescence resonance energy transfer
GAT	GGA and TOM1
GDP	Guanosine diphosphate
GFP	Green fluorescent protein
GPCR	G protein-coupled receptor
GRK	G protein-coupled receptor kinase
GST	Glutathione transferase
GTP	Guanosine triphosphate
h	Hour
HA	Haemagglutinin
HECT	Homologous to E6AP C-terminus
HEPES	4-(2-hydroxyethyl)-1-piperazineethanesulfonicacid

HER2	Human Epidermal growth factor Receptor 2
HIV	Human immunodeficiency virus
HIF	Hypoxia induced factor-1 a
HPV	Human papilloma virus
HRE	HIF-response element
HRS	Hepatocyte growth-factor regulated tyrosine kinase substrate
HEK	Human embryonic kidney
HRP	Horseradish peroxidase
IB	Immunoblotting
IL	Intracellular loop
IP	Immunoprecipitation
IP3	Inositol trisphosphate
IPTG	lsopropyl-1-thio-p-D-galactopyranoside
JAK	Janus Kinase
LAMP	Lysosomal-associated membrane protein
LE	Late endosome
LH	Leutinizing hormone
LMP2A	Latent membrane protein 2A
mAB	Monoclonal antibody
MAPK	Mitogen-activated protein kinase
MEF	Mouse embryonic fibroblasts
MIF	Macrophage migration inhibitory factor

min	Minute
MJD	Machado-josephin domain
ml	Milli-liter
mM	Milli-molar
mRNA	Messenger ribonucleic acid
MVB	Multivesicular body
N.D.	Not determined
NA	Numerical aperture
NaCI	Sodium chloride
NaOH	Sodium hydroxide
nM	Nanomolar
NEDD4	Neuronal precursor cell-expressed developmentally downregulated 4
NEM	N-ethylmaleimide
NK cells	Natural killer cells
NK1R	Neurokine 1 receptor
nm	Nanometer
pAB	Polyclonal antibody
PAFR	Platelet activating factor receptor
PAF	Platelet activating factor
PAGE	Poly-acrylamide gel electrophoresis
PAR	Protease activated receptor
PBS	Phosphate buffered saline

pDNA	Plasmid DNA
PGC	Primordial germ cell
PHD	Plant homeodomain
PI	Propidium iodide
PIP2	Phosphatidylinositol 4,5 bisphosphate
PKA	Protein kinase A
PKC	Protein kinase C
PLC	Phospholipase C
PLL	Poly L-Lysine
PMA	Phorbol 12-myristate 13-acetate
PRR	Proline rich region
Ptdlns(3)P	Phosphatidylinositol 3-phosphate
PI3K	Phosphoinositide 3-kinase.
RA	Rhematoid arthritis
Ras	Rat sarcoma
RE	Recycling endosome
RING	Really interesting new gene
Rluc	Renilla Luciferase
RT	Room temperature
s	Second
SD	Standard Deviation
SCF	Skp-Cullin-F-Box

SDF	Stromal cell derived factor
SDS	Sodium dodecyl sulfate
S.E.M.	Standard error of the mean
SH2	SRC homology 2
SH3	SRC homology 3
siRNA	Small interfering ribonucleic acid
SMURF	Smad ubiquitin regulatory factor
STAM	Signal transducing adaptor molecule
STAT	Signal transduction and activator of transcription
TBS	Tris-buffered saline
TBS-T	Tris-buffered saline with Tween-20
TF	Transcription factor
TGF	Transforming growth factor
TIRF	Total internal reflection microscopy
TM	Transmembrane
TSH	Thyroid stimulating hormone
Ub	Ubiquitin
UBC	Ubiquitin conjugating
UIM	Ubiquitin interacting motif
USP	Ubiquitin specific protease
UCH	Ubiquitin C-terminal hydrolase
V2R	V2 vasopressin receptor

VHS	Vps27p/Hrs/STAM
VPS	Vacuolar protein sorting
WHIM	Warts, Hypogammaglobulinemia, Infections, Myelokathexis
WT	Wild type
YFP	Yellow fluorescent protein

ABSTRACT

CXCR4 is a G protein-coupled receptor (GPCR) that binds to the chemokine, stromal cell-derived factor-1α (SDF-1α; a.k.a. CXCL12). The SDF-1α/CXCR4 signaling axis plays an essential role during embryogenesis in the development of the heart, brain and vasculature and in the adult mediating immune cell trafficking and stem cell homing to the bone marrow. Dysregulation of SDF-1α/CXCR4 signaling is linked to several pathological conditions, including cardiovascular disease, immunological disorders as well as cancer growth and metastasis. However, the mechanisms that govern CXCR4 signaling remain poorly understood. In this dissertation project, we attempt to further our understanding of the molecular mechanisms that regulate CXCR4 signaling.

CXCR4 signaling is tightly controlled by a complex series of events that rapidly terminates its signaling. Activated CXCR4 is rapidly phosphorylated and ubiquitinated by the E3 ubiquitin ligase AIP4 at the plasma membrane. Ubiquitinated CXCR4 is rapidly internalized onto early endosomes and targeted for lysosomal degradation, giving rise to long-term attenuation of signaling. The ubiquitin moiety on CXCR4 serves as a sorting signal for entry into the endosomal sorting complex required for transport (ESCRT) pathway. This pathway consists of four different protein complexes (ESCRT-0, I, II and III), plus several accessory factors, that act in a sequential and coordinated manner to target proteins for lysosomal degradation. Although CXCR4 is targeted into the ESCRT pathway, mechanistic insight by which this occurs remains poorly defined.

In previous work from our laboratory, it was shown that adaptor protein arrestin-2 interacts with AIP4 to regulate endosomal sorting of CXCR4 into the degradative pathway. However, the precise mechanism by which arrestin-2 performs this function remains unknown.

We set out to determine how arrestin-2 integrates with the sorting machinery on endosomes to control the amount of CXCR4 that is degraded. We show that arrestin-2 interacts with ESCRT-0 protein STAM-1. ESCRT-0 consists of two proteins: signal-transducing adaptor molecule (STAM) and hepatocyte growth factor-regulated tyrosine kinase substrate (HRS). It is the first complex that recognizes ubiquitinated CXCR4 and targets it for lysosomal degradation. We show that depletion of STAM-1 by siRNA and selective disruption of the STAM-1/arrestin-2 interaction accelerates agonist promoted degradation of CXCR4, suggesting that STAM-1 via its interaction with arrestin-2 negatively regulates CXCR4 endosomal sorting. Interestingly, disruption of this interaction also blocks agonist promoted ubiquitination of HRS, the other ESCRT-0 protein, but not ubiquitination of CXCR4 and STAM-1, suggesting that arrestin-2 via its interaction with STAM-1 mediates ubiquitination of HRS. We propose a model, whereby arrestin-2 initially recruits CXCR4 to the ESCRT machinery and subsequently interacts with ESCRT-0 to regulate its sorting function, thereby ultimately controlling the amount of CXCR4 that is degraded.

Here, we also report novel roles for AIP4 and STAM-1 in CXCR4 signaling, which are different from their roles in CXCR4 trafficking. Treatment of cells with siRNA against AIP4 and STAM-1 attenuates CXCR4-induced activation of

extracellular regulated kinase 1 and 2 (ERK-1/2). We show that STAM-1 via its SH3 domain interacts with the proline–rich region (PRR) in AIP4. AIP4 mediates STAM-1 ubiquitination and expression of AIP4-C830A, a catalytically inactive mutant that fails to ubiquitinate STAM-1, and an AIP4 mutant (AIP4-ΔPRR) that shows poor binding to STAM-1 fail to enhance CXCR4-induced ERK-1/2 activation, suggesting that interaction with STAM-1 as well as ubiquitination activity of AIP4 are important for CXCR4-induced ERK-1/2 activation. Remarkably, a discrete subpopulation of AIP4 and STAM-1 co-localize with CXCR4 at the plasma membrane and with caveolin-1, a protein that is enriched in caveolae (a specialized lipid raft). Disrupting caveolae using caveolin-1 siRNA or nystatin, a cholesterol-depleting agent, significantly attenuated CXCR4-induced ERK-1/2 activation. Based upon our data, we propose that AIP4-mediated ubiquitination of STAM-1 in caveolae coordinates CXCR4 activation of ERK-1/2 signaling.

Taken together, our study has provided novel insight into the regulation of CXCR4 both at the levels of signaling as well as trafficking. We provide novel mechanistic insight into the role of arrestin-2 in targeting CXCR4 into the degradative pathway and we have also identified a novel function for AIP4 and STAM-1 in CXCR4 signaling.

CHAPTER 1

INTRODUCTION

G PROTEIN-COUPLED RECEPTORS (GPCR)

G protein-coupled receptors (GPCRs) are the largest family of cell surface proteins encoded by the human genome. There are approximately 900 members in the family, although 50% of these are the odorant receptors (reviewed in Pierce et al., 2002). GPCRs share a common core structure that is composed of seven-transmembrane-alpha-helices (TM-1 to TM-7) connected by three intracellular loops and three extracellular loops (Figure 1.1) (reviewed in Pierce et al., 2002). GPCRs are involved in a large variety of physiological processes such as vision, smell, pain, regulation of immune system, nervous system, neurotransmission, hormone and enzyme release, cardiac- and smooth-muscle contraction and blood pressure regulation. GPCRs are important pathophysiologically as evident by the fact that more than 50% of all drugs currently on the market target GPCRs for their action (reviewed in Fredholm et al., 2007; Hislop and von Zastrow, 2011; Jacoby et al., 2006; Overington et al., 2006).

On the basis of sequence similarity the International Union of Pharmacology (IUPHAR) has classified GPCRs into four groups (http://www.iuphar-db.org/list/index.htm, (Foord et al., 2005; Fredholm et al., 2007):

Class-1 or family A: This group of GPCRs contains 272 members of rhodopsin-like and

olfactory receptors. Some of the important GPCR family members in this class include; 5-Hydroxytryptamine, acetylcholine (muscarinic), adenosine, chemokine, dopamine, opioid, protease-activated, vasopressin and oxytocin receptors among many more. Family A also contain 85 orphan receptors. Orphan receptors are receptors whose natural ligands are not known at present. Receptors in family A contain a conserved arginine in the Asp-Arg-Tyr (DRY) motif at the cytoplasmic side of the transmembrane helix (Kolakowski, 1994; Probst et al., 1992).

Class-2 or family B: This group contains 49 members of secretin receptor-like receptors. Some of the important members in this class include; calcitonin, corticotropin-releasing factor, glucagon and parathyroid hormone receptors. This group also contains around 34 orphan receptors. The DRY motif is absent in family B receptors, instead receptors in this group contain a long N-teminal domain with several cysteine residues that form a network of disulfide bridges.

Class-3 or family C: This group contains 19 members of the metabotropic $GABA_B$ and glutamate receptors as well as 7 orphan receptors. Receptors in this group have a long amino terminus (500-600 amino acids).

Frizzled family receptors: This group contains 11 members that serve as receptors in the Wnt signaling pathway.

GPCR ACTIVATION AND G PROTEIN DEPENDENT SIGNALING

GPCRs transduce information from the extracellular environment to the interior of the cell via GTP-binding proteins (G protein), which are heterotrimers of α, β, and γ subunits. Under an inactive or ligand-free basal state, the receptor is in an inactive conformation. Under this condition the G protein is inactive and is reversibly bound to guanosine
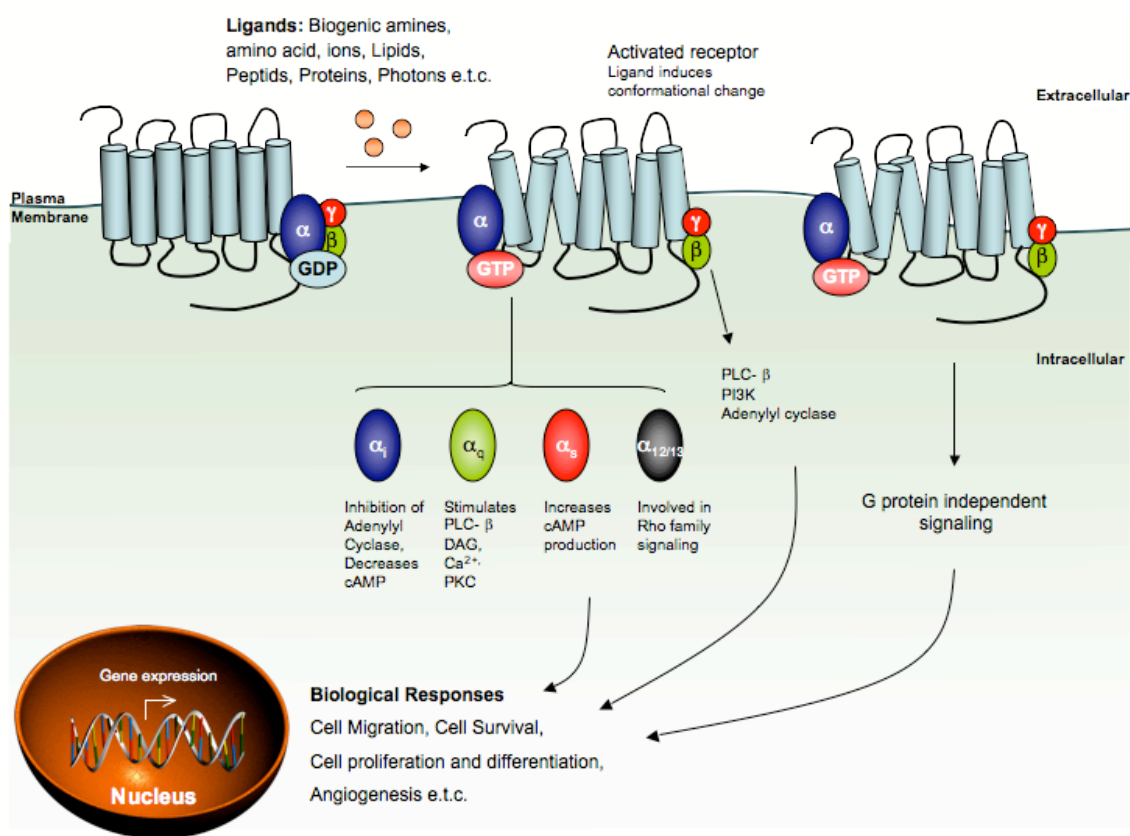
Figure 1.1: Overview of GPCR activation and signaling. GPCRs are activated by a wide variety of ligands. Agonist binding to the receptor triggers a conformational change that mediates the exchange of GDP for GDP on the α-subunit. G_s subunit stimulates adenylyl cyclase that leads to an increase in the level of cyclic AMP (cAMP) in cells. In contrast, G_i inhibits adenylyl cyclase, G_q activates phospholipase C (PLC), which is responsible for the cleavage of phosphatidylinositol bisphosphate (PIP$_2$) into second messengers diacylglycerol (DAG) and inositol trisphosphate (IP$_3$). $G_{12/13}$ regulates the actin cytoskeleton via activation

of Rho family proteins. The βγ-subunits also control a variety of intracellular signaling pathways, such as mitogen-activated protein kinase (MAPK), small GTP-binding proteins of the Ras and Rho families, c-jun N-terminal kinase (JNK) and p38. GPCRs may also signal in a G protein- independent fashion to activate these signaling pathways. Together these signaling pathways control various biological processes such as transcription, cell migration, survival, proliferation and differentiation. Abbreviations; PI3K, phosphatidylinositol 3-kinase; PKA and PKC, protein kinase A and C. Modified from Dorsam and Gutkind et al., 2007

diphosphate (GDP). Agonist binding induces conformational changes in the receptor allowing it to function as a guanine nucleotide exchange factor (GEF) by promoting the exchange of GDP for GTP on the α-subunit. Antagonist binding stabilizes different conformational states but does not promote G protein activation and hence signaling. Structural basis of ligand induced GPCR activation has been characterized for various GPCRs such as β_2 adrenergic receptor, rhodopsin and CXCR4 (Altenbach et al., 2008; Farrens et al., 1996; Scheerer et al., 2008; Wu et al., 2010; Yao et al., 2006). Irrespective of the type of GPCR, ligand binding induces conformational change, especially in the TM3 and TM6 region of the transmembrane domains, which then activates the associated G protein that further activates highly versatile signal transduction system.

Gα subunit can be divided into four families with several members in each family ($G\alpha_s$, $G\alpha_i/G\alpha_o$, $G\alpha_q/G\alpha_{11}$, and $G\alpha_{12}/G\alpha_{13}$). On the other hand, the βγ heterodiamer is made of a repertoire of 5β and 12 γ-subunits. As shown in Figure 1.1, depending upon the specific type of G protein subunit associated with the GPCR, specific signal transduction pathways will be activated (reviewed in Wettschureck and Offermanns,

2005).

G PROTEIN-INDEPENDENT SIGNALING

The first report that GPCRs can activate signaling in the absence of G protein coupling came from the studies on the adenosine 3',5'-monophosphate (cAMP) receptor (cAR) in the amoeba *Dictyostelium discoideum* (Milne and Devreotes, 1993). Since then, many GPCRs have been shown to activate cellular signaling pathways independent of G protein involvement. One of the most studied GPCRs is the β_2-adrenergic receptor (β_2AR). It has been shown that at higher doses of ligand, activation of mitogen-activated protein kinase (MAPK) pathway is independent of G protein coupling (Sun et al., 2007). Similarly, β_2AR dependent regulation of cellular pH by modulation of Na+/H+ exchanger (NHE) function is independent of G protein activation, instead it is mediated via direct binding of Na+/H+ exchanger regulatory factor (NHERF) protein via a PDZ motif present in the receptor (Hall et al., 1998).

Other GPCRs such as muscarinic, parathyroid hormone (PTH), angiotensin II type 1A, neurokinin 1 (NKR1) and type 1 metabotropic glutamate receptors have also been shown to regulate cellular functions in a G protein-independent fashion (Gesty-Palmer et al., 2006; Heuss et al., 1999; Jafri et al., 2006; Rolland et al., 2002; Seta et al., 2002; Zhai et al., 2005). However, the mechanisms of G protein-independent GPCR signaling remain largely unknown.

Role of arrestins in G protein independent signaling

The mammalian genome encodes four family members of arrestin that can be

sub-divided into two groups of visual and non-visual arrestins family (Lohse et al., 1990). Visual arrestins are composed of arrestin-1, that is found in both rod and cone cells of the visual system, and arrestin-4 (a.k.a. X-arrestin) found in cone cells. Non-visual arrestins are arrestin-2 (beta-arrestin-1) and arrestin-3 (beta-arrestin-3) and both of these proteins are ubiquitously expressed (reviewed in Gurevich and Gurevich, 2006). Arrestins have classically been shown to be involved in the termination of G protein-mediated signaling events giving rise to a process called desensitization. Arrestins were initially identified in the visual system as 48 KDa molecule that can block light induced signaling of the rhodpsin receptor, a GPCR (Wilden et al., 1986). Non visual arrestins were later discovered and shown to inhibit agonist promoted signaling of β_2AR (Lohse et al., 1990). However, in recent years there has been increasing evidence suggesting a role for non-visual arrestins in G protein-independent signal transduction mediated by seven transmembrame receptors (7TMRs) (reviewed in Krupnick and Benovic, 1998). Luttrell et al., in 1999 discovered that arrestins can directly bind to and scaffold Src family tyrosine kinases to agonist occupied activated β_2AR (Luttrell et al., 1999). The binding is mediated by the SH3 domain of Src and proline-rich PXXP region in arrestin-2. In addition, the SH2 domain of Src also interacts with N-terminal residues of arrestin-2 (Miller et al., 2000). Similar mode of binding between Src and arrestin has been reported for neurokinin-1 recepor (Barlic et al., 2000). Arrestin-mediated recruitment of Src leads to phosphorylation of ERK-1/2, phosphorylation of dynamin and stimulation of neutrophil degranulation (Barlic et al., 2000; DeFea et al., 2000a; Miller et al., 2000). Since then many more GPCRs have been shown to utilize arrestins as adaptors to

regulate signaling (Lefkowitz and Shenoy, 2005).

One of the best characterized role for arrestin in 7TMR signaling is the activation of the MAP kinase cascade. Mammalian cells contain three major classes of MAP kinase: Extracellular signal-regulated kinases (ERK), c-Jun N-terminal kinases/ stress-activated protein kinase (JNK/SAPK) and p38. Both arrestin-2 and 3 have been shown to bind to the components of the ERK cascade such as Raf-1, MEK, and ERK, subsequently leading to the activation of ERK (Lefkowitz and Shenoy, 2005). Unlike G protein-dependent ERK-1/2 activation, arrestin-dependent ERK activation is more prolonged (Ahn et al., 2004). Agonist promoted internalization of protease activated receptor (PAR)-2 in KNRK cells induces the assembly of multiprotein complex composed of arrestin-2, Raf-1, activated ERK and the receptor. A receptor mutant deficient in binding to arrestin, as well as an arrestin mutant deficient in promoting endocytosis, does not activate ERK, suggesting that the assembly of this complex is necessary for receptor mediated activation of ERK (DeFea et al., 2000b). The complex also retains activated ERK in the cytoplasm. Similarly, in case of angiotensin II type 1a receptors (AT1aR) ligand stimulation leads to redistribution of ERK cascade proteins such as Raf-1, MEK1 and ERK2 into endosomal vesicles containing AT1aR-arrestin complex (Luttrell et al., 2001). In case of the NK1 neurokinin receptor, activation by substance P leads to the formation of complexes comprising of internalized receptor, arrestin, Src and ERK1/2 (DeFea et al., 2000a).

Arrestin-mediated signaling is more diverse and is involved in scaffolding other signaling components. Arrestins also interact with members of Src family kinases such as

Hck, Frg, Yes (Imamura et al., 2001). Arrestins can also scaffold phosphodiesterase 4 (PDE4), AKT and PI3 kinases (Beaulieu et al., 2005; Schmid and Bohn, 2010). Arrestins are also known to bind and activate other MAPK proteins such as p38 and c-Jun N-terminal kinase (JNK3) (Miller et al., 2001; Song et al., 2009).

REGULATION OF GPCR SIGNALING

In order to avoid prolonged receptor activation and to maintain the signaling with in the physiological limit, three important processes regulate GPCR signaling:

1. Desensitization: a rapid (within seconds) but transient inactivation of signaling via uncoupling of G proteins.

2. Internalization: a slow (minutes) but long-term inhibition of signaling via sequestration of receptor from the plasma membrane.

3. Downregulation: a reduction in the total cellular pool of receptor via endosomal sorting and degradation via lysosomes. Downregulation can take from several hours to days.

Desensitization

Upon activation of GPCRs, the G protein α-subunit is activated through an exchange of GDP to GTP. Activated α-subunit have their own intrinsic GTP hydrolysis ability that can terminate signaling. Several accessory proteins such as regulators of G protein signaling (RGS) can bind to G proteins and accelerate the rate of GTP hydrolysis. (Ross and Wilkie, 2000). Signal termination can also take place at the level of receptor. This process requires phosphorylation of the receptor by serine-threonine protein kinases

known as G protein-coupled receptor kinases (GRKs) and second messenger-dependent kinases such as protein kinase A (PKA) and protein kinase C (PKC).

There are two main types of desensitization observed following the activation of receptors: homologous and heterologous desensitization. **Homologous desensitization** is a process whereby there is a loss of agonist responsiveness specifically in the GPCR that is activated by ligand. This type of desensitization is mediated by GRK phosphorylation and subsequent binding of arrestins that sterically hinder G protein coupling to the receptor. In contrast, **heterologous desensitization** leads to a generalized effect; involving loss in agonist responsiveness to multiple GPCR subtypes. It is caused by the phosphorylation of receptors upon activation of different receptor and is mediated by the activation of second messenger protein kinases such as PKC and PKA.

Ligand binding induces conformational changes in the receptor that facilitates the binding of GRKs. GRKs phosphorylate serine/threonine residues present in the carboxyl terminal tail (C-tail) as well as third intracellular loop of activated receptors (reviewed in Krupnick and Benovic, 1998). Phosphorylation of GPCRs by GRKs is insufficient to produce complete desensitization (reviewed in Pitcher et al., 1998), but requires recruitment of protein called arrestins. Arrestins bind to GRK phosphorylated receptor and upcouple G proteins by steric hindrance to prevent further signaling (Lohse et al., 1990). The ability of GRKs to specifically phosphorylate agonist-occupied GPCRs is an important hallmark of homologous desensitization.

Heterologous desensitization of GPCRs is mediated via second messenger dependent protein kinsases such as PKC and PKA. Certain GPCRs primarily undergo

second-messenger mediated desensitization and do not require GRKs. For example the Gq-coupled purinergic receptor P2Y(1) (Hardy et al., 2005) and D(3) dopamine receptor (D(3)R) (Cho et al., 2007), desensitization following activation is independent of GRK/arrestin recruitment and is mainly mediated by PKC-dependent phosphorylation. For Gα$_i$-coupled metabotropic glutamate receptor 4 (mGluR4), desensitization and internalization solely depends on the activation of PKC or by coexpression of neurokinin 3 receptor (NK3R) (a PKC activating Gα$_i$-coupled GPCR) (Mathiesen and Ramirez, 2006). Since PKA/PKC mediated phosphorylation does not recruit arrestins, the mechanism of desensitization remains unclear. However, in case of certain GPCRs such as the D2 dopamine receptors and the delta-opioid receptor (DOR), PKC mediated phosphorylation leads to recruitment of arrestins (Namkung and Sibley, 2004).

Role of arrestins in GPCR desensitization

The process of arrestin recruitment to activated and phosphorylated receptor was first identified in the visual system (Gurevich and Benovic, 1993). Recruitment of arrestins to the phosphorylated receptor leads to uncoupling of G protiens, thereby leading to desensitization. Activation of arrestins and recruitment to activated receptor has been extensively charaterized. Arrestins are made of two distinct domains (N and C terminal) linked by a polar core. Under basal/inactive state, arrestins are in a compact state with the negatively charged residues in the C domain anchored to the positively charged residues in the N domain. Under this state, arrestins have weak binding affinity for the receptor. The polar core contains charged residues (Asp26, Argl69, Asp290,

Asp297 and Arg393 in arrestin-2, and Asp29, Argl70, Asp291, Asp298 and Arg394 in arrestin-3) that further helps to stabilize the basal state of arrestins (Han et al., 2001; Hirsch et al., 1999). Upon activation by ligand, GPCRs are rapidly phosphorylated by GRKs increasing the negative charge on the receptor. Once phosphorylated, arrestins are recruited to the receptor through their charged residues. Phosphate recognition has been narrowed down to amino acid residues Arg-18, Lys-20, Lys-55, Arg-55 in the N-terminal domain and Lys-300 in the C-terminal domain of arrestin (Han et al., 2001). Rearrangement of the N and C domains of arrestin following the binding to phosphorylated receptor exposes the C-tail that further bind to proteins such as clathrin and AP-2 and initiates the process of internalization (reviewed in (Moore et al., 2007) (Figure 1.2).
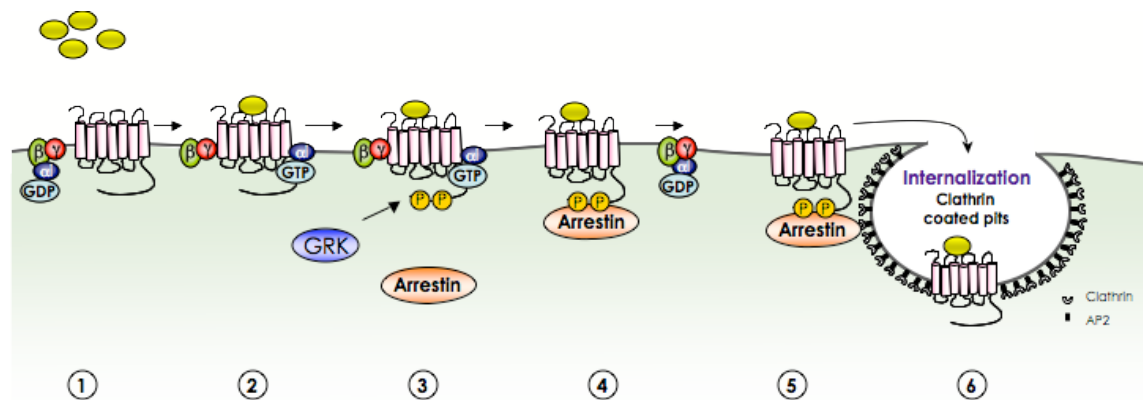
Figure 1.2 GPCR desensitization and internalization

1) Under basal condition the heterotrimeric GTP binding protein (G protein), which is comprised of an α-subunit (Gα) and a tightly associated dimer of β and γ-subunits (Gβγ), is bound to GDP and is in an inactive conformation. **2)** Upon binding to its cognate ligand (yellow oval), conformational changes in the GPCR induce the exchange of GDP for GTP on the α-subunit (Gα) leading to its activation and

dissociation from the βγ subunits. The activated α-subunit (Gα-GTP) and βγ subunits activate downstream effector molecules contributing to GPCR signaling. **3)** Signaling is rapidly terminated in part by GPCR kinase (GRK) recruitment to the activated receptor, which phosphorylates the receptor on serine and/or threonine residues that are located within the carboxy-terminal tail and/or on the intracellular loops. **4)** Arrestins are rapidly recruited to the phosphorylated receptor, which upon binding uncouple the receptor from the associated Gα subunit via steric hindrance, contributing to signal termination and to the phenomenon known as desensitization. **5)** Arrestins subsequently interact with clathrin and AP2, two important components of the internalization machinery. **6)** This results in the internalization of activated and phosphorylated receptors via clathrin coated pits.

Internalization

Apart from rapid attenuation of signaling via desensitization, agonist-induced internalization of GPCRs is an important mediator of receptor regulation. Arrestins play an important role in promoting GPCR internalization through clathrin-coated pits based on their ability to bind to components of the internalization machinery (Goodman et al., 1996; Laporte et al., 1999).

Role of arrestins in GPCR internalization

In addition to their role in the uncoupling of G protein from activated GPCRs, arrestins also facilitate endocytosis of many receptors through their interaction with proteins of the internalization machinery such as clathrin and AP2 (Goodman et al., 1996). Upon binding to the activated receptor, arrestins undergoe a conformational change exposing their carboxy-terminal clathrin-binding box motif (376-LIELD-380)

and an AP2 binding site. Other clathrin binding proteins involved in the endocytosis of GPCRs such as AP2 (Shih et al., 1995), AP180 (Morris et al., 1993), amphiphysin (Ramjaun et al., 1997), and epsin (Drake et al., 2000) also contain similar consensus motif $L\phi X\phi(D/E)$ (where ϕ is a bulky hydrophobic residue, and X represents any polar amino acid) (Laporte et al., 1999). Mutating the consensus binding site disrupts interaction between arrestins and calthrin and hence the endocytosis of receptors (Kim and Benovic, 2002; Krupnick et al., 1997).

Several post-translational modifications of arrestins also regulate their ability to modulate internalization of GPCRs. S-nitrosylation of arrestin-3 has been linked to its ability to regulate the internalization of β_2AR. It has been shown that S-nitrosylation of cysteine residue 409 in arrestin-3 increases its ability to interact with clathrin and hence promote the internalization of β_2AR (Ozawa et al., 2008). Recently, SUMOylation of arrestin-3 on lysine residue 400 has also been shown to have role in β_2AR internalization, likely by facilitating the interaction with AP2. Although the mechanism remains unclear, overexpression of SUMO deficient mutant of arrestin-3 inhibits agonist promoted internalization of β_2AR (Wyatt et al., 2011). Ubiquitination of arrestin-2 by mdm2 can indirectly regulate the endocytosis of β_2AR. Depletion of mdm2 or expression of ubiquitin deficient arrestin-3 mutant inhibits endocytosis of both β_2AR and vasopressin 2 receptor (Shenoy et al., 2007; Shenoy et al., 2001).

Role of ubiquitin in receptor trafficking

The role of ubiquitin in the endocytosis of GPCRs was initially demonstrated in the budding yeast *Saccharomyces cereviciae*. A ubiquitination-deficient α-factor receptor

Ste2P mutant that lacks a critical lysine residue in the C-tail is defective in endocytosis upon addition of α-mating factor (Hicke and Riezman, 1996). It was later shown that endocytosis is mediated by the interaction of ubiquitinated receptor with the ubiquitin interaction motif (UIM) domain of adaptor proteins such as Epsin and Eps15 (Shih et al., 2002). A similar role of ubiquitin was also observed in the case of another yeast α-factor receptor Ste3. However, in this case, only constitutive endocytosis was dependent on ubiquitination (Chen and Davis, 2002; Roth and Davis, 2000). A recent study has demonstrated that Ste3 does not require ubiquitination for its internalization, however, in the absence of the ubiquitin moiety the receptor recycles back to the plasma membrane and does not degrade efficiently (Stringer and Piper, 2011). Unlike yeast, ubiquitination of GPCRs in mammalian cells has little or no role in endocytosis. Many mammalian GPCRs are endocytosed via a clathrin-dependent pathway and some are endocytosed via lipid rafts (Chen and Davis, 2002). GPCRs such as β_2AR, DOR, CXCR4 as well as NK1R do not require ubiquitination for their internalization, however, ubiquitination is critical for their lysosomal degradation (Cottrell et al., 2006; Marchese and Benovic, 2001; Shenoy et al., 2001; Tanowitz and Von Zastrow, 2002). In the case of protease activated receptor-1 (PAR-1), a ubiquitination-deficient receptor shows increased constitutive endocytosis, suggesting a negative role of ubiquitination on internalization (Wolfe et al., 2007).

Clathrin-mediated endocytosis is one of the most characterized pathway for GPCR internalization. The key components of this pathway is the AP2 complex. This protein complex binds directly to clathrin as well as to the cargo to initiate the formation

of clathrin-coated pits (CCPs). The AP2 complex, which is composed of four subunits α, β2, μ2, and σ2, can bind to cargo proteins that contain tyrosine (TYR) or di-leucine (di-Leu) based motifs. PAR1 receptor contains a tyrosine-based motif (Y[420]KKL[423]) in the C-tail that can directly bind to μ2 subunit of the AP2 complex resulting in CCP mediated constitutive internalization (Paing et al., 2006). β2AR also contains a di-leucine motif (Leu 339, 340) that plays a critical role in the internalization of receptor (Gabilondo et al., 1997). For the chemokine receptor CXCR4 and CXCR2, the amino acid sequence LLKIL in the carboxyl terminus is required for its internalization (Orsini et. al., 1999; Fan et al., 2001).

Non-classical/clathrin-independent endocytosis

Several receptors follow non-classical/clathrin-independent pathway for internalization. One of the most distinguishing features of this pathway is the sensitivity towards cholesterol depleting agents, suggesting a role of lipid rafts (Parton and Richards, 2003). Caveolae, a specialized lipid raft enriched in the protein caveolin-1, are shown to be important in the internalization of many GPCRs. In the case of the D1 dopamine receptor, mutation of the caveolin binding motif in the receptor significantly attenuates caveolae-mediated endocytosis (Kong et al., 2007). Section 1.9 discusses lipid rafts, caveolae and their role in trafficking as well as signaling in greater details.

GPCR RECYCLING

The β2AR is known to efficiently recycle back to the plasma membrane after it has internalized onto endosomes (Hanyaloglu et al., 2005). One such recycling

determinant is the PDZ [post synaptic density protein (PSD95), *Drosophila* disc large tumor suppressor (DLG), and zonula occludens-1 protein (zo-1)] ligands/motifs (Marchese et al., 2008). PDZ motifs are present at the C-terminal end of the receptor tail and are recognized by the PDZ domains. For β_2AR, PDZ motif present in the C-tail is important for its binding to phosphoprotein EBP50 (for ezrin–radixin–moesin (ERM)-binding phosphoprotein-50), which interacts with the actin cytoskeleton to promote active recycling (Cao et al., 1999). A large number of GPCRs have been predicted to contain PDZ ligands, but whether these GPCRs undergo recycling similar to β_2AR remain to be determined (Marchese et al., 2008). The ESCRT-0 protein hepatocyte growth factor regulated tyrosine kinase substrate (HRS) has also been shown to play an important role in recycling of certain GPCRs. Although the mechanism is unclear, it has been shown that overexpression or siRNA-mediated knockdown of HRS, which leads to enlarged endosomes, inhibits recycling of β_2AR, MOR, PAR2 and calcitonin receptor like receptors (Hanyaloglu et al., 2005; Hasdemir et al., 2007). Interestingly, neither the UIM domain of HRS, nor the ubiquitination status of the receptor, is required for efficient recycling. As discussed later, HRS is also a key protein of the transport machinery involved in the degradation of GPCRs. Suggesting that HRS-mediated recycling of certain GPCRs may occur at an early stage of ESCRT-mediated sorting.

Role of arrestins in GPCR recycling

Arrestins may also mediate receptor recycling at a post-internalization step by playing a direct role on endosomes. For a subset of GPCRs, arrestins may co-internalize

with the receptor into an endocytic compartment (Oakley et al., 1999; Oakley et al., 2001). The ability of arrestins to co-internalize with GPCRs is due to their ability to form stable complexes with the GPCR. For many GPCRs, once arrestins bind and desensitization and receptor internalization have initiated, the two proteins disassociate while the receptor internalizes onto endosomes. However, for a subset of GPCRs, not only does arrestin binding promote desensitization and internalization, arrestins may co-internalize with the receptor onto endosomes (Oakley et al., 2000). These receptors tend to have multiple serine/threonine residue clusters near the end of their C-tail. Phosphorylation of these clusters promote high affinity arrestin binding that stabilizes its binding to the receptor, thereby allowing it to remain bound to the receptor while internalization onto endosomes occurs. Ubiquitination of arrestins have also been shown to regulate their affinity to bind to activated receptor. A constitutively ubiquitinated arrestin mutant can alter the kinetics of β_2AR internalization and make it behave like a class B receptor (Shenoy and Lefkowitz, 2003; Shenoy et al., 2001). For these receptors, arrestins can be found to co-localize with the receptor on endosomes. This stable interaction affects receptor recycling because it slows down the recycling of the receptor, likely by preventing the receptor from efficiently entering into the recycling pathway.

Arrestins may also play a role in GPCR recycling independent of its role in promoting GPCR internalization. Although arrestins are not required for internalization of the N-formyl peptide receptor (FPR), they are required for promoting FPR recycling. Agonist-induced internalization of FPR occurs in an arrestin-independent fashion, as FPR internalization was not altered in mouse embryonic fibroblast cells isolated from

arrestin-2 and arrestin-3 knockout out mice (Vines et al., 2003). However, recycling of the receptor was impaired in the knock-out MEFs and restored in cells in which arrestin-2 and arrestin-3 were re-expressed. Although not required for internalization, agonist activation promotes arrestin binding to FPR and its co-internalization with the receptor onto endosomes. Once on endosomes, arrestins promote recycling through a mechanism that remains to be determined. In case of the bradykinin (BK) type 2 receptor (B2R), dissociation of arrestin following internalization is critical for efficient recycling of receptor. Receptor mutants that show increased affinity for arrestin fail to recycle back to the plasma membrane (Simaan et al., 2005). It has been shown that the recycling of A_{2B} adenosine receptor ($A_{2B}AR$) depends on the presence of endogenous arrestins. HEK293 cells with stable knockdown for arrestin-2 and arrestin-3 show impaired $A_{2B}AR$ recycling, which can be rescued upon reconstitution of either arrestin-2 or arrestin-3 (Mundell et al., 2000).

GPCR DOWNREGULATION

Following endocytosis, activated GPCRs may be degraded in lysosomes giving rise to a process termed downregulation (Figure 1.3). Ubiquitination plays an important role in the trafficking of receptors after their endocytosis by regulating the sorting of cargo from the early endosomes to late endosomes. Ubiquitination is important for cargo entry into multivesicular bodies (MVBs), which also requires conserved machinery called the *E*ndosomal *S*orting *C*omplex *R*equired for *T*ransport (ESCRT) machinery.

Ubiquitination as a signal for degradation

A role for ubiquitin in the downregulation of mammalian GPCRs was initially revealed in studies examining downregulation of β₂AR (Shenoy et al., 2001) and the chemokine receptor CXCR4 (Marchese and Benovic, 2001). Agonist stimulation promotes ubiquitination of the β₂AR, which is important for its downregulation, however, the pathway was undefined (Shenoy et al., 2001). Downregulation of CXCR4 also depends on ubiquitination and ubiquitin moiety present on lysine residues in the C-tail are important for endosomal sorting to the lysosomes (Marchese et al., 2003). Several other GPCRs such as V2 vasopressin receptor (V2R), PAR2, NK1R and kappa-opioid receptor (KOR) have been shown to depend on ubiquitination for their degradation. (Cottrell et al., 2006; Jacob et al., 2005; Li et al., 2008; Martin et al., 2003)
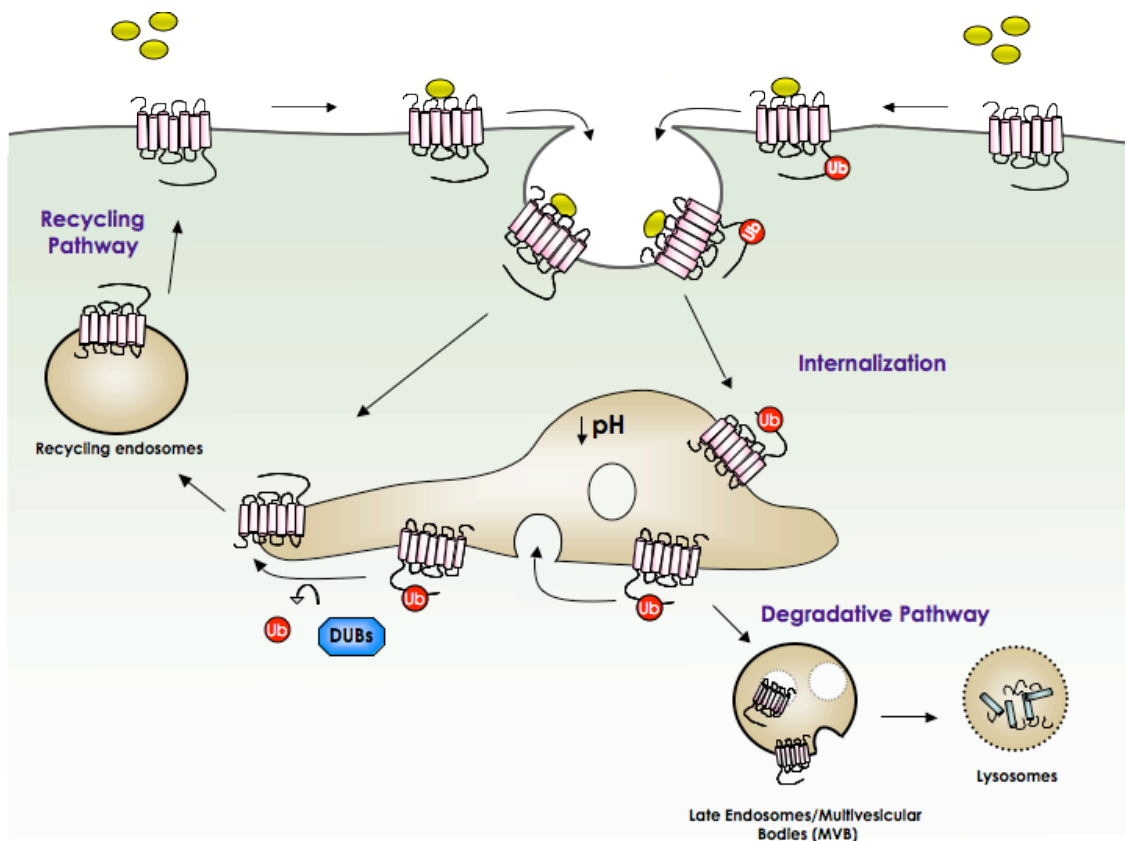
Figure 1.3. Trafficking of GPCRs. Upon activation by its cognate ligand (oval), GPCRs are typically sequestered into specialized microdomains of the plasma membrane that are responsible for endocytosis. These areas of the plasma membrane pinch off, forming vesicle that eventually fuse with early endosomes to where the receptors are delivered. Some receptors may be modified with ubiquitin moieties at the plasma membrane, although the ubiquitin moiety is not required to promote receptor internalization. Once on early endosomes, GPCRs are sorted for either entering the recycling or degradative pathway. GPCRs that enter the degradative pathway are typically modified by ubiquitin, which serves as a signal for sorting into multivesicular bodies (MVBs). MVBs fuse with lysosomes where degradation of the receptor occurs. GPCRs that are not ubiquitinated may enter the recycling pathway and are returned to the plasma membrane via recycling endosomes, giving rise to functional resensitization of signaling. The ubiquitin moieties on some receptors may be removed by the action of deubiquitinating enzymes (DUBs), which may occur on endosomes, and redirect receptors targeted for the degradative pathway into the recycling pathway.

Endosomal Sorting Complex Required for Transport (ESCRT) machinery

Sorting of ubiquitinated cargo proteins into the MVBs is executed by protein complex composed of class E (vaculor protein sorting) VPS proteins called ESCRT (Endosomal sorting complex required for transport (Figure 1.4) . Genetic and biochemical approaches have revealed that the ESCRT machinery can be subdivided into four complexes, ESCRT-0, -I, -II and -III, and several accessory components (Babst et al., 2002a; Babst et al., 2002b; Bache et al., 2003; Katzmann et al., 2001; Katzmann et al., 2003). The four ESCRT complexes are thought to act in a coordinated fashion to sort the ubiquitinated cargo into the intraluminal compartment of the MVBs (reviewed in Williams and Urbe, 2007). Table 1.1 lists the proteins that form the ESCRT complexes plus additional associated proteins.

Table 1.1 ESCRT pathway proteins. Names of all the ESCRT pathway proteins identified in yeast *Saccharomyces cerevisiae* and their human orthologues.

Complex	Yeast Proteins	Human Proteins	Important Domains
ESCRT-0	Vps 27	HRS	FYVE, UIM, VHS
	Hse1	STAM-1, STAM-2	UIM, SH3, VHS
ESCRT-I	Vps 23	Tsg101	UEV
	Vps28	Vps28	
	Vps37	Vps37A, B, C, D	Coiled-coil
	Mvb12	MVB12A, B	
ESCRT-II	Vps22	EAP30	Coiled-coil, WH
	Vps25	EAP25	PPXY, WH
	Vps36	EAP45	GLUE, NZF, WH
ESCRT-III	Vps2	CHMP2A, B	Coiled-coil
	Vsp20	CHMP6	Coiled-coil
	Vps24	CHMP3	Coiled-coil, MIR
	Snf7/Vps32	CHMP4A, B, C	Coiled-coil
	Vps60	CHMP5	Coiled-coil
	Did2	CHMP1A, B	Coiled-coil
Other	Vps4	VPS4A, B	
	Vta1	LIP5	
	Ist1	IST1	
	Bro1	ALIX	Bro1

ESCRT-0 is composed of HRS and signal transduction adaptor molecule (STAM). This complex is essential for the initial recognition of the ubiquitinated cargo. HRS contains several important domains that are required for its function. FYVE (Fab1, YOTB, Vac1 and early endosome antigen-1 (EEA1)) domain of HRS interacts with phosphatidylinositol-3-phosphate (PtdIns3P), a phospholipid that is enriched on the endosomal membrane (Burd and Emr, 1998). HRS also interacts with ubiquitinated cargo via its UIM to recruit ubiquitinated cargo to the endosomal membrane. HRS also binds to clathrin via a clathrin binding box motif (Leu-Ile-Ser-Phe-Asp) present at its C terminus. Another important function of ESCRT-0 is to recruit the downstream

ESCRT machinery to the ubiquitinated cargo. A PSAP motif present in HRS can directly interact with the ubiquitin E2 varient (UEV) domain found in ESCRT-1 protein Tsg-101. A similar motif is also present in Vps27, the yeast ortholog of Hrs (Pornillos et al., 2002; Ren and Hurley, 2011).
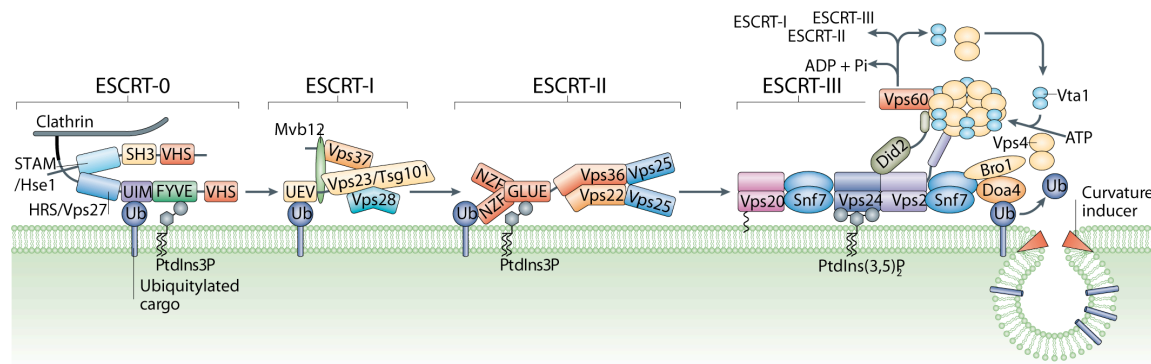
Adapted from William and Urbe, 2007

Figure 1.4. Schematic representation of ESCRT complex required for sorting of ubiquitinated cargo. Ubiquitinated cargo is recognized by ESCRT-0 protein complex protein HRS that binds to phosphatidylinositol-3-phophate (PtdIns3P) via the FYVE domain. Other domains such as GLUE domain of Vps36 and ability of Vps24 to bind to PtdIns(3,5)P2 can also contribute to the assembly of the complex to the endosomes. ESCRT-0, I and II also bind to ubiquitin via UIM, UEV or GLUE domains to facilitate cargo sorting. ESCRT-III complex, which is recruited by ESCRT-II, is required for final sorting process whereby, the receptor is deubiquitinated and concentrated into invaginations that lead to the formation of multivesicular bodies (MVB). Finally, AAA ATPase Vps4 is recruited which disassembles the complex and releases the proteins for another round of sorting. (Williams and Urbe, 2007)

The other member of ESCRT-0 is STAM. The STAM protein possesses a UIM domain that is found in number of proteins involved in endocytosis and protein trafficking such as HRS, Eps15 and Epsin. These domains are known to bind to both monoubiquitin, as well as polyubiquitin chains, and are shown to cooperate in the

recognition of ubiquitinated proteins (Bilodeau et al., 2002). Yeast Hse1 (mammalian orthologue of STAM) interacts with Vps27p (mammalian orthologue of HRS) to form a complex that binds to ubiquitin and regulates the endosomal sorting of cargo proteins (Asao et al., 1997; Endo et al., 2000; Pandey et al., 2000; Takeshita et al., 1996).

The STAM family is composed of two members STAM-1 and STAM-2 that share approximately 53% amino acid sequence homology (Endo et al., 2000). As shown in Figure 1.5, both STAMs are structurally identical and show 89% amino acid identity in each of the respektive domains (Prag et al., 2007; Ren et al., 2009). STAM contains an N-terminal VHS (Vps27, HRS and STAM homology) domain, UIM, SH3 domain, immunoreceptor-based tyrosine activation motif (ITAM) and coiled-coil region (Yamada et al., 2002; Yamada et al., 2001). Studies done on STAM knockout mice indicates that a double knockout of STAM-1 and STAM-2 is embryonic lethal (Takeshita et al., 1997). However, STAM-1 knockout alone shows growth retardation and defects in hippocampal CA3 pyramidal neurons compared to wild type littermates (Yamada et al., 2001).
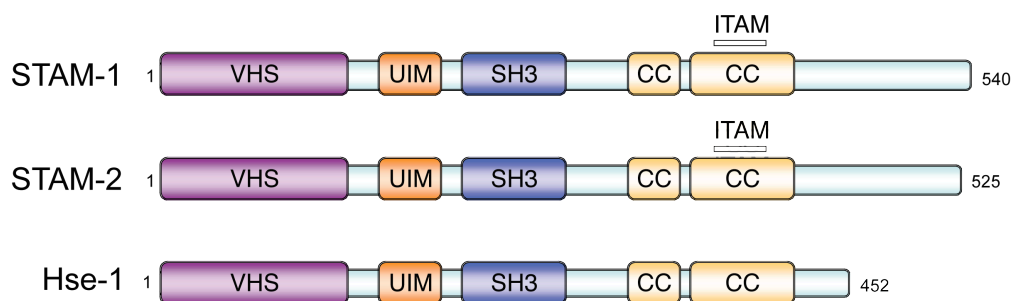
Figure 1.5 Schematic representation of the domain organization of STAM-1, STAM-2 and yeast ortholog Hse1. Both STAM-1 and STAM-2, as well as Hse1 are structurally identical and they contain VHS, UIM, SH3 and CC domains. Abbreviations; VHS: Vps27, HRS and STAM homology, UIM:

ubiquitin interacting motif, SH3: SRC homology 3, CC: coiled-coil, ITAM: immunoreceptor-based tyrosine activation motif.

Role of STAM in signal transduction: STAMs were initially characterized as signaling molecules due to their ability to be phosphorylated upon stimulation with a variety of interleukins and growth factors (Isakov, 1997; Pandey et al., 2000). Both STAM-1 and 2 have been shown to associate with tyrosine kinases Jak2 and Jak3 to regulate IL-2 and granulocyte macrophage colony-stimulating factor (GM-CSF) mediated signaling. Association with Jak2 and 3 is mediated by the SH3 and ITAM motifs (Endo et al., 2000; Takeshita et al., 1997).

STAMs have also been shown to interact with AMSH (associated molecule with the SH3 domain of STAM). Although AMSH is a deubiquitinating enzyme and has been linked to trafficking, it has also been shown to play role in IL-2 and GM-CSF mediated c-myc induction and DNA synthesis (Tanaka et al., 1999). AMSH is also involved in bone morphogenesis protein (BMP) signaling. AMSH binds to Smad6 which is an antagonist of BMP-Smad signaling thereby, promotes signaling (Itoh et al., 2001; Tanaka et al., 1999).

STAM as an endosomal sorting molecule: Both STAM-1 and STAM-2 are tightly associated with ESCRT-0 protein HRS (Hepatocyte growth factor regulated tyrosine kinase substrate) via their coiled coil region (Asao et. al., 1997; Bache et. al., 2003). One of the key domains present in STAM is the VHS domain. It is an evolutionarily conserved domain found in several proteins involved in endocytosis and vesicular

trafficking such as HRS, GGA (Golgi-localized ear–containing, ADP ribosylation factor–binding proteins) and Tom1 (Target of Myb 1) proteins (Puertollano et al., 2001). The VHS domain of GGAs has also been implicated in the trafficking of the Manose-6-phosphate receptor from golgi to endosomes (Puertollano et. al., 2001). STAM also binds to other proteins that are involved in the endosomal sorting machinery such as AMSH and USP8. STAMs have also been implicated in ER-to-Golgi trafficking through their interaction with the COPII (coat protein II) protein on the endoplasmic reticulum (Rismanchi et. al., 2009). STAMs have also been shown to bind to ubiquitin via its VHS and UIM domains (Ren and Hurley 2010)

ESCRT-I: In mammalian cells, ESCRT-I consists of Tsg101 (Vps23p in yeast), VPS28, one of four isotypes of VPS37 (VPS37A–D) and MVB12A/B (Chu et al., 2006). The central component of ESCRT-I complex is Tsg101, which is recruited to the endosomal membrane by ESCRT-0 (Katzmann et al., 2001). Tsg101 plays an important role in MVB sorting via recognition of ubiquitinated cargo by its UEV domain (Sundquist et al., 2004). Depletion of Tsg101 as well as mutations in the UEV domain that disrupts its binding to ubiquitin, inhibit MVB sorting (Babst et al., 2000; Sundquist et al., 2004). Both Tsg101, as well as Vps28, are also required to link ESCRT-I with the downstream ESCRT-II complex (Babst et al., 2002b).

ESCRT-II: The ESCRT-II complex, which is composed of Vps22, Vps25 and Vps36, is mainly involved in the recruitment of ESCRT-III complex proteins to the endosomal membranes. Proteins in this complex contain a winged-helix domain (WH), which is a protein–protein and protein–DNA interaction domain. The WH domain of Vps25 can

directly interact with ESCRT-III protein Vps20 and hence plays an important role in the assembly of ESCRT-III complex. (Babst et al., 2002a; Teo et al., 2004). Vps36 also contains a GLUE domain (GRAM-like ubiquitin-binding in EAP45) that can bind to ubiquitin as well as subset of 3-phosphoinositides present on the endosomal membranes (Slagsvold et al., 2005).

ESCRT-III and related proteins: ESCRT-III and related proteins such as Vps4 are directly responsible for membrane scission and formation of intraluminal vesicles (ILVs). The ESCRT-III complex is composed of Vps20, Snf7, Vps24 and Vps2. Several other proteins such as Vps60, Did2 and Ist1 are also known to be in ESCRT-III complex (Rue et al., 2008). All these subunits are retained in the cytosol as soluble monomers. Upon activation/membrane binding, the C-termini of ESCRT-III subunits are exposed, allowing them to bind to the microtubule-interacting and transport (MIT) domains of downstream effector proteins that lead to the formation of a detergent-insoluble complex on the endosomal membrane (Babst et al., 2002a). Vps24 contains a MIT-interacting region (MIR) that can interact with and recruit proteins required for disassembly of ESCRT machinery from endosomal membrane, such as deubiquitinating enzyme AMSH (Agromayor and Martin-Serrano, 2006) and the AAA ATPase Vps4 (Scott et al., 2005). The disassembly of the ESCRT machinery and formation of MVBs depends on protein Vps4. A Vps4 mutant that cannot hydrolyze ATP acts as a dominant negative and blocks the formation of ILV and hence leads to accumulation of cargo proteins on endosomes (Fujita et al., 2003; Sachse et al., 2004). Vps4 also hydrolyzes ATP to drive the recycling of ESCRT-III subunits back to their soluble monomeric form.

Role of arrestins as mediators of endosomal sorting

Arrestins may serve as an adaptor to recruit E3 ubiquitin ligases directly to activated receptors to mediate their ubiquitination. The ubiquitin moiety serves as a sorting signal on endosomes for targeting the receptor into the degradative pathway. A role for arrestins as an E3 ubiquitin ligase adaptor was first suggested in studies examining the regulation of β_2AR. Agonist-promoted ubiquitination of β_2AR is impaired in MEF cells isolated from arrestin-3 knock-out mice, suggesting that arrestin-3 mediates ubiquitination of β_2AR. In contrast, arrestin-2 is not involved in β_2AR ubiquitination. Arrestin-3 also interacts with the HECT-domain E3 ubiquitin ligase Nedd4 (Shenoy et al., 2008). Depletion of Nedd4 by siRNA attenuates β_2AR ubiquitination and lysosomal targeting. The interaction between β_2AR and Nedd4 is dependent upon the presence of arrestin-3. This is consistent for a role of arrestin-3 serving as an adaptor to recruit Nedd4 to β_2AR.

Interestingly, Nedd4 may be recruited to β_2AR in an arrestin-3 independent manner involving the arrestin domain-containing protein ARRDC3. ARRDs are a family of 6 mammalian proteins related to yeast proteins called arrestin-related trafficking (ART) adaptor proteins that were first characterized in the yeast *Saccharomyces cerevisiae* (Lin et al., 2008). Collectively, these proteins have been referred to as alpha-arrestins to distinguish them from arrestins (Alvarez, 2008). Although sharing very little amino acid sequence identity with mammalian arrestins, bioinformatics modeling revealed that alpha-arrestins have an arrestin-fold consisting of N and C domains. One key distinguishing feature present in ARRDs but not found in non-visual arrestins or visual

arrestins is that ARRDs have a long carboxy-terminal domain harboring two PY motifs. PY motifs are short stretches of amino acids typically found in the context of PPxY and PPPY, where P is a proline residue, x is any amino acid and Y is a tyrosine residue. PY motifs are typically recognized by WW domains, which are domains of approximately 30 amino acids containing two highly conserved tryptophan residues. The Nedd4-like family of HECT-domain E3 ubiquitin ligases, comprised of 9 members in the human genome, is characterized by the presence of 3-4 tandemly linked WW domains. Substrates that have PY motifs interact directly with their cognate E3s via the WW domains, however, many substrates do not have PY motifs and are believed to interact indirectly with these E3s through an adaptor protein that harbors a PY motif (Shearwin-Whyatt et al., 2006). Recently, it was reported that ARRDC3 interacts with the β_2AR and serves as an adaptor for Nedd4-dependent ubiquitination of the receptor. Depletion of ARRDC3 attenuates agonist-induced degradation and ubiquitination of β_2AR (Nabhan et al., 2010). Co-immunoprecipitation studies reveal that ARRDC3 interacts with the β_2AR in an agonist-dependent manner, suggesting that it may serve as an adaptor for Nedd4 mediated ubiquitination of β_2AR (Nabhan et al., 2010). Although ARRDC3 is predicted to bind directly to Nedd4 via its PY motif, it is not known how it interacts with β_2AR. Mammalian arrestins do not contain PY motifs, therefore it remains unclear how Nedd4 interacts with arrestin-3. In addition, it remains to be determined how the actions of arrestin-3 and ARRDC3 are coordinated to mediate β_2AR ubiquitination.

Interestingly, arrestin-2 interacts with another member of the Nedd4-like family of E3 ubiquitin ligases known as AIP4 (Bhandari et al., 2007). The interaction between

arrestin-2 and AIP4 is direct and it is mediated by AIP4 WW domains I and II. In addition to interacting with PY motifs, WW domains are also known to interact with phosphorylated serine or threonine residues in the presence of an adjacent proline residue (pS/TP) (Verdecia et al., 2000). Presently, it remains to be determined how the AIP4 WW-domains interact with arrestin-2. Interestingly, non-canonical WW-mediated interactions involving AIP4 have been recently reported. For example, the WW domains of AIP4 have been shown to interact with phosphorylated serine residues in the absence of nearby proline residues. Phosphorylation of serine residues within the C-tail of the CXCR4 mediate a direct interaction with AIP4 via WW domains I and II (Bhandari et al., 2009). A receptor mutant in which C-tail serine residues 324 and 325 were changed to alanine residues (S324/5A) attenuate binding to AIP4 (Bhandari et al., 2009; Marchese and Benovic, 2001). Accordingly the S324/5A mutant showed defective ubiquitination and degradation. Agonist-promoted phosphorylation of these residues occurred at the plasma membrane leading to AIP4 recruitment to the plasma membrane where the receptor is ubiquitinated. Therefore for CXCR4 ubiquitination, an adaptor is not required because the Nedd4-like E3 AIP4 can interact directly with the receptor. Similar to the mechanism of the interaction between AIP4 and CXCR4, the WW domains of Nedd4 may also interact with its substrates via phosphorylated serine residues in the absence of nearby proline residues (Edwin et al., 2010). Therefore, phosphorylated serine residues in the absence of proline residues may represent a general recognition motif for WW domains.

CHEMOKINE RECEPTORS

Chemokine (*Chemo*attractant cyto*kine*) receptors belong to the class A subfamily of GPCRs. There are 19 distinct chemokine receptors identified in mammals. Chemokine receptors are activated by 8-10 kDa small protein ligands known as chemokines (Zlotnik et al., 2006). Based upon the organization of the first two amino terminal cysteine residues, chemokines are divided into four classes- CXC (seven members), CC (ten members), XC (one member, XCR1) and CX3C chemokine (one member, CX3CR1) (Zlotnik and Yoshie, 2000). The receptors are also named according to the type of chemokine that they bind. For example, receptors that bind to CXC type of chemokine are called CXC receptors (CXCR)

CHEMOKINE RECEPTOR 4 (CXCR4)

One of the most studied chemokine receptor is CXCR4, also known as fusin or CD184 (cluster of differentiation 184) (Moriuchi et al., 1997; Wegner et al., 1998). It is one of the 7 known CXC-receptors and is activated by the chemokine ligand CXCL12 (a.k.a. stromal cell–derived factor 1alpha, SDF-1α).

Until recently, CXCL12 was the only known ligand for CXCR4, however, recent evidence demonstrates that ubiquitin, a small (76 amino acid) protein highly conserved among eukaryotic cells, and the cytokine MIF (macrophage migrating inhibitory factor) can also serve as ligands for CXCR4 (Bernhagen et al., 2007; Saini et al., 2010). MIF has been shown to function as a non-cognate ligand for both CXCR2 and CXCR4 chemokine receptors and trigger Gα_i and integrin-dependent chemotaxis of monocytes

and T cells (Bernhagen et al., 2007). The chemokine receptor CXCR7 (a.k.a RDC1) has been shown to bind to both CXCL12 and CXCL11. However, unlike CXCR4, CXCR7 fails to induce classical chemokine responses, such as cell migration and intracellular signaling. CXCR7 has been shown to act as a scavenger for CXCL12, thereby regulating CXCL12 mediated CXCR4 activation and function (Dambly-Chaudiere et al., 2007; Naumann et al., 2010).

CXCR4 oligomerization

CXCR4 forms both homo as well as heterodimers. Homodimerization of CXCR4 has been shown to play role in activation of JAK/STAT pathway as well as enhanced response to the ligand CXCL12 (Vila-Coro et al., 1999). Crystal structure of CXCR4 bound to antagonist IT1t also indicates that receptor is present as a homodimer (Wu et. al. 2010). Heterodimerization with CCR2 and CD4 has been shown to be important for HIV infection (Rodriguez-Frade et al., 2004; Toth et al., 2004). CXCR4 also dimerizes with T Cell Receptor (TCR) to activate the ERK pathway via the ZAP-70 tyrosine kinase (Kumar et al., 2006). CXCR4 is also present in a hetero-oligomeric complex with CCR2 and CCR5 (Sohy et al., 2007; Sohy et al., 2009). Recently, CXCR4 has also been shown to heterooligomerize with CXCR7. This heterodimer constitutively recruits arrestin and hence, preferentially activates arrestin-mediated signaling pathways such as ERK1/2, p38 MAPK, and SAPK over G protein-dependent pathways. As a result, the CXCR4/CXCR7 heterodimer has a more potent ability to promote cell migration (Decaillot et al., 2011). Taken together, the ability of CXCR4 to

homo/heterodimerize diversifies its ability to activate signaling by alternate and non-classical pathways.

Biological role of CXCR4

CXCR4/CXCL12 chemokine axis plays an important role in hematopoiesis, where CXCL12 acts as a critical chemokine attractant for immature and mature hematopoietic cells. This is important for the homing of hematopoietic stem cells to the bone marrow as well as their survival and proliferation (Broxmeyer et al., 2003; Lataillade et al., 2000). The following section will discuss some of the most important conditions that arise due to abnormal expression or regulation of CXCR4.

CXCR4 and Immunodeficiency Diseases

Dysregulation of CXCR4/CXCL12 signaling axis has been shown to be associated with two rare human immunodeficiencies, WHIM syndrome, which is associated with a gain of CXCR4 function and the Idiopathic CD4(+) T-cell lymphocytopenia, which is associated with a loss of CXCR4 function.

WHIM Syndrome: WHIM (Warts, Hypogammaglobulinemia, infection and Myelokathexis) syndrome is a rare immunodeficiency disorder characterized by chronic neutropenia (abnormally low number of neutrophils) (Gorlin et al., 2000; Kawai and Malech, 2009). It is linked to a gain of function mutation in CXCR4 that causes retention and apoptosis of the neutrophils in the bone marrow, leading to neutropenia. Mutations identified include one frame shift (S339fs342X) and several non-sense

(R334X, G336X, S338X, E343X) mutations. Irrespective of the type, all the mutations lead to the truncation of CXCR4 C-tail, which causes improper regulation of CXCR4 signaling and hence lack of desensitization, enhanced chemotaxis, increase in calcium mobilization, increase in F-actin polymerization and decreased internalization (Alapi et al., 2007; Diaz, 2005; Hernandez et al., 2003). In one WHIM patient, no mutations were found in CXCR4, suggesting that the downstream regulators of CXCR4 signaling such as GRKs and arrestins may also be involved. This is interesting because GRK6 and arrestin-3 knockout mice also show defects in neutrophil migration as seen in WHIM patients (Fong et al., 2002a; Vroon et al., 2004)

Idiopathic CD4(+) T-cell Lymphocytopenia (ICL): ICL is characterized by a defect in the CD4(+) T-cell population predisposing a patient to opportunistic infections (Luo and Li, 2008). Although the pathogenesis of ICL is unclear, alteration in CXCR4 surface expression has been shown to be involved. CD4(+)T lymphocytes from ICL patients display low membrane expression of CXCR4 as well as abnormal intracellular CXCR4 and CXCL12 expression that lead to impaired chemotaxis of CD4(+)T lymphocytes towards a gradient of CXCL12 (Scott-Algara et al., 2009).

CXCR4 and cancer

CXCR4 is typically over-expressed by cancer cells. Dysregulation of CXCR4 signaling and trafficking has been shown in more than 23 types of cancers ranging from epithelial, mesenchymal to hematopoietic origin (Balkwill, 2004; Busillo and Benovic, 2007). CXCR4 activates a variety of cellular pathways leading to chemotaxis, invasion,

and adhesion, all of which correlate with metastatic behavior of cancers such as breast cancers, thyroid cancers, hepatocellular carcinomas and small cell lung cancers. Metastasis to organs that express the ligand CXCL12 at high concentrations such as lymph node, liver, bone marrow and lung have been shown in the case of breast cancer (Muller et al., 2001). Consistent with this observation, overexpression of CXCR4 alone is sufficient to significantly increase the metastasis of parental MDA-MB-231 cells to bone marrow (Kang et al., 2003). Activation of CXCR4 also stimulates the production of matrix metalloproteinases (MMP). CXCR4-mediated expression of MMP2 and MMP9 is required for proper homing of human hematopoietic progenitor cells (Janowska-Wieczorek et al., 2000). MMP secretion has also been linked to the property of tumor cells to metastasize from the site of origin to distant organs. Yu et. al., recently showed that in oral squamous cell carcinoma, CXCR4 activation upregulates the production of MMP9 and MMP13 via activation of the ERK signaling pathway that in turn increases the migration and invasion potential of these cells (Yu et al., 2011). Similar observations were also seen in head and neck squamous cell carcinomas (HNSCC) (Samara et al., 2004).

Other factors can also regulate the expression of CXCR4 in tumor cells at the level of transcription. For example, in HER2 positive breast cancers, the receptor tyrosine kinase HER2 upregulates the expression of CXCR4 through inhibition of ubiquitination as well as an increase in translation (Li et al., 2004). Hypoxia also regulates the expression of CXCR4, it has been shown that hypoxia inducible factor 1 (HIF1) can directly regulate the expression of CXCR4 mRNA (Schioppa et al., 2003; Staller et al., 2003).

Other factors such as vascular endothelial growth factor (VEGF), nuclear factor kappa B (NF-κB), oncoproteins like PAX3-FKHR and RET/PTC can also regulate the expression of CXCR4 during cancer progression (Busillo and Benovic, 2007; Helbig et al., 2003).

Although the specific role of the CXCR4/CXCL12 chemokine axis in cancers remain to be fully defined, several CXCR4 antagonists are being used to inhibit CXCR4-mediated metastasis of cancer cells. A CXCR4 peptide antagonist that mimics the CXCL12 binding site has been shown to inhibit the migration of breast cancer cells in a mouse model (Liang et al., 2004). Compound MDX-1338 (BMS 936564), a specific CXCR4 antagonist from Bristol-Myers Squibb is currently in Phase I clinical trials to treat patients of Acute Myelogenous Leukemia (AML) (http://clinicaltrials.gov/ct2/show/NCT01120457). Another selective CXCR4 antagonist, (Substance BKT-140 from Biokine Therapeutics Ltd) is currently under phase II clinical trials to treat patients with Multiple Myeloma (http://clinicaltrials.gov/ct2/show/NCT01010880).

CXCR4 and Cardiovascular Disease

CXCR4 and its cognate ligand CXCL12 play an important role in the development of the heart and vasculature (Tachibana et al., 1998; Nagasawa et al., 1996). CXCR4 knock-out mice show high embryonic mortality due to cardiac ventricular septum defects and poor development of the vasculature in the gastrointestinal tract (Tachibana et al., 1998). Similar findings were also observed in mice lacking CXCL12

(Tachibana et al., 1998; Zhang et al., 2008). Enhanced expression of CXCR4 has been demonstrated in the failing myocardium (Damas et al., 2000). Recently, it has been shown that functional CXCR4 present on cardiac myocytes can modulate L-type Ca^{2+} channel activity which may lead to heart failure (Pyo et al., 2006). Impaired CXCR4 signaling can lead to alteration in angiogenic activity and homing capacity of endothelial progenitor cells (EPC) leading to aberrant neovascularization in coronary artery disease (Krapp, 1992). Using a nude mice hind limb animal model, it has been shown that mononuclear cells derived from bone marrow of patients with chronic ischemic heart disease showed impaired capacity for neovascularization compared to cells isolated from healthy control subjects, possible due in part to CXCR4 dysregulation (Heeschen et al., 2004).

Despite the importance of CXCR4 in normal physiological processes, as well as in a variety of pathological conditions, the mechanisms by which it is regulated remain poorly understood. Understanding the molecular mechanisms that regulate CXCR4 signaling as well as trafficking will help us better understand various pathological conditions associated with CXCR4 dysregulation.

CXCR4 activation and signal transduction

The first step in the activation of CXCR4 is the binding of CXCL12. The extracellular N-terminal domain of CXCR4 (amino acid residue 1-36) is important for binding to CXCL12. Ligand binding to the amino-terminus promotes a conformational change in the receptor that further facilitates additional binding between ligand and

receptor. Post-translational modification by sulfation at three tyrosine residues (Tyr7, Tyr12, and Tyr21) in the N-terminal domain of CXCR4 is necessary for high affinity binding to CXCL12 (Doranz et al., 1999; Farzan et al., 2002; Veldkamp et al., 2006). Similar to CXCR4 other chemokine receptors such as CCR5, CCR2B, and CX3CR1, are also modified by sulfation at one or more tyrosine residues (Farzan et al., 1999; Fong et al., 2002a; Preobrazhensky et al., 2000). Consistent with this observation, cleaving the N-terminal tail of CXCR4 abrogates its binding with CXCL12 and renders it non-functional. Several biological molecules such as neutrophil cathepsin, neutrophil elastase and cell surface protease dipeptidase 26 (CD26) can cleave CXCR4 N-terminal tail and hence can modulate CXCR4 signaling response (Christopherson et al., 2002; Delgado et al., 2001; Valenzuela-Fernandez et al., 2002).

G protein-dependent CXCR4 signaling. Ligand binding to CXCR4 can activate a variety of signaling pathways (Figure 1.6). Most of the signaling pathways activated by CXCR4 depend on the coupling with $G\alpha_i$ G proteins. Treatment with pertussis toxin (PTX), which ADP-ribosylate $G\alpha_i$ and prevents its interaction with the receptor, can block the majority of CXCR4 promoted signaling events (Busillo and Benovic, 2007; Thelen, 2001). Coupling to G_{13} have also been reported in the literature. Tan et al. showed that coupling to $G\alpha_{13}$ is important for Rho-dependent cell migration of Jurkat T-cells (Tan et al., 2006). Recently, $G\alpha_{13}$ has also been linked to the ability of CXCR4 to recycle back to the cell surface. $G\alpha_{13}$ and Rho-mediated actin polymerization is necessary for the trafficking of CXCR4 into a Rab11 compartment (Kumar et al., 2006).

As shown in Figure-1.6, activated CXCR4 mediates the dissociation of Gαi from the heterotrimeric G protein by facilitating the exchange of GTP for GDP. Once released, $G\alpha_i$ inhibit adenylyl cyclase (AC) resulting in the reduction of cAMP levels (Yang et al., 2007). Gαi can directly stimulate Src family kinase that in turn activates H-Ras-Raf-1-MEK1/2-ERK1/2 pathway (Ganju et al., 1998; Ma et al., 2000). $G\alpha_i$ can also stimulate various focal adhesion proteins such as FAK, paxillin, p130 and Crk (Dutt et al., 1998; Wang et al., 2000). Liberated βγ activates phospholipase C-β (PLC-β) which results in the formation of inositol-1,4,5-trisphosphate (IP$_3$) via the cleavage of inositol-4,5-bisphosphate (PIP2). IP3 is important for increase in intracellular calcium. Diacylglycerol (DAG) generated in this process can subsequently activate protein kinase C (PKC). Together these downstream messengers regulate a variety of cellular processes such as migraton and transcription.

G protein-independent CXCR4 signaling. Activation of CXCR4 also activates Janus Kinase (JAK) and Signal transducer and activator of transcription (STAT) signaling pathway. Pretreatment with PTX does not inhibit JAK/STAT signaling, suggesting that it is independent of G protein activation. (Vila-Coro et al., 1999).

Non-visual arrestins are also involved in CXCR4 signaling. Lymphocytes isolated from arrestin-3 knockout mice showed impaired chemotaxis towards the ligand in a transwell migration assay (Fong et al., 2002b). Consistent with the role of arrestins in CXCR4 signaling, it has also been shown that arrestins can sequester a number of MAPK components such as ERK and p38. siRNA mediated knockdown of arrestin-3,

block CXCL12 promoted cell migration and chemotaxis that has been previously linked

to p38 MAPK signaling (Cheng et al., 2000; Sun et al., 2002)
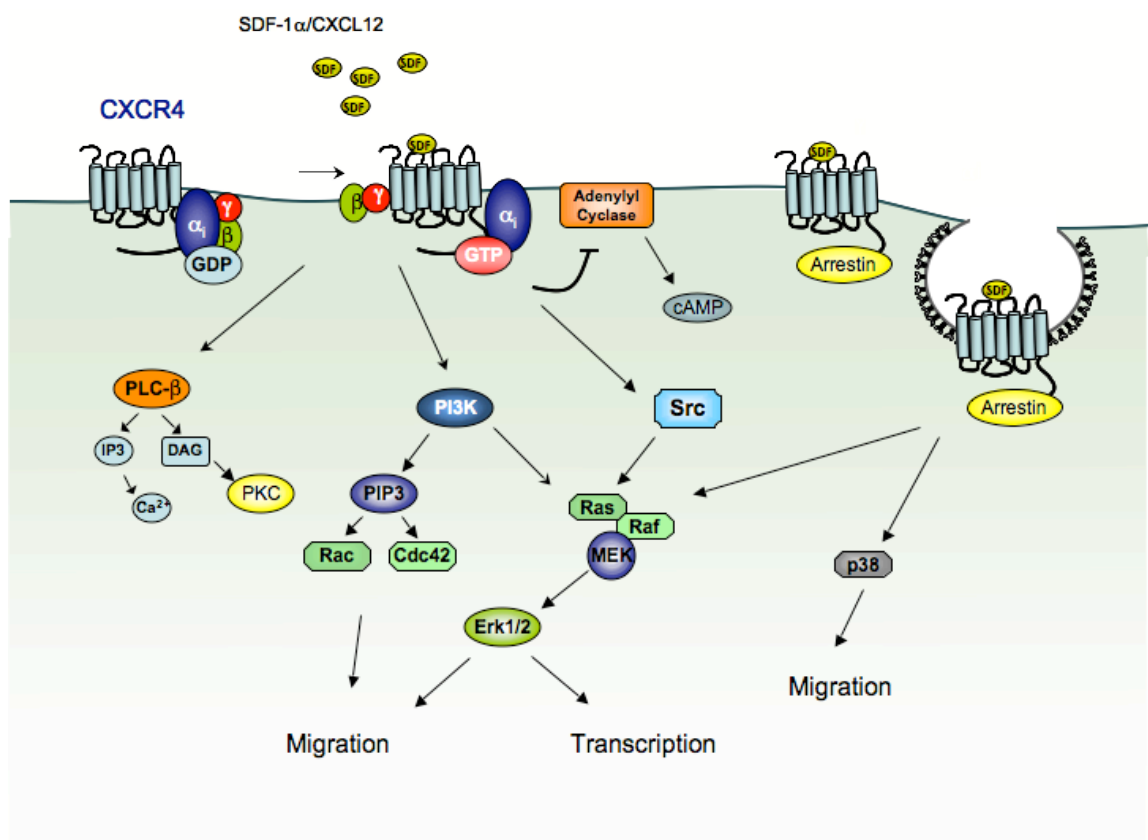
Figure 1.6. Signaling pathways activated by CXCR4. SDF binding to CXCR4 activates a wide variety of

G protein dependent and G protein independent (arrestin dependent) signaling pathways. These signaling

events regulate various biological processes such as migration, proliferation and transcription.

Regulation of CXCR4 signaling

To limit the activation of CXCR4 signaling, it is tightly regulated. Similar to other GPCRs (as described before), CXCR4 is also regulated by three main processes; desensitization, internalization and downregulation. The following section describes these regulatory mechanisms in detail.

Desensitization of CXCR4 signaling

CXCR4 contains 15 serine and 3 threonine residues in its 45-amino acid C-tail. Upon activation by CXCL12, CXCR4 is rapidly phosphorylated on multiple serine and threonine residues in the C-tail by GRKs and PKC. Several GRKs, such as GRK2 (Jimenez-Sainz et al., 2006), GRK3 (Balabanian et al., 2008) and GRK6 (Busillo et al., 2010) have been shown to phosphorylate CXCR4. Bone marrow-derived neutrophils from GRK6-deficient mice show impaired desensitization of the calcium response as well as significantly enhanced chemotaxis to CXCL12, suggesting that GRK6 is involved in CXCR4 desensitization (Fong et al., 2002b; Vroon et al., 2004). Residues that are phosphorylated have been identified by mass-spectrometry and phospho-specific antibodies. Upon CXCL12 treatment, serine resides 324 and 325 are rapidly phosphorylated by protein kinase C and GRK6, whereas Ser-339 is specifically and rapidly phosphorylated by GRK6 only. Other residue like Ser-330 is also phosphorylated by GRK6 (Busillo et al., 2010).

CXCR4 also undergoes heterologous desensitization upon phosphorylation of

serine residues by PKC. Treatment with PMA, a phorbol ester that can directly activate PKC, leads to desensitization and internalization of activated receptor (Signoret et al., 1997). Other physiological stimuli that can activate PKC such as activation of TCR (Peacock and Jirik, 1999), formyl-peptide receptor (Li et al., 2001), CXCR1 activation as well as CXCR2 activation can also induce cross desensitization and internalization of CXCR4 (Suratt et al., 2004).

Internalization of CXCR4

CXCR4 undergoes dynamin-1 dependent internalization in response to stimulation with both CXCL12 as well as PMA (through activation of protein kinase C) (Haribabu et al., 1997; Signoret et al., 1997). The serine/threonine rich C-tail of CXCR4 plays a critical role in internalization of CXCR4. Individual mutation of a stretch of residues in the C-tail (S324, S325, I328, L329, S338, S339) impairs the ability of CXCR4 to be internalized in response to both CXCL12 and PMA (Marchese and Benovic, 2001; Orsini et al., 2000). In recent studies done by Barker and Benovic, it has been shown that GRK5 can regulate the internalization of CXCR4 by phosphorylating Hsp70 interacting protein (Hip) at serine residue 346 (Barker and Benovic, 2011).
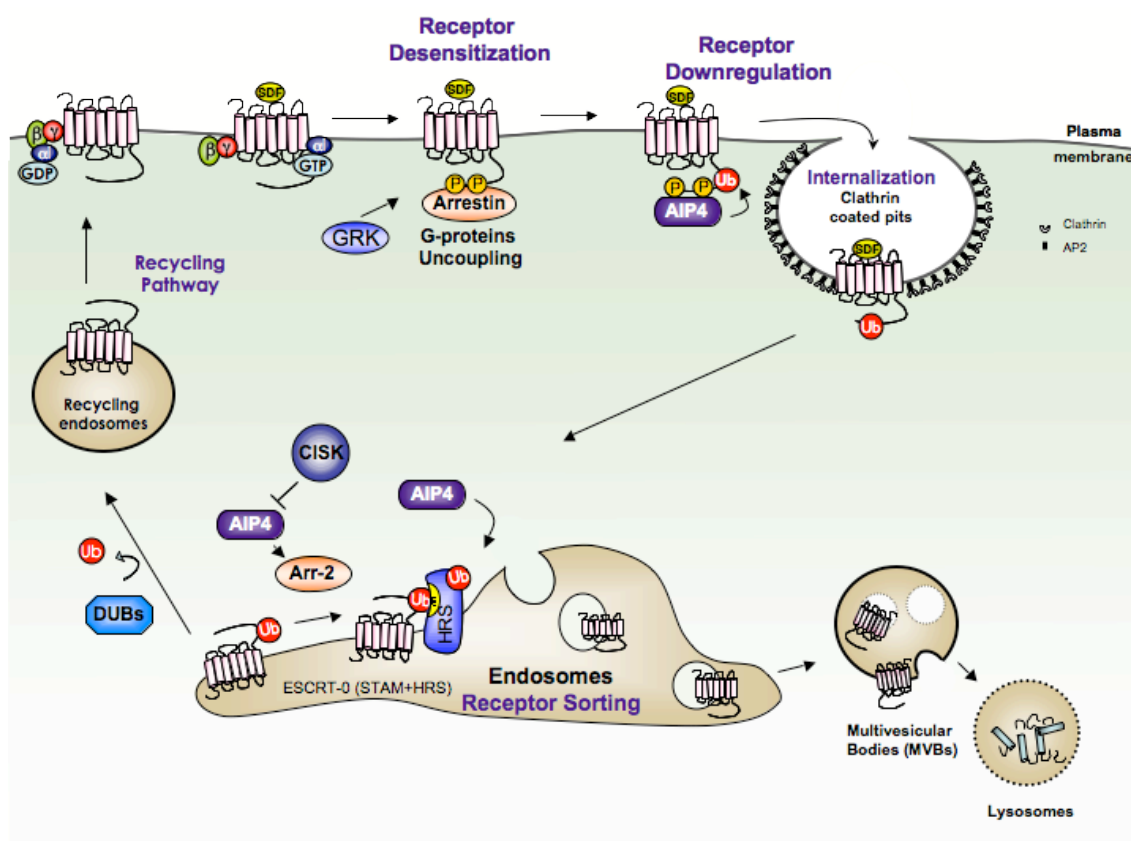
Figure 1.7 Regulation of CXCR4 signaling. CXCR4 is rapidly phosphorylated by GRKs upon agonist stimulation. Arrestin recruitment leads to uncoupling of G protein and hence desensitization of receptor signaling. Phosphorylation also recruits AIP4 that ubiquitinates the receptor. The receptor is recruited into clathrin-coated pits and internalized in a dynamin dependent and ubiquitination independent fashion. Receptor appears on early endosomes where it undergoes sorting into the multivesicular bodies (MVB) via the help of ESCRT complex protein HRS. MVB fuses with lysosomes to complete the degradation process. Receptor can get deubiquitinated and recycle back to the plasma membrane.

Ubiquitination and downregulation of CXCR4

Upon activation by CXCL12, CXCR4 is rapidly phosphorylated on two serine residues 324 and 325 in the C-tail which serve as a docking site for Ned4-like E3

ubiquitin ligase AIP4 (Bhandari et al., 2009; Busillo et al., 2010). AIP directly interacts with these serine residues via its WW domains and monoubiquitinates on one of the three-lysine residues K327, K331 and K333 (Figure 1.4) in the C-tail (Bhandari et al., 2009; Benovic and Marchese 2001). Ubiquitinated receptor is endocytosed in an arrestin-independent fashion and appears on early endosomes where it is recognized by ESCRT-0. A lysine mutant of CXCR4 (CXCR4-3K/R), that cannot be ubiquitinated can still internalize upon agonist stimulation, suggesting that internalization of CXCR4 is independent of its ubiquitination. Nevertheless, ubiquitination of CXCR4 is critical for its recruitment into the ESCRT pathway. AIP4 is also present on the endosomes where it colocalize with HRS. AIP4 ubiquitinates HRS in an agonist-dependent fashion and this ubiquitination event is important for sorting and degradation of CXCR4, however, the molecular mechanism remains to be determined (Marchese et al., 2003). The AAA ATPase Vps4 also plays role in the sorting of CXCR4 into the MVBs. Overexpression of dominant negative Vps4-E228Q (defective in ATP hydrolysis) blocks CXCR4 degradation (Marchese et al., 2003). Although CXCR4 is poorly recycled to the plasma membrane, it has been shown to be deubiquitinated by *u*biquitin *s*pecific *p*rotease 14 (USP14). USP14 plays an important role in the CXCR4 degradation, as RNAi induced knockdown blocks agonist promoted degradation of CXCR4 (Mines et al., 2009). Taken together, CXCR4 ubiquitination, as well as the downstream sorting machinery play a crucial role in the downregulation of CXCR4. However, molecular details of this process are still unclear.

LIPID RAFTS AND CAVEOLAE

Lipid rafts are specialized membrane domains that are enriched in cholesterol and glycosphingolipids (reviewed in Simons and Ikonen, 1997). Several cytoplasmic and membrane proteins have been shown to be associated with these lipid rafts. Proteins such as glycosylphosphatidylinositol (GPI)-anchored proteins 1,7, doubly acylated (N-myristoylation and palmitoylation) proteins such as Src-family kinases and α-subunits of heterotrimeric G proteins (Resh, 1999), and cholesterol linked proteins such as Hedgehog show preferential association with lipid rafts (Rietveld et al., 1999). Palmitoylation of proteins serves as one of the most important mechanisms for association with the lipid rafts. In the case of Ras family proteins, palmitoylation of the C-terminal hypervariable region targets Ras to caveolin-1 rich lipid rafts (Hancock et. al. 1990).

Modification with lipid is not the only mechanism by which protein are targeted to the lipid-rafts. Interaction with proteins associated with lipid-rafts such as caveolin, flotillin and annexin, also serve as an important mechanism to recruit proteins to lipid rafts (Le Roy and Wrana, 2005). Although why proteins are recruited to these domain is not clear, increasing evidence in the literature suggests that recruitment is crucial for the activation of many signal transduction pathways (Le Roy and Wrana, 2005).

Caveolae

Caveolae are a specialized subset of the lipid rafts that form a flask shape invagination of the plasma membrane (Patel et al., 2008). Caveolae are composed of three major components caveolin, cavin and cholesterol. Caveolin is a 21-kDa membrane

protein that forms a hairpin structure in the membrane with both N- and C-termini facing the cytoplasm. There are three types of caveolin present in cells. Caveolin-1 (CAV1) and CAV2 are abundant in non-muscle cells, whereas CAV3 expression is restricted to skeletal and some smooth-muscle cells (Tang et al., 1996). CAV1 is the major constituent of caveolae in non-muscle cells. CAV2 is also present in caveolae but to a ratio of less than half that of CAV1. Another important component of the caveolar structure is the cavin protein. Cavin is composed of polymerase I and transcript release factor (PTRF or cavin-1), serum deprivation protein response (SDPR, SDR or cavin-2), sdr related gene product that binds to C-kinase (SRBC or cavin-3) and muscle restricted coiled-coil protein (MURC or cavin-4) (Hayer et al., 2010; Hill et al., 2008)

Role of lipid rafts in GPCR signaling

Lipid rafts and caveolae have been shown to regulate a wide variety of GPCR signaling cascades. GPCRs, heterotrimeric G proteins, and their various effectors can differentially partition into caveolae (reviewed in Patel et al., 2008). The preserved caveolin scaffolding domain (CSD, amino acids 82–101 of CAV1) found in caveolins can interact with a wide variety of signaling molecules (Li et al., 1996). G proteins, specifically Gα, have been shown to interact with caveolae (Li et al., 1996). Small GTP-binding protein of the Ras superfamily, H-Ras, also associates with caveolae. Palmitoylation of H-Ras increases its association with caveolae and hence keeps it in an inactive state. Exchange of GTP for GDP releases H-Ras from the lipid rafts and leads to activation of downstream Raf that leads to activation of MEK and ERK (Prior et al.,

2001; Song et al., 1996). Consistent with this observation, mutation of Ras (G12V) that prevents its association with caveolae makes it constitutively active.

Caveolae and CXCR4

Although, there are no palmitoylation sites in CXCR4, various reports in the literature suggest that CXCR4 associate with lipid rafts. In MDA-MB-231 breast cancer cell line, CXCR4 has been shown to be associated with the lipid raft compartment (Altenburg and Siddiqui, 2009). Treatment with Omega-3 unsaturated fatty acid (docosahexaenoic acid and eicosapentaenoic acid) disrupts lipid rafts resulting in decreased expression of CXCR4 on the cell membrane and hence the ability of these cells to migrate. CXCR4 has been shown to be present in the GM3 positive lipid rafts that are associated with the leading edge of a migrating/polarized T lymphocytes (Gomez-Mouton et al., 2001). It has been shown that the initial interaction of HIV protein gp120 with CD4 activates clustering of lipid rafts resulting in an increased association of CXCR4, which in turn facilitates viral entry. Consistent with this observation, disruption of lipid rafts result in inhibition of viral infection (Manes et al., 2000).

UBIQUITIN CONJUGATION

Ubiquitination reactions are carried out by the sequential activity of three distinct enzymes. The first enzyme is called a ubiquitin activating enzyme (E1) that activates ubiquitin in a two step process using ATP as an energy source. In the first step, ubiquitin is activated by ATP forming a ubiquitin-adenylate intermediate. In the second step, ubiquitin is transferred to an active cysteine residue on the E1 by formation of thio ester linkage between the terminal glycine residue carboxyl group in ubiquitin and sulfhydryl

group of the active site cysteine residue. Ubiquitin is then transferred to a cysteine residue in the second enzyme called a ubiquitin conjugating (UBC) enzyme (E2). Finally, ubiquitin is transferred to the epsilon amine group of a lysine residue in the substrate with the help of a third class of enzyme called the ubiquitin ligase enzyme (E3) (reviewed in Pickart, 2001). A description of the process of ubiquitination is described in Figure 1.8. The human genome is estimated to encode ~2 E1s, ~30 E2s and ~600-1000 E3s (Rotin and Kumar, 2009; Ye and Rape, 2009).

E3 ubiquitin ligases play an important role in the process of ubiquitination as they provide the specificity to the reaction by recognizing the substrate. Based upon the mechanism of transfer of ubiquitin to the substrate, these enzymes can be divided into two classes; 1) *H*omologous to *E*6-AP *c*arboxy *t*erminus (HECT) E3 ligases; 2) *R*eally *i*nteresting *n*ew *g*ene (RING) family E3 ligases. HECT domain containing E3 ligases such as AIP4 accept the ubiquitin from the E2 and directly transfer it to the substrate. In contrast, RING domain-containing ligases such as Cbl, SCF (SKP1-CUL1-F-box protein) act as scaffolds to mediate the interaction between E2 and the substrate (Figure 1.8).
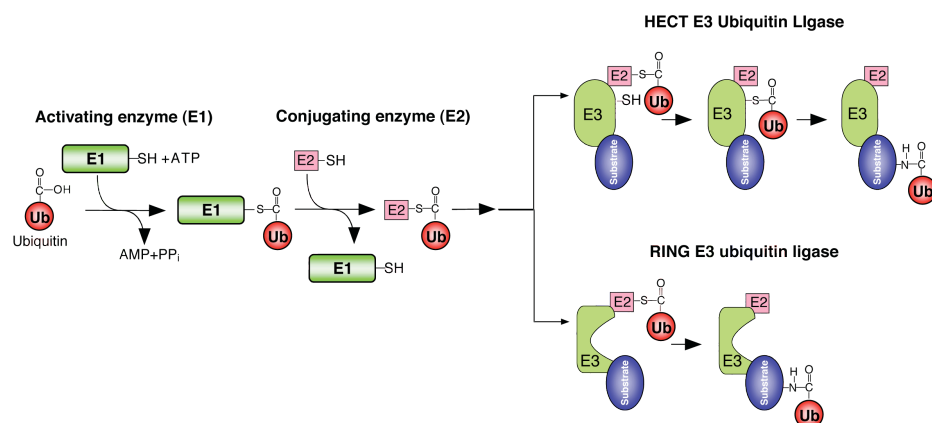
Figure 1.8. Schematic representation of the ubiquitination machinery. Ubiquitination of a substrate requires three enzymatic steps. In first step, an activating enzyme (E1) hydrolyzes ATP to activate ubiquitin by forming a thiolester linkage between its active site cysteine and the carboxyl-terminal glycine residue of ubiquitin. In second step, the activated Ub is passed from the E1 to a Cys residue of an E2-conjugating enzyme. Finally, the Ub-charged E2 is recruited by an E3 ligase, which also binds to the substrate. There are two main types of E3 ligases called HECT and RING E3s. HECT E3s form a thiol ester intermediate with Ub before transfering it to the target. RING E3 ligases act as an adaptor to bring the substrate and the Ub-charged E2-conjugating enzyme into close proximity, promoting Ub transfer directly from the E2 to the target. (Modified from Bowerman and Kurz, 2006)

Ubiquitination is a reversible process; proteins called deubiquitinating enzymes (DUBs) are proteases that mediate the removal of ubiquitin. There are approximately 100 DUBs encoded by the human genome. These enzymes can be further divided into five families; the ubiquitin specific proteinase (USP), the ovarian tumor domain (OUT), the ubiquitin C-terminal hydrolase (UCH), the machado-josephin domain (MJD) and the JAB1/MPN/Mov34 (JAMM) domain (Amerik and Hochstrasser, 2004).

Atrophin-interacting protein 4 (AIP4)

AIP is an E3 ubiquitin ligase that was initially identified in a yeast-two hybrid screen as a protein that interacts with Atrophin-1. Mutation in atrophin-1 is a major cause of a autosomal dominant spinocerebellar degeneration disease called dentotobular-pallidoluysian atrophy (DRPLA) also known as Haw River Syndrome and Naito-Oyanagi disease (Yang et al., 2006). AIP4 is a HECT domain containing E3 ubiquitin

ligase that belongs to the Nedd4 family E3 ligases. Other ligases in this family include Nedd4 (a.k.a. Nedd4.1), Nedd4.3, Smurf1, Smurf2, BUl1, NEDl2, WWP1 (a.k.a. AIP5) and WWP2 (a.k.a. AIP2). AIP4 has a modular structure and contain an N-terminal **C2 domain,** which can bind to membrane phospholipids and is known to play a role in membrane targeting (Gao et al., 2004), a **proline rich region** that binds to SH3 domain containing proteins such as Endophilin-A and β-PIX (Angers et al., 2004; Janz et al., 2007), four tandem **WW-domains**, that recognize and binds to proline rich PY (PPXY, PPPY) motifs as well as phospho-serine/threonine based motifs (Ingham et al., 2005), and a large C-terminal catalytic **HECT domain** that associates with the E2 enzyme of ubiquitination cascade (Figure 1.9).
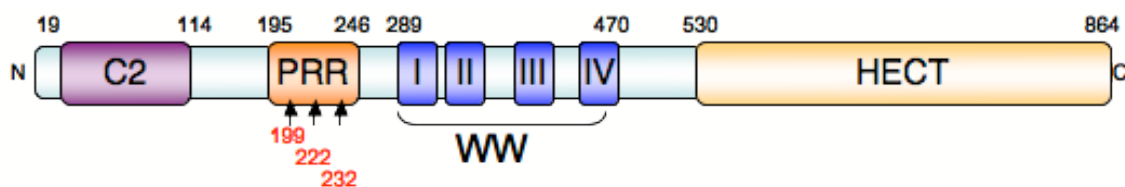
Figure 1.9. **Schematic representation of AIP4 structure.** AIP4 contains N-terminal C2 domain, proline-rich region (PRR), four tandemly linked WW domains (I, II, III and IV) and a C-terminal catalytic HECT domain. Numbers indicate the start and end position of domains. Serine residues phosphorylated by JNK1 are shown in red (199, 222 and 232).

AIP4 substrates: A large number of substrates have been identified for AIP4. For example, ubiquitination and degradation of cFLIP, p73, p63 by AIP4 regulate apoptosis (Chang et al., 2006; Rossi et al., 2005; Rossi et al., 2006). Adaptor proteins such as E3 ligase Deltex (DTX), Endophilin and HRS are ubiquitinated by AIP4 (Angers et al.,

2004; Chastagner et al., 2006; Marchese et al., 2003). Other protein such as c-Jun, JunB (Qiu et al., 2000), Notch (Qiu et al., 2000), Viral infectivity factor (VIF) (Dussart et al., 2004) and Gli1(Di Marcotullio et al., 2006; Di Marcotullio et al., 2011) are also regulated by AIP4. Mostly AIP4 targets its substrates to degradation, however, in case of TRP channels, AIP4 mediated ubiquitination regulates the cell surface expression (Gallagher et al., 2006). Similar to other E3 ubiquitin ligases, AIP4 is also auto-ubiquitinated. Both mono as well as polyubiquitination (both K29 as well as K63) is found. AIP4 also associates with the deubiquitinating enzyme FAM(USP9X) that protects it from degradation following auto-ubiquitination (Dupont et. al., 2009).

Regulation of AIP4 activity: AIP is subjected to regulation by a number of mechanisms including phosphorylation and ubiquitination. JNK1 kinase dependent phosphorylation of S199, T222 and S232 in the proline rich region of AIP is important for its activation. This phosphorylation event disrupts an auto-inhibitory conformation formed by interaction between the HECT domain and the PRR and WW domains of AIP4 increasing its enzymatic activity (Mund and Pelham, 2009). Similarly, binding of Nedd4 family-interacting proteins (Ndfip)-1 and 2, also relieve the intra-molecular self-inhibitory interaction (Yang et al., 2006). AIP is also a target of Src family kinase Fyn. Fyn leads to phosphorylation of AIP4 on tyrosine residue 371 which reduces the interaction of AIP4 with its substrate JunB (Gao et al., 2004). In contrast, phosphorylation by MEKK1-JNK1 kinases on Ser/Thr residues enhances AIP4 activity on junB (Lallemand et al., 2005). Recently, binding of Numb via PTB domain to WW1-

2 of AIP4 has also been shown to relieve the auto-inhibitory intra-molecular interaction and activate AIP4 (Di Marcotullio et al., 2011).

Role of AIP4 in Signaling: AIP4 has been shown to inhibit transforming growth factor-α signaling. Although the catalytic activity of AIP4 is not required for this function, its ability to act as an adaptor to link Smad7 to activated receptor is critical (Takeshita et al., 1996; Takeshita et al., 1997). AIP4 has also been shown to interact with another RING finger type ubiquitin ligase, CBLC. This interaction regulates both down-regulation and signaling of EGFR (Courbard et al., 2002).

RATIONALE AND RESEARCH OBJECTIVES

The receptor/chemokine signaling axis formed by the chemokine receptor CXCR4 and its cognate ligand CXCL12 play a major role in normal mammalian physiology and dysregulation of CXCR4 signaling and trafficking has been linked to several pathological conditions. However, the molecular and cellular mechanisms that regulate CXCR4 signaling and trafficking remain poorly understood.

Our laboratory has previously shown that arrestin-2 mediates endosomal sorting of CXCR4 by interacting with the E3 ubiquitin ligase AIP4, to direct CXCR4 into the degradative pathway. However, the precise mechanism by which arrestin-2 function on the endosomes remain unknown. CXCR4 has been shown to be targeted to lysosomes via the ESCRT pathway. HRS and STAM form the ESCRT-0 complex that can directly bind to the endosomal membrane and recruit ubiquitinated cargo to regulate its sorting

into MVBs. STAM is a unique protein that contains domains important for signal transduction (such as SH3 domains and ITAM motifs) as well as for endosomal sorting (UIM domain), suggesting their role in both signaling as well as endosomal sorting of proteins. Our data show that both arrestin-2 and AIP4 can interact with STAM and siRNA mediated knockdown of STAMs had effect on both CXCR4 signaling and downregulation. Since, both arrestin-2 and AIP4 are important for trafficking of CXCR4 to lysosomes, we hypothesize that STAM interacts with AIP4 and arrestin-2 to play a critical role in CXCR4 regulation. With an objective to further our understanding of the molecular mechanisms that regulate CXCR4 signaling and trafficking the following aims were proposed.

1. To determine the role of arrestin-2 in endosomal sorting and downregulation of the chemokine receptor CXCR4.

2. To determine the role of AIP4 and STAM-1 in CXCR4 signaling.

The results from this study would help us understand additional mechanisms that regulate CXCR4 signaling and trafficking and explain how CXCR4 dysregulation contributes to various biological disorders.

CHAPTER 2

MATERIALS AND METHODS

2.1 Cell lines, Transfections, Reagents

Human embryonic kidney (HEK) 293 cells (Microbix, Toronto, ON, Canada), HEK293-WT#2 (stably expressing HA-CXCR4) cells, human cervical cancer cell line, HeLa (American Type Culture Collection, Manassas, VA), human breast cancer cell lines BT474 (kindly provided by Dr. Bruce Quevas, Loyola University Chicago) and SKBR3 (kindly provided by Dr. Clodia Osipo, Loyola University Chicago) were maintained in Dulbecco's Modified Eagle Medium (DMEM) (HyClone Laboratories, Logan, UT) supplemented with 10% fetal bovine serum (FBS; HyClone Laboratories), hereafter called DMEM-complete, at 37°C in a humidified atmosphere containing 5% CO_2.

Plasmid DNA and siRNA transfections were performed using *Trans*IT®-LT1 (Mirus, Madison, WI) and Lipofectamine™2000 (Invitrogen) transfection reagents respectively, following manufacturers instruction as described below.

2.1.1 Transfection of plasmid DNA using *Trans*IT®-LT1 transfection reagent

DNA transfections were performed on cells cultured in 10-cm, 6-cm, 6-well and 24-well culture dishes using *Trans*IT®-LT1 transfection reagent as described below. For DNA transfections in a 10-cm dish, 10 μg of total plasmid DNA was aliquoted into a

microcentrifuge tube and diluted by adding 1 ml of Opti-MEM (Reduced Serum Minimum Essential Media, Gibco). Thirty microliter (μl) (1:3 ration i.e. 3 μl of LT1 for every microgram of DNA) of warm *Trans*IT®-LT1 transfection reagent was added to the DNA/Opti-MEM mixture. For DNA transfections in a 6-cm dish, 5 μg of total plasmid DNA was aliquoted into a microcentrifuge tube and diluted by adding 500 μl of Opti-MEM. Fifteen μl of *Trans*IT®-LT1 transfection reagent was added to the DNA/Opti-MEM mixture. For DNA transfections in each well of a 6-well culture dish, 2.5 μg of total plasmid DNA was aliquoted into a microcentrifuge tube and diluted by adding 250 μl of Opti-MEM. Seven and half μl of warm *Trans*IT®-LT1 transfection reagent was added to the DNA/Opti-MEM mixture. For DNA transfections in each well of a 24-well dish, 0.5 μg of total plasmid DNA was aliquoted into a microcentrifuge tube and diluted by adding 50 μl of Opti-MEM. One and half μl of warm *Trans*IT®-LT1 transfection reagent was added to the DNA/Opti-MEM mixture. *Trans*IT®-LT1/DNA/Opti-MEM mixture was vortexed briefly (2-3 sec at low speed) and incubated for 20 min at room temperature (RT). Media from dishes/wells to be transfected was removed by aspiration and replaced with warm DMEM-complete media (9, 4, 2, 0.5 ml for 10-cm, 6-cm, 6-well and 24 well dishes, respectively). Following incubation, DNA/transfection reagent complexes were added drop wise to different areas of the plate/well and gently rocked back-and-forth and from side-to-side to evenly distribute the complexes. The plates were incubated at 37°C for 24-48 hr depending on the experiment and plasmid DNA transfected.

Transfection of siRNA with Lipofectamine™2000 transfection reagent

Transfections with siRNA were performed on cells cultured in 10-cm or 6-cm dishes as described below. For transfections in a 10-cm dish, 600 picomoles (pmol) of siRNA (30 μl siRNA from a working stock of 20 μM) were aliquoted into a microcentrifuge tube and diluted by adding 1 ml Opti-MEM. In a 15 ml conical tube, 30 μl Lipofectamine™2000 reagent was diluted in 1 ml Opti-MEM. For transfections in a 6-cm dish, 200 pmol of siRNA (10 μl siRNA from a stock of 20 μM) was aliquoted into a microcentrifuge tube and diluted in 250 μl Opti-MEM. In a separate microcentrifuge tube, 10 μl Lipofectamine™2000 was diluted in 250 μl Opti-MEM. Both tubes were incubated for 5 min at RT and then solutions were mixed together carefully, vortexed briefly (2-3 sec at low speed) and incubated for another 20 min at RT to allow formation of complexes between siRNA and transfection reagent. Media from dishes containing cells to be transfected was replaced with 8 ml (for 10-cm dish) or 3.5 ml (for 6 cm dish) warm DMEM-complete media. siRNA/transfection reagent complexes were added drop wise to different areas of the plate and gently rocked back-and-forth and from side-to-side to evenly distribute the complexes. The plates were incubated at 37°C for 48-72 hr depending on the experiment and siRNA transfected.

Antibodies, Reagents and DNA constructs

List of all antibodies, reagents, kits, DNA constructs, siRNA and primers used in this study are compiled in Table 2.1-2.6.

Sodium dodecyl sulfate polyacrylamide gel electrophoresis (SDS-PAGE) and Western Blotting

Samples to be analyzed by western blotting were mixed with 2x sample buffer (0.75 M Tris-HCl pH-6.5, 10% SDS, 10% glycerol, 5% beta-Mercaptoethanol, 0.005 % (wt/vol) bromophenol blue) and loaded onto 7.5%, 10% or 12%, SDS-polyacrylamide gel along with a molecular weight marker (prestained SDS-PAGE low range standards, Bio-Rad, Cat. No. 161-0305). Samples were electrophoresed at 160 volts for 1 hr at RT using Mini-PROTEAN 3 system (Bio-Rad). Separated proteins were electrophoretically transferred onto 0.45 μm nitrocellulose membrane (Bio-Rad) using transfer buffer (0.25 mM Tris-HCl pH 7.5, 0.192 M glycine and 20% (vol/vol) methanol) at 100 volts for 1 hr at RT. After the transfer, membranes were incubated with 10 ml Ponceau S stain to estimate the efficiency of transfer. Membranes were rinsed once with TBST (Tris-buffered saline containing Tween®20; 20 mM Tris pH 7.5, 150 mM NaCl, 0.05% (vol/vol) Tween®20) to remove excess Ponceau S stain and incubated with 10 ml 5% (wt/vol) non-fat milk made in TBS-T for 30 min at RT while rocking. Membranes were then incubated with appropriate primary antibody diluted in 7.5 ml 5% milk-TBST for 1 hr at RT or overnight at 4°C while rocking. Following incubation, the membranes were washed 3 times (5 min each) with 10 ml TBST and then incubated with 10 ml appropriate secondary antibody conjugated with horse radish peroxidase (HRP) made in 5% milk-TBST for 30 min at RT. Finally blots were washed 5 times (10 min each) with 10 ml TBST at RT and developed by incubating with enhanced chemiluminescence (ECL) reagent on autoradiography films (Phenix Research) using automated film

processor. Depending upon the sensitivity of primary antibody, ECL of different sensitivity were used i.e. Pico, Dura and Femto (Pierce)

Treatment with ligand

To stimulate the cells with ligand, appropriate concentration of ligands (CXCL12, carbachol, EGF) was prepared in DMEM incomplete media supplemented with 20 mM HEPES (e.g. to achieve final concentration of 30 nM CXCL12, 3μl from a stock solution of 10 μM was added to 1 ml DMEM incomplete media). To stimulate cells, media from the plates were removed by aspiration and slowly replaced with media containing appropriate dilution of ligand. Plates were gently rocked back-and-forth and from side-to-side to evenly distribute the media and incubated at 37℃ for different time points depending on experiment.

GST-fusion protein purification and quantification

Five ml of Luria Broth containing 100 μg/ml ampicillin (LB-amp) was inoculated from a glycerol stock of *Escherichia coli* (*E.coli*) BL21 cells transformed with GST-fusion protein constructs or empty vector (pGEX-4T2) and grown overnight at 37℃ in an orbital shaker (model 4518, Forma Scientific) at 250 rpm. The next day, 30 ml LB-amp in a 50 ml conical tube was inoculated with 750 μl of the overnight culture and incubated at 37℃ until an OD_{600} of 0.35–0.40 was reached (~2 hr). To induce protein production, 30 μl of 1 M isopropyl-1-thio-β-D-galactopyranoside (IPTG) (final concentration 0.1 mM) was added and tubes were incubated for 2 hr at 18℃ in an orbital shaker. After

induction, cells were pelleted by centrifugation at 4500 rpm for 15 min at 4°C in a Beckman Coulter J6-HC centrifuge. The supernatant was discarded by pouring and the pellet was resuspended in 1 ml binding buffer (20 mM Tris-HCl pH 7.4, 150 mM NaCl, 0.1% Triton X-100 (vol/vol), 1 mM dithiothreitol, 10 μg/ml leupeptin, 10 μg/ml aprotinin, and 10 μg/ml pepstatin-A). Samples were subjected to sonication using a Branson Digital Sonifier® (Model 450, Branson Ultrasonic corp.) once at amplitude of 11% for 10 sec on ice, followed by centrifugation at 14,000 rpm for 20 min at 4°C (Eppendorf Centrifuge; 5417R). To equilibrate glutathione-sepharose 4B resin with binding buffer, 100 μl resin was aliquoted in a microcentrifuge tube and 750 μl binding buffer was added. Tubes were inverted 5-6 times and then centrifuged at 4500 rpm for 5-7 sec to pellet resin. Buffer was discarded by aspiration and this step was repeated two times. After final centrifugation step, buffer was aspirated and the beads were resuspended in 100 μl binding buffer.

Fusion proteins were immobilized by incubating cleared lysate with 100 μl equilibrated glutathione-sepharose 4B resin overnight (15-17 hr) at 4°C while rocking. After incubation, samples were centrifuged at 4000 rpm for 5-10 sec and the supernatant was discarded by aspiration. Samples were washed by adding 750 μl binding buffer, incubated while rocking for 10 min at 4°C followed by centrifugation at 4000 rpm for 5-10 sec. Supernatant was discarded by aspiration and samples were washed second time by adding 750 μl binding buffer and gently inverting the tube 5-6 times followed by centrifugation at 4000 rpm for 5-10 sec. A third wash was done in similar fashion to the second wash and finally the beads were resuspended in 100 μl binding buffer.

To determine the protein amount, 15 μl sepharose beads were collected in a microcentrifuge tube, centrifuged at 4000 rpm for 5-10 sec, and buffer was discarded by aspiration. Ten μl 2x sample buffer was added to the beads and the bound protein was eluted by incubating at 100°C for 10 min. Samples were analyzed by 10% SDS-PAGE with known amounts (0.5, 1.0, 2.0 and 3.0μg) of purified bovine serum albumin (Fraction V; Roche Diagnostics, Indianapolis, IN). Gel was washed three times (5 min each) with 20-30 ml distilled water and incubated with 15 ml GelCode®Blue stain at RT on a rotary shaker for 30 to 60 min. After staining, gel was washed 3-5 times (5 min each) with 20-30 ml distilled water to de-stain. To estimate the concentration of fusion protein, band intensities between know BSA amounts and fusion protein were compared (Figure 2.1). Various GST-fusion proteins purified using this protocol are summarized in table 1.7.

GelCode Blue Staining
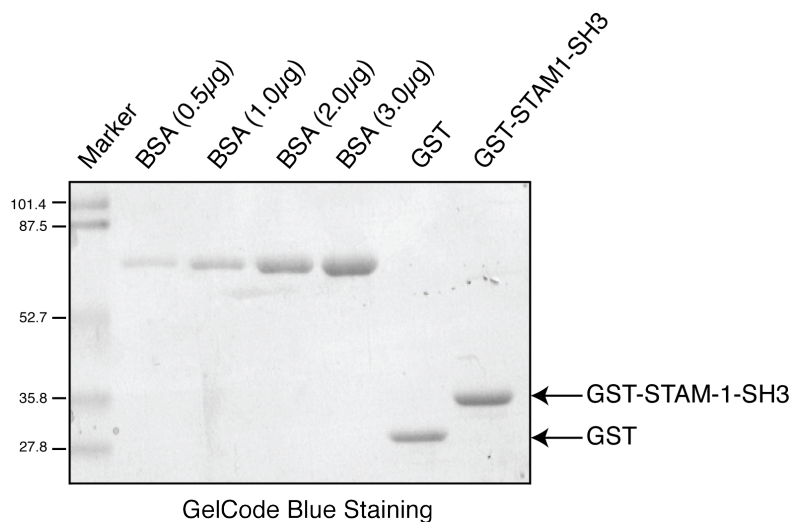
Figure 2.1 Quantification of amounts of GST-fusion proteins purified by immobilizing to glutathione-sepharose beads. Show is an example of typical GST-fusion protein purification. Fifteen μl of sepharose beads bound to fusion protein were taken in microcentrifuge tubes. Fusion proteins were eluted in 15 μl 2x sample bluffer by incubating at 100°C for 10 min and loaded onto 10% SDS-PAGE gel with known

amounts of BSA. Following electrophoresis, gel was washed with water and stained with GelCode®Blue.

Shown is a representative gel stained with GelCode®Blue to estimate the amount of protein purified by

comparing it with know amounts of BSA (0.5-3.0 μg). In this example, GST was estimated to be around

1.5 μg/15μl of beads and GST-STAM-1-SH3 was estimated to be 2 μg/15μl of beads.

Table 2.7 List of all the GST-fusion proteins purified for this study

S. No.	Fusion Protein
1.	GST
2.	GST-STAM-1
3.	GST-STAM-2
4.	GST-STAM-1
5.	GST-STAM-1-CC
6.	GST-STAM-1-SH3
7.	GST-arrestin-2
8.	GST-arrestin-2-(25-161)
9.	GST-AIP4
10.	GST-AIP4-ΔWW-I-IV
11.	GST-AIP4-HECT
12.	GST-AIP4-WW-I-IV

Purification of HIS-tagged STAM-1

Thirty ml of LB-amp was inoculated from a glycerol stock of *Escherichia coli*

(*E.coli*) BL21 cells transformed with HIS-STAM-1 and grown overnight at 37°C in an

orbital shaker (model 4518, Forma Scientific) at 250 rpm. The next day, 500 ml LB-amp

in a 1 L Erlenmeyer flask was inoculated with 30 ml of the overnight culture and

incubated at 37°C until an OD_{600} of 0.43 was reached. Protein induction was initiated by adding 500 µl of 1 M IPTG (final concentration 0.1 mM) and incubating for 2 hr at 18°C in an orbital shaker at 250 rpm. After induction, cells were pelleted by centrifugation at 4500 rpm in Beckman Coulter J6-HC centrifuge for 15 min at 4°C. The supernatant was discarded and the pellet was resuspended in 10 ml binding buffer (20 mM Tris-HCl pH 7.5, 150 mM NaCl, 0.1% Triton X-100 (vol/vol), 1 mM dithiothreitol, 10 µg/ml leupeptin, 10 µg/ml aprotinin, 10 µg/ml pepstatin-A and 10 mM Imidazole). Samples were subjected to sonication three times using a Branson Digital Sonifier® at amplitude of 11% for 10 sec on ice. Sample was sub-divided into 10 microcentrifuge tubes and centrifuged at 14000 rpm for 20 min at 4°C (Eppendorf Centrifuge; 5417R). The supernatant from all the tubes was pooled in a 15 ml conical tube and passed through a 0.25 µm syringe filter to remove any cellular debris. A 0.8 x 4 cm Poly-Prep Chromatography columns (Bio-Rad, cat. no. 731-1550) was loaded with 1 ml of His-Select Nickel Affinity Gel (Sigma, cat. no. P6611) and left undisturbed at 4°C for 30-45 min. The column was washed with 5 bed volumes (5 ml) of cold binding buffer before loading filtered cell lysate. A flow rate of 10-20 µl/sec was achieved by adjusting the pressure on the column cap. The flow-through was collected in a 15 ml conical tube and loaded again on the same column. The column was washed with 10 bed volumes (10 ml) of cold binding buffer to remove unbound proteins. To elute bound proteins, 10 ml elution buffer (binding buffer with 150 mM Imidazole) was added and 7 fractions of 500 µl each were collected in microcentrifuge tubes on ice. A 20 µl aliquot from each fraction was collected in a microcentrifuge tube and diluted by adding 20 µl sample buffer.

Remaining fractions were snap frozen and stored at -80°C. Samples (10 µl) were analyzed

by 10% SDS-PAGE and GelCode®Blue staining. Figure 2.2 shows the purity of

different fractions.
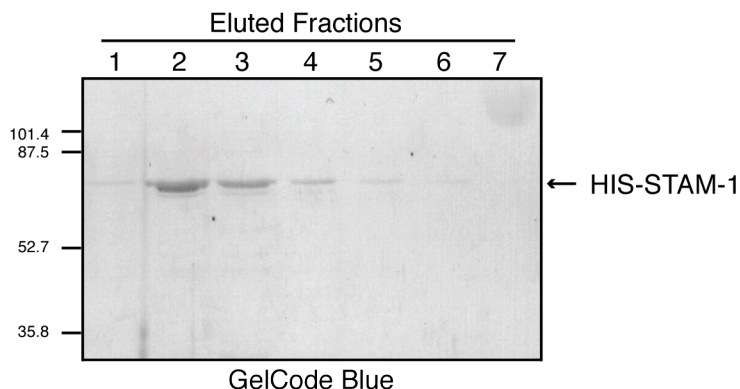
Figure 2.2. GelCode®Blue staining of different fractions of HIS-STAM-1 eluted from His-Select Nickel Affinity Gel column using 150 mM Imidiazole. An aliquot of 10 µl from each eluted fraction was mixed with 10 µl 2x sample buffer and incubated at 100°C for 10 min. Ten µl from each aliquot (5 µl sample) was analyzed by 10% SDS-PAGE. Gel washed with water and stained with GelCode®Blue.

Binding assay with GST-fusion proteins

Cell lysates were prepared from HEK293 and HeLa cells expressing the desired

DNA constructs cultured in 6-well plates as described below. Cells were transfected with

desired DNA constructs using *Trans*IT®-LT1 transfection reagent as described in section

2.1.1. After 48 hr, plates were placed on ice and media was removed by aspiration. Cells

were washed once with 2.5 ml cold PBS and 500 µl binding buffer was added to each

plate. Cells were collected in a microcentrifuge tube by scraping and then sonicated once

at amplitude of 11% for 10 sec on ice using a Branson Digital Sonifier®. Cleared cell

lysate (CCL) was prepared by centrifugation at 14000 rpm for 20 min at 4°C. For binding assays, equimolar amounts of purified GST and GST-fusion proteins were incubated with 100 μl of CCL and then incubated for 2–18 hr at 4°C while rocking. For binding experiments using purified arrestin-2, GST fusion proteins were incubated with 500 ng purified arrestin-2 in 100 μl of binding buffer for 1 hr at 4°C. After incubation, samples were washed three times with 750 μl binding buffer and then eluted in 20 μl 2x sample buffer by incubating at 100°C for 10 min. Bound proteins were detected by 10% SDS-PAGE followed by immunoblotting against desired protein. After the protein transfer, nitrocellulose membrane was stained with Ponceau S stain to determine the presence of fusion proteins.

For GST pulldown experiment between STAM-1-SH3 and AIP4, GST-STAM-1-SH3 and GST were purified from bacterial cells exactly as described above. GST and GST-STAM-1-SH3 were eluted from glutathione sepharose beads by incubating with 100 μl elution buffer (binding buffer+20 mM glutathione) for 1 hr at RT. Beads were spun down at 4000 rpm for 1 min and supernatant was collected in a fresh tube and labeled as elution1. Hundred microliters of elution buffer was added again to the remaining beads and incubated at RT for 1 hr and elution 2 was collected as described above. Ten μl of remaining beads and 10 μl of each elution was analyzed by SDS-PAGE and amount of protein eluted was determined by staining with Gel-code blue (Figure 2.2). For binding reaction, equimolar amounts of GST and GST-STAM-1-SH3 were added to lysates prepared from HeLa cells expressing FLAG-AIP4 and incubated overnight at 4°C. Next day 20 μl equilibrated glutathione beads were added to

the tubes and incubated for another 1 hr. Beads were washed and bound protein was eluted and analyzed as described above.
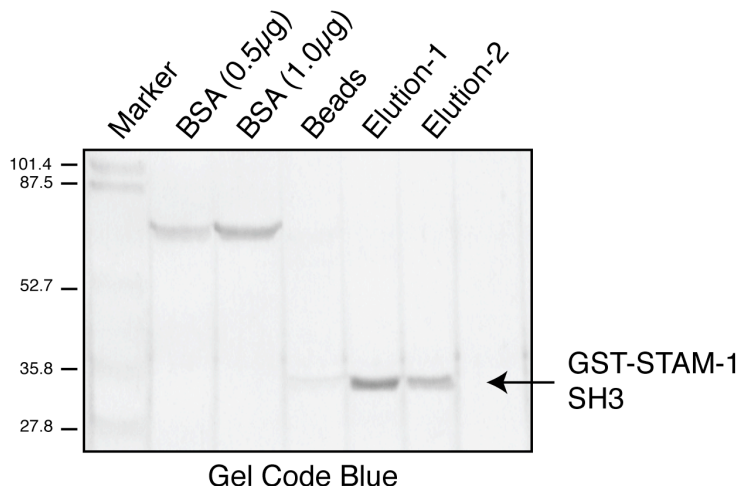
Figure 2.3. Elution of GST-STAM-1-SH3. GST-STAM-1-SH3 bound to glutathione beads was eluted twice with binding buffer containing 20 mM glutathione. Ten microliters of remaining beads and 10 μl of each fraction were analyzed by 10% SDS-PAGE and stained with Gel-code blue.

CXCR4 degradation assay

CXCR4 degradation assay was performed using either HEK293 cells stable expressing HA-CXCR4 (HEK293-WT#2) or HeLa cells that express detectable levels of endogenous CXCR4. HEK293-WT#2 and HeLa cells cultured in 10-cm dishes to a confluency of 70-80% were transfected with 600 pmol STAM-1, AMSH and GAPDH siRNA using Lipofectamine™2000 transfection reagent as described in section 2.1.2. To assess the role of disrupting STAM-1/arrestin-2 interaction by expressing STAM-1 and arrestin-2 minigene constructs on CXCR4 degradation, HEK293 cells cultured in 10-cm dishes were co-transfected with 1 μg HA-CXCR4 and 9 μg FLAG-STAM-1-CC-(296-

380), FLAG-arrestin-2-(25-161) and empty vector (pCMV-10) using *Trans*IT®-LT1 transfection reagent as described in section 2.1.1. Twenty-four hours later, cells were passaged onto Poly-L-Lysine (PLL) coated 24-well plates (HEK293 cells) or six-well plates (HeLa cells) and grown for an additional 18–24 hr. To coat plates with PLL, 5 mg PLL (Sigma-Aldrich) was diluted in 50 ml distilled water to achieve a final concentration of 0.1 mg/ml. Working solution of PLL (0.1 mg/ml) was pipetted to the bottom of the plate and incubated for 5 min at RT. PLL was removed and plates were allowed to air dry at RT (~30-45 min). Cells were washed once with DMEM containing 10% FBS and then incubated with 50 μg/ml cyclohexamide (made in DMEM containing 10% FBS) to stop protein synthesis for 15 min at 37°C. Cells were then incubated with the same medium containing 30 nM CXCL12 or vehicle (PBS+0.1% bovine serum albumin [BSA]) for 1, 2, and 3 hr. Cells were washed once with PBS and collected in 300 μl of 2x sample buffer and then sonicated once at amplitude of 11% for 10 sec using a Branson Digital Sonifier®. Receptor amounts were determined by 7.5% SDS-PAGE followed by immunoblotting using an anti-HA antibody to detect HA-CXCR4 in HEK293-WT#2 cells and anti-CXCR4 antibody (2B11) to detect endogenous CXCR4 in HeLa cells.

To assess the effect of inhibiting the STAM-1/arrestin-2 interaction on EGFR degradation, HeLa cells cultured in 6-well plates were transfected with 3 μg of FLAG-STAM-1-CC, FLAG-arrestin-2-(25-161) and empty vector (pCMV-10) using *Trans*IT®-LT1 transfection reagent as describe in section 2.1.1. Forty-eight hours later, cells were washed once with DMEM containing 10% FBS and then incubated with 50 μg/ml cyclohexamide for 15 min at 37°C. Cells were then incubated with the same

medium containing 100 ng/ml epidermal growth factor (EGF) or vehicle (PBS+0.1% BSA) for 1 hr. Cells were processed exactly as described above for CXCR4 degradation. Receptor amounts were determined by 10% SDS-PAGE followed by immunoblotting using an anti-EGFR antibody.

Co-immunoprecipitation

HeLa cells cultured in 10-cm dishes were transiently transfected with HA-arrestin-2, HA-arrestin-3 and empty vector (pcDNA3) using *Trans*IT®-LT1 transfection reagent as described in section 2.1.1. Forty-eight hours later, cells were washed with 10 ml cold PBS, scraped and collected in 1.0 ml immunoprecipitation buffer [20 mM Na_2PO_4 pH 6.5, 150 mM NaCl, 1% (vol/vol) Triton-X 100, 10 μg/ml leupeptin, 10 μg/ml aprotinin, and 10 μg/ml pepstatin A] and incubated at 4°C for 30 min while rocking. CCLs were prepared by sonicating the samples once at amplitude of 11% for 10 sec using a Branson Digital Sonifier® followed by centrifugation at 14000 rpm for 20 min at 4°C. CCLs were then incubated with an anti-HA mouse monoclonal antibody (101R) or isotype control antibody (mouse IgG1) at 1:150 dilution (1μl antibody for 150 μl CCL) for overnight at 4°C while rocking. After incubation, 25 μl of protein-G agarose beads, equilibrated with IP buffer were added to each tube and incubated for additional 1 hr. After incubation, agarose beads were pelleted down by centrifugation at 4000 rpm for 1 min and supernatant was discarded by aspiration. Samples were washed 3 times by inverting 5-6 times with 750 μl IP buffer and after final wash 20 μl 2x sample buffer was added. Immunoprecipitates (IPs) were incubated at 100°C for 10 min and aliquotes of 10

μl were analyzed by 7-10 % SDS-PAGE followed by western blotting to detect bound endogenous STAM-1 and HRS.

To assess the effect of the STAM-1-CC minigene on the interaction between STAM-1 and arrestin-2, HeLa cells were transfected with plasmid DNA encoding HA-arrestin-2 and FLAG-STAM-1-CC or pCMV. CCLs were prepared as described above and were incubated with an anti-HA (101R) or isotype control antibody. IPs were subjected to immunobloting to detect endogenous STAM-1. To assess the effect of the arrestin-2-(25-161) minigene on the interaction between STAM-1 and arrestin-2, HeLa cells were transfected with T7-STAM-1, HA-arrestin-2, and FLAG-arrestin-2-(25-161) or pCMV. CCLs were prepared as described above and were incubated with an anti-T7 polyclonal or isotype control antibody. IPs were subjected to immunobloting to detect HA-arrestin-2 and endogenous HRS.

To detect interaction between endogenous arrestin, STAM-1 and HRS, CCLs were made from HeLa cells cultured in 10-cm dishes. Five hundred μl CCLs were incubated with 2.5 μl (1:200 dilution) anti-arrestin-2/3 mouse monoclonal (BD Biosciences) or isotype control antibody (mouse IgG). Immunoprecipitation was performed exactly as described above and aliquotes of 10 μl were analyzed by 10 % SDS-PAGE followed by western blotting to detect bound endogenous STAM-1 and HRS.

To detect binding between endogenous STAM-1, AIP4 and caveolin-1, 500 μl CCLs made from HeLa cells, HEK293 cells stably expressing HA-CXCR4 and BT474 cells were subjected to immunoprecipitation using 10 μl (1:50 dilution) anti-AIP4 (G11) mouse monoclonal or isotype control antibody (mouse IgG). Immunoprecipitation was

performed exactly as described above and aliquotes of 10 µl were analyzed for the presence of STAM-1 and caveolin-1 as described above.

Confocal immunofluorescence microscopy

Protein co-localization studies were done in HEK293 cells transiently transfected with HA-CXCR4-YFP and HeLa cells expressing endogenous CXCR4 by confocal immunofluoroscence microscopy. HEK293 cells cultured in 6-well dishes were transiently transfected with 1 µg HA-CXCR4-YFP using *Trans*IT®-LT1 transfection reagent as described in section 2.1.1. Transfected HEK293 and HeLa cells were passaged onto PLL coated glass coverslips and were allowed to grow to a confluency of 70-80 %. To coat, glass coverslips were placed in 24 well plate using forceps and incubated with 500 µl 0.1 mg/ml PLL for 5-10 min. PLL was removed by aspiration and the coverslips were allowed to air dry by incubating at RT for 30-45 min. Next day, cells were washed once with 500 µl warm DMEM containing 20 mM HEPES pH 7.5 and incubated in the same medium for 3–4 hr at 37℃. Serum starved cells were treated with 500 µl DMEM containing 30 nM CXCL12 or vehicle (PBS+0.1% BSA) for 30 min at 37℃. After the treatment, cells were placed on ice and washed twice with 500 µl cold PBS and then fixed by incubating with 500 µl 3.7% paraformaldehyde made in PBS for 10 min at RT. Cells were then incubated with 500 µl 0.05% (wt/vol) saponin for 10 min at RT to permeabilize cell membrane. Cells were blocked by incubating with 500 µl blocking buffer (PBS containing 0.05% saponin and 5% normal goat serum) for 30 min at 37℃. Immunostaining was performed by incubating cells with desired concentration of primary antibody made in blocking buffer at 37℃ for 1 hr in a moist chamber. Coverslips

containing cells were flipped over so that the side containing cells were placed on top of a 50 μl drop of antibody on a parafilm. After incubation, coverslip containing cells were placed back into 24 well plates and washed five times with 500 μl 0.05% saponin made in PBS (Saponin-PBS). For the last wash, coverslips were incubated with 500 μl Saponin-PBS for 15 min at 37°C. After washing, cells were incubated with appropriate Alexa-Fluor–conjugated secondary antibodies made in blocking buffer for 30 min at 37°C in a moist chamber, similar to primary antibody. Finally, cells were washed again 5 times with 500 μl Saponin-PBS as described before and coverslips were mounted onto glass slides using mounting media containing 4,6-diamidino-2-phenylindole (DAPI). Sides of the coverslips were sealed using nail polish and slides were allowed to air dry at 4°C in dark. Samples were analyzed using an LSM 510 laser scanning confocal microscope (Carl Zeiss, Thornwood, NY) equipped with a Plan-Apo 63x/1.4 oil lens objective. Images were acquired using a 1.4-megapixel cooled extended spectra range RGB digital camera set at 512 x 512 resolution (Carl Zeiss, Thornwood, NY). Acquired images were analyzed using ImageJ, version 1.41o (National Institutes of Health, Bethesda, MD) and Adobe Photoshop (CS4). Amount of colocalization between proteins were determined by calculating the Pearson coefficient using MetaMorph 7.6 (Molecular Devices, Downingtown, PA) or ImageJ.

To examine colocalization between CXCR4, arrestins and EEA1, HEK293 cells transfected with HA-CXCR4-YFP and arrestin-2-CFP or HeLa cells expressing endogenous levels of CXCR4 were processed as exactly as described above and stained with anti-EEA1 and arrestin-2/3 antibodies (HEK293) or anti-CXCR4, EEA1 and

arrestin-2/3 antibodies (HeLa). To examine colocalization between CXCR4, STAM1 and EEA1 and STAM-1, arrestins and EEA1, HEK293 cells expressing HA-CXCR4-YFP or HeLa cells were processed and stained with STAM-1 and EEA1 (HEK293) and CXCR4, STAM-1, EEA1 antibodies. To examine colocalization between CXCR4, STAM1 and α-adaptin and CXCR4, Caveolin-1 and α-adaptin, HeLa cells were co-incubated with primary antibodies against α-adaptin, CXCR4, caveolin-1, and STAM-1 for 1 hr at 37°C, followed by incubation with appropriate Alexa-Fluor conjugated secondary antibodies for 30 min at 37°C. To examine colocalization between STAM-1, caveolin-1 and α-adaptin or AIP4, caveolin-1 and α-adaptin, HeLa cells were transiently transfected with YFP-STAM-1 or YFP-AIP4, respectively and processed as described above. To examine the role of caveolin-1 in CXCR4-induced ERK-1/2 phosphorylation we employed quantitative confocal immunflouresence microscopy. HeLa cells cultured in 10-cm dish were transfected with 600 pmol caveolin-1 and GAPDH siRNA. Twenty-four hours later, cells were passaged onto PLL coated coverslips and grown to a confluency of 70-80%. Cells were serum starved as described before and were treated with 500 μl DMEM containing 10 nM CXCL12 or vehicle (PBS+0.1% BSA) for 5 min at 37°C. Following treatment, cells were processed as described above and co-stained with anti-pERK-1/2 mouse monoclonal and anti-caveolin-1 rabbit polyclonal antibodies overnight (15-17 hr) at 4°C in a moist chamber. Cells were washed and stained with Alexa-fluor-conjugated secondary antibodies for 1 hr at RT. Coverslips were mounted on glass slides and images were acquired as described above. The mean pixel intensity of pERK-1/2 and caveolin-1 staining per cell was calculated using LSM 510 image analysis

software. The average of the mean pixel intensity from 45 cells from 3 independent experiments was determined.

Antibody Dilution: Primary antibodies for STAM-1, EEA1, caveolin-1 and α-adaptin were used at 1:100 dilution (1 μl antibody in 100 μl blocking buffer) and against CXCR4, arrestin-2/3 and pERK-1/2 at a 1:50 dilution. All the Alexa-fluor-conjugated secondary antibodies were used at 1:200 dilutions.

Ubiquitination assays

CXCR4 ubiquitination assay: To examine the effect of inhibiting the STAM-1/arrestin-2 interaction on CXCR4 ubiquitination, HEK293 cells stably expressing HA-CXCR4 were cultured in 10-cm dishes to a confluency of 70-80% and transfected with 3 μg of FLAG-ubiquitin. Eight hours later, cells were transfected with 10 μg of FLAG-STAM-1-CC, FLAG-Arr2-(25-161), or empty vector (pCMV-10). The next day, cells were passaged onto 6-cm dishes and allowed to grow for an additional 24 hr. The next day, cells were washed with 5 ml DMEM containing 20 mM HEPES and serum starved by incubating in the same media for 3 hr. Cells were treated with vehicle (PBS+0.1% BSA) and 30 nM CXCL12 for 30 min. After stimulation, plates were kept on ice and cells were washed once with 5 ml cold PBS. Cells were scraped in 1 ml of lysis buffer [50 mM Tris-HCl pH 7.4, 150 mM NaCl, 5 mM EDTA, 0.5% (wt/vol) sodium deoxycholate, 1% (vol/vol) NP-40, 0.1% (wt/vol) SDS, 20 mM *N*-ethylmaleimide (NEM), and 10 μg/ml each of leupeptin, aprotinin, and pepstatin A], transferred to microcentrifuge tubes and incubated at 4°C for 30 min while rocking. CCLs were prepared by sonicating the

samples once at amplitude of 11% for 10 sec on ice using Branson Digital Sonifier®
followed by centrifugation at 14000 rpm for 20 min. CCLs were then incubated with an
anti-HA polyclonal antibody (101C) to immunoprecipitate CXCR4.
Immunoprecipitates were analyzed by subjecting to 7.5% SDS-PAGE followed by
western blotting using an anti-FLAG antibody conjugated to HRP to detect
incorporated ubiquitin. Blots were stripped and reprobed using anti-HA monoclonal
antibody (101R) to detect the amount of CXCR4 immunoprecipitated. Lysates were
analyzed by western blotting to detect expression level of HA-CXCR4, FLAG-STAM-
1-CC and FLAG-Ub.

HRS ubiquitination assay. To examine the effect of inhibiting STAM-1/arrestin-2
interaction on HRS ubiquitination, HEK293 cells stably expressing HA-CXCR4 culture
in 10-cm dishes were transfected with 3 μg of FLAG-ubiquitin. Eight hours later, cells
were co-transfected with 8 μg of FLAG-STAM-1-CC or empty vector (pCMV-10) and
2 μg of T7-tagged HRS. Twenty-four hours later, cells were passaged onto PLL coated
6-cm dishes. The next day, cells were serum starved by incubating in DMEM containing
20 mM HEPES for 4–5 hr and then treated with 30 nM CXCL12 or vehicle
(PBS+0.1%BSA) for 30 and 60 min. Cells were washed with 5 ml cold PBS and collected
in 1 ml ubiquitination buffer (20 mM Tris-HCl pH 7.5, 150 mM NaCl, 1% Triton-X
100, 5 mM EDTA, 20 mM NEM, 10 μg/ml leupeptin, 10 μg/ml aprotinin, and 10
μg/ml pepstatin-A). Samples were transferred into microcentrifuge tubes and incubated at
4°C for 30 min while rocking, followed by sonicating once at amplitude of 11% for 10 sec

on ice using Branson Digital Sonifier®. CCLs were prepared by centrifugation at 14000 rpm for 20 min. CCLs were incubated with an anti-HRS polyclonal antibody to immunoprecipitate HRS. Immunoprecipitates were analyzed by subjecting to a 7.5% SDS-PAGE followed by western blotting using an anti-FLAG antibody conjugated to HRP to detect incorporated ubiquitin. Blots were stripped and reprobed using anti-HRS polyclonal antibody to detect the amount of HRS immunoprecipitated. Lysates were analyzed by SDS-PAGE and western blotting to detect expression levels of T7-HRS and FLAG-STAM-1-CC.

STAM-1 ubiquitination assay. For STAM-1 ubiquitination experiments, HeLa cells cultured in 6-well dishes were co-transfected with 3 μg of T7-STAM-1 and 40 ng of HA-ubiquitin. Eight hours later, cells were transfected with 3 μg of FLAG-STAM-1-CC or empty vector (pCMV-10). Twenty-four hours later, cells were passaged onto PLL coated 6-cm dishes and grown to 100% confluency (~24 hr). Cells were serum starved and treated with ligand and processed as described above for HRS ubiquitination using a modified ubiquitination buffer (20 mM $NaPO_4$, pH 6.5, 150 mM NaCl, 1% Triton-X 100, 20 mM NEM, and protease inhibitor cocktail). T7-STAM-1 was immunoprecipitated by incubating CCLs with anti-T7 goat polyclonal antibody and immunoprecipitates were analyzed by 7.5% SDS-PAGE followed by immunoblotting using an anti-HA mAb to detect ubiquitinated STAM-1. Blots were stripped and reprobed using an anti-STAM-1 polyclonal antibody to detect the amount of STAM-1

immunoprecipitated. Lysates were analyzed by SDS-PAGE and western blotting to detect expression levels of T7-STAM-1 and FLAG-STAM-1-CC.

To analyze the effect of AIP4 on STAM-1 ubiquitination, HeLa cells were transfected with FLAG-STAM-1 or empty vector (pCMV-10), Myc-AIP4 or Myc-AIP4-C830A and HA-ubiquitin or empty vector (pcDNA3). Forty-eight hours later, FLAG-STAM-1 was immunoprecipitated by incubating the CCLs with anti-FLAG polyclonal antibody and immunoprecipitates were analyzed by SDS-PAGE followed by immunoblotting using an anti-HA monoclonal Ab to detect ubiquitinated STAM-1. Blots were stripped and reprobed using an anti-FLAG monoclonal antibody to detect the amount of STAM-1 immunoprecipitated. Lysates were analyzed by SDS-PAGE and western blotting to detect expression levels of Myc-AIP4/C830A and FLAG-STAM-1.

CXCR4 internalization and recycling assay by ELISA

To measure CXCR4 internalization and recycling, HEK293 cells were cultured in 10-cm dishes to a confluency of 70-80%. Cells were co-transfected with 1 µg FLAG-CXCR4 and 600 pmol STAM-1 and GAPDH siRNA using Lipofectamine™2000 transfection reagent as described in section 2.1.2. Twenty-four hours later, cells were passaged onto PLL coated 24-well plates and grown for an additional 24 hr to a confluency of 100%. A sets of 5, 24-well dishes were made i.e. total surface receptor, % internalization, t=0 (total internalization), t=30 (recovery), and t=60 (recovery). The total surface receptor dish contains extra well for secondary antibody only control. Cells were

washed once with 500 μl DMEM containing 20 mM HEPES and serum starved by incubating in same media for 3–4 hr. Plates were placed on ice, media was removed by aspiration and cells were washed once with cold 500 μl DMEM containing 0.1% BSA, 20 mM HEPES, and 1 mM Ca^{2+} and then incubated on ice in the same media for 15 min. Cell surface receptor was labeled with antibody by incubating the cells with 250 μl DMEM containing 0.1% BSA, 20 mM HEPES, 1 mM Ca^{2+} and 1:100 dilution of calcium-dependent M1 anti-FLAG antibody for 1 hr on ice. M1 anti-FLAG antibody labels all cell surface FLAG-CXCR4 receptors in a calcium dependent fashion. After incubation, media from total surface receptor plate was removed by aspiration and cells were washed once with 500 μl DMEM containing 0.1% BSA, 20 mM HEPES, and 1 mM Ca^{2+} and left in same media on ice. Media from % internalization, t=0, t=30, and t=60 plates were removed by aspiration and cells were washed once with 500 μl DMEM containing 0.1% BSA, 20 mM HEPES, and 1 mM Ca^{2+}. Cell were then treated with 30 nM CXCL12 or vehicle (PBS+0.1% BSA) made in same media for 45 min at 37°C. Treatment with agonist promotes the internalization of receptor/antibody complex. After the treatment, media from % internalization plate was removed by aspiration and cells were washed once with 500 μl DMEM containing 0.1% BSA, 20 mM HEPES, and 1 mM Ca^{2+} and left in same media on ice. Surface bound antibody from t=0, t=30, and t=60 plates, that represent un-internalized receptor, was removed by washing the cells three times with 500 μl Ca^{2+} and Mg^{2+} free PBS containing 0.04% EDTA. EDTA chelates calcium that in turn leads to uncoupling of calcium dependent M1 antibody from the receptor. Media from total surface receptor plate, % internalization plate and t=0 was

removed by aspiration and replaced with 500 μl PBS containing 3.7% paraformaldehyde (PFA) and incubated for 5 minutes at RT. After fixation, cells were washed once with 500 μl PBS with Ca^{2+} and left in the same solution on ice. To monitor receptor recycling, cells in t=30 and t=60 plates were incubated with 500 μl DMEM containing 1 mM Ca^{2+} and 10 μM AMD3100 and incubated for 30 (t=30 plate) and 60 min (t=60 plate) at 37°C. AMD3100 is a CXCR4 antagonist and is used to block the binding of any residual CXCL12 that may be present in the media in the event that it was not completely removed during the washing step. After incubation, cells were washed once with PBS containing 1 mM Ca^{2+} and then fixed with 3.7% PFA for 5 min on ice. After fixation, cells were washed three times with 500 μl PBS containing 1 mM Ca^{2+} and all the plates were incubated with 300 μl alkaline phosphatase-conjugated goat anti-mouse antibody diluted 1:1000 in PBS containing 1% BSA for 1 hr at RT. Cells were washed with 500 μl PBS-Ca^{2+} and incubated with 250 μl developing solution (*p*-nitrophenyl phosphate) diluted in diethanolamine buffer (Bio-Rad Laboratories) for 5–15 min. Reactions were stopped by adding 100 μl 0.4 N NaOH and an aliquot of 100 μl was used to measure the absorbance at 405 nm. Percentage of receptor recycled was calculated by dividing the amount of receptor internalized by the amount of receptors recovered after incubation at different time intervals. To calculate the percentage of receptor internalization, the amount of receptor remaining on the cell surface was divided by the total number of receptors present on the cell surface before treatment with agonist.

CXCR4 internalization by FACS

CXCR4 internalization was determined by analyzing the surface receptor levels before and after ligand stimulation for 20 min using FACS. To determine the effect of Nystatin treatment on CXCR4 internalization, HeLa cells cultured in 10-cm dishes were washed once with 10 ml DMEM containing 20 mM HEPES and then treated with 50 μg/ml nystatin and vehicle (DMSO) in DMEM containing 20 mM HEPES for 30 min at 37°C. After treatment, cells were washed twice with 10 ml PBS and detached from the surface of the dish by incubating the cell monolayer with 2 ml Cellstripper™ cell dissociation solution for 10 min at 37°C. Cells were then collected in 8 ml PBS containing 0.1% BSA (Media Tech, VA), centrifuged and re-suspended in 2 ml PBS-0.1% BSA. Cells were counted in a Countess® Automated cell counter using trypan blue stain (Invitrogen). Five hundred thousand cells were transferred to a fresh 5 ml polystyrene round bottom tube (BD falcon) and washed once with PBS containing 0.1% BSA and resuspended in 250 μl PBS+0.1%BSA. Cells were incubated at 37°C for 15 min and then treated with 50 nM CXCL12 for 2, 5, 10 and 20 min and with vehicle (PBS+0.1% BSA) for 20 min at 37°C (this was accomplished by directly adding 1.25 μl of 10 μM stock of SDF to appropriate tube for a final concentration of 50 nM). After 20 min, 4 ml cold PBS was added to each tube, cells were collected by centrifugation at 1000 rpm at 4°C (JOUAN GR412 centrigufe) and then fixed by resuspending the pellet in 500 μl 4% paraformaldehyde (made in PBS) and incubating for 15 min at 37°C. Cells were collected by centrifugation and washed once with 4 mL PBS and then twice with PBS+0.1%BSA. CXCR4 present on the surface was labeled by incubating the cells with PE-conjugated anti-CXCR4 or isotype control antibodies. Cell pellet was re-suspended

in 100 µl PBS+0.1%BSA (supplemented with 5% normal goat serum) containing antibody (1:100 dilution) and incubated for 1 hr at RT in dark. Following labelling, cells were washed twice with 4 ml PBS+0.1%BSA and finally resuspended in 300 µl PBS+0.1%BSA and kept in dark until analysis was done. CXCR4 surface expression was determined by flow cytometry (FACS-CANTO; Becton Dickinson) and raw data were analyzed by FlowJo v.9.3 software. Geometrical mean of the PE fluorescence intensity was calculated to quantify percent CXCR4 internalization.

ERK-1/2 phosphorylation assay

HeLa or HEK293 cells cultured in 10-cm dishes were transfected with 600 pmol siRNA against arrestin-2/3, AIP4, STAM-1, µ2 and control siRNA (GAPDH) or plasmid DNA encoding dynamin-K44A, FLAG-STAM-1-CC, FLAG-arrestin-2-(25-161). Twenty-four hours later, cells were passaged onto 24-well plates and grown to 100% confluency (~24 hr). Cells were washed with 500 µl of DMEM containing 20 mM HEPES and incubated in the same media for 3-4 hr at 37˚C. Following serum starvation, cells were treated with 10 nM CXCL12, 100 ng/ml EGF or 1 mM carbachol and vehicle (PBS+0.1% BSA) for various time points. Following incubation, media from each well was removed by aspiration and cells were lysed by directly adding 300 µl 2x sample buffer. Cells were collected in microcentrifuge tubes and lysed by sonicating for 10 sec at amplitude of 11% using Branson Digital Sonifier®. Samples were analyzed by 10% SDS-PAGE followed by immunoblotting using mouse monoclonal phosphophorylation specific ERK-1/2 antibody. Blots were striped and re-probed for total ERK-1/2 and

actin. Phosphorylation of ERK-1/2 was quantified by densitometry and normalized to total-ERK levels.

To examine the effect of nystatin on ERK-1/2 phosphorylation, HeLa cells cultured in 24 well plates were washed once with 500 µl DMEM containing 20 mM HEPES and then treated with 50 µg/ml nystatin and vehicle (DMSO) made in DMEM containing 20 mM HEPES for 30 min. After treatment, cells were washed twice with DMEM containing 20 mM HEPES and treated with 10 nM CXCL12 or 100 ng/ml EGF and vehicle (PBS+0.1% BSA) for 5 min and processed exactly as described above.

To examine the effect of STAM-1 and AIP4 interaction on ERK-1/2 phosphorylation, HeLa cells cultured in 24-well plates were grown to 80-90% confluency and transfected with 0.15 µg FLAG-STAM-1 and 0.35 µg FLAG-AIP4 or FLAG-AIP4-ΔPRR and pCMV-10 alone using *Trans*IT®-LT1 transfection reagent as described in section 2.1.1. To examine the effect of AIP4 ubiquitination activity on ERK-1/2 phosphorylation, HeLa cells cultured in 24-well plates were grown to 80-90% confluency and transfected with 0.15 µg Myc-STAM-1 and 0.35 µg Myc-AIP4 or Myc-AIP4-C830A and pcDNA-3 alone. Forty-eight hours later, cells were washed once with 500 µl DMEM containing 20 mM HEPES and then incubated in same media for 5 hr at 37°C. Cells were treated with 10 nM CXCL12 and vehicle (PBS+0.1% BSA) for 5 min at 37°C and processed exactly as described above.

Cell fractionation experiment by sucrose gradient centrifugation

HeLa cells cultured in 10-cm dishes were transfected with 1 µg FLAG-AIP4

using *Trans*IT®-LT1 transfection reagent as described in section 2.1.1. Twenty-four

hours later, each 10-cm dish was passaged into two 10-cm dishes and grown to 100%

confluency (~24 hr). Media from the dishes was removed and cells were washed once

with DMEM containing 20 mM HEPES and then serum starved in the same media for

3-4 hr at 37°C. Cells were then treated with vehicle (PBS+0.1% BSA) or 10 nM

CXCL12 for 5 min. Caveolin-1 enriched fractions were isolated using a detergent-free

procedure (Song et al., 1996). Following incubation, plates were kept on ice and washed

with 10 ml ice cold PBS. Cells were collected in 600 μl carbonate buffer (150 mM

sodium carbonate, pH 11, 1 mM EDTA, 10 μg/ml each of leupeptin, aprotinin and

pepstatin A) by scrapping and transferred to a pre-chilled 2 ml microcentrifuge tube (cells

from 2, 10-cm dishes were pooled together). Cells were lysed by passing 10 times

through a cold 2 ml dounce homogenizer, followed by passing through an 18-gauge

needle 10 times and finally sonicating 5 times at 20% while on ice using Branson Digital

Sonifier®. Eight hundred μl lysed cells were mixed with 800 μl MBS buffer (25 mM

MES, pH 6.5, 150 mM NaCl, 2 mM EDTA) containing 80% sucrose and 300 mM

sodium carbonate and pipetted to the bottom of a 12 ml prechilled ultracentrifuge tube

(Ultra-Clear tubes, Beckman). Carefully, 6 ml of 35% sucrose made in MBS buffer

containing 150 mM sodium carbonate was layered on top, which was subsequently

layered with 4 ml of 5% sucrose made in MBS buffer. Tubes were carefully placed in a

prechilled tube adaptor and attached to a prechilled SW41 swinging bucket rotor (Note:

all tubes placed in tube adaptors were weighed to an accuracy of 0.001 gm to ensure

proper balancing while centrifugation). Tubes were centrifuged at 221,000 g for 18 hr at

4°C. After centrifugation, tubes were carefully removed from the adapter using forceps and nine sequential fractions of 1.33 ml each were removed from the top of each tube. An aliquot of 250 μl from each fraction was mixed with 50 μl of 6x sample buffer and heated at 50°C for 10 min to dissolve all the sucrose. Aliquot of 35 μl from each fractions was analyzed by 10% SDS-PAGE followed by immunoblotting to detect CXCR4, α2-adaptin, caveolin-1, STAM-1, AIP4 and Gαi.

To examine the effect of STAM-1 and AIP4 knockdown on distribution of CXCR4, HeLa cells cultured in 10-cm dishes to 70-80% confluency were transfected with 600 pmoles siRNA against GAPDH, AIP4 and STAM-1. Twenty-four hours later, each 10-cm dish were passaged into two 10-cm dishes and grown to 100% confluency. Cells were treated with 10 nM CXCL12 and processed exactly as described above.

Fluorescent vector based transwell migration assay

HeLa cells cultured in 10-cm dishes to 70-80% confluency were co-transfected with 600 pmol siRNA against GAPDH, AIP4, STAM-1 or arrestin-2/3 and 2 μg pEYFP-C1 vector. Cells were grown for 48 hr to reach a confluency of 100 % and were washed once with DMEM containing 1% BSA, 0.5% FBS and 20 mM HEPES and then serum starved in same media for 16 hr at 37°C. FluoroBlok™ transwell inserts with 8 μm pores were coated on the underneath with rat-tail type I collagen by placing inserts in single well of a compatible 24 well plate (BD Biosciences Cat. No. 353504) containing 500 μl rat-tail type I collagen (50 μg/ml) made in RPMI containing 20 mM acetic acid

and incubating at 4°C for 16 hr. The following day, plates were washed once with warm 10 ml PBS and cells were detached from the plate by incubating the monolayer with 2 ml Cellstripper™ cell dissociation solution for 10 min at 37°C. Eight ml DMEM+1% BSA was added to each plate, pipetted up and down and collected in a 15 ml conical tube. Cells were pelleted down by centrifugation at 1000 rpm for 5 min at RT and re-suspended in 2 ml PBS-0.1% BSA. Cells were counted using a Countess® Automated cell counter using trypan blue stain (Invitrogen). A suspension of 500,000 cells/ml was made in DMEM containing 20 mM HEPES. Coated FluoroBlok™ transwell inserts were washed once with DMEM containing 1% BSA and then placed in 24 well plate containing 500 μl of 30 nM CXCL12 or vehicle (PBS+0.1% BSA) made in DMEM+20 mM HEPES. Two hundred μl cell suspension (i.e. 100,000 cells) was added on the top of each insert and incubated for 12 hr at 37°C. After incubation, inserts were removed and placed in single well of a 24-well dish containing 500 μl PBS. Media containing cells from the top of inserts was aspirated and cells were scraped from the top of the membrane using a cotton swab. Top of each insert was washed with 500 μl PBS to remove detached cells. Inserts were then removed and placed in wells containing 500 μl of 3.7% formaldehyde and incubated for 15 min at RT to fix cells present on the bottom of the insert. After incubation, inserts were washed again with 500 μl PBS and the membrane was removed using a scalpel blade and mounted on a slide using permount-mounting media (bottom of insert facing up). Samples were analyzed by Olympus IX81 fluorescent microscopy equipped with UPLanFI 20X objective using QCapture software (v 2.90.1). Images were acquired using a QIMAGING RETIGA EXi cooled Mono 12

bit digital camera (QCamDriver v. 1.90.1). Number of cells migrated to the bottom of the insert were quantified manually using eraser tool of Adobe Photoshop (CS4).

Propidium iodide based cell cycle analysis

HeLa cells cultured in 10-cm dishes were transfected with 600 pmol siRNA against GAPDH, AIP4, STAM-1 and arrestin-2+3. Twenty four hours later, each 10-cm plate was passaged 1:3 onto 6-cm dishes and grown for additional 24 hr to achieve a confluency of 100%. The next day, cells were washed once with DMEM+20mM HEPES and incubated in the same media for 12 hr at 37°C to serum starve the cells. Cells were treated with 100 nM CXCL12, 10% FBS and vehicle (PBS+0.1% BSA) made in DMEM+20mM HEPES for 12 hr. After the treatment, cells were trypsonized by incubating with 350 μl trypsin at 37°C for 5 min. Cells were collected in 4 ml PBS containing 5% Bovine Calf Serum (BCS), centrifuged at 1000 rpm for 5 min and re-suspended in 2 ml PBS+0.1% BSA. Cells were counted in a Countess® Automated cell counter using trypan blue stain. One million cells were transferred to a fresh 5 ml polystyrene round bottom tube (BD falcon) and washed once with 3 ml PBS+5% BCS. Cells were then fixed by adding 600 μl 100% ethanol to the cell pellet while constantly vortexing at low speed. Tubes were left on ice for 10-15 min and then washed with 3 ml PBS+5% BCS. Cell pellet was then resuspended in 250 μl of 10 μg/ml RNase A and incubated at 37°C for 15 min. Following incubation, cells were stained with propidium iodide (PI) by adding 250 μl 100 μg/ml PI to all tubes and incubated at RT for 1 hr before analyzing by FACS (FACS-CANTO; Becton Dickinson). Raw data were further

analyzed by FlowJo v.9.3 using the Watson pragmatic model for cell cycle analysis (Watson et al., 1987). Percent cell present in S, G1 and G2 phase were plotted separately by using GraphPad prism.

CXCR4 surface expression analysis by FACS

HeLa cells were passaged onto 6-cm dishes and grown until a confluency of 70-80% was reached (~24 hr). Cells were transfected with 200 pmol siRNA against GAPDH, STAM-1, AIP4 and arrestin-2+3 or were mock transfected (no siRNA) using Lipofectamine™2000 transfection reagent as described in section 2.1.2. Forty-eight hours later, media from the dishes was removed by aspiration and cells were washed once with 4 ml PBS. Cells were detached from the plate by incubating cell monolayer with 350 µl Cellstripper™ solution for 10 min at 37°C. Cells were collected in 4 ml PBS containing 0.1% BSA, centrifuged at 1000 rpm for 5 min and re-suspended in 2 ml PBS+0.1% BSA. Cells were counted in automatic Countess cell counter using trypan blue stain (Invitrogen). Five hundred thousand cells were transferred to a fresh 5 ml polystyrene round bottom tube (BD falcon) and washed once with PBS+0.1% BSA. Cells were then fixed by resuspending the pellet in 500 µl 4% paraformaldehyde (made in PBS) and incubating for 15 min at 37°C. Cells were collected by centrifugation at 1000 rpm for 5 min and washed once with 4 ml PBS and then twice with PBS-0.1%BSA. Cells were stained by re-suspending the cell pellet in 100 µl antibody dilution buffer (PBS+0.1%BSA+5% normal goat serum) containing PE-conjugated anti-CXCR4 or isotype control antibody (1:100 dilution) and incubating for 1 hr at RT in dark. Cells were mixed with antibody by agitating the tubes 5-6 times every 15 min during the

incubation. Following staining, cells were washed twice with 4 mL PBS+0.1% BSA and finally the cell pellet was resuspended in 300 μl PBS+0.1%BSA and kept in the dark until the analysis. CXCR4 surface expression was analyzed by flow cytometry (FACS-CANTO; Becton Dickinson) and all the raw data were analyzed by FlowJo v.9.3. Geometrical mean of the PE fluorescence intensity was plotted to quantify the surface expression of CXCR4.

PARP cleavage/apoptosis assay

To investigate the effect of AIP4, STAM-1 and arrestin-2/3 knockdown on PARP cleavage, HeLa cells cultured in 6-cm dishes were transfected with 200 pmol siRNA against GAPDH, STAM-1, AIP4 and arrestin-2+3 or were mock transfected (no siRNA) using Lipofectamine™2000 transfection reagent as described in section 2.1.2. Forty-eight hours later, cells were washed once with 5 ml PBS and 300 μl of 2x sample buffer was added. Cells were scraped, collected in fresh microcentrifuge tube and sonicated once for 10 sec at amplitude of 11% using Branson Digital Sonifier®. Equal volume of samples were analyzed by 10% SDS-PAGE followed by immunoblotting to detect full-length and cleaved PARP. Blots were stripped and reprobed for actin.

Statistical analysis and final figures

Data were analyzed by Student's t-test, One-way or Two-way analysis of variance (ANOVA) using GraphPad Prism 4.0 for Macintosh (GraphPad Software, San Diego, CA; www.graphpad.com). Graphs were generated by using GraphPad Prism and Adobe Illustrator CS4. All western blots and immunofluorescence figures were made using Adobe Photoshop and Adobe illustrator (Adobe Creative Suite CS4 for Macintosh).

Table 2.1: List of all antibodies used in this dissertation work

Antibody Name	Clone	Type	Catalogue no. and Source
Anti-HA	16B12	Mouse	MMS-101R, Covance (Berkeley, CA)
Anti-HA	-	Rabbit	PRB-101C, Covance (Berkeley, CA)
Anti-c-Myc	9E10	Mouse	AFC-150P, Covance (Berkeley, CA)
Anti-STAM-1	-	Rabbit	12434-1-AP, ProteinTech (Chicago, IL)
Anti-STAM-2	-	Rabbit	13009-1-AP, ProteinTech (Chicago, IL)
Anti-AMSH	-	Rabbit	11346-1-AP, ProteinTech (Chicago, IL)
Anti-FLAG	M1	Mouse	F3040, Sigma-Aldrich (St. Louis, MO)
Anti-FLAG	M2	Mouse	F1804, Sigma-Aldrich (St. Louis, MO)
Anti-FLAG-HRP	M2	Mouse	A8592, Sigma-Aldrich (St. Louis, MO)
Anti-FLAG	M2	Rabbit	F7425, Sigma-Aldrich (St. Louis, MO)
Anti-ERK1/2	-	Rabbit	M5670, Sigma-Aldrich (St. Louis, MO)
Anti-P-ERK1/2	MAPK-YT	Mouse	M8159, Sigma-Aldrich (St. Louis, MO)
Anti-T7	-	Mouse	T8823, Sigma-Aldrich (St. Louis, MO)
Anti-AIP4	D20	Goat	sc-11890, Santa Cruz (CA)
Anti-AIP4	G11	Mouse	sc-28367, Santa Cruz (CA)
Anti-Gαi	T-19	Rabbit	Santa Cruz (CA)
Anti-Dynamin-1	D5	Mouse	sc-12724, Santa Cruz (CA)
Anti-c-Myc	A-14	Rabbit	sc-789, Santa Cruz (CA)
Anti-HRS	M-79	Rabbit	sc-30221, Santa Cruz (CA)
Anti-Caveolin	N-20	Rabbit	sc-894, Santa Cruz (CA)
Anti-β-arrestin-1/2/3	H-290	Rabbit	sc-28869, Santa Cruz (CA)
Anti-β-arrestin-1/2	21-B1	Mouse	sc-53781, Santa Cruz (CA)
Anti-Clathrin-HC	TD1	Mouse	sc-12734, Santa Cruz (CA)
Anti-Clathrin-HC	-	Mouse	610499, BD Biosciences (San Jose, CA)
Anti-ITCH (AIP4)	-	Rabbit	3612-1, Epitomics (Burlingame, CA)
Anti-CXCR4 (CD184)	2B11	Rat	551852, BD Biosciences (San Jose, CA)
Anti-arrestin-2	-	Mouse	610550, BD Biosciences (San Jose, CA)
Anti-EEA1	-	Mouse	610456, BD Biosciences (San Jose, CA)
PE Anti-Human CD184	-	Mouse	555974, BD Biosciences (San Jose, CA)
PE Mouse IgG1a	-	Mouse	555574, BD Biosciences (San Jose, CA)
Anti-T7	-	Goat	Ab9138, Abcam (Cambridge, MA)
Anti-Actin	-	Mouse	691001, MP Biomedical (Aurora, OH)
Anti-β-tubulin	-	Mouse	Accurate Chemical (Westbury, NY)
Anti-β-tubulin	E7	Mouse	Iowa University
Anti-GST	-	Mouse	Sigma-Aldrich (St. Louis, MO)
Anti-EGFR	-	Mouse	Assay Designs (Ann Arbor, MI)

Anti-α-Adaptin	AP6	Mouse	Fisher Scientific (Pittsburg, PA)
Anti-arrestin-2/3	178	Rabbit	Dr. Jeffrey L. Benovic
Anti-PARP	-	Rabbit	9542, Cell Signaling

Table 2.2: List of HRP conjugated and fluorescent tagged secondary antibodies used in this dissertation work

Antibody Name	Species	Catalogus No. and Source
Anti-Mouse-HRP	Goat	PI-2000, Vector Labs (Burlingame, CA)
Anti-Rabbit-HRP	Goat	PI-1000, Vector Labs (Burlingame, CA)
Anti-Goat-HRP	Horse	PI-95000, Vector Labs (Burlingame, CA)
Anti-Rat-HRP	Goat	DC01L, Calbiochem
Fluorescent Tagged Secondary Antibodies		
Alexa-Fluor 488	Mouse	A11029, Invitrogen (Carlsbad, CA)
Alexa-Fluor 555	Mouse	A21424, Invitrogen (Carlsbad, CA)
Alexa-Fluor 594	Mouse	A11020, Invitrogen (Carlsbad, CA)
Alexa-Fluor 635	Mouse	A31575, Invitrogen (Carlsbad, CA)
Alexa-Fluor 488	Rabbit	A11070, Invitrogen (Carlsbad, CA)
Alexa-Fluor 568	Rabbit	A11036, Invitrogen (Carlsbad, CA)
Alexa-Fluor 594	Rabbit	A11072, Invitrogen (Carlsbad, CA)
Alexa-Fluor 633	Rabbit	A21071, Invitrogen (Carlsbad, CA)
Alexa-Fluor 594	Rat	A11007, Invitrogen (Carlsbad, CA)
Alexa-Fluor 633	Rat	A21094, Invitrogen (Carlsbad, CA)

Table 2.3: List of reagents, chemicals and kits used in this dissertation work

Reagent/Kit Name	Catalogue no. and Source
Glutathione-Sepharose 4B resin	17-0756-01, GE Healthcare
L Glutathione reduced	G4251, Sigma-Aldrich (St. Louis, MO)
Nystatin	N6261, Sigma-Aldrich (St. Louis, MO)
Stromal cell-derived factor-1 (CXCL12)	300-28A, PeproTech (Rocky Hill, NJ)
Epidermal growth factor (EGF)	PeproTech (Rocky Hill, NJ)
Rat tail Collagen, Type 1	354236, BD Biosciences (San Jose, CA)
HTS-FLuoroBlok Insert (8μm)	351152, BD labware (Franklin Lakes NJ)
AMD3100	A5602, Sigma-Aldrich (St. Louis, MO)
Alkaline phosphatase substrate kit	Bio-Rad Laboratories (Hercules, CA)
VECTASHIELD Mounting media (DAPI)	H-1200, Vector laboratories (CA)
Permount mounting media	SP15-100, Fisher Chemicals (NJ)
Cellstripper Cell Dissociation solution	25-056-CI, Mediatech (Manassas, VA)

Trypsin EDTA, 1X	25-052-CI, Mediatech (Herndon, VA)
Trypan Blue	T10282, Invitrogen (Carlsbad, CA)
Goat Serum	G6767, Sigma-Aldrich (St. Louis, MO)
Protein A Agarose	11134515001, Roche (Manhein, Germany)
Protein G Agarose	11243233001, Roche (Manhein, Germany)
Phosphatase Inhibitors (Cocktail 1+2)	Sigma-Aldrich (St. Louis, MO)
NEM (N-Ethylmaleimide)	E3876, Sigma-Aldrich (St. Louis, MO)
Saponin Detergent	S7900, Sigma-Aldrich (St. Louis, MO)
HEPES	SH30237.01, Hyclone
Tween-20	P9416, Sigma-Aldrich (St. Louis, MO)
Triton X-100	T8787, Sigma-Aldrich (St. Louis, MO)
Non Fat Dry Milk	Distributed by ALDI
Blue X-ray films	Phenix Research
Leupeptin	11017101001, Roche
Aprotinin	10236624001, Roche
Pepstatine	1359053001, Roche
Sodium Chloride (NaCl)	S9888, Sigma-Aldrich (St. Louis, MO)
Glycine	03117251001, Roche
Methanol	A412.20, Fisher Scientific
2-Propanol	I9516, Sigma-Aldrich (St. Louis, MO)
Tris Base	11814273001, Roche
Coverglass circular cover slips	12-545-81, Fisher Scientific
Imidazole	10125, Sigma Aldrich (St. Louis, MO)
Dimethyl Sulfoxide (DMSO)	D2650, Sigma Aldrich (St. Louis, MO)
Acrylamide/Bisacrylamide, liquid (37.5:1)	11685821001, Roche
Ammonium persulfate (APS)	A3678, Sigma Aldrich (St. Louis, MO)
TEMED	161-08-01, Bio-Rad
Ponceau S	P7180, Sigma Aldrich (St. Louis, MO)
GelCode Blue	24590, Thermo Scientific
NP-40	13344700, Roche
MES	M3671, Sigma-Aldrich (St. Louis, MO)
Sucrose	S0389, Sigma-Aldrich (St. Louis, MO)
Propidium iodide (PI)	P3566, Invitrogen
Bovine Serum Albumin Fraction V	03117057001, Roche
Isopropyl-β-D-1-thiogalactopyranoside	I5502, Sigma Aldrich (St. Louis, MO)
DL-Dithiothreitol (DTT)	43815, Sigma Aldrich (St. Louis, MO)
His-Select Nickel Affinity Gel	P6611, Sigma-Aldrich (St. Louis, MO)
Poly-Prep Chromatography columns	731-1550, Bio-Rad

Table 2.4: List of siRNA used in this dissertation work

siRNA Name	Sequence	Source

STAM-1	GAACGAAGAUCCGAUGUAU	D-001423-01 Thermo Scientific
STAM-2	CAAAGAGGAUGAAGACAUA	D-017361-02 Thermo Scientific
AIP4	GGUGACAAAGAGCCAACAGAG	
AMSH	GAGAAGCCCUCCUUAGAUG UCACUGCUCUUACCAGAUG GCAAGGAUCCACCUCUGUU AGACCUUCGAUGAGCGUUU	SMARTpool M-012202-01 Thermo Scientific
Arrestin-2+3	ACCUGCGCCUUCCGCUAUG	Dharmacon RNA technologies
Arrestin-3(1)	CAACCUCAUUGAAUUUGAU	M-007292-00-0005 Thermo Scientific
Arrestin-3(2)	CGGCGUAGACUUUGAGAUU	M-007292-00-0005 Thermo Scientific
Arrestin-3(3)	GAUGAAGGAUGACGACUAU	M-007292-00-0005 Thermo Scientific
Arrestin-3(4)	CGAACAAGAUGACCAGGUA	M-007292-00-0005 Thermo Scientific
Caveolin-1	UCAAGCGCAUGGCAGGCAU	Dr. Joann Trejo (UCSD, San Deigo, CA)
Caveolin-1	GCAAAUACGUAGACUCGGA AUUAAGAGCUUCCUGAUUG GCAGUUGUACCAUGCAUUA CUAAACACCUCAACGAUGA	SMARTPOOL M-003467-01 Thermo Scientific
μ2	UCAAGCGCAUGGCAGGCAU	Dharmacon RNA Technologies

Table 2.5: List of DNA constructs used in this dissertation work

Construct Name	Vector	Reference

CXCR4 constructs

HA-CXCR4	pcDNA3.0	Marchese and Benovic, 2001
HA-CXCR4-S330A	pcDNA3.0	Marchese and Benovic, 2001
HA-CXCR4-S324-5A	pcDNA3.0	Marchese and Benovic, 2001
HA-CXCR4-YFP-WT	pEYFP-N1	Bhandari *et. al.,* 2009
HA-CXCR4-ΔC-tail	pcDNA3.0	

STAM constructs

GST-STAM-1	pGEX-4T2	Malik and Marchese, 2010

GST-STAM-2	pGEX-4T2	Malik and Marchese, 2010
FLAG-STAM-1	pCMV-10	Malik and Marchese, 2010
Myc-STAM-1	N.A.	Malik *et. al.*, 2011 (submitted)
HIS-STAM-1	pQE30-Xa	Malik and Marchese, 2010
T7-STAM-1	N.A.	Malik and Marchese, 2010
YFP-STAM-1	pEYFP-C1	Malik and Marchese, 2010
FLAG-STAM-1-CC 296-380	pCMV-10	Malik and Marchese, 2010
FLAG-STAM-1-1-144	pCMV-10	Malik and Marchese, 2010
FLAG-STAM-1-(1-195)	pCMV-10	Malik and Marchese, 2010
FLAG-STAM-1-(1-269)	pCMV-10	Malik and Marchese, 2010
FLAG-STAM-1-(1-390)	pCMV-10	Malik and Marchese, 2010
FLAG-STAM-1-(391-540)	pCMV-10	Malik and Marchese, 2010
FLAG-STAM-1-(337-540)	pCMV-10	Malik and Marchese, 2010
FLAG-STAM-1-(270-540)	pCMV-10	Malik and Marchese, 2010
FLAG-STAM-1-(221-540)	pCMV-10	Malik and Marchese, 2010
FLAG-STAM-1-(144-540)	pCMV-10	Malik and Marchese, 2010
FLAG-STAM-1-SH3-(209-269)	pCMV-10	Malik *et. al.*, 2011 (submitted)
GST-STAM-1-SH3-(209-269)	pGEX-4T2	Malik *et. al.*, 2011 (submitted)

AIP4 constructs

FLAG-AIP4	pCMV-10	Marchese and Benovic, 2001
Myc-AIP4	pRK5	Marchese *et. al.*, 2003
Myc-AIP4-C830A	pRK5	Marchese *et. al.*, 2003
YFP-AIP4	pEYFP-C1	Bhandari *et. al.*, 2007
GST-AIP4	pGEX-4T2	Bhandari *et. al.*, 2007
GST-AIP4-ΔWWI-IV	pGEX-4T2	Bhandari *et. al.*, 2007
GST-AIP4-WW-I-IV	pGEX-4T2	Bhandari *et. al.*, 2007
GST-AIP4-HECT	pGEX-4T2	Bhandari *et. al.*, 2007
GST-AIP4-ΔPRR	pGEX-4T2	Malik *et. al.*, 2011 (submitted)
FLAG-AIP4-ΔPRR	pCMV-10	Malik *et. al.*, 2011 (submitted)

Arrestin-2/3 constructs

HA-arrestin-2	pcDNA3.0	Bhandari *et. al.*, 2007
HA-arrestin-3	pcDNA3.0	Bhandari *et. al.*, 2007
HA-arrestin-2 1-260	pcDNA3.0	Bhandari *et. al.*, 2007
HA-arrestin-2 261-418	pcDNA3.0	Bhandari *et. al.*, 2007
HA-arrestin-2 1-161	pcDNA3.0	Bhandari *et. al.*, 2007
HA-arrestin-2 1-179	pcDNA3.0	Bhandari *et. al.*, 2007
HA-arrestin-2(25-161)	pcDNA3.0	Malik and Marchese, 2010
GST-arrestin-2	pGEX-4T2	Bhandari *et. al.*, 2007
YFP-arrestin-2	pEYFP-C1	Bhandari *et. al.*, 2007
HIS-arrestin-2	pQE-30 Xa	Malik and Marchese, 2010

Ubiquitin and other protein constructs

HA-Ubiquitin	pcDNA3.0	Bhandari *et. al.*, 2007
FLAG-Ubiquitin	pCMV-10	Marchese and Benovic, 2001
FLAG-HRS	pCMV-10	Malik and Marchese, 2010
FLAG-AMSH	pCMV-10	Malik and Marchese, 2010
Dynamine-K44A	N/A	Marchese *et. al.*, 2003

- The integrity of all constructs was verified by sequencing

Table 2.6: List of the primers used to make constructs described in this dissertation work

Name	Primers (5'→3')
FLAG-STAM-1 (1-195)	*Forward:* GGAGGTCTATATAAGCAGAGC *Reverse:* ATATTCTAGATTAGGAAAGGGTGGTTGACTGCTG
FLAG-STAM-1 (1-269)	*Forward:* GGAGGTCTATATAAGCAGAGC *Reverse:* ATATTCTAGATTAAGTGAGATCTGCAGTCACAAA
FLAG-STAM-1 (1-390)	*Forward:* GGAGGTCTATATAAGCAGAGC *Reverse*: ATATTCTAGATTACTGATTCTGTAACTTTGCATA
FLAG-STAM1 (391-540)	*Forward:* ATATAAGCTTCCATATTATATGCAG *Reverse:* GGGCCAGGAGAGGCACTG
FLAG-STAM-1 (144-540/ ΔVHS)	*Forward:* ATATAAGCTTGCTATTGGCTCTCAGGCT *Reverse*: GGGCCAGGAGAGGCACTG
FLAG-STAM-1 (337-540)	*Forward:* ATATAAGCTTCACCAGATGGGACCTCTC *Reverse:* GGGCCAGGAGAGGCACTG
FLAG-STAM-1 (212-540)	*Forward:* ATATAAGCTTGGCCGAAAAGTTCGTGC *Reverse:* GGGCCAGGAGAGGCACTG
FLAG-STAM-1 (270-540)	*Forward:* ATATAAGCTTGCTGAACCAGAAATGATT *Reverse:* GGGCCAGGAGAGGCACTG
FLAG-STAM-1-Delta GAT	*Forward* *1*: TGTCACCAGATGGGACCTCTCGATCCGATGTAT TCCATGTATGC

(Δ343-377)	*Reverse 1*: GAGAGGTCCCATCTGGTGACA *Forward 2*: GGAGGTCTATATAAGCAGAGC *Reverse 2*: GGGCCAGGAGAGGCACTG
GST-STAM-1-Delta GAT (Δ343-377)	*Forward*: ATATGAATTCTGCCTCTTTTTGCCACCAATCCC *Reverse*: ATATCTCGAGCTATAGCAGAGCCTTCTG
GST-STAM-1-GAT (296-380)	*Forward*: ATATGAATTC TGGAGCCGGAACCAGCC *Reverse*: ATATCTCGAGCTACATCGGATCTTCGTTCATTAAC
FLAG-STAM-1-GAT (296-380)	*Forward*: ATAT AAG CTT GAG CCG GAA CCA GCC *Reverse*: ATATTCTAGACTACATCGGATCTTCGTTCATTAAC
YFP-STAM-1	*Forward*: ATATAAGCTTTGCCTCTTTTTGCCACCAATCCCTTC *Reverse*: ATATGGTACCCTACATCGGATCTTCGTTCATTAAC
FLAG-Arr-2-(25-161)	*Forward*: ATATAAGCTTCGGGACTTTGTGGACCAC *Reverse*: CAAACAACAGATGGCTGGCAAC
GST-Arr-2-(25-161)	*Forward*: ATATCCCGGGCGGGACTTTGTGGACCAC *Reverse*: ATATCTCGAGCTACCGCTTGTGGATCTTCTCCTCCA
FLAG-STAM-1-Delta-SH3 (209-269)	*Forward*: TCCAGTCTCTTAACTAACCACGCTGAACCAGAAAT GATTAAAAC *Reverse*: GTGGTTAGTTAAGAGAC GG
FLAG-STAM1-SH3 (209-269)	*Forward*: ATATAAGCTTCAACATGAAGGCCGAAAAG *Reverse*: ATATTCTAGATTAAGTGAGATCTGCAGTCAC
FLAG-AIP4-Delta-PRR	*Forward*: TCA AAT GGT GGT TTT AAA GCA TCT GTC AAT GG *Reverse*: TTT AAA ACC ACC ATT TGA
FLAG-AIP4-PRR	*Forward*: ATAT GCG GCC GC A CCT TCT AGA CCT CCA AGA CC *Reverse*: ATAT GGA TCC TTA TGG TCT ACG TGG GGT GGG

CHAPTER 3

RESULTS

ROLE OF ARRESTIN-2 IN ENDOSOMAL SORTING AND DEGRADATION OF CXCR4

Previous work from our laboratory indicates that arrestin-2 through an interaction with AIP4 has a role in endosomal sorting of activated CXCR4 from early endosomes to lysosomes (Bhandari et al., 2007). It was shown that siRNA-mediated knockdown of arrestin-2, but not arrestin-3, blocks agonist promoted degradation of CXCR4. Confocal microscopy revealed that arrestin-2 is important for the trafficking of CXCR4 from early endosomes to lysosomes, as in cells that lack arrestin-2, CXCR4 was trapped onto early endosomes. Arrestin-2 has also been shown to directly interact with the carboxy-terminal tail (C-tail) of CXCR4. However, the molecular mechanism behind the role of arrestin-2 in endosomal sorting of CXCR4 remains unclear.

Serine residue 330 in the C-tail of CXCR4 is important for the interaction with arrestin-2

In order to understand the role of arrestin-2 in endosomal sorting of CXCR4, we initially set out to characterize the interaction between CXCR4 and arrestin-2. To determine if the arrestin-2 binding site on CXCR4 is limited to the C-tail, we performed

GST-pulldown experiments by incubating HEK293 cell lysates expressing HA-CXCR4-full length and HA-CXCR4-ΔC-tail with bacterially purified GST-tagged arrestin-2. As shown in Figure 3.1A, GST-arrestin-2 was able to pull down full length CXCR4 from the lysates, however, no binding was seen in case of CXCR4 truncation mutant lacking the C-tail, suggesting that the binding site for arrestin-2 on CXCR4 is present in the C-tail. To further characterize this interaction we next sought to identify the receptor determinants responsible for mediating the interaction between CXCR4 and arrestin-2. It has been shown previously that a stretch of 10 amino acids in the C-tail of CXCR4 is important for targeting CXCR4 into the degradative pathway (Marchese and Benovic, 2001). As shown in Figure 3.1B, this stretch of 10 amino acid contains three serine residues (324, 325 and 330), which are potential phosphorylation sites and phosphorylated serines/threonines within GPCRs are known to mediate arrestin binding (Defea, 2008; Marchese et al., 2008). Serine residues 324/5 have been recently shown to be important for the binding to AIP4. Phosphorylation of S324/5 leads to direct binding of E3 ubiquitin ligase AIP4 to CXCR4 (Bhandari et al., 2009). To assess the importance of serine residues 324, 325 and 330 in the C tail of CXCR4 for binding with arrestin-2, we mutated them to alanine residues and assessed their ability to bind arrestin-2 by GST-pulldown experiment. As shown in figure 3.1 B and C, serine residue 330, when mutated to alanine, leads to loss of binding with GST-arrestin-2 as compared to wild-type receptor binding. No effect on binding to arrestin-2 was seen with CXCR4 S324/325A mutant (Figure 3.1C). It has been recently shown in the literature that serine residue 330 is phosphorylated in response to agonist stimulation by GRK6 suggesting

that phosphorylation of S330 might regulate CXCR4-arrestin-2 interaction (Busillo et al., 2010). Although the role of S330 phosphorylation in arrestin-2 binding remains to be determined, nevertheless, our data suggest that arrestin-2 directly interacts with CXCR4 C-tail and serine residue 330 is important for this interaction.
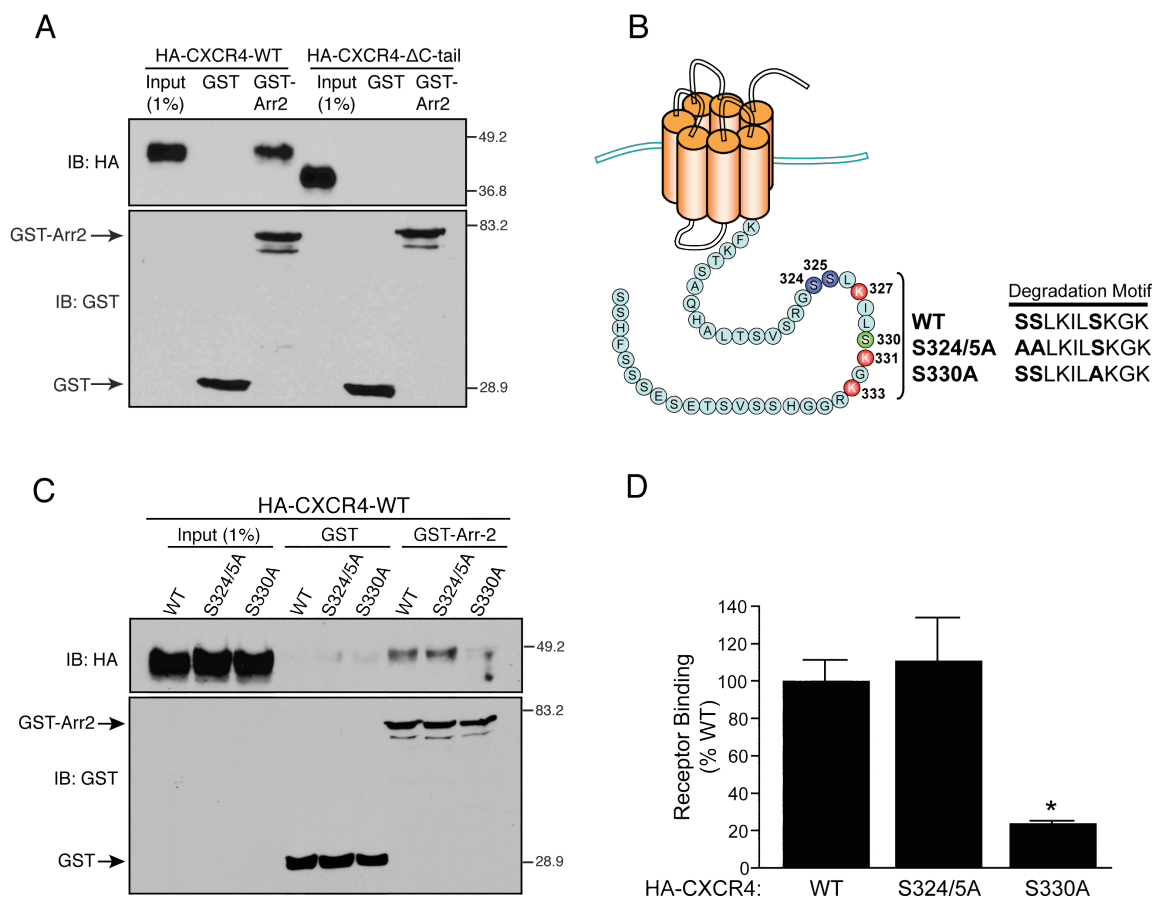
Figure 3.1: Serine residue 330 in the C-tail of CXCR4 plays an important role in CXCR4/arrestin-2 interaction. **A.** Schematic representation of the amino acid sequence of CXCR4 C-tail. The degradation motif and serine mutants are also shown **B.** Cleared cell lysates (CCL) from HEK293 cells transiently expressing HA-CXCR4 WT and HA-CXCR4-ΔC-tail (B) or HA-CXCR4 WT, HA-CXCR4 S324/325A and HA-CXCR4 S330A mutants (C) were incubated with equimolar amounts of GST alone or GST-tagged arrestin-2 bound to glutathione-Sepharose resin. Receptor binding was assessed by western blot with an anti-HA antibody. Blots were stripped and reported with anti-GST antibody **D.** Percent

receptor bound was quantified by densitometric analysis. Data were analyzed by a one-way ANOVA, followed by Bonferroni's multiple comparison test. Binding to S330A receptor was significantly reduced as compared to WT receptor, p<0.05. Shown are a representative blot from 2 (A) and 3 (C) independent experiments.

Arrestin-2 co-localizes with CXCR4 on early endosomes

Previously published results from our laboratory have shown that arrestin-2 co-localizes with AIP4 on endocytic vesicles in cells treated with CXCL12 for 30 min (Bhandari et al., 2007). Whether CXCR4 is associated with this complex remains unknown. Based upon our interaction data, we hypothesize that CXCR4 recruits arrestin-2 to endosomes where it then interacts with AIP4. To examine whether arrestin-2 co-localizes with CXCR4 on endosomes upon CXCL12 treatment we employed fixed cell confocal immunofluorescence microscopy. HEK293 cells transiently transfected with HA-CXCR4 tagged at the C-terminus with yellow fluorescent protein (YFP), a construct that we have described previously (Bhandari et al., 2009), and CFP-tagged arrestin-2 were treated with CXCL12 for 30 minutes. In vehicle treated cells, CXCR4 was primarily localized on the plasma membrane, while arrestin-2 was diffuse within the cytoplasm and did not co-localize with CXCR4 (Figure 3.2A). Upon treatment with agonist, CXCR4 staining was punctate and showed strong co-localization with the early endosomal marker EEA1 suggesting that agonist promotes CXCR4 internalization onto endosomes (Figure 3.2A). In CXCL12 treated cells, arrestin-2 also became punctate and co-localized with CXCR4 on early endosomes, suggesting that agonist activation of CXCR4 promotes arrestin-2 recruitment to CXCR4 on endosomes.

We also examined the distribution of endogenous CXCR4 and arrestin-2 in HeLa cells treated with CXCL12 for 30 min, again revealing that CXCR4 co-localizes with endogenous arrestin-2/3 on EEA1 positive early endosomes (Figure 3.2B).
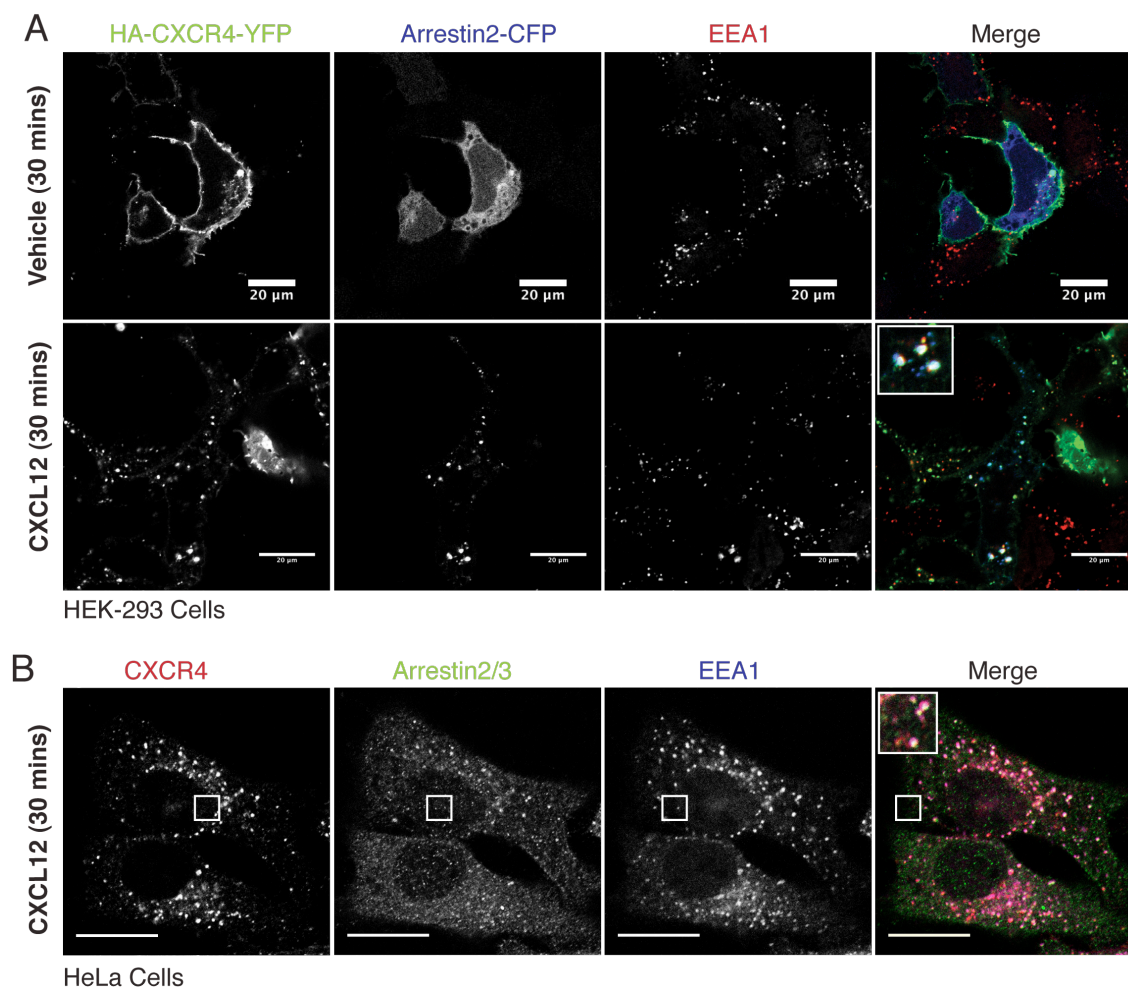
Figure 3.2: Arrestin-2 co-localizes with CXCR4 on EEA1 positive early endosomes. A. Serum starved HEK293 cells co-expressing HA-CXCR4-YFP and CFP-arrestin-2 were treated with 30nM CXCL12 or vehicle alone for 30 min. Cells were permeabilized, fixed and stained for EEA1 and analyzed by confocal microscopy. CXCR4 is shown in green, arrestin-2 is shown in blue and EEA1 is shown in red. White puncta in the merged image represent co-localization between CXCR4, EEA1 and arrestin-2. Some of the receptors only co-localizes with EEA1 (yellow). **B.** Serum-starved HeLa cells were treated with 30 nM CXCL12 for 30 min. Cells were fixed, permeabilized, and triple stained with anti-CXCR4 (red), anti-

arrestin-2/3 (green), and anti-EEA1 (blue) antibodies. White puncta in the merged images represent colocalization between all three proteins. Co-localization between CXCR4 and arrestin was quantified as described in *Materials and Methods* and was found to be 30.7%. Inset represents 4–8x the size of the boxed region. Shown are representative micrographs from three independent experiments. Bars, 20 μm.

Arrestin-2 interacts with ESCRT-0

Although we have shown previously that HRS and arrestin-2 mediate endosomal sorting of CXCR4 into the degradative pathway (Bhandari et al., 2007; Marchese et al., 2003), the molecular mechanism by which this occurs remains poorly understood. To gain mechanistic insight into this process we initially examined whether arrestin-2 interacts with the ESCRT-0 complex that contains HRS and STAM (STAM has two isoforms STAM-1 and 2). Lysate prepared from HEK293 cells expressing FLAG-tagged STAM-1, STAM-2 and HRS were incubated with bacterially purified GST-arrestin-2 and GST immobilized on glutathione-Sepharose 4A resin. As shown in Figure 3.3A, arrestin-2 bound to STAM-1 and HRS but only weakly to STAM-2. To rule out the possibility of an intermediate protein mediating the interaction with STAM-1, similar experiments were performed using purified arrestin-2. As shown in Figure 3.3B, GST-STAM-1, but not GST-STAM-2 and GST, bound to purified arrestin-2, indicating that the interaction between arrestin-2 and STAM-1 is direct and that arrestin-2 binds poorly to STAM-2. To determine whether arrestin-2 associates with ESCRT-0 in cells, HA-arrestin-2, HA-arrestin-3 and empty vector (pcDNA3) were transfected into HeLa cells followed by immunoprecipitation and immunoblotting to detect the presence of endogenous STAM-1 and HRS. Both STAM-1 and HRS were detected in the

immunoprecipitates from cells expressing HA-arrestin-2, suggesting that arrestin-2 associates with HRS and STAM-1 in cells (Figure 3.3C), whereas HRS, but not STAM-1, was detected in the HA-arrestin-3 immunoprecipitates. Similarly, endogenous arrestins also co-immunoprecipitated with endogenous STAM-1 and HRS in HeLa cells (Figure 3.3D). Together, these data show that the interaction between STAM-1 and non-visual arrestins is limited to arrestin-2 and that HRS interacts with both arrestin-2 and arrestin-3. In addition, our data suggest that arrestin-2 exists in complex with a subpopulation of ESCRT-0 that includes STAM-1 and HRS but not STAM-2.
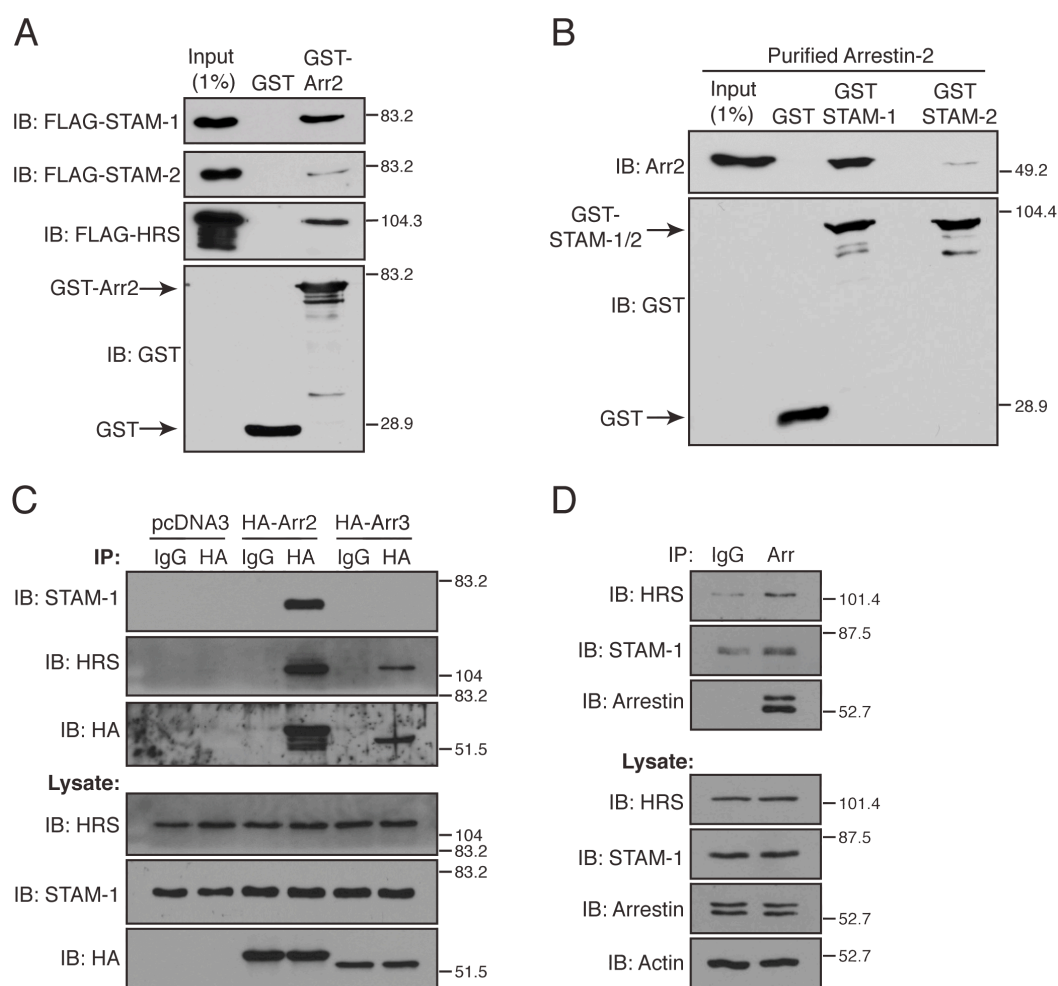
Figure 3.3. Arrestin-2 interacts with ESCRT-0 proteins STAM-1 and HRS. A. Equimolar amounts (134 nM) of GST-arrestin-2 and GST immobilized on glutathione-Sepharose resin were incubated with lysates from HEK293 cells transiently transfected with FLAG-STAM-1, FLAG-STAM-2, and FLAG-HRS. Bound proteins were detected by immunoblotting using the M2 anti-FLAG antibody. **B.** Equimolar amounts (117 nM) of GST-STAM-1, GST-STAM-2, and GST immobilized on glutathione-Sepharose resin were incubated with purified arrestin-2 (212 nM). Bound arrestin-2 was detected using an anti-arrestin-2 mouse monoclonal antibody (mAB). Blots were stripped and re-probed using an anti-GST antibody to determine the levels of the GST fusion proteins used in the binding assays. **C-D.** Lysates from HeLa cells either transiently transfected with HA-arrestin-2, HA-arrestin-3 and empty vector (pcDNA3) (C) or untransfected (D) were incubated with antibodies to immunoprecipitate transfected (C) or endogenous arrestins (D), as described in *Materials and Methods*. Immunoprecipitates (IP) and lysates were analyzed by SDS-PAGE and immunoblotting as indicated. Shown are representative blots from one of three (A–C) and four (D) independent experiment.

CXCR4 activation enhances the interaction between arrestin-2 and STAM-1

Next, we examined whether the interaction between STAM-1 and arrestin-2 was regulated by activation of CXCR4. HeLa cells, which endogenously express CXCR4 and STAM-1 were transfected with HA-arrestin-2. Cells were serum-starved and then treated with CXCL12 (30 nM) or vehicle (0.05% BSA-PBS) for 30 and 60 min followed by immunoprecipitation of tagged arrestin-2 and immunoblotting to detect bound endogenous STAM-1. As shown in Figure 3.4A, activation of CXCR4 enhanced the interaction between STAM-1 and arrestin-2 30-60 min after agonist treatment, suggesting that receptor activation may promote the interaction between STAM-1 and arrestin-2. Because STAM-1 and STAM-2 have been shown to be ubiquitinated

(McCullough *et al.*, 2004), we next assessed whether CXCR4 activation promotes ubiquitination of STAM-1 and STAM-2. HEK293 cells transfected with FLAG-tagged STAM-1 or STAM-2 and HA-tagged ubiquitin were treated with CXCL12 (100 nM) or vehicle (0.05% BSA-PBS) for 30 min followed by immunoprecipitation of tagged STAM proteins and immunoblotting to detect incorporation of tagged ubiquitin. As shown in Figure 3.4B, STAM-1 was ubiquitinated by agonist activation of CXCR4. Consistent with the previous data that STAM-2 does not interact with arrestin-2, we found out that receptor activation does not promote STAM-2 ubiquitination.
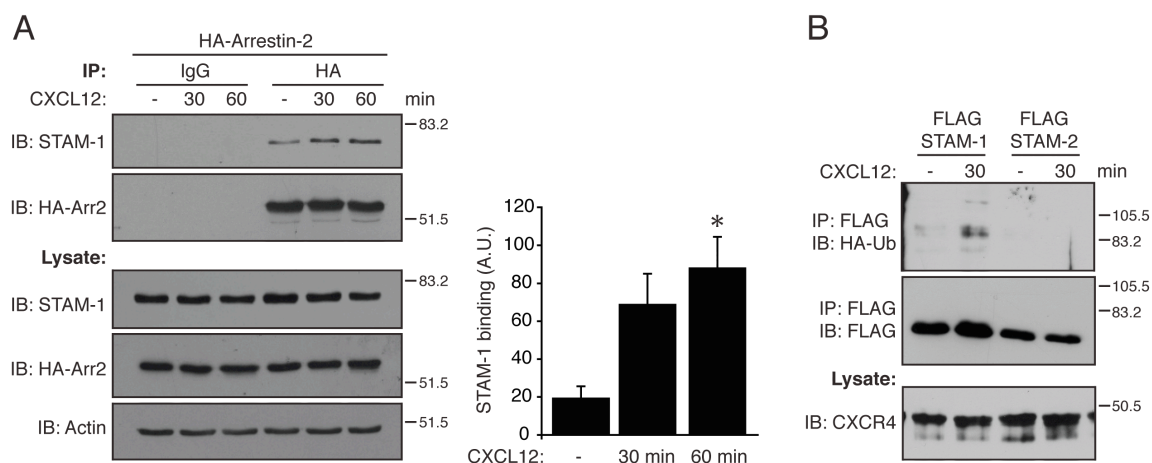
Figure 3.4. CXCR4 regulates the STAM-1/arrestin-2 interaction and STAM-1 ubiquitination. A. HeLa cells transiently transfected with HA-arrestin-2 were serum starved as described in *Materials and Methods*, followed by treatment with 30 nM CXCL12 for 30 and 60 min. Cell lysates were subject to immunoprecipitation using monoclonal anti-HA and isotype control antibodies. Immunoprecipitates and lysates were analyzed by SDS-PAGE and immunoblotting to detect endogenous STAM-1 and HA-arrestin-2. Immunoblots were subject to densitometric analysis, and the bar graph represents the average STAM-1 binding ± SEM normalized to the level of HA-arrestin-2 in the immunoprecipitates. STAM-1

binding to arrestin-2 was significantly increased upon agonist treatment as compared with vehicle. Data were analyzed by one-way ANOVA followed by a Bonferroni's post hoc test (*p < 0.05). **B. STAM-1 is ubiquitinated upon CXCR4 activation.** HEK293 cells co-transfected with HA-CXCR4, FLAG-STAM-1, and FLAG-STAM-2 and HA-ubiquitin were treated with 100 nM CXCL12 for 30 min. FLAG-STAM-1/2 were immunoprecipitated using an anti-FLAG rabbit polyclonal antibody (pAB), followed by 7.5% SDS-PAGE and immunoblotting to detect incorporated HA-ubiquitin. Blots were stripped and reprobed for FLAG-STAM-1/2 to assess loading. Cell lysates were analyzed for the presence of HA-CXCR4. Shown are representative blots from one of three independent experiments.

CXCR4 co-localizes with STAM-1 and arrestin-2 on early endosomes

To confirm that arrestin-2 and STAM-1 were found within the same intracellular compartment, we examined their distribution in cells by confocal immunofluorescence microscopy. As shown in Figure 3.5A, in HEK293 cells transfected with yellow fluorescent protein (YFP)-tagged CXCR4, CXCR4 was mainly localized to the plasma membrane in vehicle treated cells, whereas endogenous STAM-1 was mainly localized to punctate vesicles distributed throughout the cytoplasm, many of which also co-localized with EEA1, used here as a marker for early endosomes. In contrast, upon agonist treatment, CXCR4 distributed into an intracellular punctate pattern, indicating that it had internalized into vesicles and these vesicles also contained STAM-1 and EEA1 (Figure 3.5A, bottom). We also examined the distribution of endogenous CXCR4 in HeLa cells treated with CXCL12 for 30 min, revealing that CXCR4 co-localized with endogenous STAM-1 (Figure 3.5B) on EEA1-positive early endosomes. CXCR4 activation also promoted co-localization of arrestin-2/3 and YFP-tagged STAM-1 on

early endosomes in HeLa cells (Figure 3.5C). Together, our data indicate that upon

internalization CXCR4 appears on early endosomes with arrestin-2 and STAM-1.
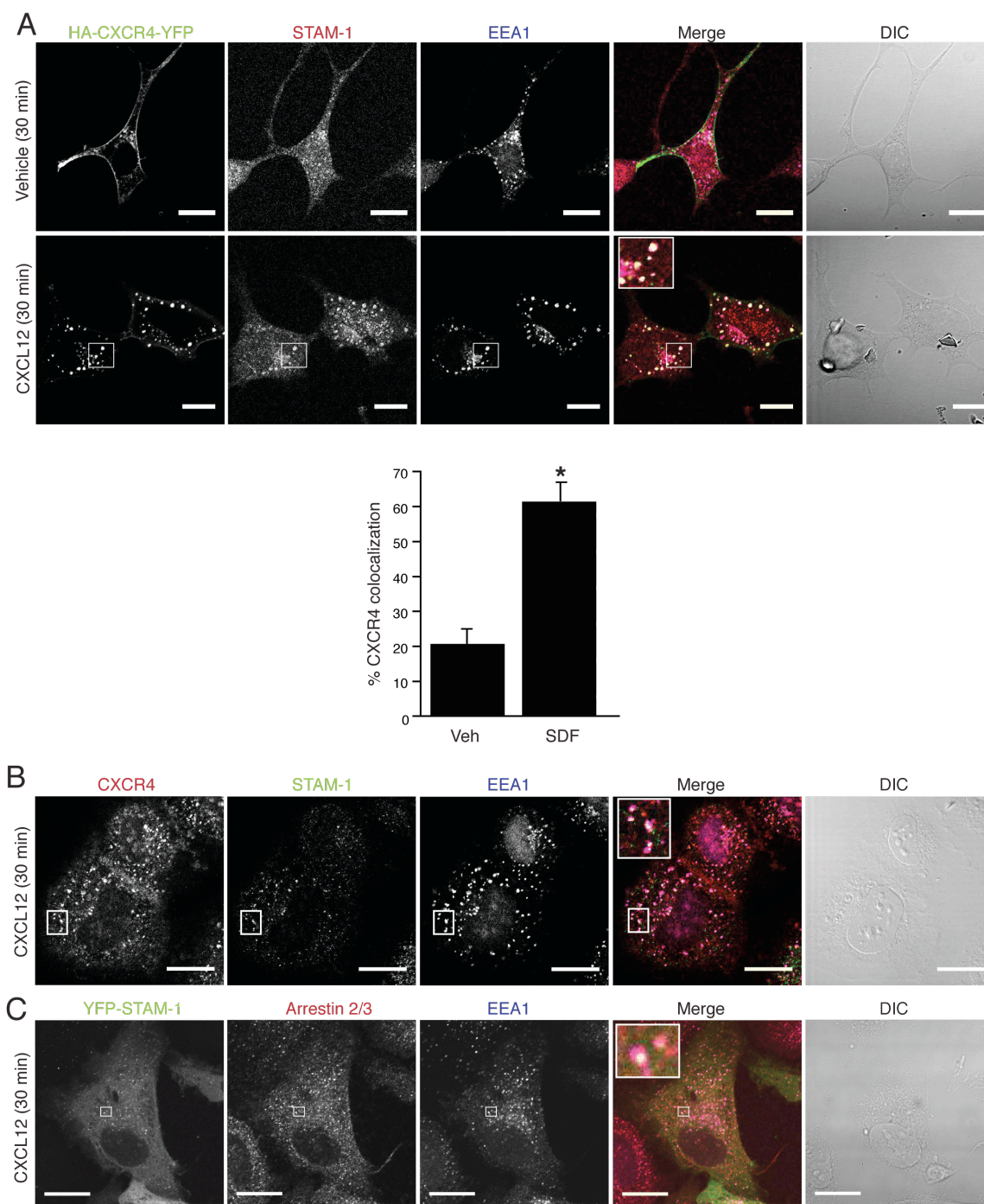
Figure 3.5. Arrestin-2, STAM-1 and CXCR4 co-localize on early endosomes. A. Serum-starved HEK293 cells expressing HA-CXCR4-YFP were treated with 30 nM CXCL12 or vehicle for 30 min. Cells were fixed, permeabilized and double stained with anti-STAM-1 pAb (red) and anti-EEA1 mAb (blue). White puncta in the merged images represents co-localization between all three proteins. The percentage of colocalization between CXCR4-YFP and STAM-1 was quantified as described in *Materials and Methods*. Bar graph represents the percent co-localization between CXCR4-YFP and STAM-1 in vehicle and SDF-treated cells ± SEM from 10 cells. Data were analyzed by Student's *t* test *p < 0.0001. (B–C) Serum-starved HeLa cells were treated with 30 nM CXCL12 or vehicle for 30 min. Cells were fixed, permeabilized, and triple stained with anti-STAM-1 rabbit pAB (green), anti-EEA1 mouse mAb (blue), and anti-CXCR4 (red) rat mAb (2B11) (B); and HeLa cells expressing YFP-STAM-1 were double stained with arrestin-2/3 rabbit pAB (red) and mouse mAb EEA1 (blue) **C.** White puncta in the merged images represent co-localization between all three proteins. Co-localization between CXCR4 and STAM-1 (B; 20%) and YFP-STAM-1 and arrestin-2 (D; 26%) were quantified as described in *Materials and Methods*. Inset represents 4–8x the size of the boxed region. Differential interference contrast (DIC) images are shown. Shown are representative micrographs from three independent experiments. Bars, 20 μm.

STAM-1 negatively regulates degradation of CXCR4

Since arrestin-2 interacts with STAM-1, and our data suggest that STAM-1 has a role in endosoma sorting of CXCR4, we examined agonist promoted degradation of CXCR4 in cells that were depeleted of STAM-1 by RNA interference. HEK293 cells stably expressing HA-CXCR4 were transfected with control and STAM-1 siRNA, followed by treatment with CXCL12 (30 nM) for 3 hr, and receptor degradation was assessed by immunoblot analysis, as described previously (Marchese et al., 2003). As shown in Figure 3.6A, siRNA-mediated depletion of STAM-1 lead to a statistically

significant increase in CXCR4 degradation (90±3.2%), compared with control siRNA-treated cells (68±5.9%), suggesting that STAM-1 negatively regulates agonist promoted degradation of CXCR4. As the amount of receptor that is degraded is in part a function of the rate of receptor internalization and recycling, we also examined the effect of depleting STAM-1 on CXCR4 internalization and recycling. Cell surface FLAG-tagged CXCR4 was labeled with the M1 anti-FLAG antibody on ice in the presence of 1 mM Ca^{2+}. The M1 antibody binds to the FLAG epitope in a calcium-dependent manner. Cells were washed to remove unbound antibody, and the media were replaced with DMEM containing CXCL12 (30 nM) in the continued presence of 1 mM Ca^{2+} and placed at 37°C for 45 min to allow for internalization of the M1 antibody/CXCR4 complexes. Antibody remaining on the surface, mostly representing un-internalized receptor, was removed by incubating cells with PBS containing EDTA (0.04%), a calcium-chelating agent. The amount of receptor-antibody complex that recycled back to the cell surface after 30 and 60 min was quantified by cell surface enzyme-linked immunosorbent assay (ELISA). In control siRNA treated cells, 20% of internalized CXCR4 recycled back to the cell surface after 30 and 60 min, similar to what we observed in STAM-1–depleted cells, suggesting that STAM-1 depletion had no effect on recycling of CXCR4 (Figure 3.6B). In addition, agonist-promoted internalization of CXCR4 was similar in STAM-1–depleted cells, compared with control siRNA-treated cells, suggesting that STAM-1 is not involved in CXCR4 internalization (Figure 3.6C). We also examined the role of AMSH on agonist promoted degradation of CXCR4. AMSH is a deubiquitinating enzyme that interacts with STAM-1 and negatively

regulates endosomal sorting of the EGFR (McCullough *et al.*, 2004). As shown in Figure 3.6D, siRNA-mediated depletion of AMSH did not effect agonist promoted degradation of CXCR4 in HeLa cells, suggesting that AMSH does not regulate endosomal sorting of activated CXCR4. However, CXCR4 levels were elevated in vehicle treated cells transfected with AMSH siRNA (Figure 3.6D), suggesting that AMSH may regulate degradation of constitutively internalized CXCR4, similar to what has been reported recently (Sierra *et al.*, 2010). Together, our data suggest that STAM-1 negatively regulates CXCR4 degradation likely through a mechanism that directly attenuates endosomal sorting.
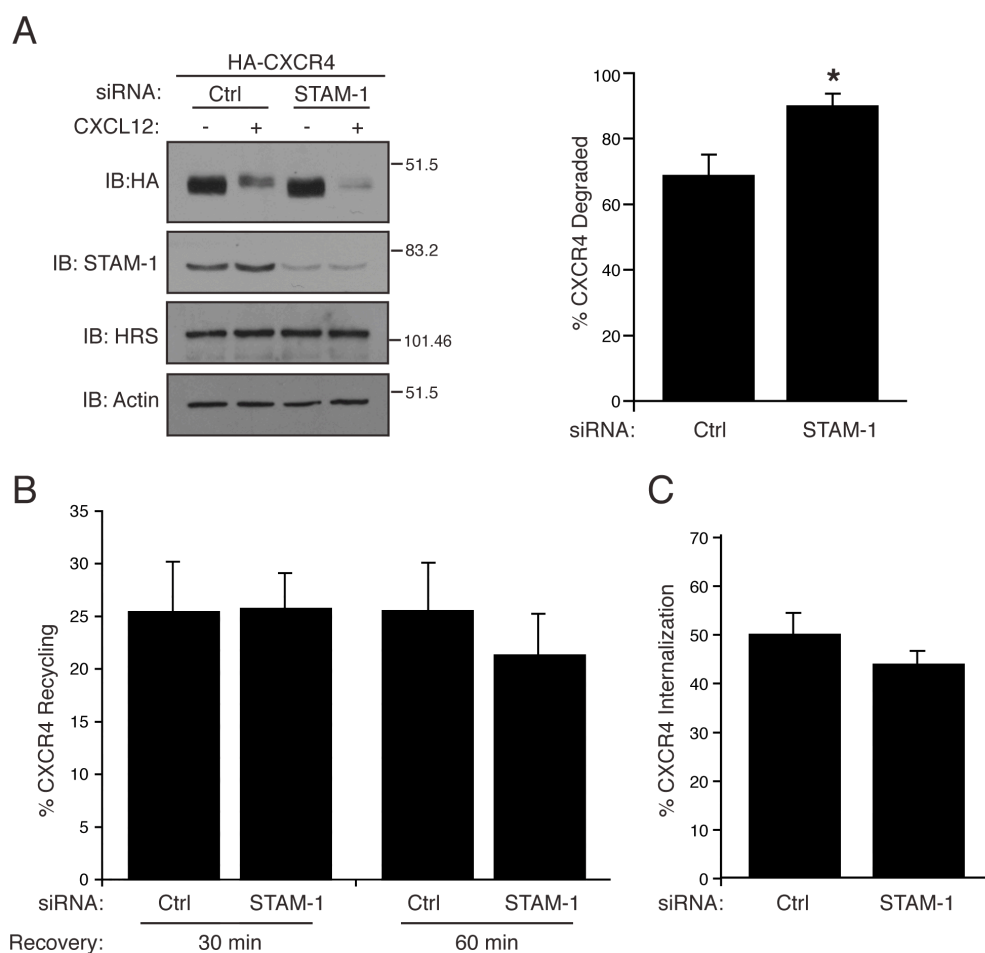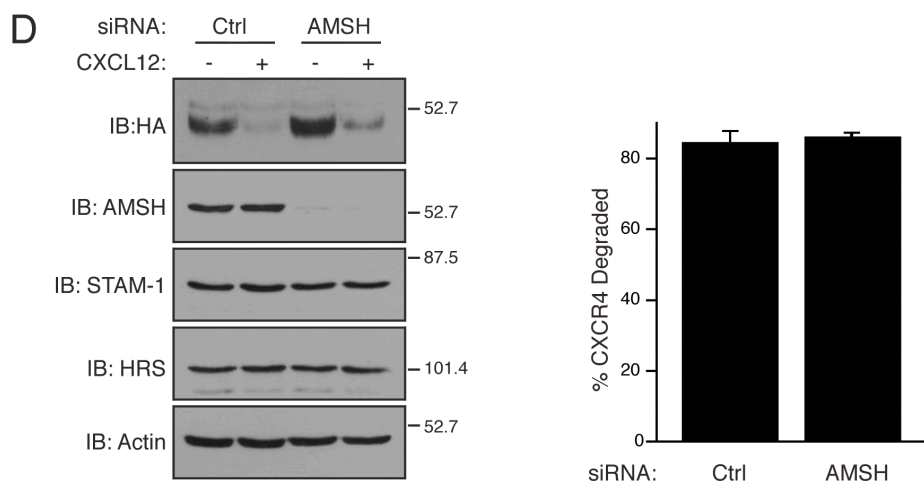
Figure 3.6. STAM-1 negatively regulates CXCR4 degradation. **A.** HEK293 cells stably expressing HA-CXCR4 were transfected with control (GAPDH) and STAM-1 siRNA as described in *Materials and Methods*. Cells were treated with vehicle (PBS containing 0.01% BSA) or 30 nM CXCL12 for 3 h and receptor levels were determined by immunoblotting followed by densitometric analysis. Bars represent the percentage amounts of CXCR4 degraded ± SEM from three independent experiments. *p < 0.05, unpaired *t* test. **B-C. Effect of STAM-1 knockdown on CXCR4 internalization and recycling**. CXCR4 recycling was measured in HEK293 cells transfected with FLAG-CXCR4 and siRNA as described in A. Surface receptors were labeled with the M1 anti-FLAG antibody followed by treatment with 30 nM CXCL12 for 45 min in DMEM containing 0.1% BSA, 20 mM HEPES, pH 7.4, and 1 mM Ca^{2+}. Antibody remaining on the cell surface was stripped by two rapid washes with Ca^{2+}/Mg^{2+} free PBS containing 0.04% EDTA. Cells were then incubated in DMEM containing 1 mM Ca^{2+} and 10 μM AMD3100 (CXCR4 antagonist) and incubated at 37°C for 30 and 60 min. The amount of antibody reappearing on the cell surface was quantified by ELISA, as described in *Materials and Methods*, and used as an indicator of receptor recycling. Bars represent the percentage of internalized receptor that recycled ± SEM from three independent experiments. **C.** Bars represent the percentage of cell surface receptors internalized in cells treated with CXCL12 compared with vehicle treated cells. The error bars represent SEM from three independent experiments. **D. Effect of AMSH knockdown on CXCR4 degradation**. HeLa cells were transfected with

GAPDH and AMSH siRNA and treated and analyzed as described in A. Bars represent the percentage amounts of CXCR4 degraded ± SEM from three independent experiments.

Mapping the arrestin-2 binding site on STAM-1

We recently reported that arrestin-2 positively regulates CXCR4 sorting into the degradative pathway. To gain insight into the function of the arrestin-2/STAM-1 interaction on CXCR4 trafficking, we initially set out to determine the mechanism of the interaction. To accomplish this we mapped the arrestin-2 binding region on STAM-1 by truncation mutagenesis. As shown in figure 3.7A, STAM contains multiple domains; an amino-terminal Vps27, HRS, STAM homology (VHS) domain, ubiquitin interaction motif (UIM), Src homology domain (SH3), immunoreceptor based tyrosine activation motif (ITAM), and a GGA and TOM1 homologous (GAT) domain that partially overlaps with the ITAM (Prag *et al.*, 2007; Ren *et al.*, 2009). We created several STAM-1 N-terminal and C-terminal truncation mutants, according to its domain organization, tagged with the FLAG epitope on the amino-terminal end (Figure 3.7). GST-arrestin-2 and GST immobilized on glutathione-Sepharose-4B resin were incubated with HeLa cell lysates expressing the various STAM-1 truncation mutants, and bound proteins were detected by immunoblotting. The results from these experiments are summarized in Figure 3.7A and the data are shown in Figure 3.7 B-F. The arrestin-2 binding region was determined to reside between amino acid residues 296-380 on STAM-1. This region has been shown to form two tandem coiled-coil (CC) domains (amino-acid residues 301–377) (Prag *et al.*, 2007; Ren *et al.*, 2009). To further confirm that the CC domain

mediates binding to arrestin-2, we made a STAM-1 mutant lacking the CC region using truncation mutagenesis. As shown in Figure 3.7G, GST-arrestin-2 was unable to pull-down FLAG-STAM-1-ΔCC from CCL. Consistent with this, we also show that purified GST-tagged STAM-1-CC domain was able to pull-down FLAG-arrestin-2 from CCL (Figure 3.7H). Taken together our data suggest that STAM-1-CC is both necessary and sufficient to bind to arrestin-2.

D FLAG-STAM-1

1-540 (FL) | 1-390 | 337-540

Input (1%) | GST | GST-Arr2 ...

IB: FLAG

83.2
50.4
36.8

GST Arr2 →
GST →
83.2
28.9

Ponceau-S

E FLAG-STAM-1

212-540 | 270-540

IB: FLAG — 50.4

GST Arr2 → 83.2
GST → 28.9

Ponceau-S

F FLAG-STAM-1

1-540 (FL) | ΔVHS (144-540)

IB: FLAG

83.2
83.2

GST Arr2
GST →
28.9

Ponceau-S

G FLAG-STAM-1

WT | ΔCC

IB:FLAG 83.2

GST-Arr2 → 83.2
GST → 28.9

Ponceau-S

H FLAG-Arr2

Input (0.5%) | GST | GST-S-1 | GST CC

IB: FLAG — 50.4

GST-STAM-1 →
104.4
94.6
51.5

GST-STAM-1-CC → 36.8

GST → 28.9

Ponceau-S

Figure 3.7: The STAM-1 coiled-coil domain is both necessary and sufficient for arrestin-2 binding. A. STAM-1 truncation mutants are represented schematically. Binding or no binding to GST-arrestin-2 is represented by + and – symbols, respectively, on the right as assessed by data shown in Figures 3.7 B-H. **B-G**. Binding reactions were performed by incubating equimolar amounts (600 nM) of GST-arrestin-2 and GST immobilized on glutathione-Sepharose resin with lysates from HEK293 cells transiently transfected with various STAM-1 constructs **H.** Equimolar amounts (117 nM) of (GST-STAM-1,) GST-STAM-1-GAT and GST were incubated with lysates from HEK293 cells transiently transfected with FLAG-tagged arrestin-2. In B-H, bound proteins were detected by immunoblotting using the anti-FLAG M2 mAb, followed by staining with Ponceau-S (C-H) or immunoblotting for GST (B) to assess the amount of GST fusion proteins used in the binding assays. Shown are representative blots from one of three independent experiments.

STAM-1/arrestin-2 interaction negatively regulates CXCR4 degradation

To determine whether the interaction between STAM-1 and arrestin-2 is important for CXCR4 trafficking, we initially expressed the STAM-1-CC domain as a minigene in cells and assessed whether it disrupted the STAM-1/arrestin-2 interaction. HeLa cells transfected with FLAG-S1-CC and HA-arrestin-2 were subjected to immunoprecipitation using an anti-HA mAb followed by immunoblotting to detect the presence of endogenous STAM-1 in the immunoprecipitates. As shown in Figure 3.8A, expression of the CC domain disrupted the STAM-1/arrestin-2 interaction. To determine the function of the STAM-1/arrestin-2 interaction on lysosomal targeting of CXCR4, we examined the effect of expressing the CC domain on CXCR4 degradation. Remarkably, expression of the CC domain significantly accelerated CXCR4 degradation after agonist treatment as compared with empty vector (Figure 3.8 B and C). Together,

these data suggest that the STAM-1/arrestin-2 interaction negatively regulates CXCR4 sorting to lysosomes.
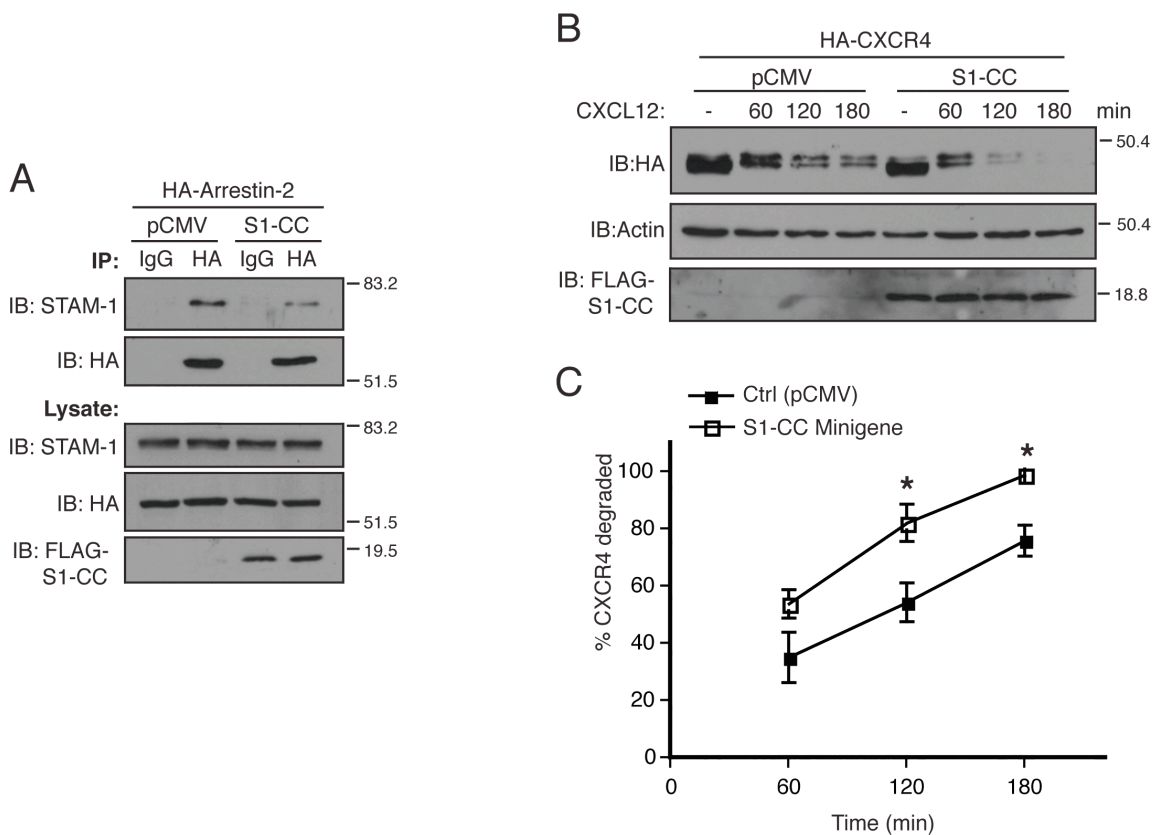
Figure 3.8. Expression of the STAM-1 coiled-coil domain disrupts the STAM-1/arrestin-2 interaction and accelerates CXCR4 degradation. A. Lysates from HeLa cells co-transfected with HA-arrestin-2 and FLAG-STAM-1-CC (S1-CC) or empty vector (pCMV) were incubated with anti-HA mAb and isotype control antibody. Immunoprecipitates were analyzed by immunoblotting to detect bound endogenous STAM-1, and lysates were analyzed to assess expression of the various constructs. Shown are representative blots from one of three independent experiments. **B.** HA-CXCR4 degradation was assessed in HEK293 cells stably expressing HA-CXCR4 and transiently expressing FLAG-STAM-1-CC or empty vector

(pCMV) as described in *Materials and Methods*. **C.** Graphical representation of average percentage of receptor degraded three independent experiments. Data were analyzed by two-way ANOVA and followed by a Bonferroni's post hoc test. (*$p < 0.0001$). Shown are representative blots from one of three independent experiments.

Mapping the STAM-1 binding site on arrestin-2

To gain greater insight into this process of STAM1-arrestin-2 mediated CXCR4 sorting, we next set out to identify the STAM-1 binding region on arrestin-2 by truncation mutagenesis. Schematic representations of the arrestin-2 truncation mutants used are shown in Figure 3.9A; most have been described previously (Bhandari et al., 2009). GST-STAM-1 and GST were incubated with lysates prepared from HEK293 cells expressing various HA-tagged arrestin-2 truncation mutants. The results from these binding experiments are summarized in Figure 3.9A, and the data is shown in Figure 3.9 B and C. Both the N- and C-terminal regions of arrestin-2 bound to GST-STAM1, but not GST, although binding to the N-terminal region seemed to be stronger, suggesting that it represented the main binding region. Further deletion of this region revealed that the STAM-1 binding site on arrestin-2 is between amino acid residues 1–161 (Figure 3.9C). We next determined whether expression of this region as a minigene in cells also disrupted the STAM-1/arrestin-2 interaction. However, when expressed in cells the arrestin-2-(1-161) minigene completely blocked CXCR4 degradation (Figure 3.9D). The N-terminal lysine residues within arrestin-2 are predicted to serve as phosphosensors and recognize phosphates attached to receptors (Kern et al., 2009), analogous to what has been observed for arrestin-1 (Vishnivetskiy et al., 2000); therefore, the arrestin-2-(1-161)

construct may bind to CXCR4 and have a dominant-negative effect on CXCR4 internalization. To rule out any effects at the level of internalization, the first 24 amino acids from the N terminus of arrestin-2 were deleted to create arrestin-2-(25-161), and we initially tested the ability of this mutant to bind to STAM-1. As shown in Figure 3.9E, GST fused to arrestin-2-(25-161), but not GST alone, efficiently bound to FLAG-STAM-1 expressed in cells. A FLAG-tagged construct of arrestin-2-(25-161) when expressed in HEK293 cells also bound to GST-STAM-1-CC, suggesting that the STAM-1/CC domain binding site on arrestin-2 is located between amino acid residues 25-161 (Figure 3.9F).

		Binding to STAM-1
HA————————————————418	Arr-2 (1-418)	+
HA——————————260	Arr-2 (1-260)	+++
HA————418	Arr-2 (261-418)	+
HA—————240	Arr-2 (1-240)	++
HA————179	Arr-2 (1-179)	++
HA————161	Arr-2 (1-161)	++
FLAG²⁵————161	Arr-2 (25-161)	++
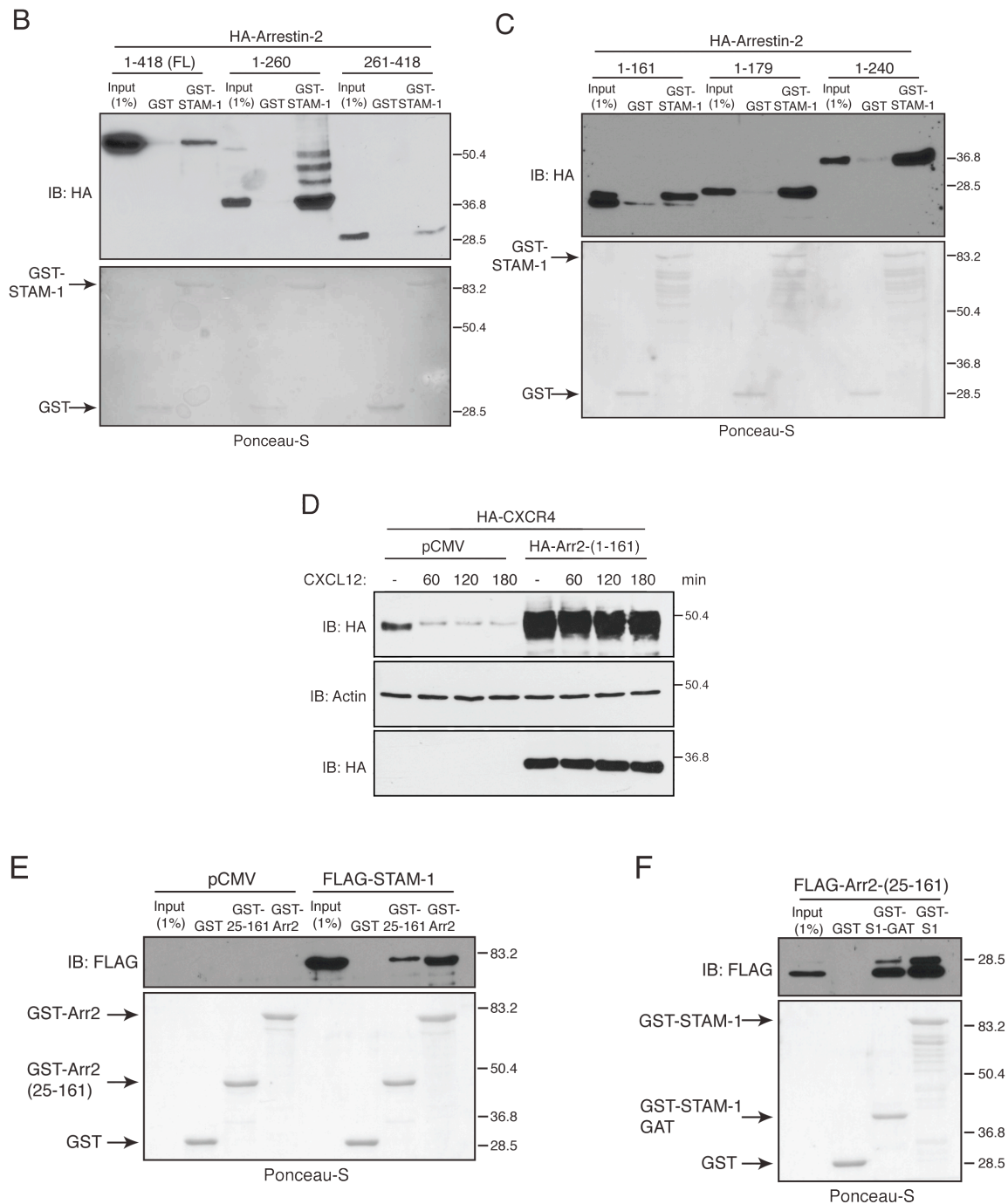
Figure 3.9. Mapping of the STAM-1 binding domain on arrestin-2. A. Arrestin-2 truncation mutants used in the binding studies are represented schematically. Binding between GST-STAM-1 and HA-tagged arrestin-2 truncation mutants is shown as weak (+), intermediate (++), and strong (+++) on the right. **B-C.** Equimolar amounts (117 nM) of GST-STAM-1 and GST immobilized on glutathione-

Sepharose resin were incubated with lysates from HEK293 cells transiently transfected with HA-arrestin-2 constructs shown in A. Bound proteins were detected by immunoblotting using the anti-HA mAb followed by staining with Ponceau-S to assess the amount of GST fusion proteins used in the binding assay. **D.** CXCR4 degradation was assessed in HEK293 cells stable expressing HA-CXCR4 and transiently transfected with FLAG-Arr2-(1-161) and empty vector (pCMV) as described in *Materials and Methods.* **E.** Equimolar amounts (234 nM) of GST-arrestin-2, GST-Arr2-(25-161), and GST were incubated with lysates from HEK293 cells transiently transfected with FLAG-STAM-1 and empty vector (pCMV-10). **F.** Equimolar amounts (276 nM) of GST-STAM-1, GST-STAM-1-CC, and GST alone were incubated with lysates from HEK293 cells transiently transfected with FLAG-Arr-2-(25-161). In E and F, bound proteins were detected by immunoblotting using an M2 anti-FLAG mAb conjugated to HRP and blots were stained with Ponceau-S to assess the amount of GST-tagged protein used in the binding assay. Shown are representative blots from one of three independent experiments.

Disrupting STAM-1/arrestin-2 interaction negatively regulates CXCR4 degradation

We next examined whether expression of arrestin-2-(25-161) disrupted the STAM-1/arrestin-2 interaction and modulated CXCR4 degradation. As shown in Figure 3.10A, expression of FLAG-arrestin-2-(25-161) in increasing concentration markedly disrupted the interaction between arrestin-2 and STAM-1. Overexpression of FLAG-arrestin-2-(25-161) in HeLa cells significantly accelerated agonist promoted degradation of CXCR4 (Figure 3.10 B and C), similar to what was observed with the overexpression of STAM-1-CC domain. Together these data further indicate that the interaction between STAM-1 and arrestin-2 attenuates CXCR4 trafficking into the degradative pathway. This interaction may be specific to modulating CXCR4 and/or GPCR sorting, as EGFR degradation was not altered by expression of the STAM-1-CC domain and

arrestin-2-(25-161) (Figure 3.10D).
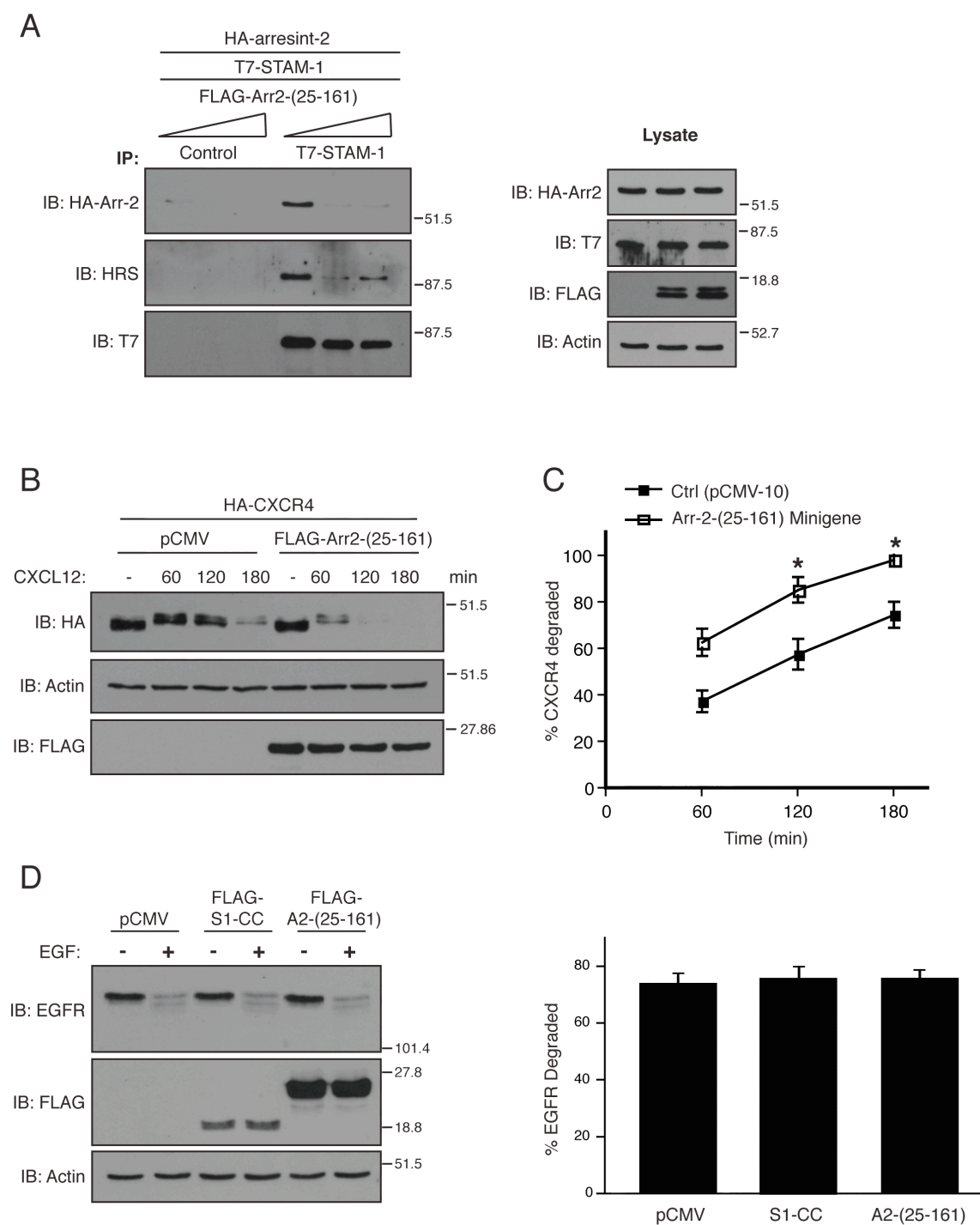
Figure 3.10. Expression of arrestin-2-(25-161) disrupts the STAM-1/arrestin-2 interaction and

accelerates CXCR4 degradation. A. Lysates were prepared from HeLa cells co-transfected with T7-STAM-1, HA-arrestin-2 and increasing amounts (0, 1, and 2.5 μg) of FLAG-Arr2 (25-161). Lysates were divided into equal aliquots and incubated with either an anti-T7 pAb or protein-G agarose alone (control). Immunoprecipitates were analyzed by immunoblotting to detect bound HA-arrestin-2 and endogenous HRS and lysates were analyzed to assess the expression of the various constructs. Blots were stripped and reporbed with anti-T7 mAb to detect immunoprecipitated STAM-1. Shown are representative blots from one of three independent experiments. **B.** CXCR4 degradation was assessed in HEK293 cells stable expressing HA-CXCR4 and transiently transfected with FLAG-Arr2-(25-161) or empty vector (pCMV) as described in *Materials and Methods*. **C.** Graphical representation of average percent receptor degraded. Error bars represent SEM from three independent experiments. Data were analyzed by two-way ANOVA and followed by a Bonferroni's post hoc test. (*$p < 0.0001$). **D.** EGFR degradation was assessed in HeLa cells transfected with FLAG-STAM-1-CC, FLAG-Arr-2-(25-161) or pCMV. Cells were treated with 100 ng/ml EFG for 1 hr followed by immunobloting as described in *Materials and Methods*. Bar graph represents the average percent amount of EGFR degraded in EGFR treated cells as compared to vehicle treated cells ± S.E.M. from three independent experiments. Data were analyzed by one-way analysis of variance and were found not to be significantly different. Shown are representative immunoblots from one of three independent experiments

Role of the STAM-1/arrestin-2 interaction on the ubiquitination status of CXCR4, STAM-1 and HRS

STAM, through its interaction with several deubiquitinating enzymes, may regulate the ubiquitination status of both cargo and of itself (McCullough et al., 2006; Row et al., 2006). Therefore, one possibility is that the STAM-1/arrestin-2 interaction regulates the ubiquitination status of CXCR4 and STAM-1, thereby modulating CXCR4 trafficking into the degradative pathway. To examine this possibility we examined the

effect of expressing the STAM-1-CC domain on the ubiquitination status of both CXCR4 and STAM-1. Surprisingly, expression of the CC, compared with empty vector, did not significantly change the ubiquitination status of CXCR4 (Figure 3.11A) and STAM-1 (Figure 3.11B), suggesting that the STAM-1/arrestin-2 interaction does not regulate their ubiquitination status. In sharp contrast, expression of the CC domain blocked CXCR4 mediated ubiquitination of HRS (Figure 3.11C). Therefore, together our data show that the STAM-1/arrestin-2 interaction is critical for modulating ubiquitination of HRS, which is likely to be important for regulating sorting of CXCR4 into the degradative pathway.
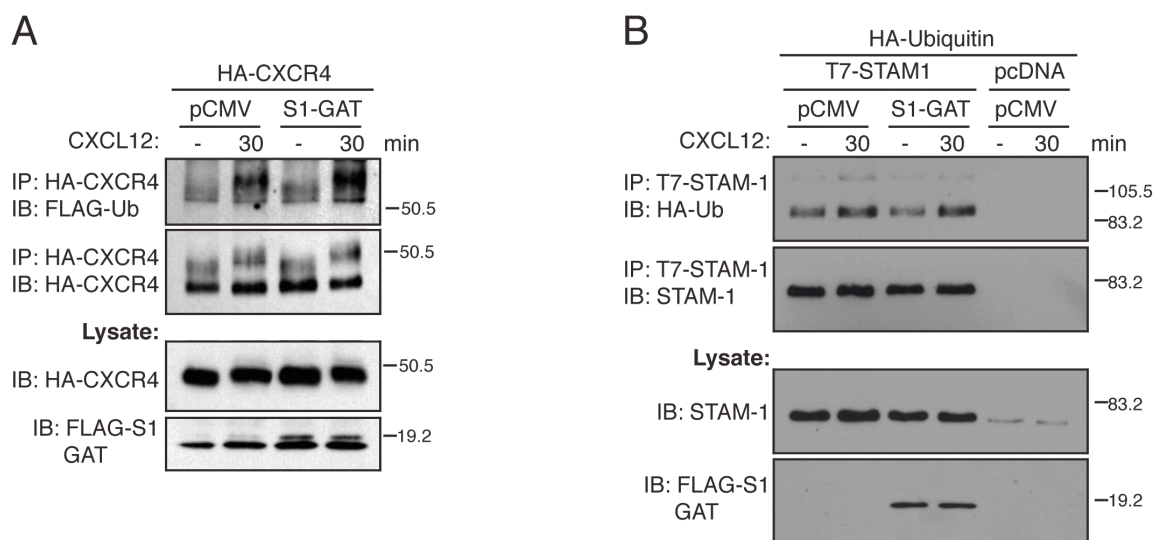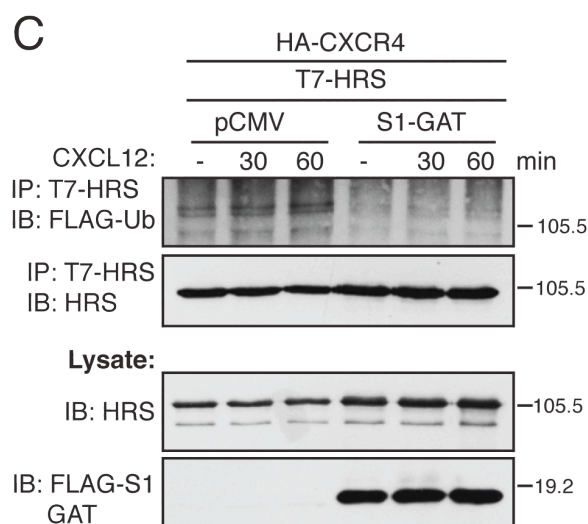
Figure 3.11. Disrupting the STAM-1/arrestin-2 interaction inhibits HRS ubiquitination but does not effect CXCR4 and STAM-1 ubiquitination. A. HEK293 cells stably expressing HA-CXCR4 were transfected with FLAG-ubiquitin and STAM-1-GAT domain or pCMV. **B.** HeLa cells were transfected with HA-ubiquitin, T7-STAM-1, and STAM-1-GAT or pCMV. **C.** Cells were transfected as in A, except T7-HRS was also transfected. Cells were serum starved and treated with 30 nM CXCL12 for 30–60 min, followed by immunoprecipitation and immunoblotting to detect incorporated ubiquitin as described in *Materials and Methods*. Shown are representative blots from six (A) and three (B and C) independent experiments.

Role of STAM-1, arrestins and AIP4 in CXCR4 mediated migration of HeLa cells

Because STAM-1, arrestin-2 and AIP4 can modulate the levels of CXCR4 in cells, we next looked at the effect of STAM-1, arrestin-2 and AIP4 knockdown on migration of HeLa cells in response to CXCL12 as a chemoattractant. HeLa cells were co-transfected with siRNA against STAM-1, arrestin-2/3, AIP4 or control siRNA (GAPDH) and pEYFP empty vector. Cells were serum starved and seeded onto FluroBlok inserts coated with collagen at the bottom surface as described in *Materials and*

Method section. Inserts were placed in wells containing 30nM CXCL12 and incubated

for 12 hours. Number of cells that migrated to the bottom of the well were fixed with

PFA and counted under a fluorescent microscope. As shown in Figure 3.12A-B,

knockdown of STAM-1 and arrestin-2/3 significantly inhibited the number of cells that

migrated towards the ligand, however, AIP4 knock down had no effect on HeLa cells

migration.
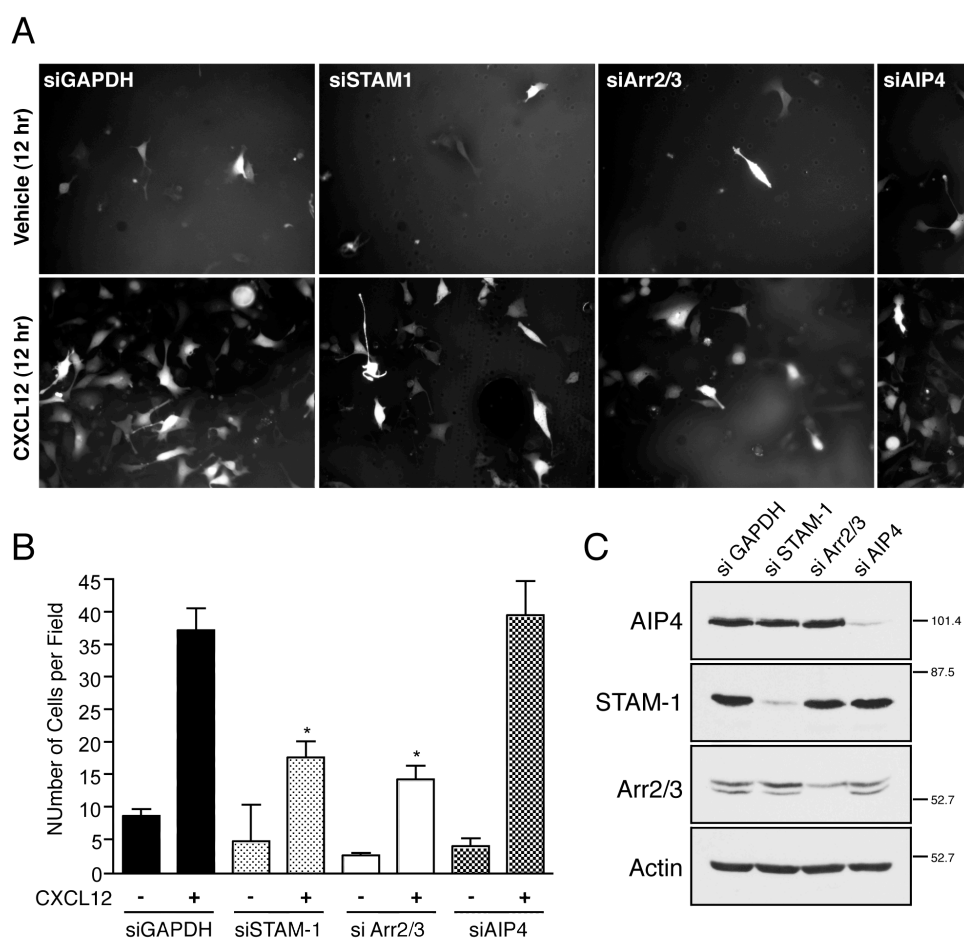
Figure 3.12: Role of STAM-1, arrestins and AIP4 in CXCR4 mediated migration of HeLa cells. A. One

hundred thousand HeLa cells co-transfected with siRNA against STAM-1, AIP4, arrestin-2/3 or

GAPDH and pEYFP-C1 were serum starved and seeded onto FluroBlok transwell inserts pre-coated with collagen. Inserts were placed in wells containing 500μl DMEM containing 30nM CXCL12 or vehicle (0.1% BSA) and incubated at 37°C for 12 hr. Cells from top of the membrane were scrapped and the inserts were fixed with PFA and mounted onto glass slides using permount mounting media. Number of cells that migrated to the bottom of the inserts were counted by observing the slides under fluorescent microscope. Shown are representative micrographs taken from three independent experiments **B.** Cells from 5 fields each from three independent experiments were counted and plotted as mean number of cells per 20× field. Data was analyzed by two-way ANOVA followed by bonferroni's post-hoc test. (*P<0.001). Error bar represents SD. **C.** Equal number of cells used in the migration experiment were subject to immunoblot analysis to analyze the level of STAM1, arr-2/3 and AIP4 knockdown. Actin was used as a loading control. Shown are representative immunoblots from three independent experiments.

Effect of STAM-1, AIP4 and arrestin-2/3 knockdown on surface expression of CXCR4

Migration of cells can be a directly correlated with the amount of receptor present on the cell surface. Since STAM-1, arrestin-2 as well as AIP4 can regulate CXCR4 levels in cells, effect on cell migration can be indirectly due to effect on cell surface CXCR4 expression. In order to determine whether STAM-1, AIP4 and arrestin-2 knockdown regulate CXCR4 surface expression, we analyzed CXCR4 surface expression following protein knockdown suing FACS analysis. HeLa cells were mock transfected or transfected with siRNA against GAPDH, STAM-1, AIP4 and arrestin-2/3 and cell surface expression of CXCR4 was determined by surface labeling of CXCR4 followed by FACS analysis. As shown in Figure 3.13 A and B, no significant difference in the surface expression of CXCR4 was observed in mock transfected as compared with GAPDH, STAM-1 and arrestin-2/3 transfected cells. However, cells depleted for AIP4 showed a

significant increase in CXCR4 surface levels. This is consistent with previous published

data from the lab, which suggests that AIP4 is required for ubiquitination and subsequent

degradation of CXCR4. siRNA mediated knockdown of AIP4 would block CXCR4

degradation as a results would increases the total pool of CXCR4 in the cells.
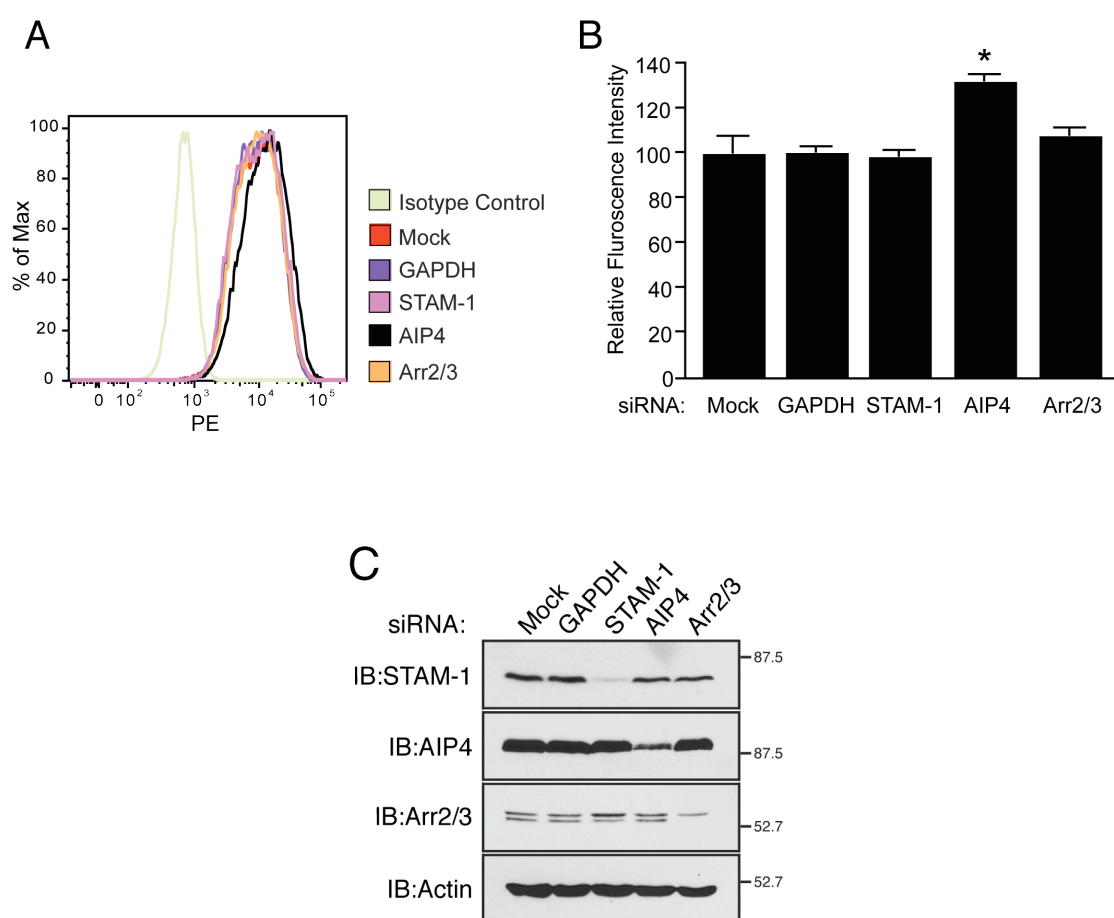
Figure 3.13: Effect of STAM-1, AIP4 and arrestin-2/3 knockdown on surface expression of CXCR4. A.
HeLa cells mock transfected or transfected with siRNA against STAM-1, AIP4, arrestin-2/3 and control

siRNA (GAPDH) were fixed and stained with anti-PE conjugated anti-CXCR4 antibody or isotype control antibody (IgG2aκ). FACS was used to quantify the amount of antibody bound receptor present on the cell surface. **B.** Geometrical mean of the PE florescent intensity relative to mock-transfected cells from three independent experiments was plotted and the data were analyzed by one-way ANOVA followed by Bonferroni's post hoc test (*=p<0.05). Error bar represents ±S.E.M. from three independent experiments performed. **C.** Amount of protein knockdown was determined by SDS-PAGE followed by immunoblotting to detect STAM-1, AIP4, and arresitn-2/3. Actin was used as a loading control.

ROLE OF STAM AND AIP4 IN CXCR4-INDUCED PHOSPHORYLATION OF ERK-1/2

Our data show that arrestin-2 is present on endosomes where it regulates the endosomal sorting of CXCR4 into the degradative pathway through interactions with AIP4 and STAM-1. Arrestins have been shown to scaffold several signaling molecules including Akt and the components of the mitogen-activated protein kinase (MAPK) cascade, such as Raf, MEK1 and ERK-1/2 (Beaulieu et al., 2005; Luttrell et al., 2001). Both arrestin-2 and arrestin-3 have been linked to CXCR4-induced ERK-1/2 activation (Busillo et al., 2010; Sun et al., 2002), but whether STAM-1 and/or AIP4 are also involved in signaling via ERK-1/2 pathway remains unknown.

STAM and AIP4 are required for CXCR4-induced activation of ERK-1/2

In order to investigate the role of arrestins, STAM-1 and AIP4 in CXCR4 mediated signaling via MAPK cascade we utilized the approach of RNA interference in

HeLa and HEK-293 cells. Cells were transfected with siRNA targeting STAM-1, AIP4, arrestin-2/3 or control (GAPDH) siRNA. Cells were serum starved and treated with 10 nM CXCL12 (2, 5, 10 and 15 min) and phosphorylated ERK (pERK-1/2) levels were determined by immunoblotting. As shown in Figure 3.14A, CXCL12 induced a similar rapid and transient increase in pERK-1/2 levels in both the control GAPDH and arrestin-2/3 siRNA treated HeLa cells which is identical to what is observed in either mock or untransfected HeLa cells (Figure 3.14C). However, the levels of pERK-1/2 were significantly increased in the arrestin-2/3 depleted cells. This enhanced signaling is consistent with a defect in signal termination and is consistent for a role of arrestins in CXCR4 desensitization (Busillo and Benovic, 2007). We also observed that CXCR4-induced ERK-1/2 activation was enhanced in mouse embryonic fibroblast (MEF) cells isolated from double arrestin-2/3 knockout animals as compared to MEFs isolated from matched WT animals (Figure 3.14B).

We next examined the roles of STAM-1 and AIP4 in CXCR4-induced ERK-1/2 activation. In contrast to arrestin-2/3 knockdown, depletion of STAM-1 using siRNA in HeLa cells significantly attenuated CXCR4 induced pERK-1/2, as compared to GAPDH siRNA transfected cells (Figure 3.14D). We also investigated the role of STAM-2 in CXCR4 promoted ERK-1/2 phosphorylation. HEK293 cells were transfected with siRNA against STAM-1, STAM-2, STAM1+2 and GAPDH and treated with 10 nM CXCL12 or vehicle for 2, 5, 10 min. As shown in Figure 3.14E, consistent with HeLa cells data, STAM-1 knockdown significantly attenuated ERK-1/2 phosphorylation. Double STAM-1/2 knockdown further inhibited ERK-1/2

phosphorylation. However, STAM-2 knockdown had no significant effect on ERK-1/2 phosphorylation, suggesting that STAM-1 plays a prominent role in CXCR4 mediated MAPK signaling. Similar to STAM-1, AIP4 depletion in HeLa cells using siRNA also significantly attenuated CXCR4-induced pERK-1/2 (Figure 3.14F). We next examined if this role of AIP4 was exclusive to CXCR4 signaling. HeLa cells were transfected with siRNA against AIP4 or control siRNA (GAPDH) and treated with carbachol, a non-selective muscarinic receptor agonist, and epidermal growth factor (EGF), an agonist for tyrosine kinase receptor EGFR. As shown in Figure 3.14G, carbachol induced pERK-1/2 levels were also attenuated in AIP4 depleted cells. However, epidermal growth factor promoted ERK-1/2 phosphorylation was unaffected upon AIP4 depletion (Figure 3.14H), suggesting that AIP4 may have a general role in GPCR signaling. Expression of STAM-1-CC as well as arrestin-2-(25-161), that disrupts STAM-1/arrestin-2 also had no effect on ERK-1/2 phosphorylation (Figure 3.14 I and J). Taken together, our data suggest that STAM-1 and AIP4, but not arrestin-2/3, are downstream of CXCR4 in the pathway that leads to agonist activation of the ERK-1/2 signaling cascade.

E

F

G

H

I

CXCL12 (min): pCMV FLAG-S1(296-380)

J

CXCL12 (min): pCMV FLAG-Arr2(25-161)
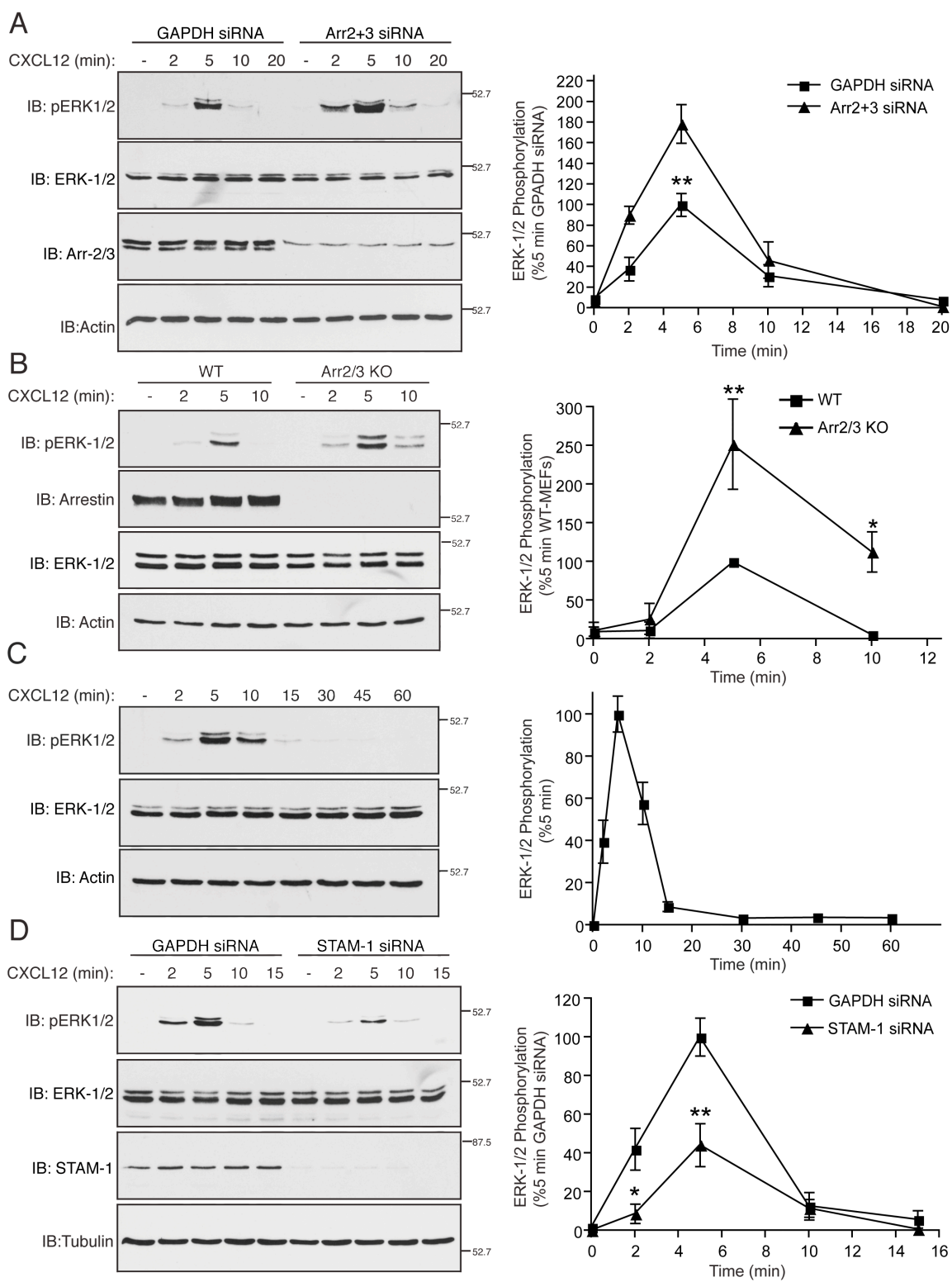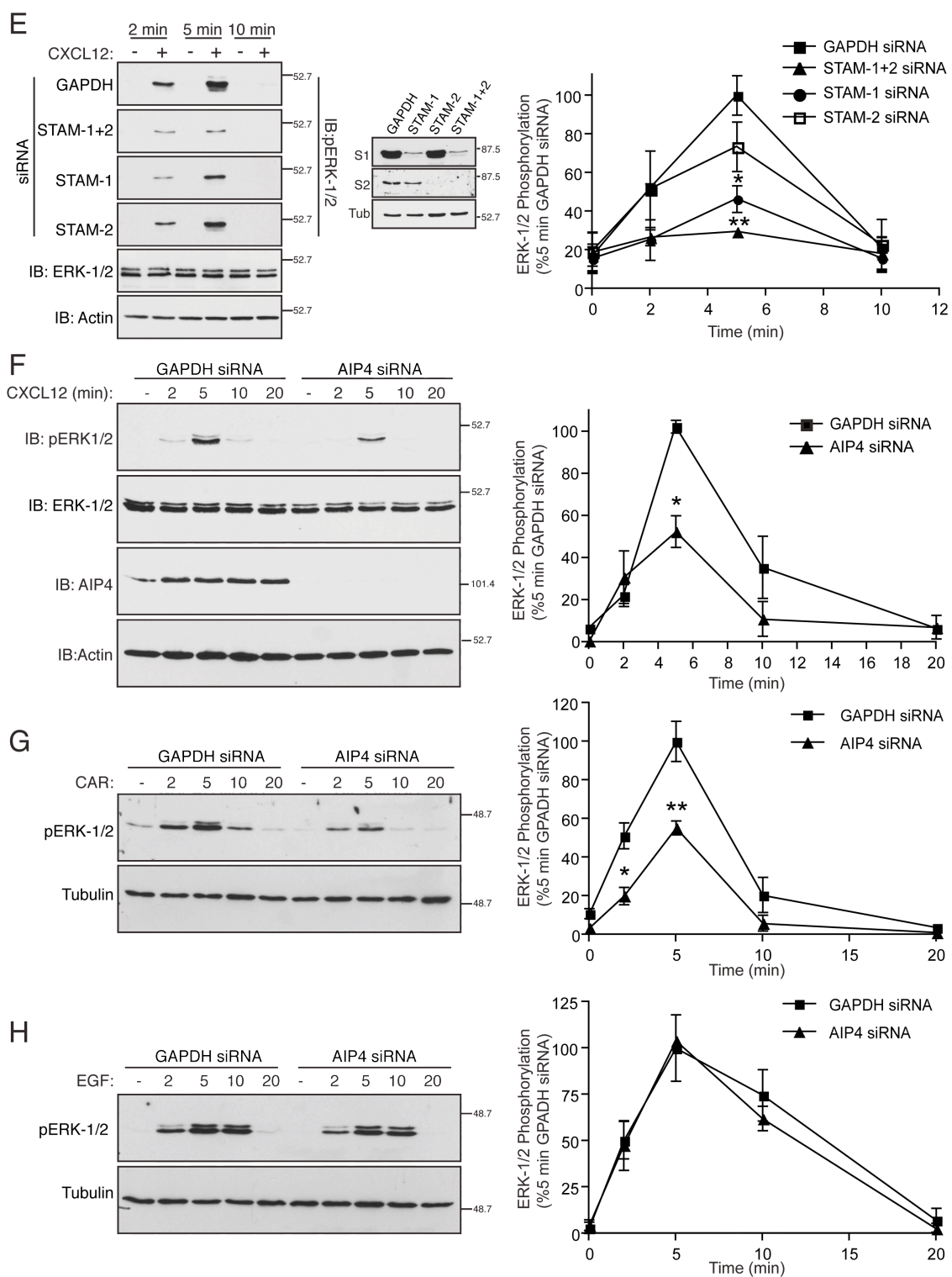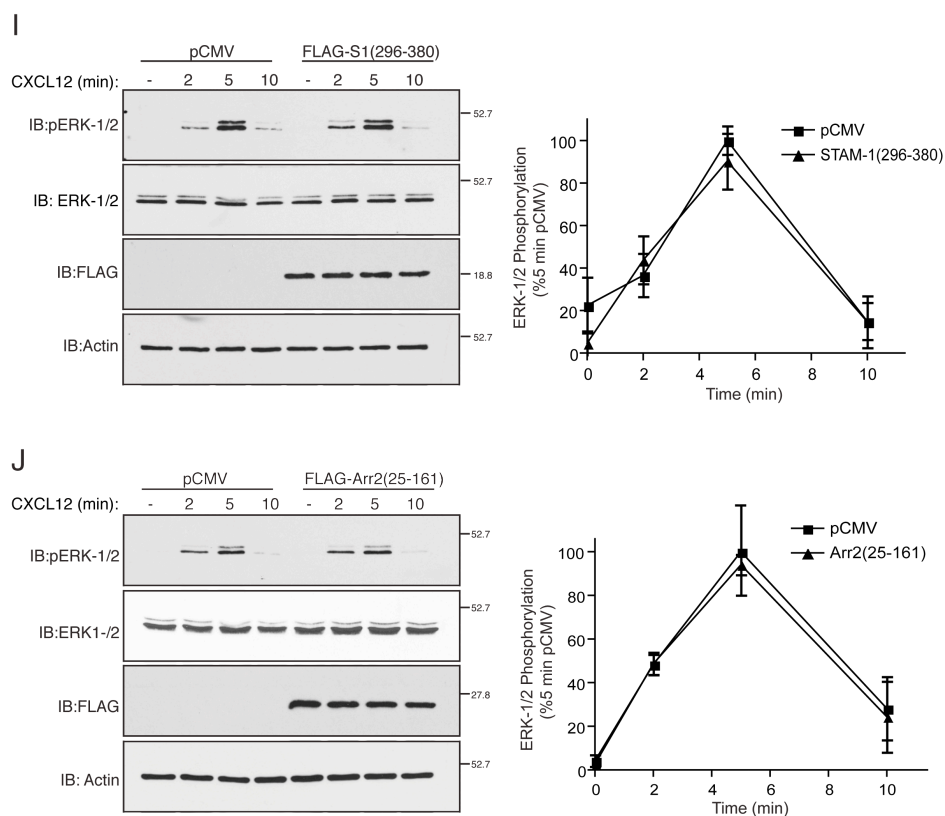
Figure 3.14. STAM-1 and AIP4 but not arrestin-2/3 are required for CXCR4-induced ERK-1/2 phosphorylation. A. HeLa cells transfected with siRNA against arrestin-2/3 or control siRNA (GAPDH) were serum starved and treated with 10 nM CXCL12 for 2, 5, 10, 20 min. ERK-1/2 phosphorylation was determined by SDS-PAGE followed by immunoblot (IB) analysis. Bolts were stripped and reprobed for total ERK and actin to assess loading. Phosphorylated ERK-1/2 levels were determined by densitometric analysis and normalized to total ERK-1/2 levels. Bars represent the percent ERK-1/2 phosphorylation compared to maximal pERK-1/2 levels (5 min) in GAPDH transfected cells. Data were analyzed by two-way ANOVA followed by Bonferroni's post hoc test (*=$p<0.05$, **=$p<0.01$). Error bars represent the standard error of the mean. Shown are representative blots from one of four independent experiments **B.** WT and arrestin2/3 knockout MEFs were serum starved and treated with 10 nM CXCL12 for the indicated time and ERK-1/2 phosphorylation was determined as described in A. **C.** CXCR4-induced ERK-1/2 phosphorylation was examined in HeLa cells treated with 10 nM CXCL12 for the 0, 2, 5, 10 , 15, 30 and 60 min. ERK-1/2 phosphorylation was determined as described in A. **D-E.** HeLa cells

transfected with siRNA against STAM-1 or control siRNA (GAPDH) (C) or HEK-293 cells transfected with siRNA against STAM-1, STAM-2, STAM1+2 or control siRNA (GAPDH) and were serum starved and treated with 10 nM CXCL12 and vehicle for 2, 5 and 10 min. ERK-1/2 phosphorylation was determined as described in A. **F-H.** HeLa cells transfected with siRNA against AIP4 and control siRNA (GAPDH) were serum starved and treated with 10 nM CXCL12 (F), 100 nM Carbachol (G) and 100 ng/mL EGF (H) for 2, 5, 10 and 20 min. ERK-1/2 phosphorylation was determined as described in A. **I-J.** ERK-1/2 phosphorylation was examined in HeLa cells transfected with FLAG-Arr2-(25-161) (**I**) FLAG-STAM-1-coiled-coil-296-380 (**J**) and empty vector (pCMV). Cells were treated with 10 nM CXCL12 for the indicated times and ERK-1/2 phosphorylation was determined as described in A. Shown are representative blots from one of three independent experiments.

STAM-1 interacts directly with AIP4

To determine the mechanism by which STAM-1 and AIP4 mediate CXCR4 activation of ERK-1/2 we initially examined whether these proteins associate with each other in cells. Cell lysates prepared from HeLa cells expressing FLAG-AIP4 were incubated with bacterially purified GST STAM-1, GST-STAM-2 and GST immobilized on glutathione Sepharose resin and bound FLAG AIP4 was detected by immunoblotting. Both GST-STAM-1 and GST-STAM-2, but not GST, bound to FLAG-AIP4, suggesting that AIP4 interacts with both STAM-1 and STAM-2 (Figure 3.15A,B). We also performed reciprocal pull-down experiments in which purified GST-AIP4 was incubated with cell lysates expressing FLAG-STAM-1 or FLAG-STAM-2. These experiments also revealed that both STAM-1 and STAM-2 interact with AIP4 (Figure 3.15C). To rule out the possibility of an intermediate protein mediating this interaction

We also performed reciprocal pull-down experiments in which purified GST-

AIP4 was incubated with cell lysates expressing FLAG-STAM-1 or FLAG-STAM-2. These experiments also revealed that both STAM-1 and STAM-2 interact with AIP4 (Figure 3.15C). To rule out the possibility of an intermediate protein mediating this interaction we performed binding experiments using purified proteins. As shown in Figure 3.15D, bacterially purified GST-AIP4 was able to interact with purified HIS-tagged STAM-1, indicating that STAM-1 interacts directly with AIP4. Next, we examined the interaction between endogenous proteins in HEK293 and BT474 cells, both of which endogenously express STAM-1 and AIP4. BT474 cells are a breast cancer tumor cell line that expresses high levels of CXCR4 (Li et al., 2004) (Figure 3.15E). As shown in Figure 3.15F, endogenous STAM-1 was detected in samples in which endogenous AIP4 was immunoprecipitated, but not in control IgG immunoprecipitated samples, indicating that native AIP4 and STAM-1 are part of a complex in cells. Similarly, heterologously expressed FLAG-tagged STAM-1 co-immunoprecipitated with Myc-tagged AIP4 (Figure 3.15G). Upon exposure of the immunoblot for longer time (approx 5 min with ECL Dura), higher molecular weight FLAG-STAM-1 species were evident, possibly representing ubiquitinated STAM-1 and consistent with the notion that AIP4 mediates STAM-1 ubiquitination (Fig. 3.15G). To test this, we examined the ubiquitination status of FLAG-STAM-1 in HeLa cells that were co-transfected with Myc-tagged wild-type AIP4 and the AIP4 C830A catalytically inactive mutant, which we have previously shown acts as a dominant-negative when expressed in cells (Marchese et al., 2003). As shown in Figure 3.15H, ubiquitination of FLAG-STAM-1 was completely abolished in cells expressing the AIP4 C830A mutant, as

compared to the wild-type expressing cells, suggesting that AIP4 ubiquitinates STAM-1.
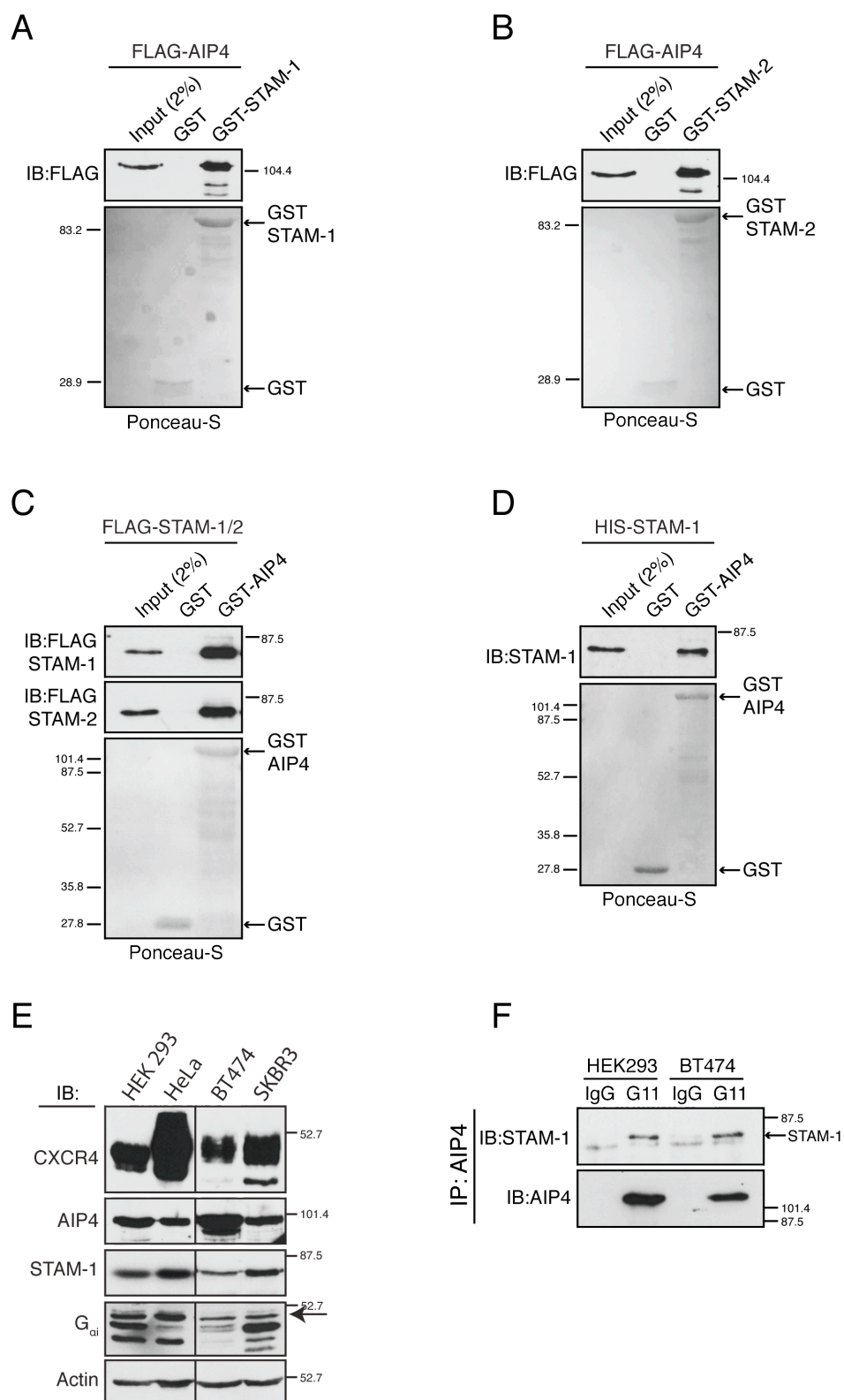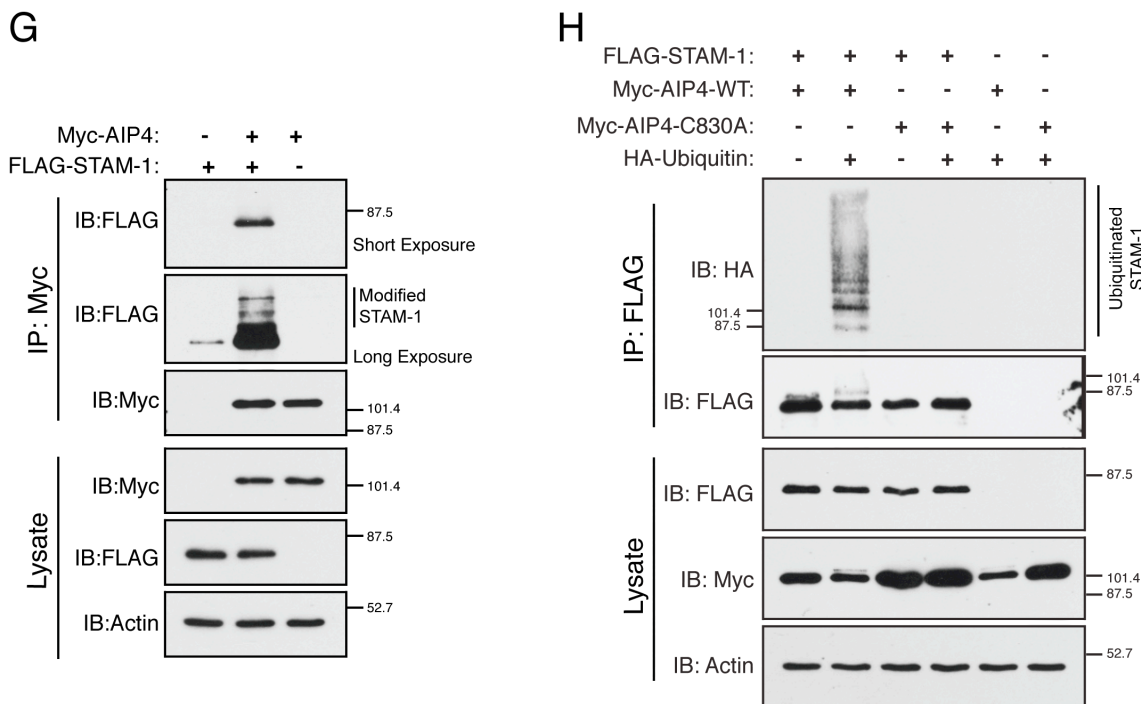
Figure 3.15. STAM-1 interacts directly with AIP4. A-B. Equimolar amounts (117 nM) of GST-STAM-1 (A), GST-STAM-2 (B) and GST alone immobilized on glutathione sepharose resin were incubated with lysates from HeLa cells transiently transfected with FLAG-AIP4. Bound proteins were detected by immunoblotting with an anti-FLAG antibody. **C-D.** Equimolar amounts of GST-AIP4 (186 nM) and GST alone immobilized on glutathione sepharose resin were incubated with lysates from HeLa cells transiently transfected with FLAG-STAM-1 or FLAG-STAM-2 **(C)** or 500 ng purified HIS-STAM-1 **(D).** Bound proteins were detected by SDS-PAGE followed by immunoblotting using anti-FLAG antibody **(C)** or anti-STAM-1 **(D)** antibodies. Blots were stained with Ponceau-S to detect the level of GST fusion protein used in the binding reactions. **E.** Endogenous AIP4 was immunoprecipitated from HEK293 and BT474 cells and samples were analyzed for the presence of endogenous STAM-1 by

immunoblotting. **F.** Equal amounts (10 g) of cleared lysates from HeLa, HEK293, BT474 and SKBR3 cells were subject to SDS-PAGE followed by immunoblotting to detect CXCR4, AIP4, STAM-1, Gα$_i$ and actin. **G.** HeLa cells were transfected with Myc-AIP4 and FLAG-STAM-1 together or alone with empty vector (pcDNA) and Myc-AIP4 was subject to immunoprecipitation (IP) followed by SDS-PAGE and immunoblotting to detect FLAG-STAM-1. A longer exposure of the FLAG-STAM-1 IB reveals the presence of high molecular weight bands that likely represent ubiquitinated species **H.** HeLa cells were transfected with FLAG-STAM-1, Myc-AIP4-WT, Myc-AIP4-C830A, HA-ubiquitin and empty vector (pcDNA or pCMV10). FLAG-STAM-1 was immunoprecipitated and samples were analyzed by SDS-PAGE followed by immunoblotting to detect incorporated HA-ubiquitin. Shown are representative blots from one of three independent experiments performed.

The SH3 domain in STAM-1 interacts with the proline-rich region in AIP4

To define the STAM-1 interaction surface on AIP4 we employed truncation mutagenesis and assessed the ability of AIP4 truncation mutants to bind to STAM-1 (Figure 3.16A). The AIP4 truncations were made based on the domain organization of AIP4. Initially we focused on the four tandemly linked WW domains and the HECT domain. The WW domains are protein-protein interaction modules that typically interact with PP*x*Y and PPPY motifs in binding partners (Macias et al., 1996; Macias et al., 2002). Although STAM-1 does not encode a bonafide PP*x*Y motif we have recently shown that the AIP4 WW domains may also interact with non-canonical motifs (Bhandari et al., 2009). The HECT domain iteracts with the E2 enzyme and has the catalytic cysteine residue that forms the direct thiolester intermediate with ubiquitin before transfer to a target protein (Scheffner et al., 1995). Lysates from HeLa cells

expressing FLAG-STAM-1 were incubated with GST-fusion proteins of full-length AIP4, a deletion mutant in which the four WW domains were removed (AIP4-ΔWW-I-IV), the four WW domains alone (WW-I-IV) and the HECT domain alone. As shown in Figure 16B, bound FLAG-STAM-1 was detected in samples incubated with GST-AIP4 and GST-ΔWW-I-IV, but not with GST-WW-I-IV and GST-HECT domain, suggesting that the STAM-1 binding region on AIP4 does not include the WW domains and nor the HECT domain. These data suggest that the STAM-1 binding region likely resides within the amino terminal region of AIP4. The amino terminal region of AIP4 includes a C2 domain, mostly known as a phospholipid binding domain (Dunn et al., 2004; Plant et al., 1997; Wiesner et al., 2007), and a proline-rich region. The proline-rich region in AIP4 has been shown to bind to a subset of SH3 domains (Angers et al., 2004), which are domains of approximately 60 amino acids that bind to P*xx*P motifs in proteins, where P represents a proline residue and *x* represents any amino acid (Li, 2005). As shown in Figure 3.16C, the proline-rich deletion mutant of AIP4 (ΔPRR) showed almost no binding to GST-STAM-1 when compared to full-length AIP4 (FL), suggesting that the proline-rich region represents the major binding site for STAM-1. Deletion of the SH3 domain in STAM-1 reduced binding to AIP4 by approximately 50% (Figure 3.16D), while the SH3 domain alone was sufficient for binding to AIP4 (Figure 3.16E). Taken together these data indicate that the SH3 domain of STAM-1 is sufficient for interacting with the proline-rich region on AIP4.
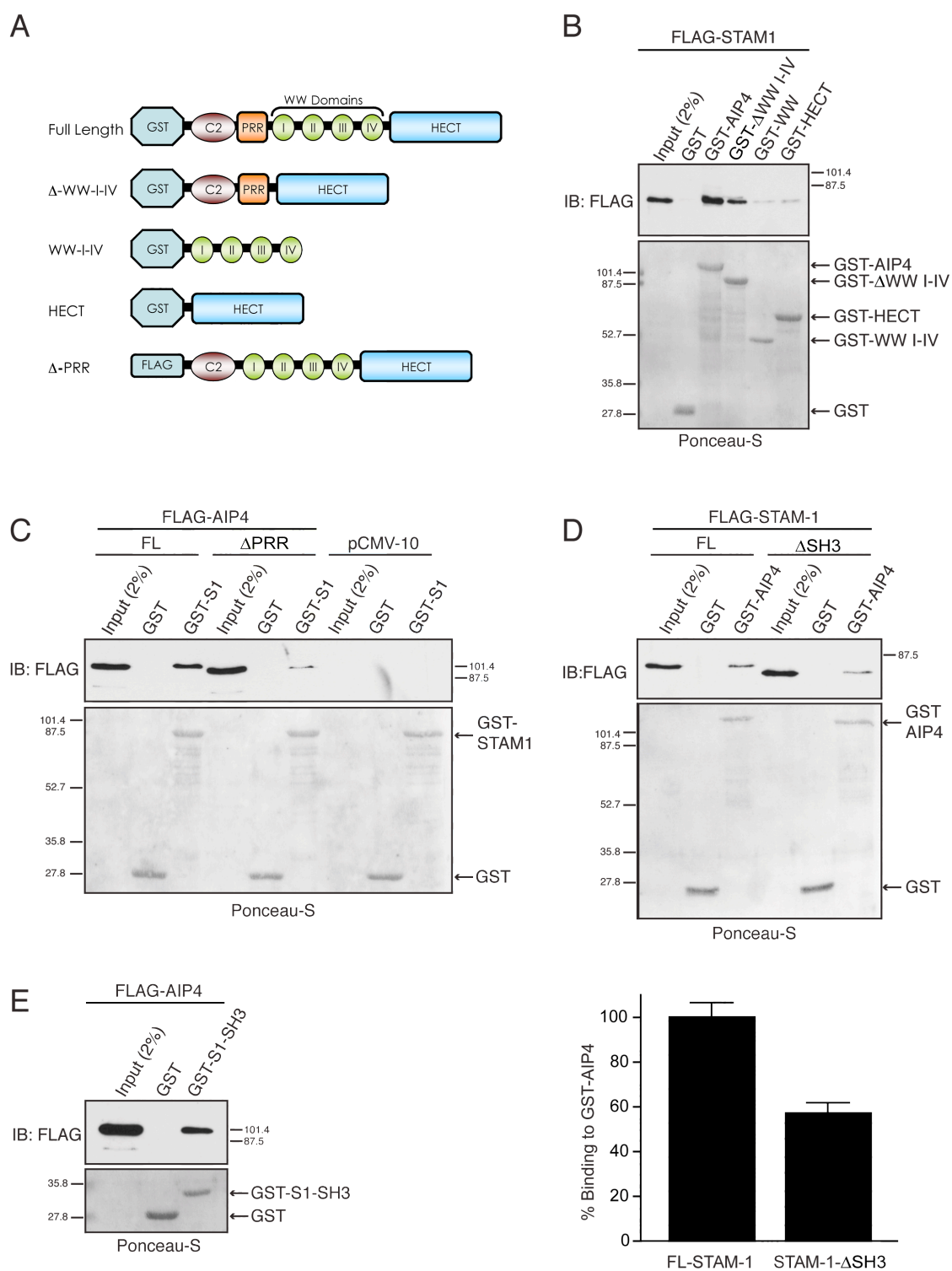
Figure 3.16. AIP4 proline-rich region interacts with the SH3 domain of STAM-1. A. Schematic

representation of AIP4 truncation mutants. The C2 domain, the proline-rich region (PRR), the WW

domains (I-IV) and the HECT domain are indicated. **B.** Equimolar amounts of GST-AIP4, GST-AIP4-ΔWW-I-IV, GST-WW-I-IV, GST-AIP4-HECT and GST immobilized on glutathione sepharose resin were incubated with lysates from HeLa cells expressing FLAG-STAM-1. Samples were subject to immunoblot (IB) analysis to detect bound FLAG-STAM-1. **C.** Equimolar amounts of GST-STAM-1 and GST immobilized on glutathione sepharose resin were incubated with lysates from HeLa cells expressing FLAG-tagged full-length AIP4 (FL), FLAG-AIP4-ΔPRR (ΔPRR) and empty vector (pCMV). Input shows the amount of wild-type and ΔPRR AIP4 used in the binding reactions. Samples were analyzed by IB to detect bound FLAG-AIP4. **D.** Equimolar amounts of GST-AIP4 and GST immobilized on glutathione sepharose resin were incubated with lysates from HeLa cells expressing FLAG-tagged full-length STAM-1 (FL) and FLAG-STAM-1-ΔSH3 (ΔSH3). Samples were subject to IB analysis to detect bound FL and ΔSH3. Bars represent the average percent bound compared to FL as determined by densitometric analysis. The error bars represent the standard deviation from two independent experiments. **E.** GST-STAM-1-SH3 and GST were purified from bacterial call lysate and eluted from the beads as described in *Materials and Methods* section. Equimolar amounts of GST-STAM-1-SH3 and GST were incubated with HeLa cell lysate expressing FLAG-AIP4. After incubation, glutathione sepharose beads were added and incubated for additional 1 hr. Samples were subject to IB analysis to detect bound FLAG-AIP4. Blots were stained with Ponceau-S to assess the amount of GST fusion protein used in the binding reactions. IBs are from one of three independent experiments performed.

Interaction between STAM-1 and AIP4 and ubiquitination activity of AIP4 is important for CXCR4 mediated ERK-1/2 activation

To determine whether the interaction between AIP4 and STAM-1 functions in CXCR4-induced ERK-1/2 phosphorylation, we transiently expressed an AIP4 mutant in which the proline-rich region was deleted (AIP4-ΔPRR) and hence was unable to bind to STAM-1. HeLa cells were transfected with STAM-1 and WT-AIP4 or AIP4-ΔPRR

and stimulated with 10nM CXCL12 for 5 mins, the time when maximal ERK-1/2 phosphorylation was observed (Figure 3.14). As shown in figure 3.17A, over-expression of WT-AIP4 and STAM-1 led to a 3 fold increase in ERK-1/2 phosphorylation levels as compared to cells transfected with vector alone. This is consistent with our finding that knockdown of STAM-1 and AIP4 reduces CXCR4 mediate ERK-1/2 phosphorylation (Figure 3.14A-E). Remarkably, overexpression of AIP4-ΔPRR mutant failed to enhance ERK-1/2 phosphorylation similar to WT-AIP4, suggesting that the interaction between AIP4 and STAM is necessary for mediating CXCR4-induced ERK-1/2 activation. We next assessed whether the ubiquitin ligase activity of AIP4 was required for CXCR4 promoted ERK-1/2 phosphorylation. As shown in Figure 3.17B, over-expression of the catalytically inactive C830A mutant of AIP4 failed to enhance ERK-1/2 phosphorylation, as compared to wild-type AIP4, suggesting that the ubiquitin ligase activity of AIP4 is necessary for CXCR4-induced ERK-1/2 activation. We also examined the effect of CXCR4 activation on STAM-1 ubiquitination. HeLa cells were transfected with T7-STAM-1 and HA-Ubiquitin. Cells were serum-starved and stimulated with 100nM CXCL12 for 5 min. As shown in figure 3.17 C, CXCR4-promoted STAM-1 ubiquitination was enhanced at 5 min after agonist treatment. This is in line with when ERK-1/2 activation is maximal. Taken together our data suggest that AIP4 interacts with and ubiquitinates STAM-1 as early as 5 mins after agonist stimulation. Interaction with STAM-1 as well as AIP4 ubiquitination activity is important for CXCR4 promoted ERK-1/2 phophopration; raising the possibility that STAM-1 ubiquitination is required for this process.
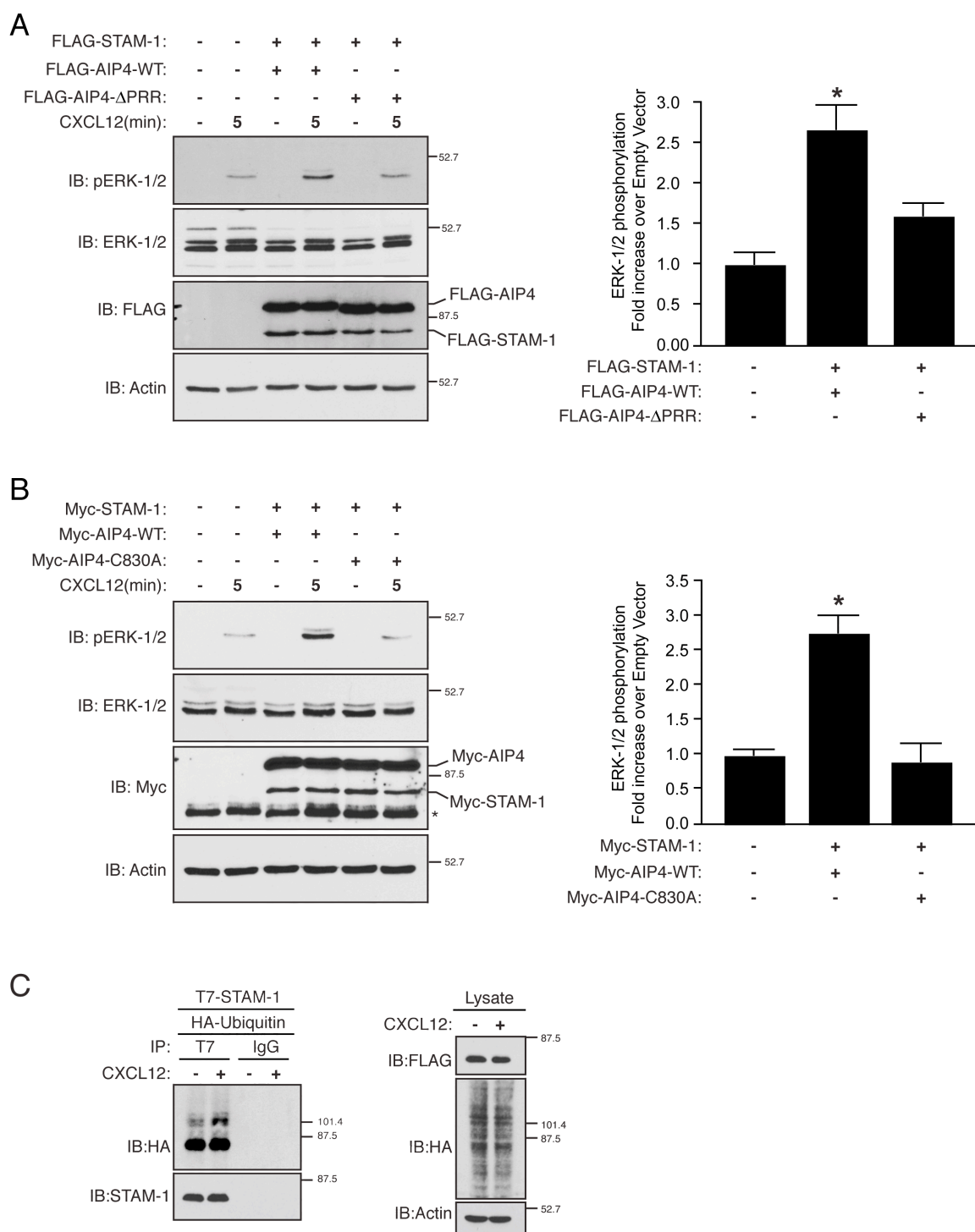
Figure 3.17. The role of AIP4 in CXCR4-induced ERK-1/2 phosphorylation. A-B. HeLa cells grown in

24 well plates were transfected with 300 ng FLAG-STAM-1 and 200ng FLAG-AIP4 or FLAG-AIP4-

ΔPRR **(A)** or 300 ng Myc-STAM-1 and 200ng Myc-AIP4 or Myc-AIP4- C830A, the catalytically

inactive mutant **(B)**. Cells were treated with vehicle (PBS with 0.01% BSA) or 10 nM CXCL12 for 5 min.

The degree of ERK-1/2 phosphorylation (pERK-1/2) was determined by IB analysis and quantified by

densitometry and normalization to actin levels. Data represent the average pERK- 1/2 levels ± S.E.M. from

3 independent experiments and are expressed as fold increase in pERK-1/2 levels in CXCL12 as compared

to empty vector transfected cells. Data were analyzed by a one-way ANOVA. pERK-1/2 levels were

significantly different between wild-type AIP4 and mutant AIP4 expressing cells in both (A) and (B). *, $p <$

0.05. **C.** HeLa cells transfected with T7-STAM-1 and HA-ubiquitin were treated with vehicle (PBS with

0.01% BSA) or 100 nM CXCL12 for 5 min. Samples were subject to IP (T7 and Goat-IgG control) and

analyzed by IB to detect incorporated HA-ubiquitin. Shown are representative blots from one of three

independent experiments.

CXCR4 internalization is not required for ERK-1/2 phosphorylation

We have previously shown that internalized CXCR4 co-localizes with both AIP4

and STAM-1 on endosomes, suggesting that endocytosis and the presence of CXCR4 on

endosomes may be required for ERK-1/2 activation. Expression of dynamin K44A, a

dominant negative mutant of dynamin that blocks CXCR4 internalization (Marchese

and Benovic, 2001), had no effect on CXCR4-induced ERK-1/2 phosphorylation,

suggesting that CXCR4 internalization is not required for ERK-1/2 activation (Figure

3.18A). To confirm this, HeLa cells were treated with siRNA targeting μ2, a subunit of

the heterotetrameric protein complex AP2, which is involved in GPCR internalization

through clathrin-coated pits (Kim and Benovic, 2002; Laporte et al., 1999) and which

co-localizes with CXCR4 upon agonist activation (Marchese et al., 2003). Treatment of

HeLa cells with μ2 siRNA, significantly attenuated agonist-induced internalization of

endogenous CXCR4, as compared to GAPDH siRNA treated cells, indicating that AP2 is required for CXCR4 internalization (Figure 3.18B). Next, we examined CXCR4 induced ERK-1/2 phosphorylation in the same cells that were used for the internalization experiments. As shown in Figure 3.18C, μ2 siRNA did not affect CXCR4-induced ERK-1/2 phosphorylation compared to GAPDH siRNA, suggesting that CXCR4 internalization is not required for ERK-1/2 activation.
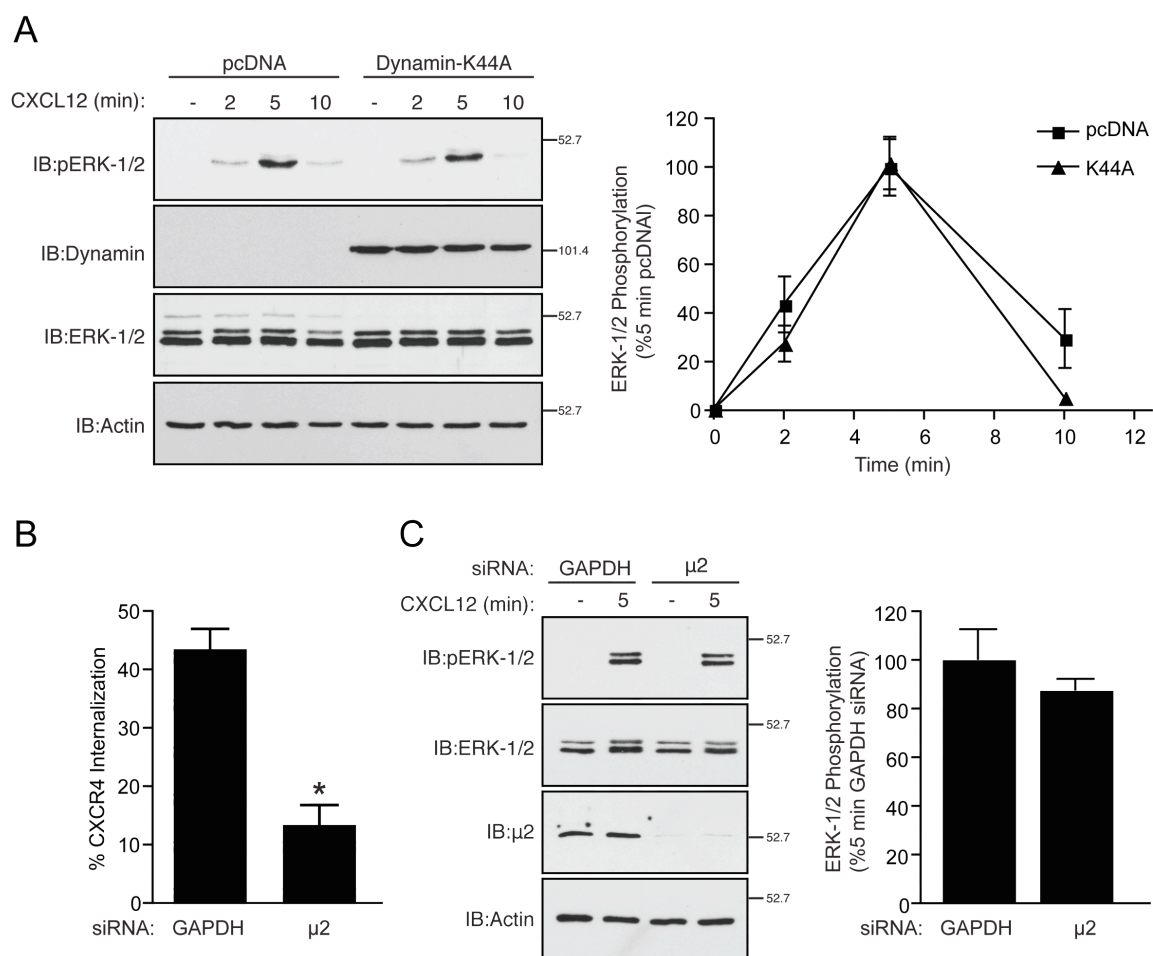
Figure 3.18. The role of endocytosis in CXCR4-induced ERK-1/2 phosphorylation. A. HeLa cells transfected with dynamin-K44A and empty vector (pcDNA) were treated with 10 nM CXCL12 for the indicated time points. pERK-1/2 levels were determined by immunoblot (IB) analysis and quantified as described in the legend to Figure 1. Data were analyzed by a two-way ANOVA followed by Bonferroni's post hoc test and were not found to be statistically significant. **B.** HeLa cells were transfected with μ2 siRNA and treated with vehicle and 10 nM CXCL12 for 20 min. Endogenous CXCR4 cell surface levels were quantified by FACS analysis, as described under Materials and methods. Data represent the mean ± S.E.M. from four independent experiments. Data were analyzed by a student's t-test (*=p<0.05). **C.** CXCL12 promoted ERK-1/2 phosphorylation was determined in the same cells used in the experiments described in (B). Data were analyzed by a student's t-test and were not found to be statistically significant.

STAM-1 colocalizes with CXCR4 on the plasma membrane

Given that internalization is not required for ERK-1/2 activation and because the kinetics of ERK-1/2 phosphorylation are rapid and transient (peak ERK-1/2 phosphorylation at 5 min), it is likely that the molecular events responsible for ERK-1/2 signaling occur proximal to the receptor at the plasma membrane. We have previously shown that in addition to endosomal co-localization with CXCR4, AIP4 also colocalizes with CXCR4 at the plasma membrane, but whether STAM-1 is found at the plasma membrane remains unknown (Marchese et al., 2003). To determine whether STAM-1 is also localized with CXCR4 at the plasma membrane we applied confocal immunofluorescence microscopy. To ensure that we focused only at the plasma membrane we also co-stained cells for AP2, which is only found at the plasma membrane. In HeLa cells treated with CXCL12, endogenous CXCR4 staining was punctate and many puncta co-localized with AP2 (Figure 3.19, arrow heads), consistent

with CXCR4 being recruited to clathrin-coated pits for internalization, as we have previously reported (Marchese et al., 2003). STAM-1 staining was also punctate but it showed only a limited amount of co-localization with CXCR4 and AP2 (Figure 3.19, lines). Surprisingly, some STAM-1 puncta that co-localized with CXCR4 were devoid of AP2 (Figure 3.19, arrows), suggesting that CXCR4 and STAM-1 exist in microdomains distinct from clathrin-coated pits at the plasma membrane.
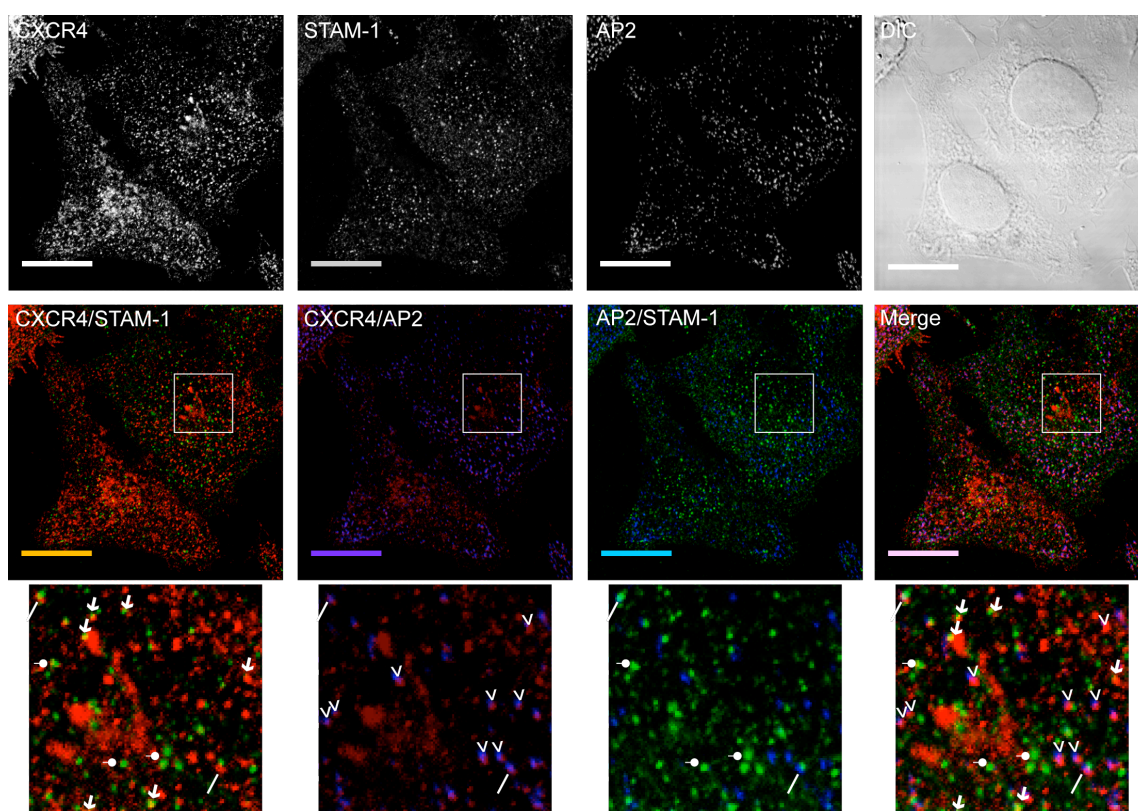
Figure 3.19. STAM-1 co-localizes with CXCR4 at the plasma membrane. HeLa cells grown on cover slips were treated with 10 nM CXCL12 for 5 min. Cells were then fixed, permeabilized and stained with anti-CXCR4 (red), anti-STAM-1 (green) and anti-AP2 (blue). Arrows point to puncta that show co-localization between CXCR4 and STAM-1. Arrowheads point to puncta that show co-localization

between CXCR4 and AP2. The white line indicates puncta that show co-localization between CXCR4, AP2 and STAM-1. The line with the circle indicates STAM-1 puncta that do no contain CXCR4 and AP2. Differential interference contrast (DIC) image is shown. Representative area (boxed) from each image is enlarged 4× and shown below in the bottom panels. Shown are representative micrographs from three independent experiments (5 images per experiment). Bars, 20 μm

Biochemical distribution of CXCR4

CXCR4 has been shown to distribute into cholesterol- and sphingolipid-rich microdomains known as lipid rafts in T cells (Nguyen and Taub, 2002), raising the possibility that CXCR4 and STAM-1 may be found together in this compartment. One particular lipid raft microdomain contains the protein caveolin, forming structures known as cavealae, to which many GPCRs and their downstream effector signaling molecules are localized (Patel et al., 2008). To verify the presence of CXCR4, STAM-1 and AIP4 within lipid rafts we utilized detergent free sucrose gradient membrane fractionation protocol (Song et al., 1996). HeLa cells transfected with FLAG-AIP4 (Because of the limitations in detecting endogenous AIP4, we transiently expressed FLAG-AIP4 ~2-fold above endogenous) were serum starved and treated with CXCL12 or vechicle alone for 5 min. Caveolar membranes were separated from the remainder of the membranes by sucrose gradient centrigufation. Purity of the frationation was determined by immunoblotting. Caveolin-1 fractionates in buoyant fractions near the top of the gradient and is used as a marker of caveolae. The heavy fractions or later fractions contain other cellular membranes and here we used α2-adaptin as a marker of this fraction. As shown in Figure 3.20A, CXCR4 was found in a fraction that was enriched in α2-adaptin,

consistent with the immunofluorescence microscopy data that showed that CXCR4 mostly co-localizes with α2-adaptin (see Figure 3.19). In addition, CXCR4 was found in fractions enriched with caveolin-1, suggesting the presence of CXCR4 within caveolae and/or lipid rafts. We also examined these fractions for the presence of FLAG-AIP4 and STAM-1. STAM-1 and FLAG-AIP4 were mainly in the fraction that contained α2-adaptin, consistent with their presence in non-caveolar membrane compartments, but a pool of both STAM-1 and AIP4 were also present in the caveolin-1 enriched fraction (Figure 3.20A). As CXCR4-induced ERK-1/2 phosphorylation requires coupling to the heterotrimeric G protein Gαi (data not shown), we also show that Gα_i also co-fractionates in the caveolin-1 enriched fraction (Figure 3.20A). A similar pattern of distribution among the fractions was observed in vehicle treated cells (Figure 3.20A), suggesting that agonist stimulation has no effect on the distribution of proteins to caveolae. To complement these data, we next examined the distribution of CXCR4, STAM and AIP4 relative to caveolin-1 by confocal microscopy. HeLa cells expressing endogenous CXCR4 were serum starved and treated with CXCL12 for 5 mins. Cells were fixed and stained with CXCR4, caveolin-1 and AP2. As shown in Figure 3.20B, CXCR4 colocalizes with caveolin-1 (arrow heads) as well as AP2. To examine the distribution of AIP4 and STAM-1, HeLa cells transiently transfected with YFP-AIP4 (Figure 3.20C) and YFP-STAM-1 (Figure 3.20D) were stimulated with CXCL12 for 5 min, fixed and stained with caveolin-1 and AP2. Both AIP4 and STAM-1 were found to co-localize with caveolin-1 at the plasma membrane, as assessed by confocal microscopy (Figures 3.20 C and D). We next examined whether caveolin-1 exists in a complex with

AIP4 and STAM-1 in cells by co-immunoprecipitation experiments. Endogenous AIP4 was immunoprecipitated from HEK293 (Figure 3.20E) and HeLa (Figure 3.20F) cells and samples were analyzed by immunoblotting for the presence of endogenous caveolin-1 and STAM-1. As shown in Figure 3.20E,F, both caveolin-1 and STAM-1 were found to co-immunoprecipitate with AIP4, suggesting that AIP4 and STAM-1 exist in a complex with caveolin-1 in cells. When taken together, our data suggest that STAM-1 and AIP4 may co-localize with CXCR4 at the plasma membrane in caveolae and/or lipid rafts.

C

YFP-AIP4 Caveolin-1 AP2 Merge

D

YFP-STAM-1 Caveolin-1 AP2 Merge
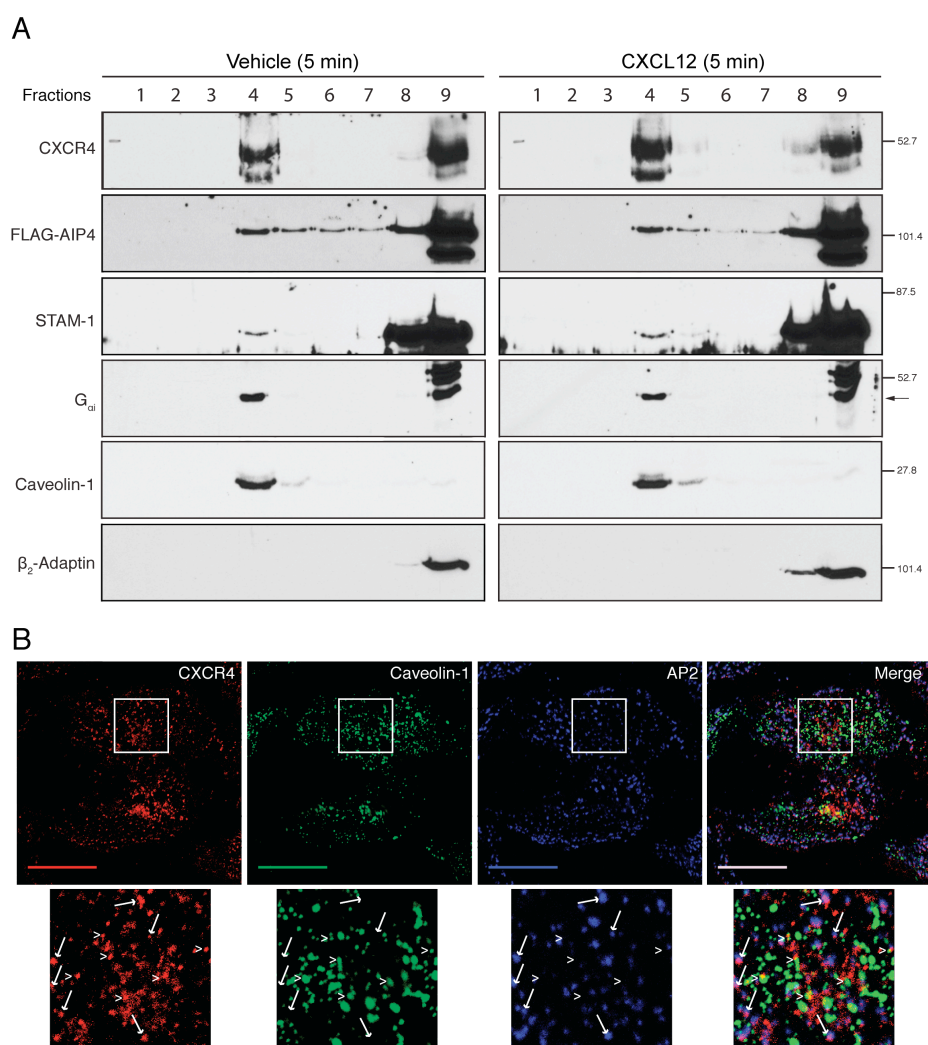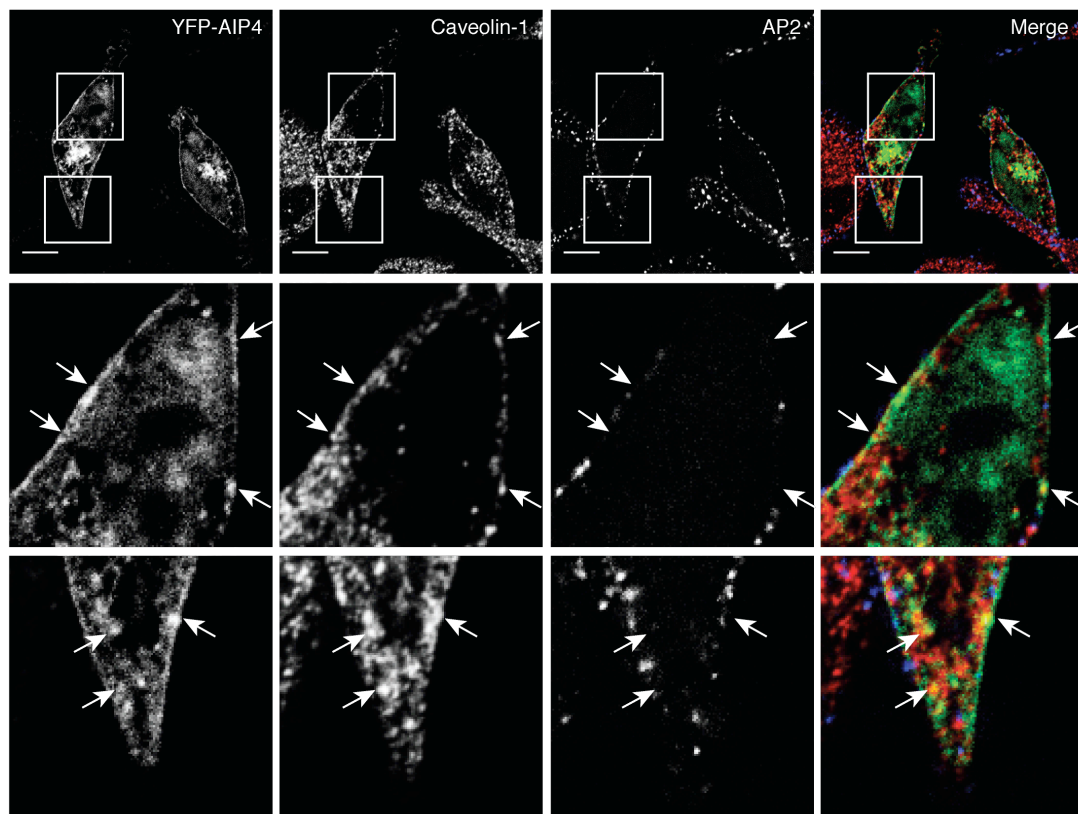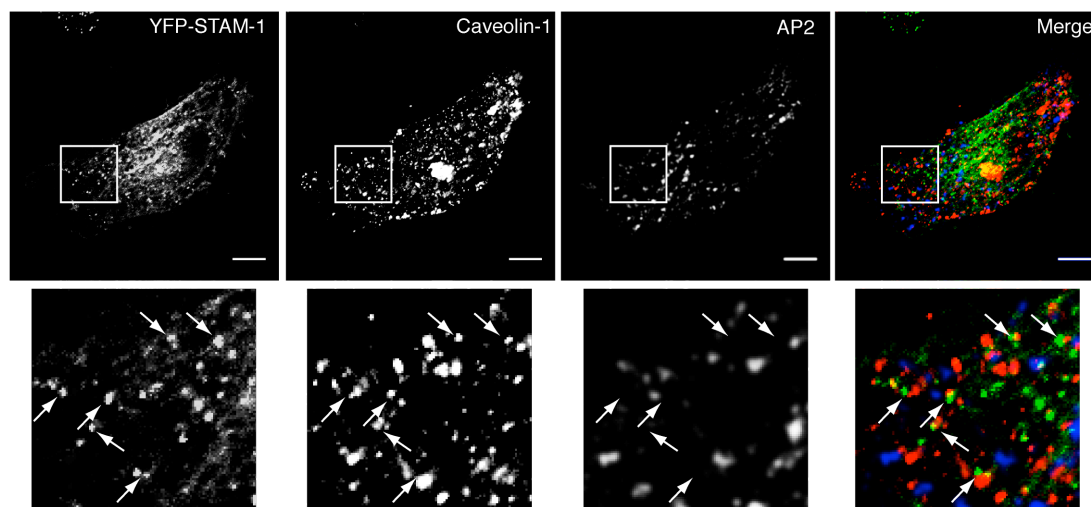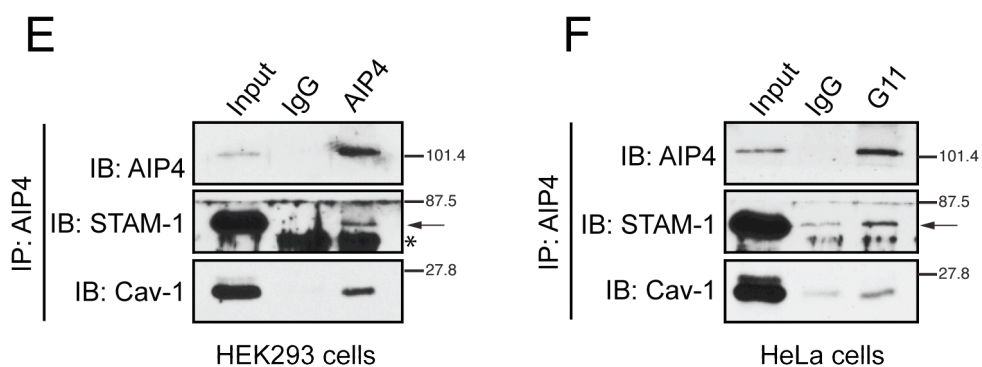
Figure 3.20. CXCR4 co-fractionates with AIP4, STAM-1 and caveolin-1. A. HeLa cells were transfected with low amounts of FLAG-AIP4 and were treated with vehicle (PBS with 0.01% BSA) and 10 nM CXCL12 for 5 min. Sucrose gradient centrifugation was performed, as described under Materials and methods. Nine fractions were collected and subject to immunoblot (IB) analysis for the presence of caveolin-1, CXCR4, FLAG-AIP4, STAM-1, Gαi and β2 adaptin. Shown are representative blots from one of three experiments. **B.** HeLa cells grown on cover slips were serum starved and treated with 10 nM CXCL12 for 5 min. Cells were then fixed, permeabilized and stained with anti-CXCR4 (red), anti-caveolin-1 (green) and anti- -adaptin (clone AP6; blue) antibodies. Arrowheads indicate puncta that show colocalization between CXCR4 and caveolin-1 and arows indicate puncta that show colocalization between CXCR4 and AP2. **C-D.** HeLa cells transfected with YFP-AIP4 (C) or YFP-STAM-1 (D) grown on cover slips were serum starved and treated with10 nM CXCL12 for 5 min. Cells were then fixed, permeabilized and stained with anti-caveolin-1(red) and anti-β-adaptin (clone AP6; blue) antibodies. Arrows indicate puncta that show colocalization between YFP-AIP4 (B) or YFP-STAM1(D) and caveolin-1. Boxed region from each image is enlarged 4 and shown in the bottom panels. Representative micrographs from three independent experiments are shown. Micrograph showing AP2 staining in D was processed in Adobe Photoshop by applying a Gaussian blur (Gaussian blur of 1 pixel). Bars, 20 μm. **E-F.** Cell lysates from HEK293 cells stably expressing HA-CXCR4 (B) and HeLa cells (C) were subject to immunoprecipitation (IP) using an anti-AIP4 antibody (G11, Santa Cruz). Coimmunoprecipitated bound endogenous STAM-1 and caveolin-1 were detected by IB. Shown are representative blots from one of three experiments. The asterisk (*) indicates heavy chain of IgG.

We next investigated whether STAM-1 and AIP4 were involved in the recruitment of CXCR4 into the caveolar compartment. STAM-1 and AIP4 were depleted from HeLa cells using siRNA and sucrose fractionation experiment were performed to isolate caveolar fractions similar to as described previously. As shown in Figure 3.21, depletion of both STAM-1 as well as AIP4 had no effect on the recruitment of CXCR4 to the caveolar fraction (fraction 4). When taken together, our data suggest that STAM-1 and AIP4 co-localize with CXCR4 at the plasma membrane in caveolae and/or lipid rafts and are consistent with the notion that CXCR4 induced signaling via STAM-1 and AIP4 likely occurs from this compartment.
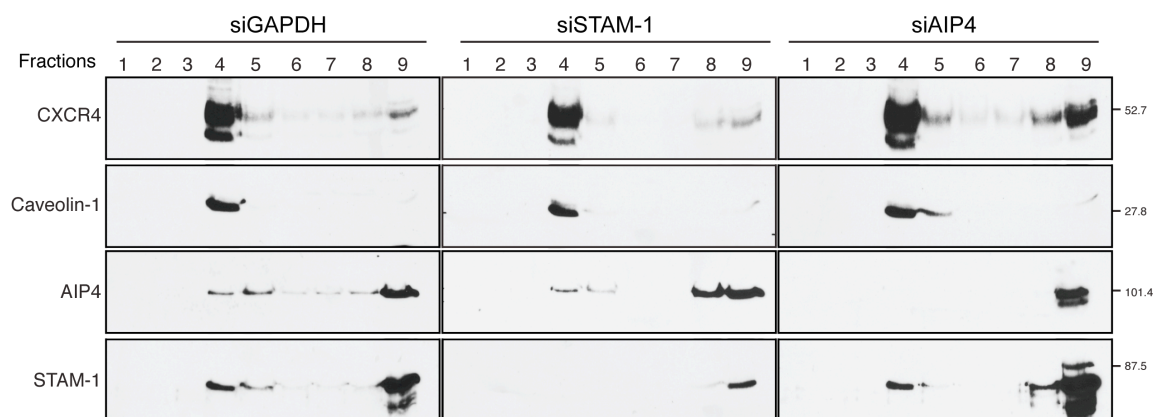
Figure 3.21. Depletion of AIP4 and STAM-1 have no effect on recruitment of CXCR4 to caveolae. HeLa cells were transfected with 600pmoles of siRNA against GAPDH, STAM-1 and AIP4 and were treated with 10 nM CXCL12 for 5 min. Sucrose gradient centrifugation was performed, as described under *Materials and methods*. Nine fractions were collected and subject to immunoblot (IB) analysis for the presence of caveolin-1, CXCR4, AIP4 and STAM-1. Shown are representative blots from one of three experiments.

Caveolin-1 is required for CXCR4-induced ERK-1/2 activation

To confirm a role for caveolae and/or lipid rafts in CXCR4-induced ERK-1/2 activation we initially tested the effect of the cholesterol sequestering drug nystatin, which disrupts lipid rafts. HeLa cells were serum starved and treated with 50 μg/ml nystatin or DMSO for 30 min at 37°C. Cells were treatment with CXCL12 or vehicle for 5 min and ERK-1/2 phosphorylation was analyzed by immunoblotting. As shown in Figure 3.22A, treatment with Nystatin attenuated CXCL12 induced ERK-1/2 phosphorylation as compared to DMSO treated cells. In contrast, Nystatin treatment had no effect on EGF-induced ERK-1/2 phosphorylation, suggesting that nystatin does not globally affect plasma membrane signaling (Figure 3.22A). We also examined the effect of Nystatin treatment on receptor internalization and found that Nystatin treatment only modestly inhibited CXCR4 internalization (Figure 3.22B). Consistent with HeLa cells, Nystatin treatment also significantly attenuated CXCR4-induced ERK-1/2 phosphorylation in SKBR3 cells, a breast cancer cell line that expresses high levels of CXCR4 (Figure 3.15E), but not that induced by EGF (Figure 3.22C).

As caveolin-1 is a major constituent of caveolae, we examined its role in CXCR4-induced ERK-1/2 activation. We examined ERK-1/2 phosphorylation by quantitative confocal immunofluorescence microscopy because it allowed us to focus on individual cells and to determine the distribution of pERK-1/2 in activated cells. HeLa cells transiently transfected with GAPDH or caveolin-1 siRNA were treated with CXCL12 or vehicle for 5 min, fixed and co-stained for caveolin-1 and pERK-1/2, as described under *Materials and methods*. In control siRNA transfected cells, CXCL12 treatment

significantly enhanced pERK-1/2 staining, which was mostly nuclear, as compared to vehicle treated cells (Figure 3.22D,E). In contrast, in caveolin-1 siRNA transfected cells, pERK-1/2 staining was significantly attenuated, as compared to vehicle treated cells. Caveolin-1 levels were significantly reduced in caveolin-1 siRNA transfected cells as compared to GAPDH transfected cells (Figure 3.22F,G). Taken together, these data suggest that caveolin-1 and caveolae are important for CXCR4-induced activation of ERK-1/2.

A

B

C

Nystatin — — + + — — + +
CXCL12 — + — + — — — —
EGF — — — — — + — +

IB:pERK-1/2

IB: Actin

IB:ERK-1/2

SKBR3 Cells

D

Vehicle | CXCL12 (5min)

siControl — Caveolin-1 / pERK1/2

siCAV-1 — Caveolin-1 / pERK1/2

E

F

G

siRNA: GAPDH | Caveolin-1

IB: Cav-1

IB: Actin
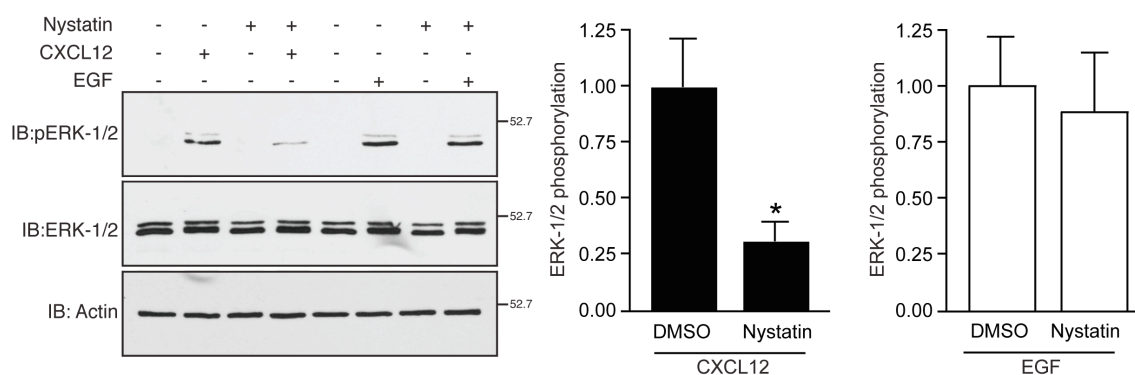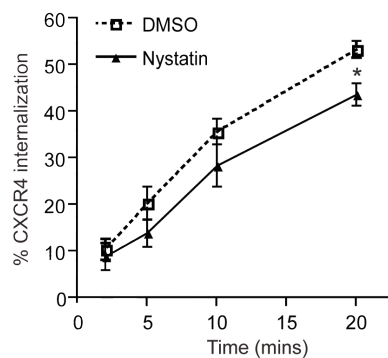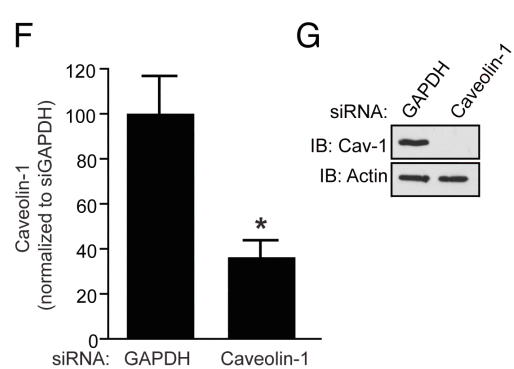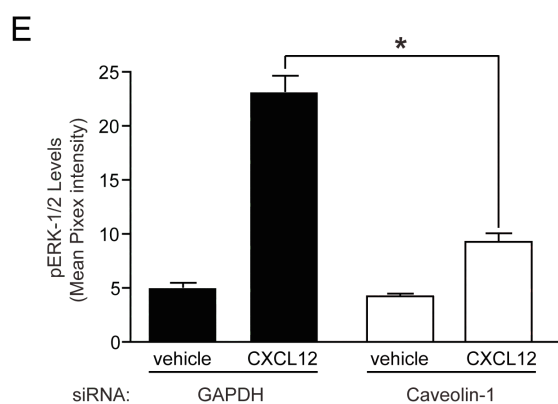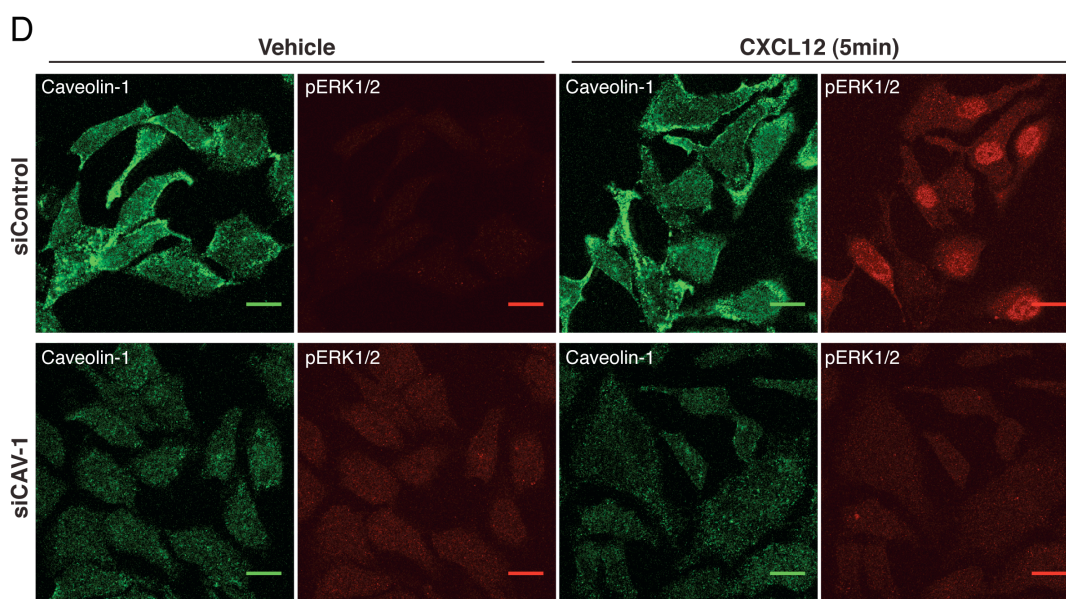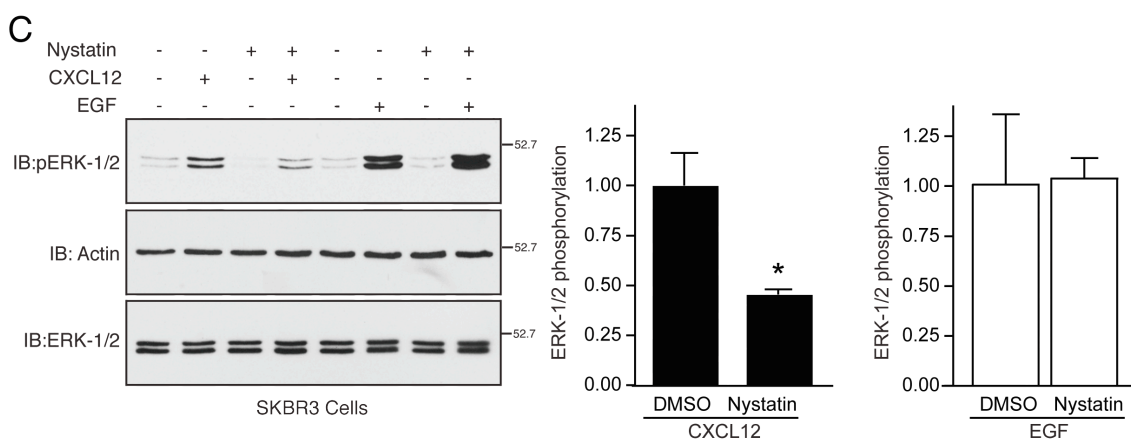
Figure 3.22. Caveolin-1 is essential for CXCR4-induced ERK-1/2 phosphorylation. A. Serum starved HeLa cells were treated with 50 μg/mL nystatin for 30 min followed by treatment with 10 nM CXCL12, 100 ng/mL EGF and vehicle (PBS with 0.01% BSA) for 5 min. ERK-1/2 phosphorylation was determined by immunoblotting and pERK-1/2 levels were quantified by densitometry and normalized to total ERK levels. Bars represent the average pERK-1/2 levels ± S.E.M. from 3 independent experiments and are expressed as fold increase in CXCL12 compared to vehicle treated cells normalized to pERK-1/2 levels in DMSO treated cells. Data were analyzed by a student's t-test (*=p<0.05). Shown are representative blots from one of three independent experiments performed. **B.** HeLa cells treated with vehicle (DMSO) or 50 g/ml nystatin were treated with vehicle (PBS with 0.01% BSA) or 10 nM CXCL12 for the indicated time points. Cell were then fixed and stained with anti-PE conjugated anti-CXCR4 antibody. Amount of receptor internalized upon stimulation was quantified using FACS and the data were analyzed by two-way ANOVA followed by Bonferroni's post hoc test (*=p<0.05). Error bar represents ±S.E.M. from three independent experiments performed. **C.** Serum starved SKBr3 cells were treated with 50 g/ml nystatin for 30 min followed by treatment with 10 nM CXCL12, 100 n g/mL EGF and vehicle (PBS with 0.01% BSA) for 5 min. ERK-1/2 phosphorylation was determined by immunoblotting and pERK-1/2 levels were quantified as described above. Data were analyzed by student's t-test (*=p<0.05). Error bar represents ± S.E.M. Shown are representative blots from one of three independent experiments performed. **D.** HeLa cells transfected with GAPDH and caveolin-1 siRNA were treated with 10 nM CXCL12 for 5 min. Cells were processed as described under *Material and Methods* and stained for pERK-1/2 and caveolin-1. Shown are micrographs from one of three independent experiments. Bar, 20 μm. **E-F.** The levels of pERK-1/2 (E) and caveolin-1 (F) were determined by calculating the mean pixel intensity of pERK-1/2 and caveolin-1 staining using Zeiss LSM 510 image analysis software. The bars represent the average of the mean pixel intensity of pERK-1/2 (E) or caveolin-1 (F) in GAPDH and caveolin-1 siRNA transfected cells treated with vehicle and 10nM CXCL12. A total of 45 cells from 3 independent experiments were used in the analysis. Data in (E) were analyzed using a two-way ANOVA followed by a Bonferroni posthoc test

(*,p<0.001). Data in (D) were analyzed by a Student's *t*-test. Error bars represent S.E.M. **G.** Level of caveolin-1 knockdown was determined by western blotting.

STAM-1, AIP4 and arrestin-2/3 do not regulate CXCR4-mediated cell proliferation

CXCR4 promoted MAPK activation has been shown to promote cellular proliferation (Shen et al., 2010). In order investigate the biological significance of STAM-1 and AIP4 mediated regulation ERK-1/2, we examined the effect of STAM-1 and AIP4 knockdown on proliferation of HeLa cells. Proliferation was measured by quantifying the DNA content by staining the cells with DNA intercalating drug propidium iodide (PI). HeLa cells transfected with siRNA against STAM-1, AIP4 and arrestin-2/3 were treated with vehicle, 30 nM CXCL12 and 10% FBS for 12 hr. Cells were fixed, stained with propidium iodide (PI) and analyzed by flow cytometry. The amount of cells present in each phase of the cell cycle were quantified using "Watson Pragmatic" model (Watson et al., 1987). As shown in Figure 3.23A-D, CXCL12 treatment promotes cell proliferation as percent number of cell present in the S-phase increased from 16±1.7% to 22±1.7% after CXCL12 treatment. Treatment with 10% FBS had a much greater effect on proliferation as number of cell present in S-phase were 31±1.9%. However, knock down of STAM-1, AIP4 as well as arrestin-2/3 had no effect on the cell present in the S-phase as well as in the G1 phase of cell cycle (Figure 3.23E-G). Taken together our data suggest that AIP4, STAM-1 and arrestin-2/3 does not regulate proliferation of HeLa cells.

A siGAPDH

Vehicle
%G1 = 67.9
%S = 19.6
%G2 = 6.47

30nM CXCL12
%G1 = 64.1
%S = 24.9
%G2 = 3.99

10% Serum
%G1 = 57.4
%S = 33.9
%G2 = 4.52

B siSTAM-1

Vehicle
%G1 = 58.7
%S = 22.7
%G2 = 6.81

30nM CXCL12
%G1 = 60.4
%S = 26.9
%G2 = 7.66

10% Serum
%G1 = 55.2
%S = 34.8
%G2 = 5.65

C siAIP4

Vehicle
%G1 = 63.3
%S = 19.9
%G2 = 7.7

30nM CXCL12
%G1 = 56.5
%S = 28.8
%G2 = 6.98

10% Serum
%G1 = 46.9
%S = 35.3
%G2 = 6.83

D siArrestin2/3

Vehicle
%G1 = 62.3
%S = 20.8
%G2 = 8.64

30nM CXCL12
%G1 = 65.5
%S = 24.2
%G2 = 5.6

10% Serum
%G1 = 55.6
%S = 34.3
%G2 = 4.91
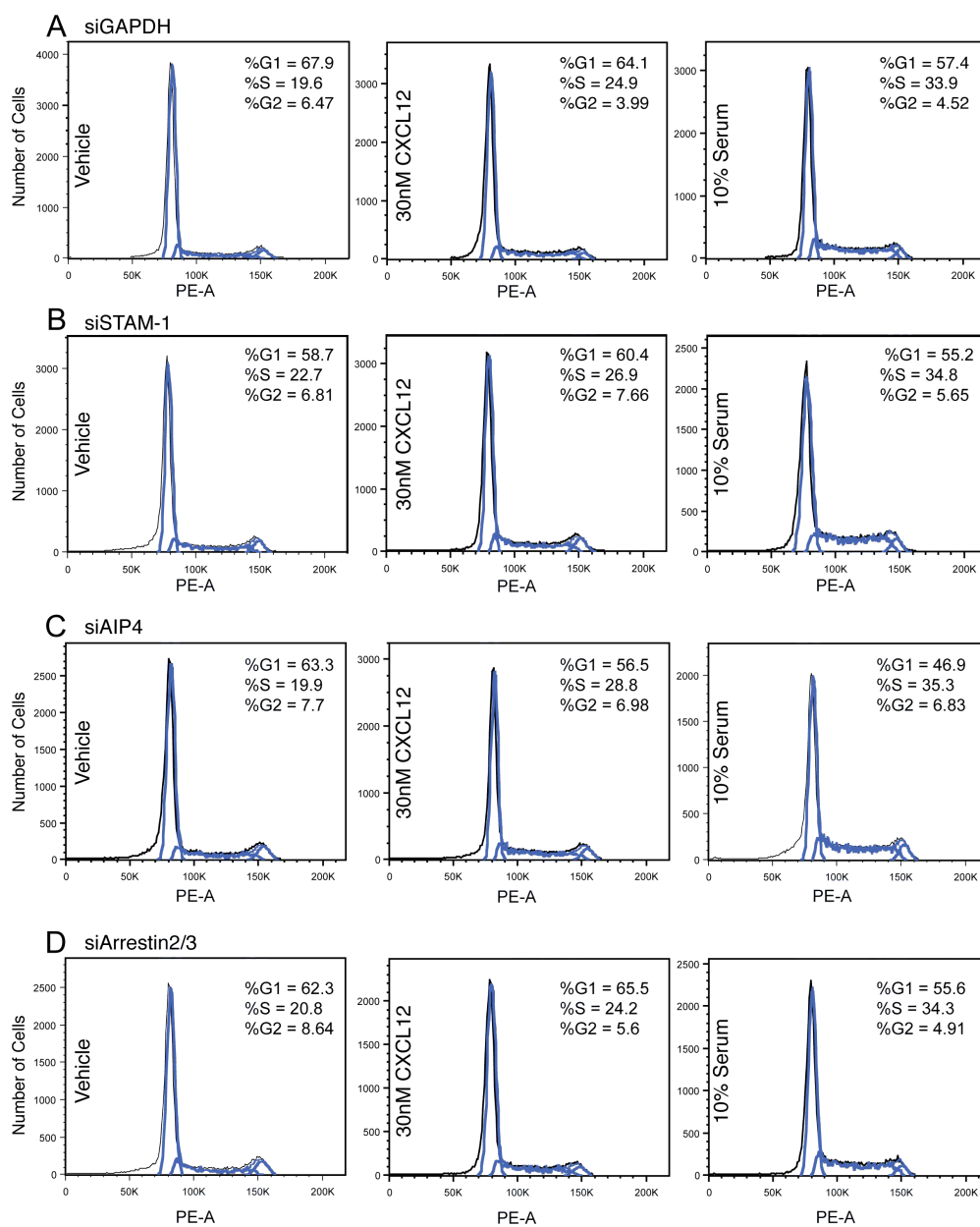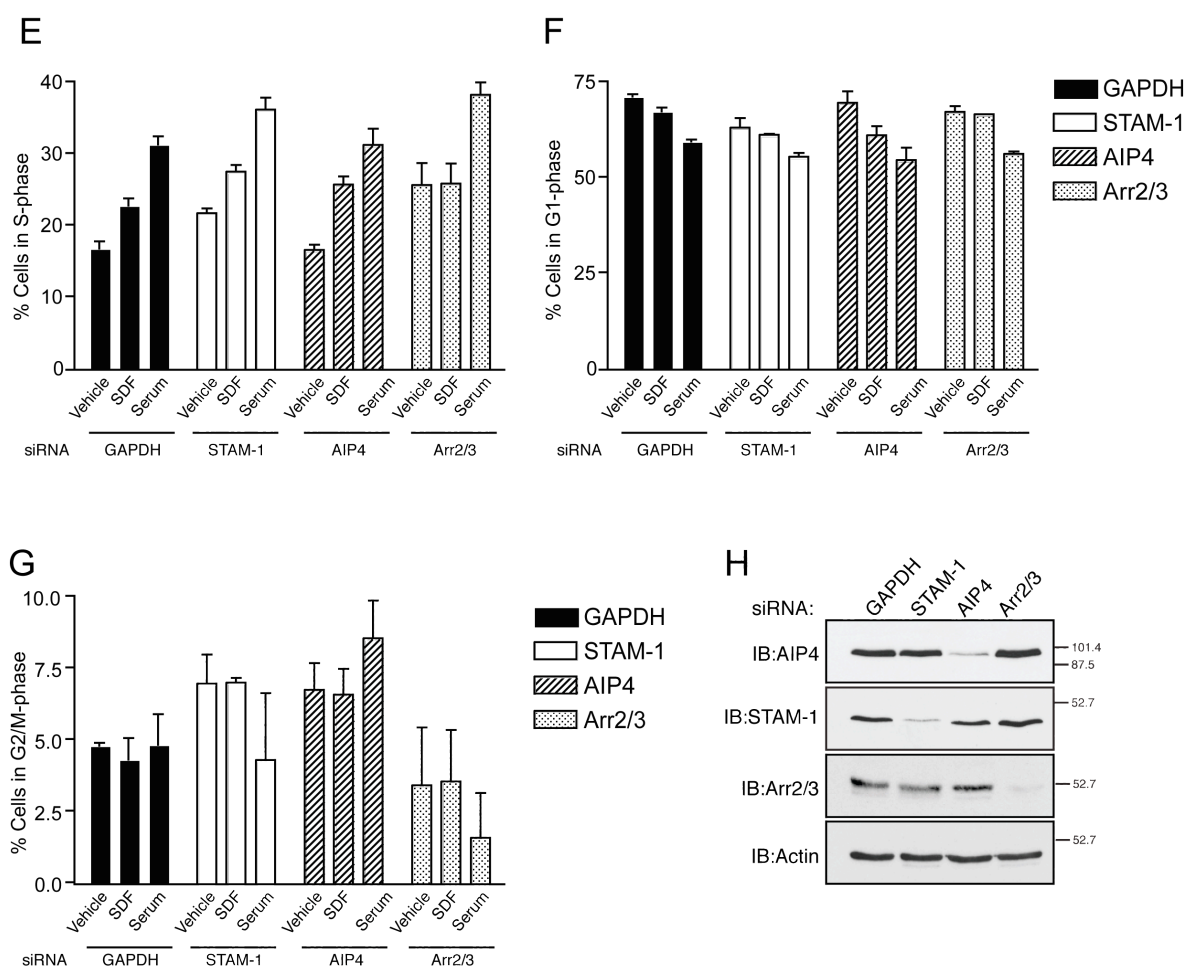
Figure 3.23. Role of STAM-1, AIP4 and arrestin-2/3 in CXCR4 promoted proliferation of HeLa cells.

A-D. HeLa cells transfected with control siRNA (GAPDH)(A) or siRNA against STAM-1(B), AIP4(C) or arrestin-2/3(D) or were serum starved and treated with 30nM CXCL12, 10% FBS or vehicle (PBS with 0.1% BSA) for 12 hours. Cells were then fixed with ethanol and stained with propidium iodide as described in *Materials and methods*. Cells were analyzed by FACS to determine the percent cells in S, G1 and G2 phase. **E-G.** Percent cell in S-phase (E), G1-phase (F) and G2-phase (G) were determined by Watson pragmatic cell cycle analysis model using FlowJo v.9.3 and the data were analyzed by two-way ANOVA followed by Bonferroni's post hoc test (*=$p<0.05$). Error bar represents ±S.E.M. from three independent experiments performed. **H.** Protein knockdown was determined by SDS-PAGE and immunoblotting for STAM-1, AIP4 and arrestin-2/3.

Effect of STAM-1, AIP4 and arrestin-2/3 knockdown on PARP cleavage

We also examined the effect of STAM-1, AIP4 and arrestin-2/3 knockdown on apoptosis by looking at PARP cleavage. PARP is a 116 kDa nuclear poly (ADP-ribose) polymerase which is involved in DNA repair in response to various kind stress (Satoh and Lindahl, 1992). PARP is cleaved between Asp214 and Gly215, by caspase-3, which separates the PARP amino-terminal DNA binding domain (24 kDa) from the carboxy-terminal catalytic domain (89 kDa) (Lazebnik et al., 1994). Cleavage of PARP facilitates cellular disassembly and serves as a marker of cells undergoing apoptosis. As shown in figure 3.24, knockdown of STAM-1, AIP4 and arrestin-2/3 had no effect on PARP cleavage suggesting that these proteins are not involved in the apoptosis pathway. However, a more detailed analysis of the effects on apoptosis is required such as TUNNEL assay or Annexin-V staining.
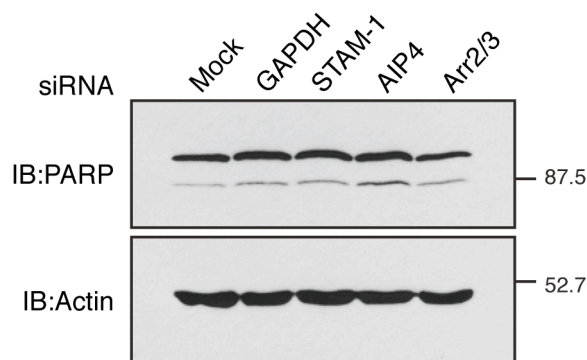
Figure 3.24: Effect of STAM-1, AIP4, arrestin-2/3 knocdown on PARP cleavage. Mock transfected HeLa cells or HeLa cells transfected with control siRNA (GAPDH) or siRNA against STAM-1, arrestin-2/3 or AIP4 were collected in sample buffer and analyzed by SDS-PAGE followed by immunoblotting for PARP. Blot was stripped and reprobed for actin. Shown are representative blots from one of three independent experiments performed.

CHAPTER 4

DISCUSSION

The present study provides mechanistic insights into signaling and downregulation of the chemokine receptor CXCR4. We have identified an unprecedented role of arrestin-2 in trafficking and downregulation of CXCR4 through multiple interactions with ESCRT-0. We reveal here that ESCRT-0 protein STAM-1 via interaction with arrestin-2 regulates the ubiquitination status of HRS, which is critical for sorting ubiquitinated CXCR4 into the degradative pathway. In addition, we have also identified novel roles for AIP4 and STAM-1 in CXCR4 signaling, which are different from their roles in CXCR4 trafficking. Our data show that STAM-1 interacts with AIP4 to mediate CXCR4-induced phosphorylation of ERK-1/2. Remarkably, a discrete subpopulation of AIP4 and STAM-1 that resides in caveolae with CXCR4 is responsible for this signaling event. We propose that the AIP4/STAM-1 interaction, as well as ubiquitin ligase activity of AIP4 in caveolae coordinates activation of ERK signaling.

Role of arrestins in CXCR4 regulation

Non-visual arrestins (arrestin-2 and 3) are generally known for their ability to mediate GPCR desensitization, trafficking and signaling (Ferguson et al., 1996; Goodman et al., 1996; Kovacs et al., 2009; Luttrell and Lefkowitz, 2002). Arrestin-2 interacts with AIP4 and mediates endosomal sorting of CXCR4 into the degradative

158

pathway (Bhandari et al., 2007). Previous work done in the lab and the present study show that both arrestin-2 as well as AIP4 can directly interact with CXCR4-C-tail and co-localizes with the receptor on early endosomes (Figure 3.1 and 3.2) (Bhandari et al., 2009; Marchese et al., 2003). However, mechanistic insight into the role of arrestin-2 as well as AIP4 in endosomal sorting of CXCR4 remains to be determined. Here we extend these findings and provide further insight into this unprecedented role of arrestin-2.

Arrestin-2 interacts with ESCRT-0

ESCRT proteins are required for the sorting of ubiquitinated cargo into the degradative pathway. ESCRT-0, which is composed of HRS and STAM, is the most proximal complex that recognizes the ubiquitinated cargo and recruits it into the sorting machinery. Our data suggest that arrestin-2 mediates multiple interactions with ESCRT-0 on early endosomes. Arrestin-2 interacts directly with STAM-1, but not to its close isoform STAM-2 (Figure 3.3 A and B). The differential binding was somewhat surprising as STAM-1 and STAM-2 share strong overall sequence identity (~53% amino acid identity), especially within the coiled coil domain (71% amino acid identity), which is the region that binds to arrestin-2. The C-terminal domains (24% amino acid identity) represent the most divergent regions between STAM-1 and STAM-2, but surprisingly, arrestin-2 binding to a STAM-1 truncation mutant deleted of the C-terminal end was similar to binding to full-length STAM-1 (Figure 3.7 A and C) or when the C-terminal end was expressed alone we did not detect any binding to arrestin-2 (Figure 3.7C). We also observed that activation of CXCR4 selectively enhances STAM-

1 ubiquitination, but not STAM-2 ubiquitination (Figure 3.4B), thus further supporting the selectivity of STAM-1 towards CXCR4. This suggests that arrestin-2 likely restricts CXCR4 sorting to ESCRT-0 complexes that have STAM-1 but not STAM-2. Our data clearly show that arrestin-2 binds to STAM-1 and that the coiled-coil domain of STAM-1 (296-380) and amino acid residues 25-161 of arrestin-2 form the respective minimal binding regions. The precise molecular determinants that are responsible for preferential binding to STAM-1 but not to STAM-2 remain unknown, however, it is likely due to the amino acid residues that are different between STAM-1 and STAM-2, rather than a structural component. There also appears to be specificity with respect to arrestin-2 versus arrestin-3 binding. We were unable to detect arrestin-3 binding to STAM-1 by co-immunoprecipitation, although it bound somewhat to HRS (Figure 3.3C). This is consistent with our previous finding, where it was shown that knockdown of arrestin-2 blocked CXCR4 degradation more efficiently than arrestin-3 (Bhandari et al., 2007).

Remarkably, linking GPCRs to the ESCRT machinery may be an evolutionary conserved function of arrestins. Rim8, an arrestin-like molecule in yeast *Saccharomyces cerevisiae* related to PalF, an arrestin-like molecule in the fungus *Aspergillus nidulans*, interacts with components of the ESCRT machinery (Herrador et al., 2010). Sequence homology predicts that both Rim8 and PalF share a limited amount of sequence identity with mammalian arrestins. In fungi, PalF may interact with a putative seven transmembrane domain (7TM) receptor in an analogous manner to which arrestins interact with ligand activated GPCRs (Herranz et al., 2005). Both Rim8 and PalF are

involved in a signaling cascade that senses the pH of the environment. In fungi, pH is recognized in part by the putative 7TM receptor called PalH. Akaline pH is thought to activate PalH and promotes its binding to PalF. The predicted cytoplasmic tail of PalH interacts with PalF and this interaction may be necessary to activate the intracellular signaling pathway necessary for pH sensing. Intriguingly, genetic screens in fungi have revealed that components of the ESCRT machinery, including ESCRT-I, ESCRT-II and ESCRT-III subunits Snf7 and Vps20, but not ESCRT-III subunits Vps2 and Vps24 are also necessary for pH sensing (Xu et al., 2004). Alkaline pH sensing may also be conserved in Rim8 (*Saccharomyces cerevisiae* orthologue of PalF) that binds to Rim21, a 7TM receptor with pH sensing capabilities (Herrador et al., 2010). The arrestin-like molecule Rim8 not only interacts with the receptor Rim21, it also interacts with the ESCRT machinery. Rim8 interacts with ESCRT-I subunits Vps23 and Vps28. Genetic evidence suggests that ESCRT-0 is not involved in pH sensing signaling, therefore the arrestin-like protein Rim8 may link the 7TM receptor Rim21 directly to ESCRT-I. This raises the intriguing possibility that arrestin mediated recruitment of GPCRs to the ESCRT machinery may represent a conserved function.

Role of STAM-1/arrestin-2 complex in CXCR4 sorting and degradation

Our data show that knockdown of STAM-1 significantly accelerated CXCR4 degradation, suggesting that STAM-1 in cells is a negative regulator of CXCR4 degradation (Figure 3.6A). Consistent with this, we found that depletion of STAM-1 had no effect on CXCR4 internalization and recycling that can also regulate the amount

of receptor that is degraded (Figure 3.6 B and C). In contrast, we have previously shown that arrestin-2 promotes CXCR4 degradation (Bhandari et al., 2007). We further investigated the role of STAM-1/arrestin-2 interaction and showed that disrupting this interaction by expressing minimal binding regions of both protein as minigenes enhanced agonist promoted degradation of CXCR4 (Figure 3.8B and 3.10B). Taken together our results suggest that arrestin-2 and STAM-1 act in concert to reduce the amount of CXCR4 that is degraded.

Role of arrestin-2 in CXCR4 degradation

We believe that arrestin-2 acts at multiple steps in the sorting process and may initially act upstream of STAM-1 to positively regulate sorting of CXCR4 into the degradative pathway. This is consistent with our previous model of CXCR4 recruitment into ESCRT pathway by arrestin-2. Arrestin-2 interacts directly with phosphorylated serine residue 330 in the C-tail of CXCR4 (Figure 3.1 C and D) and links it to downstream elements of the ESCRT-0 through an interaction with either HRS and/or STAM-1. Our data are consistent with a model in which arrestin-2 exerts both positive and negative effects on CXCR4 sorting and it is a balance of these two activities that dictate the extent to which CXCR4 is degraded.

Role of STAM-1/arrestin-2 interaction in CXCR4 degradation

CXCR4 undergo rapid agonist-promoted ubiquitination by E3 ligase AIP4 that is important for proper sorting and lysosomal degradation. (Marchese and Benovic, 2001;

Marchese et al., 2003). We also observed that activation of CXCR4 selectively enhances STAM-1 ubiquitination (Figure 3.4B). STAMs are also known to interact with deubiquitinating enzymes (DUBs), such as AMSH and UBPY, which play important role in regulating the ubiquitination status of cargo (e.g. EGFR) and/or of STAM itself (McCullough et al., 2004; Row et al., 2006). Therefore, one mechanism by which STAM-1/arrestin-2 interaction may regulates CXCR4 degradation is by modulating ubiquitination status of the cargo and/or STAM-1. Our data show that disrupting STAM-1/arrestin-2 interaction by expressing the STAM-1-CC minigene had no effect on either CXCR4 or STAM-1 ubiquitination (Figure 13.11 A and B). Therefore, although arrestin-2 interacts with STAM-1, arrestin-2 may not be involved in STAM-1 ubiquitination. Consistent with these findings, AMSH knockdown also had no effect on CXCR4 degradation (Figure 3.6D). Taken together, our data suggest that STAM-1/arrestin-2 complex does not regulate CXCR4 degradation via regulating ubiquitination/deubiquitination of CXCR4 and STAM-1 (Figure 3.11A).

We have previously shown (Marchese et al., 2003), and confirm here (Figure. 3.11C), that activation of CXCR4 enhances ubiquitination of HRS. HRS contains a UIM domain that mediates binding to multiple ubiquitin moieties simultaneously and is thought to bind to ubiquitin moieties on cargo to recruit them into the degradative pathway (Hirano et al., 2006). Interestingly, monoubiquitination of UBD containing proteins, such as HRS and Eps15, is thought to induce an intramolecular interaction between the ubiquitin moiety and the internal UBD. This interaction promotes the formation of an auto inhibitory conformation culminating in an inability of these proteins

to bind to ubiquitin moieties on cargo (Hoeller et al., 2006). Conceivably, in cells where STAM-1/arrestin-2 interaction was inhibited by expressing the STAM-1-CC domain, HRS ubiquitination was inhibited as well (Figure 3.11 C). Under this state, HRS could somehow enhance its sorting function possibly by facilitating interactions with ubiquitinated CXCR4 thus leading to enhanced degradation. Therefore we propose that the STAM-1/arrestin-2 interaction promotes ubiquitination of HRS, in part, to inhibit its sorting activity. As agonist activation of CXCR4 promotes ubiquitination of HRS, it would seem that CXCR4 blocks its own sorting by inhibiting HRS sorting activity. We speculate that ubiquitination of HRS also release it from ubiquitinated CXCR4 while linking it to the ESCRT-I machinery. Therefore, our data are consistent with a model whereby arrestin-2 interacts with STAM-1 to promote ubiquitination of HRS resulting in termination of its sorting function.

While HRS ubiquitination appears to regulate the amount of CXCR4 that is degraded, presently it is not clear what is the role of STAM-1 ubiquitination on CXCR4 trafficking. Polyubiquitination of STAM has been shown to promote its degradation (Row et al., 2006), however it is doubtful that CXCR4 regulates STAM-1 stability, as we did not observe any differences in STAM-1 levels in cells treated with CXCL12 (data not shown). Alternatively, ubiquitination of STAM-1 may have a role in some other aspect of CXCR4 related functions. We show that AIP4 ubiquitinates STAM-1 and that the ubiquitination activity of AIP4, as well as interaction with STAM-1, is important for CXCR4-mediated phosphorylation of ERK-1/2. This would suggest that ubiquitinated STAM-1 might regulate CXCR4 signaling via the MAPK pathway.

Role of STAM-1/arrestin-2 complex in ubiquitination of HRS

Arrestin-2 interacts with AIP4 and regulates endosomal sorting of CXCR4 (Bhandari et al., 2007). Therofore, arrestin-2 through its interaction with STAM-1 may serve as an adaptor to bridge AIP4 and HRS, which facilitates ubiquitination of HRS. There is evidence in the literature to support our model whereby arrestins can recruit a ligase to the cargo. A role for arrestins as an E3 ubiquitin ligase adaptor for receptor ubiquitination was first suggested in studies examining the regulation of β_2AR. Agonist-promoted ubiquitination of β_2AR is impaired in MEFs isolated from arrestin-3 knock-out mice, suggesting that arrestin-3 mediates ubiquitination of β_2AR. In contrast, arrestin-2 is not involved in β_2AR ubiquitination. Arrestin-3 interacts with the HECT-domain E3 ubiquitin ligase Nedd4, which mediates ubiquitination of β_2AR. Although arrestin-3 interacts with Mdm2, it does not mediate ubiquitination of β_2AR. Depletion of Nedd4 by siRNA attenuates β_2AR ubiquitination and lysosomal targeting and the interaction between β_2AR and Nedd4 is dependent upon the presence of arrestin-3. This is consistent with a role of arrestin-3 serving as an adaptor to recruit Nedd4 to β_2AR. (Shenoy et al., 2008). Similarly, yeast proteins called arrestin-related trafficking adaptors (ARTs) could recruit the E3 ligase Rsp5/Nedd4-like ubiquitin ligase to the cargo. This interaction can serve as a mechanism to provide specificity (Lin et al., 2008). Mammalian proteins called Arrestin domain-containing protein (ARRDs) also referred to as alpha-arrestins are a family of 6 mammalian proteins related to yeast ART proteins. Recently, *ARRDC3,* that has an arrestin-like domain at the N-terminus and PPXY motifs at the

C-terminus is reported to interact with β_2AR and serve as an adaptor for Nedd4-dependent ubiquitination of the receptor. Depletion of ARRDC3 attenuates agonist-induced ubiquitination and lysosomal targeting of β_2AR (Nabhan et al., 2010).

Taken together, our data are consistent with a model (Figure 4.1) in which upon activation of CXCR4, arrestin-2, through an interaction with STAM-1, promotes ubiquitination of HRS, possibly by recruiting AIP4. Thus, it appears that arrestin-2 serves as a critical molecule in regulating the interactions with, and the activities of, AIP4, HRS and STAM-1, in order to regulate the amount of CXCR4 that is degraded. However, the mechanism by which these proteins are coordinated and integrated to regulate the events that sort ubiquitinated CXCR4 into the degradative pathway remains unknown. It is also possible that arrestin-2 may be required for other events relating to the sorting process.
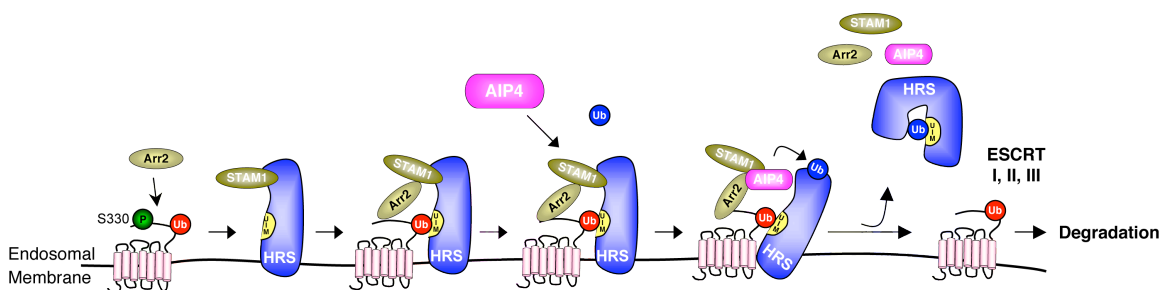
Figure 4.1. Proposed mechanism for the role of the STAM-1/arrestin-2 complex in endosomal sorting of CXCR4. CXCR4 is ubiquitinated by the E3 ubiquitin ligase AIP4 at the plasma membrane, after which it is internalized onto early endosomes, although, ubiquitination is not required for this process. Once on endosomes ubiquitinated CXCR4 is recognized by HRS, likely by an interaction involving the ubiquitin

moiety (red) on CXCR4 and the UIM of HRS, and possibly via an interaction with arrestin-2. Arrestin-2 then interacts with STAM-1, which serves to recruit AIP4 culminating in the ubiquitination of HRS. We speculate that this triggers a conformational change in HRS induced by an interaction between the ubiquitin moiety (blue) and the internal UIM. CXCR4 is subsequently committed to downstream interactions with ESCRT-I-III, whereas arrestin-2, STAM-1, AIP4, and autoinhibited HRS are recycled for an another round of sorting to take place.

Role of STAM-1, arrestin-2 and AIP4 in CXCR4 mediated cell migration

CXCR4 signaling is normally under very tight regulation, however, dysregulated CXCR4 signaling and expression levels have been linked to several pathologies including WHIM syndrome and cancers (Balabanian et al., 2005; Li et al., 2004). In particular, in a subset of breast cancers, defective ubiquitination and endosomal sorting of CXCR4 has been associated with increased CXCR4 levels and metastatic potential of tumor cells (Li et al., 2004). Our data suggest that both STAM-1 and arrestin-2 are important for CXCR4-mediated migration of HeLa cells (Figure 3.12). However, the mechanism remains to be determined. Interestingly, disrupting STAM-1/arrestin-2 interaction also inhibits CXCR4-mediated HeLa cell migration (data not shown). We have shown that CXCR4 is negatively regulated by STAM-1 in cells (Figure 3.6A), hence one possible explanation for inhibition of cell migration could be an effect of STAM-1 knockdown on CXCR4 protein levels/surface expression. However, we do not think that CXCR4 protein levels regulate migration because: (1) although arrestin-2 knockdown inhibits CXCR4 degradation (Bhandari et al., 2007), it blocks CXCR4 mediated migration (Figure 3.12), (2) No effect of STAM-1 and arrestin-2 knockdown was observed on

surface expression of CXCR4, as compared to control siRNA treated cells (Figure 3.13). Taken together, our data suggest that STAM-1 and arrestin-2 regulate CXCR4 promoted cell migration via signaling pathways independent of CXCR4 protein levels.

CXCR4 promoted ERK signaling has been linked to cell migration. Yu et al., showed that CXCR4 promoted ERK activation induces expression of MMP-9 and 13 that are required for migration of oral squamous carcinoma cells (Yu et al., 2011). Our data suggest that inhibition of CXCR4-mediated cell migration is independent of its effects on ERK-1/2 phosphorylation. Some of the key observations that support this data are: (1) AIP4 knockdown inhibits ERK-1/2 phosphorylation, but has no effect on migration of HeLa cells (Figure 3.12A and 3.14F), (2) Arrestin-2 knockdown inhibits cell migration but has an opposite effect on ERK-1/2 phosphorylation (Figure 3.14A and B), (3) Disrupting the STAM-1/arrestin-2 interaction inhibits migration, but does not affect ERK-1/2 phosphorylation (Figure 3.14 I and J). Taken together, these observations suggest that a signaling pathway other than ERK is responsible for STAM-1/arrestin-2 promoted cell migration. Consistent with our findings, Mines et al, reported that CXCR4-mediated migration is independent of ERK activation. These authors have shown that a ubiquitination deficient CXCR4 mutant (3KR) is defective in promoting cell migration, however, activation of ERK was indistinguishable between wild type CXCR4 and CXCR4-3K/R mutant, suggesting that chemotaxis in response to CXCL12 is independent of the ERK cascade (Mines et al., 2009). Interestingly, in *Drosophila melanogaster*, STAM is required for migration of tracheal cells to air sac primordium. Both STAM and HRS are required for efficient FGFR signaling during cell migration in

the air sac primordium and during the formation of fine cytoplasmic extensions in terminal cells (Chanut-Delalande et al., 2010), suggesting a role of ESCRT-0 in cellular migration.

Role of STAM-1 and AIP4 in CXCR4 mediated ERK-1/2 phosphorylation

Agonist binding to CXCR4 stimulates multiple downstream signaling pathways such as Akt and ERK-1/2, which mediate CXCR4-induced cell survival and migration (Busillo and Benovic, 2007). Despite the importance of CXCR4 signaling in development and disease, the molecular mechanisms mediating CXCR4 signaling remain poorly understood. Here, we show that a discrete subpopulation of STAM-1 and AIP4, but not arrestin, mediates ERK signaling upon activation of CXCR4 (Figure 3.13). We delineated a novel molecular mechanism by which the chemokine receptor CXCR4 promotes activation of the ERK signaling cascade. Interaction between E3 ubiquitin ligase AIP4 and the STAM-1 acts as a positive regulator of ERK-1/2 phosphorylation. Both proteins have previously been shown to help sort CXCR4 and other cargo on endosomes for lysosomal degradation. However, their role in signaling is likely mediated by a subpopulation that is restricted in distribution to caveolae. Interestingly, AIP4 binding to, and ubiquitination of STAM-1, may be required for this process, suggesting a novel role for ubiquitin in cell signaling. We propose a model whereby spatial segregation of AIP4-mediated ubiquitination of STAM-1 in caveolae is required for CXCR4 signaling and possibly signaling mediated by other GPCRs.

Interaction between STAM-1 and AIP4

Our data suggest that AIP4, through an interaction with STAM-1, mediates CXCR4-induced ERK-1/2 phosphorylation (Figure 3.17A). Over-expression of wild-type AIP4 and STAM-1 led to a significant increase in ERK-1/2 phosphorylation. Remarkably, over-expression of AIP4-ΔPRR, a mutant that does not bind to STAM-1, failed to enhance ERK-1/2 phosphorylation, suggesting that the interaction between AIP4 and STAM-1 is necessary for mediating CXCR4-induced ERK-1/2 activation. We also show that the ubiquitin ligase activity of AIP4 is required for this process, as expression of a catalytically inactive AIP4 mutant (C830A) failed to enhance ERK-1/2 phosphorylation (Figure 3.17B). One possible role of the interaction between AIP4 and STAM-1 may be to activate and/or enhance AIP4 ligase activity. AIP4 exists in an auto-inhibitory conformation via an intra-molecular interaction between the HECT-domain and the WW domains (Gallagher et al., 2006). Phosphorylation of serine/threonine residues within the proline-rich region releases the intra-molecular inhibition thereby enabling AIP4 to interact with and ubiquitinate target substrates. STAM-1 binding to AIP4 may function in an analogous manner by alleviating the auto-inhibited state, resulting in ubiquitination of other target substrates that remains to be identified. One possible substrate can be STAM-1 itself. Consistent with this, we show that CXCR4 promoted STAM-1 ubiquitination was observed at 5 min after agonist treatment, in line with when ERK-1/2 activation is maximal, raising the possibility that STAM-1 ubiquitination is required for this process (Figure 3.17C). However, the mechanism by which ubiquitination of STAM-1 may promote ERK-1/2 activation remains to be

determined. STAM-1 ubiquitination does not appear to be required for CXCR4 endosomal sorting and STAM-1 protein levels do not change after CXCR4 activation (Malik and Marchese, 2010), therefore, it is unlikely that ubiquitination mediates degradation of STAM-1. Interestingly, STAM also binds to the deubiquitinating enzymes AMSH and USP8 via its SH3 domain (Kato et al., 2000), but whether they are involved in CXCR4 signaling remains to be determined. We have recently shown that AMSH does not mediate agonist-induced degradation of CXCR4 (Malik and Marchese, 2010). Ubiquitin has previously been shown to play a role in GPCR-induced ERK signaling. Ubiquitination of arrestin-3 by the E3 ligase Mdm2 induces a stable association between arrestin-3 and phosphorylated ERK-1/2 following activation of a subset of GPCRs (Shenoy et al., 2007). Ubiquitinated arrestin-3 co-internalizes with the GPCR and pERK-1/2 onto endosomes, retaining bound pERK-1/2 on endosomes to act on cytosolic factors (DeWire et al., 2007). Although, we have previously shown that arrestins interact with STAM-1, our data indicate that arrestins do not regulate ERK-1/2 signaling (Figure 3.13 A and B). To our knowledge, this present study represents the first to report a direct link between ubiquitin and an ESCRT protein in the regulation of GPCR stimulated ERK-1/2 signaling.

STAM-1 and AIP4 mediated signaling originates proximal to the plasma membrane

CXCR4 induced phosphorylation of ERK-1/2 is rapid and transient reaching a maximum response at 5 min after treatment with agonist and returning to basal levels by 10 min of agonist treatment. A time course (0-60 min) of agonist stimulation also

indicates that phosphorylation of ERK-1/2 peaks at 5 min and returns to basal levels by 10 min and remaining for up to 60 min after agonist treatment (Figure 3.14C), however, there is no second peak of ERK-1/2 activation/phosphorylation. Taken together, our data suggest that ERK signaling initiates proximal to the receptor at the plasma membrane. However, signaling can be sustained on endosomes, as we see phosphorylated ERK-1/2 species even 60 min after activation. For some GPCRs, such as the angiotensin AT_{1A} receptor, agonist induced ERK-1/2 activation is also a rapid process, but in contrast to what is observed for CXCR4, ERK-1/2 activation remains sustained for 90 min following receptor activation (Ahn et al., 2004). The early and late elements of ERK-1/2 activation are mechanistically distinct occurring through G protein-dependent and independent mechanisms. The initial signal is G protein-dependent and leads to nuclear localization of pERK-1/2, while the later sustained signal is arrestin-dependent and sequesters pERK-1/2 on endosomes in the cytoplasm (Ahn et al., 2004).

The transient nature of ERK-1/2 activation induced by CXCR4 and the rapid appearance of pERK-1/2 in the nucleus following receptor activation is consistent with G protein-dependent signaling occurring proximal to the receptor at the plasma membrane. In addition, CXCR4-induced pERK-1/2 signaling is completely blocked by pretreatment with pertussis toxin, an inhibitor of $G\alpha_i$ (data not shown). A lack of sustained pERK-1/2 levels argues against a later endosomal associated signaling event and inhibiting endocytosis using siRNA against μ2 subunit of AP2 complex and expression of dynamin K44A mutant has no effect on CXCR4 induced ERK-1/2 activation (Figure 3.18). However, we cannot rule out the possibility that an endosomal associated signaling event

may occur rapidly through the action of a second messenger and/or some other molecule. Our data also reveals that arrestins are not directly involved in CXCR4 mediated ERK signaling (Figure. 3.14 A and B). It was recently reported that siRNA mediated depletion of arrestin-2, and perhaps to a lesser degree arrestin-3, attenuated CXCR4-induced ERK-1/2 activation in HEK293 cells, suggesting that arrestin-2 regulates CXCR4 mediated ERK signaling (Busillo et al., 2010; Sun et al., 2002). This discrepancy with our study is likely a consequence of differences in experimental design as we performed our experiments using HeLa cells in which both non-visual arrestins were depleted simultaneously and in arrestin-2/3 double knockout MEFs. Nevertheless, we do not believe that arrestin-2 interacts with STAM-1 to modulate CXCR4-induced ERK-1/2 activation, as expression of minigenes (STAM-CC and arrestin-2-25-161) that disrupt this interaction do not affect CXCR4-induced ERK-1/2 activation (Figure 3.14 I and J). However, the possibility that arrestins can modulate CXCR4 signaling on endosomes cannot be ruled out since depleting arrestins in cells is a limiting step as arrestins are involved in initial desensitization of receptor signaling. Nevertheless, our data are consistent with the idea that CXCR4 signaling is regulated by STAM-1 and AIP4 possibly proxial to the plasma membrane.

Role of caveolae in GPCR signaling

Lipids rafts have been implicated in CXCR4 signaling in T cells (Nguyen and Taub, 2002), as well as in prostate cancer cell lines where CXCR4 induces transactivation of receptor tyrosine kinase HER2 in lipid rafts (Chinni et al., 2008). Caveolae, a subset

of lipid raft microdomains that contain caveolin proteins, help to organize several signal transduction systems (Patel et al., 2008). Caveolin-1, a major component of caveolae, is thought to scaffold components of G protein signaling pathways, including heterotrimeric G proteins and their effector molecules (Oh and Schnitzer, 2001). Caveolin is also found to be upregulated in hepatocellular carcinoma cells where a positive correlation between caveolin-1 expression and invasion, metastasis and recurrence has been shown. Overexpression of caveolin-1 in HepG2 cells protects cell from apoptosis, as well as increases expression of MMP-2, MMP-9 and VGEF that lead to increase in migration and invasion (Tang et al., 2011).

Here we show that CXCR4 and its cognate G protein Gαi, along with both AIP4 and STAM-1, co-fractionate with caveolin-1 in buoyant membrane fractions suggesting that they are localized to caveolae (Figure 3.20 A). We also show by confocal microscopy that CXCR4, AIP4 and STAM-1 co-localize with caveolin-1 at the plasma membrane (Figure 3.20 B and D) as well as co-immunoprecipitate in HEK293 and HeLa cell (Figure 3.20 E and F). Depletion of caveolin-1 by siRNA, or treatment of cells with the cholesterol sequestering drug nystatin, attenuated CXCR4-induced phosphorylation of ERK-1/2 suggesting that caveolae are important for CXCR4 signaling. We propose that a subpopulation of AIP4 and STAM-1 localized to caveolae and/or lipid rafts is essential for CXCR4-induced ERK-1/2 activation. It is possible that within caveolae AIP4 and STAM-1 facilitate or stabilize receptor/G protein interactions and consequently facilitate downstream signaling. Alternatively, AIP4 and STAM-1 may be directly involved in receptor/G protein signaling.

AIP4 and STAM-1 segregate into caveolae and/or lipid rafts

Agonist treatment had no effect on the relative amounts of CXCR4, STAM-1, and AIP4 that cofractionated with caveolin-1, suggesting that they may be constitutively associated with caveolae. AIP4 belongs to the Nedd4-family of E3 ubiquitin ligase and one important feature of this family is that they encode a C2 domain (Ingham et al., 2004). The C2 domain of AIP4 has been shown to have a role in membrane targeting (Angers et al., 2004; Jadwin et al., 2010). The C2-domain of other members of the Nedd4-like family has been shown to bind to membrane phospholipids (Dunn et al., 2004; Wiesner et al., 2007). Interestingly, caveolin-1 was co-immunoprecipitated with AIP4 and STAM-1, suggesting that AIP4 and STAM-1 may be scaffolded by caveolin-1 and thus may be recruited to caveolae through this interaction (Figure 3.20 E and F). Lipid rafts have been implicated in CXCR4 signaling in T cell lines and in prostate cancer cell lines where CXCR4-induced transactivation of the receptor tyrosine kinase HER2 contributes to Akt activation and potentially to tumor invasiveness (Chinni et al., 2006; Chinni et al., 2008; Nguyen and Taub, 2002). Therefore, segregation of CXCR4 into caveolae and/or lipid rafts may be required for multiple signaling pathways and its role in cancer biology and possibly other diseases. Although depletion of STAM-1 and AIP4 had no effect on the recruitment of CXCR4 into the caveolar compartment (Figure 3.21), it is possible that STAM-1 and AIP4 are required for the assembly of the downstream components in the caveolar compartment. Interestingly, AIP4 has been shown to interact with Jun amino-terminal kinase 1 (JNK1) via a MAP kinase docking domain located within its HECT domain (Gallagher et al., 2006). T cell receptor-

induced JNK1-mediated phosphorylation of AIP4 leads to ubiquitination and proteasomal degradation of the Jun transcription factor, which regulates cytokine production in T cells (Gao et al., 2004). AIP4 may also negatively regulate JNK signaling following sorbitol induced stress by mediating ubiquitination and degradation of MKK4, the upstream activator of JNK (Ahn and Kurie, 2009). Our data are consistent for a   role of AIP4 in positively regulating ERK-1/2 activation induced by a GPCR. Although, the precise mechanism remains unknown, the role that AIP4 plays in this process appears to require an interaction with STAM-1.

Clathrin-coated pit-associated CXCR4 is not involved in ERK-1/2 phosphorylation

CXCR4, STAM-1 and AIP4 also co-fractionate with heavy membrane fractions, consistent with their presence in clathrin-coated pits and/or endosomal membranes (Figure 3.20A). However, their presence in clathrin-coated pits and internalization onto endosomes are not required for ERK signaling, as depletion of the µ2 subunit of AP2, as well as over-expression of catalytically inactive dynamin (K44A) mutant, had no effect on CXCR4 mediated ERK-1/2 phosphorylation (Figure 3.18 A and C). We also observed minimal co-localization between STAM-1 and AP2 in our confocal microscopy studies (Figure 3.19). STAM-1 co-fractionated with heavy membrane fractions containing AP2 (Figure 3.20A), however, these fractions also contain endosomal membranes, where we have shown that STAM-1 co-localizes with CXCR4 (Figure 3.5 A and B). Therefore, the pool of STAM-1 that is localized to the plasma membrane may be restricted to caveolae and/or lipids rafts. It may be targeted to this compartment because of its ability

to associate with caveolin-1 and/or AIP4 (Figure 3.20 E and F). STAM-1 is mostly known for its role as a component of ESCRT-0, an endosomal associated protein complex involved in targeting ubiquitinated CXCR4 and other ubiquitinated cargo into the degradative pathway. STAM-1 and STAM-2 were originally identified as substrates for tyrosine phosphorylation downstream of several cytokine and growth factor receptors (Endo et al., 2000; Lohi and Lehto, 1998; Takeshita et al., 1996; Takeshita et al., 1997). They were shown to play a role in cytokine-induced T-cell development and survival, possibly through an interaction with Janus kinases but not via ERK-1/2 and Akt activation (Yamada et al., 2002). Our study reveal a novel role for STAM-1 in cell signaling and whether other components of the ESCRT machinery are involved remains to be determined.

Summary and current model for CXCR4 signaling and downregulation

Our current understanding of CXCR4 signaling and downregulation is summarized in figure 4.3. We have identified a novel role of arrestin-2 through its interaction with STAM-1 in endosomal sorting and degradation of CXCR4. An interaction between arrestin-2 and STAM-1 serves to recruit AIP4 that in-turn regulates the ubiquitination status of HRS. Together this complex is required for sorting and downregualtion of CXCR4. We have also identified a novel function for the AIP4/STAM-1 complex in CXCR4-mediated phosphorylation of ERK-1/2, which is different from their roles in endosomal trafficking. AIP4 binding to, and ubiquitination of STAM-1, may occur in caveolae and not in clathrin-coated pits and/or endosomes,

where AIP4 and STAM-1 have been previously shown to be located. This interaction is important for CXCR4-mediated activation of MAPK signaling, which is associated with cancer metastasis and tumor growth (Busillo and Benovic, 2007; Rubin et al., 2003; Yu et al., 2011).

The information from this study may provide useful insight into the development of novel therapeutic targets for treating diseases in which CXCR4 is involved.
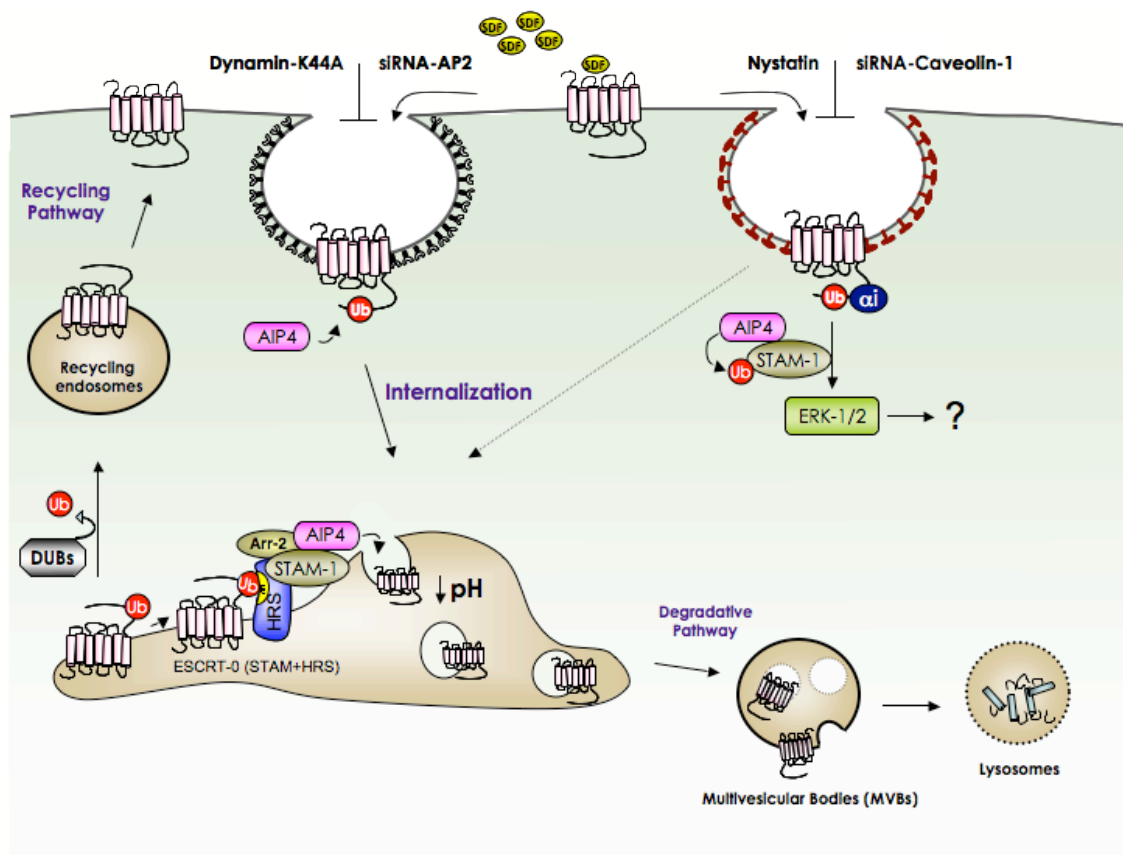
Figure 4.2 Model for the regulation of CXCR4 signaling and downregualtion

Upon activation by its cognate ligand CXCL12, CXCR4 can be sequestered into specialized microdomains of the plasma membrane such as clathrin coated pits (CCPs) and caveolae. Caveolar pool of CXCR4 interacts with STAM-1 and AIP4 to activate ERK-1/2. Intereaction between AIP4 and STAM-1 as well

as ligase activity of AIP4 play an important role in CXCR4 mediated ERK-1/2 phosphorylation. Ubiquitinated CXCR4 is sequestered in the clathrin coated pits and endocytosed. Receptor is delivered to early endosomes where it gets sorted into the multivesicular bodies. Protein complex composed of STAM-1, arrestin-2 play an important role in the sorting process. STAM-1/arrestin-2 complex recruits AIP4 on endosomes that inturn ubiquitinates HRS. Ubiquitination of HRS is a key process in the trafficking of CXCR4 to the downstream ESCRT complexes. Receptor is ultimately sequestered into the MVBs which fuses with the lysosomes to complete the degradation process. Some receptors may get deubiquitinated and are redirected into the recycling pathway that delivers the receptor back to the plasma membrane.

FUTURE DIECTIONS

This study was focused on understanding the role of arestin-2 in endosomal sorting and degradation of CXCR4. Although the importance of arestin-2/STAM-1 interaction in CXCR4 endosomal sorting was clarified, there are several critical questions that remain to be explored in order to completely understand this novel role of arrestin-2. Some of the important future directions are discussed below.

Recruitment of arrestin-2 to the receptor following agonist stimulation

We show that arrestin-2 directly interacts with STAM-1 on endosomes to possibly recruit the E3 ubiquitin ligase AIP4. Together with AIP4, the STAM-1/arrestin-2 complex regulates CXCR4 sorting and degradation. However, whether arrestin-2 traffics with the receptor to endosomes, or is recruited directly to the endosomal bound receptor remains to be investigated. Previous work, and work done in this study, suggests that arrestin-2 can directly interact with CXCR4, and that the C- tail

is important for this interaction (Figure 3.1B). We also show that serine residue 330 in the C-tail of CXCR4 is critical for interaction with arrestin-2 (Figure 3.1C). Since it is a serine residue it is logical to speculate that phosphorylation may modulate this interaction. In fact, it has been recently shown by Busillo et al., that serine residue 330 is phosphorylated by GRK6 in response to agonist stimulation (Busillo et al., 2010). The time frame in which the receptor gets phosphorylated (15-20 min) is consistent with the time required for the receptor to internalize and appear on early endosomes. Taken together, we popose a model whereby, phosphorylation of the receptor at serine residue 330 by GRK6, post internalization, recruits arrestin-2 directly on the endosomes. Once recruited, arrestin-2 can interact with and recruit the receptor into the ESCRT machinery (Figure 4.2). Although, we did not test this hypothesis directly, we provide evidence that arrestin-2 co-localizes with the receptor on early endosomes upon agonist stimulation for 30 min (Figure 3.2 A, B).
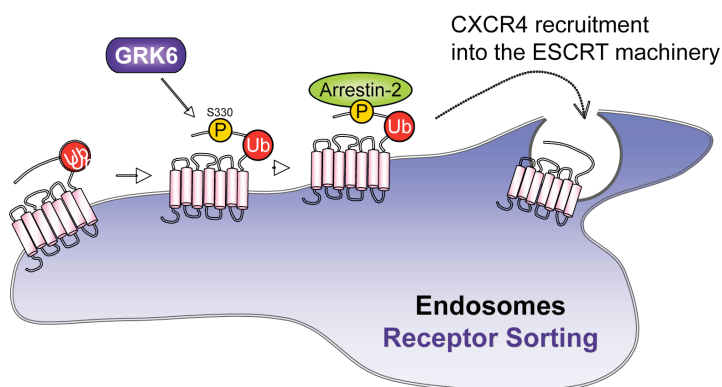
Figure 4.3 Proposed model for the role of arresitn-2 in recruitment of CXCR4 into the ESCRT pathway. Arrestin-2 interacts directly with receptor via phosphorylation of serine residue 330 in the C-tail of

receptor possible on the endosomes. Further, aarrestin-2 interacts with ESCRT-0 proteins and recruits the receptor into the ESCRT sotting pathway.

However, several key questions remain to be addressed: 1) Is Serine residue 330 phosphorylated on endosomes?; 3) Does GRK6 co-localize with arrestin-2 on endosomes, and if GRK6 is the kinase for S330 phosphorylation, what is the role of GRK6 in endosomal trafficking of CXCR4?

Our data indicate that arrestin-2 interacts with ESCRT-0. Whether arrestin-2 also interacts with other ESCRT proteins reamains to be determined. Whether arrestins are required for the transfer of the receptor to downstream ESCRT components remains to be determined.

Role of the STAM-1/arrestin-2 interaction in cell migration

We show that the STAM-1/arrestin-2 interaction regulates CXCR4 degradation by negatively regulating the process of endosoal sorting. Why CXCR4 is retained on the early endosomes remain to be determined. One possible role for CXCR4 on endosomes might be to regulate signaling pathways involved in cellular migration. We show that both STAM-1 and arrestin-2 knockdown, as well as inhibition of the STAM-1/arrestin-2 complex accelerates CXCR4 degradation and in-turn inhibits migration of HeLa cells. This sugests that the signaling pathway originating from endosomes can regulate cellular migration. Infact, the family of small Rho-like GTPases such as Cdc42, Rac1, and RhoA have been shown to play role in migration of cells. These GTPases activate a variety of

signaling pathways that control cell migration by regulating cytoskeletal rearrangements such as formation of filopodia, lamellipodia and actin rearrangment. Ral, which is another member of the Ras family of small GTPases, has been shown to induce CXCL12-promoted migration of B cells and multiple myeloma cells (de Gorter et al., 2008). Rac has been shown to be activated by Tiam-1, a guanidine nucleotide exchange factor (GEF) for Rac, on endosomes. Inhibition of Rab5-dependent endocytosis prevents Rac activation and hence migration (Palamidessi et. al., 2008) One possible mechanism by which STAM-1/arrestin-2 complex promotes cell migration is via regulating the small GTPase-mediated cytoskeletal rearrangement.

Role of AIP4 ubiquitination activity and AIP4/STAM-1 interaction in ERK signaling

Our data suggest that both STAM-1 and AIP4 are important for CXCR4 promoted ERK-1/2 phosphorylation. Interaction between STAM-1/AIP4 is important for ERK-1/2 phosphorylation, however, the mechanism by which this complex functions to regulate signaling via ERK-1/2 remains to be determined. Our data suggest that ERK-1/2 co-immunoprecipitated in complex with STAM-1 and AIP4 (data not shown). Whether STAM-1/AIP4 complex merely serves as a scaffold to bring the upstream MAPKK (i.e MEK) closer to the substrate (ERK) or whether the complex directly regulates the phosphorylation of ERK-1/2 remains to be determined.

We also show that the ligase activity of AIP4 is important for CXCR4 promoted ERK-1/2 phosphorylation. AIP4 ubiquitinates STAM-1 within 5 min of agonist stimulation. However, the precise role of AIP4 ubiquitination activity, as well as the role

of ubiquitinated STAM-1 in CXCR4 signaling remains unclear. One approach to address the role of ubiquitinated STAM-1 in signaling would be to identify the lysine residues on STAM-1 that are ubiquitinated by AIP4. Expression of STAM-1 ubiquitination-deficient mutant in cells would provide insight into the role of STAM-1 ubiquitination in ERK-1/2 phosphorylation.

ERK-1/2 has been shown to be ubiquitinated. The PHD domain of MEKK1 acts as an E3 ligase to ubiquitinate ERK-1/2 to promote its degradation (Lu et al., 2002). Whether ubiquitination of ERK-1/2 is mediated by AIP4 in context to CXCR4 stimulation remain to be determined.

CONCLUSION

The present study provides mechanistic insight into the role of arrestin-2 in downregulation of chemokine receptor CXCR4. We show that in addition to their role in GPCR desensitization, internalization and recycling, arrestins also function in endosomal sorting of CXCR4. We also identified a novel pathway composed of STAM-1 and AIP4 that regulates CXCR4 signaling in speciliazed microdomains called caveolae. We also show that the ligase activity of AIP4 is critical for this process. To our knowledge this is the first report demonstrating the role of ubiquitin in GPCR signaing. Overall, this study provides insight into the regulation of CXCR4 biology with potantial implicitations for designing novel interventions in pathologies related to CXCR4 dysfunction.

BIBLIOGRAPHY

Agromayor, M., and Martin-Serrano, J. (2006). Interaction of AMSH with ESCRT-III and deubiquitination of endosomal cargo. The Journal of biological chemistry *281*, 23083-23091.

Ahn, S., Shenoy, S. K., Wei, H., and Lefkowitz, R. J. (2004). Differential kinetic and spatial patterns of beta-arrestin and G protein-mediated ERK activation by the angiotensin II receptor. The Journal of biological chemistry *279*, 35518-35525.

Ahn, Y. H., and Kurie, J. M. (2009). MKK4/SEK1 is negatively regulated through a feedback loop involving the E3 ubiquitin ligase itch. The Journal of biological chemistry *284*, 29399-29404.

Alapi, K., Erdos, M., Kovacs, G., and Marodi, L. (2007). Recurrent CXCR4 sequence variation in a girl with WHIM syndrome. European journal of haematology *78*, 86-88.

Altenbach, C., Kusnetzow, A. K., Ernst, O. P., Hofmann, K. P., and Hubbell, W. L. (2008). High-resolution distance mapping in rhodopsin reveals the pattern of helix movement due to activation. Proceedings of the National Academy of Sciences of the United States of America *105*, 7439-7444.

Altenburg, J. D., and Siddiqui, R. A. (2009). Omega-3 polyunsaturated fatty acids down-modulate CXCR4 expression and function in MDA-MB-231 breast cancer cells. Mol Cancer Res *7*, 1013-1020.

Amerik, A. Y., and Hochstrasser, M. (2004). Mechanism and function of deubiquitinating enzymes. Biochim Biophys Acta *1695*, 189-207.

Angers, A., Ramjaun, A. R., and McPherson, P. S. (2004). The HECT domain ligase itch ubiquitinates endophilin and localizes to the trans-Golgi network and endosomal system. The Journal of biological chemistry *279*, 11471-11479.

Asao, H., Sasaki, Y., Arita, T., Tanaka, N., Endo, K., Kasai, H., Takeshita, T., Endo, Y., Fujita, T., and Sugamura, K. (1997). Hrs is associated with STAM, a signal-transducing adaptor molecule. Its suppressive effect on cytokine-induced cell growth. The Journal of biological chemistry *272*, 32785-32791.

Babst, M., Katzmann, D. J., Estepa-Sabal, E. J., Meerloo, T., and Emr, S. D. (2002a). Escrt-III: an endosome-associated heterooligomeric protein complex required for mvb sorting. Developmental cell *3*, 271-282.

Babst, M., Katzmann, D. J., Snyder, W. B., Wendland, B., and Emr, S. D. (2002b). Endosome-associated complex, ESCRT-II, recruits transport machinery for protein sorting at the multivesicular body. Developmental cell *3*, 283-289.

Babst, M., Odorizzi, G., Estepa, E. J., and Emr, S. D. (2000). Mammalian tumor susceptibility gene 101 (TSG101) and the yeast homologue, Vps23p, both function in late endosomal trafficking. Traffic (Copenhagen, Denmark) *1*, 248-258.

Bache, K. G., Brech, A., Mehlum, A., and Stenmark, H. (2003). Hrs regulates multivesicular body formation via ESCRT recruitment to endosomes. J Cell Biol *162*, 435-442.

Balabanian, K., Lagane, B., Pablos, J. L., Laurent, L., Planchenault, T., Verola, O., Lebbe, C., Kerob, D., Dupuy, A., Hermine, O., *et al.* (2005). WHIM syndromes with different genetic anomalies are accounted for by impaired CXCR4 desensitization to CXCL12. Blood *105*, 2449-2457.

Balabanian, K., Levoye, A., Klemm, L., Lagane, B., Hermine, O., Harriague, J., Baleux, F., Arenzana-Seisdedos, F., and Bachelerie, F. (2008). Leukocyte analysis from WHIM syndrome patients reveals a pivotal role for GRK3 in CXCR4 signaling. J Clin Invest *118*, 1074-1084.

Balkwill, F. (2004). The significance of cancer cell expression of the chemokine receptor CXCR4. Semin Cancer Biol *14*, 171-179.

Barker, B. L., and Benovic, J. L. (2011). G protein-coupled receptor kinase 5 phosphorylation of hip regulates internalization of the chemokine receptor CXCR4. Biochemistry *50*, 6933-6941.

Barlic, J., Andrews, J. D., Kelvin, A. A., Bosinger, S. E., DeVries, M. E., Xu, L., Dobransky, T., Feldman, R. D., Ferguson, S. S., and Kelvin, D. J. (2000). Regulation of tyrosine kinase activation and granule release through beta-arrestin by CXCRI. Nat Immunol *1*, 227-233.

Beaulieu, J. M., Sotnikova, T. D., Marion, S., Lefkowitz, R. J., Gainetdinov, R. R., and Caron, M. G. (2005). An Akt/beta-arrestin 2/PP2A signaling complex mediates dopaminergic neurotransmission and behavior. Cell *122*, 261-273.

Bernhagen, J., Krohn, R., Lue, H., Gregory, J. L., Zernecke, A., Koenen, R. R., Dewor, M., Georgiev, I., Schober, A., Leng, L., *et al.* (2007). MIF is a noncognate ligand of CXC chemokine receptors in inflammatory and atherogenic cell recruitment. Nat Med *13*, 587-596.

Bhandari, D., Robia, S. L., and Marchese, A. (2009). The E3 ubiquitin ligase atrophin interacting protein 4 binds directly to the chemokine receptor CXCR4 via a novel WW domain-mediated interaction. Molecular biology of the cell *20*, 1324-1339.

Bhandari, D., Trejo, J., Benovic, J. L., and Marchese, A. (2007). Arrestin-2 interacts with the ubiquitin-protein isopeptide ligase atrophin-interacting protein 4 and mediates endosomal sorting of the chemokine receptor CXCR4. The Journal of biological chemistry *282*, 36971-36979.

Bilodeau, P. S., Urbanowski, J. L., Winistorfer, S. C., and Piper, R. C. (2002). The Vps27p Hse1p complex binds ubiquitin and mediates endosomal protein sorting. Nat Cell Biol *4*, 534-539.

Bowerman, B., and Kurz, T. (2006). Degrade to create: developmental requirements for ubiquitin-mediated proteolysis during early C. elegans embryogenesis. Development (Cambridge, England) *133*, 773-784.

Broxmeyer, H. E., Cooper, S., Kohli, L., Hangoc, G., Lee, Y., Mantel, C., Clapp, D. W., and Kim, C. H. (2003). Transgenic expression of stromal cell-derived factor-1/CXC chemokine ligand 12 enhances myeloid progenitor cell survival/antiapoptosis in vitro in response to growth factor withdrawal and enhances myelopoiesis in vivo. J Immunol *170*, 421-429.

Burd, C. G., and Emr, S. D. (1998). Phosphatidylinositol(3)-phosphate signaling mediated by specific binding to RING FYVE domains. Mol Cell *2*, 157-162.

Busillo, J. M., Armando, S., Sengupta, R., Meucci, O., Bouvier, M., and Benovic, J. L. (2010). Site-specific phosphorylation of CXCR4 is dynamically regulated by multiple kinases and results in differential modulation of CXCR4 signaling. The Journal of biological chemistry.

Busillo, J. M., and Benovic, J. L. (2007). Regulation of CXCR4 signaling. Biochim Biophys Acta *1768*, 952-963.

Cao, T. T., Deacon, H. W., Reczek, D., Bretscher, A., and von Zastrow, M. (1999). A kinase-regulated PDZ-domain interaction controls endocytic sorting of the beta2-adrenergic receptor. Nature *401*, 286-290.

Chang, L., Kamata, H., Solinas, G., Luo, J. L., Maeda, S., Venuprasad, K., Liu, Y. C., and Karin, M. (2006). The E3 ubiquitin ligase itch couples JNK activation to TNFalpha-induced cell death by inducing c-FLIP(L) turnover. Cell *124*, 601-613.

Chanut-Delalande, H., Jung, A. C., Baer, M. M., Lin, L., Payre, F., and Affolter, M. (2010). The Hrs/Stam complex acts as a positive and negative regulator of RTK signaling during Drosophila development. PloS one *5*, e10245.

Chastagner, P., Israel, A., and Brou, C. (2006). Itch/AIP4 mediates Deltex degradation through the formation of K29-linked polyubiquitin chains. EMBO Rep *7*, 1147-1153.

Chen, L., and Davis, N. G. (2002). Ubiquitin-independent entry into the yeast recycling pathway. Traffic (Copenhagen, Denmark) *3*, 110-123.

Cheng, Z. J., Zhao, J., Sun, Y., Hu, W., Wu, Y. L., Cen, B., Wu, G. X., and Pei, G. (2000). beta-arrestin differentially regulates the chemokine receptor CXCR4-mediated signaling and receptor internalization, and this implicates multiple interaction sites between beta-arrestin and CXCR4. The Journal of biological chemistry *275*, 2479-2485.

Chinni, S. R., Sivalogan, S., Dong, Z., Filho, J. C., Deng, X., Bonfil, R. D., and Cher, M. L. (2006). CXCL12/CXCR4 signaling activates Akt-1 and MMP-9 expression in prostate cancer cells: the role of bone microenvironment-associated CXCL12. The Prostate *66*, 32-48.

Chinni, S. R., Yamamoto, H., Dong, Z., Sabbota, A., Bonfil, R. D., and Cher, M. L. (2008). CXCL12/CXCR4 transactivates HER2 in lipid rafts of prostate cancer cells and promotes growth of metastatic deposits in bone. Mol Cancer Res *6*, 446-457.

Cho, E. Y., Cho, D. I., Park, J. H., Kurose, H., Caron, M. G., and Kim, K. M. (2007). Roles of protein kinase C and actin-binding protein 280 in the regulation of intracellular trafficking of dopamine D3 receptor. Mol Endocrinol *21*, 2242-2254.

Christopherson, K. W., 2nd, Hangoc, G., and Broxmeyer, H. E. (2002). Cell surface peptidase CD26/dipeptidylpeptidase IV regulates CXCL12/stromal cell-derived factor-1 alpha-mediated chemotaxis of human cord blood CD34+ progenitor cells. J Immunol *169*, 7000-7008.

Chu, T., Sun, J., Saksena, S., and Emr, S. D. (2006). New component of ESCRT-I regulates endosomal sorting complex assembly. J Cell Biol *175*, 815-823.

Cottrell, G. S., Padilla, B., Pikios, S., Roosterman, D., Steinhoff, M., Gehringer, D., Grady, E. F., and Bunnett, N. W. (2006). Ubiquitin-dependent down-regulation of the neurokinin-1 receptor. The Journal of biological chemistry *281*, 27773-27783.

Courbard, J. R., Fiore, F., Adelaide, J., Borg, J. P., Birnbaum, D., and Ollendorff, V. (2002). Interaction between two ubiquitin-protein isopeptide ligases of different classes, CBLC and AIP4/ITCH. The Journal of biological chemistry *277*, 45267-45275.

Damas, J. K., Eiken, H. G., Oie, E., Bjerkeli, V., Yndestad, A., Ueland, T., Tonnessen, T., Geiran, O. R., Aass, H., Simonsen, S.*, et al.* (2000). Myocardial expression of CC- and CXC-chemokines and their receptors in human end-stage heart failure. Cardiovasc Res *47*, 778-787.

Dambly-Chaudiere, C., Cubedo, N., and Ghysen, A. (2007). Control of cell migration in the development of the posterior lateral line: antagonistic interactions between the chemokine receptors CXCR4 and CXCR7/RDC1. BMC developmental biology *7*, 23.

de Gorter, D. J., Reijmers, R. M., Beuling, E. A., Naber, H. P., Kuil, A., Kersten, M. J., Pals, S. T., and Spaargaren, M. (2008). The small GTPase Ral mediates SDF-1-induced migration of B cells and multiple myeloma cells. Blood *111*, 3364-3372.

Decaillot, F. M., Kazmi, M. A., Lin, Y., Ray-Saha, S., Sakmar, T. P., and Sachdev, P. (2011). CXCR7/CXCR4 heterodimer constitutively recruits {beta}-arrestin to enhance cell migration. The Journal of biological chemistry.

Defea, K. (2008). Beta-arrestins and heterotrimeric G-proteins: collaborators and competitors in signal transduction. Br J Pharmacol *153 Suppl 1*, S298-309.

DeFea, K. A., Vaughn, Z. D., O'Bryan, E. M., Nishijima, D., Dery, O., and Bunnett, N. W. (2000a). The proliferative and antiapoptotic effects of substance P are facilitated by formation of a beta -arrestin-dependent scaffolding complex. Proceedings of the National Academy of Sciences of the United States of America *97*, 11086-11091.

DeFea, K. A., Zalevsky, J., Thoma, M. S., Dery, O., Mullins, R. D., and Bunnett, N. W. (2000b). beta-arrestin-dependent endocytosis of proteinase-activated receptor 2 is required for intracellular targeting of activated ERK1/2. J Cell Biol *148*, 1267-1281.

Delgado, M. B., Clark-Lewis, I., Loetscher, P., Langen, H., Thelen, M., Baggiolini, M., and Wolf, M. (2001). Rapid inactivation of stromal cell-derived factor-1 by cathepsin G associated with lymphocytes. European journal of immunology *31*, 699-707.

DeWire, S. M., Ahn, S., Lefkowitz, R. J., and Shenoy, S. K. (2007). Beta-arrestins and cell signaling. Annu Rev Physiol *69*, 483-510.

Di Marcotullio, L., Ferretti, E., Greco, A., De Smaele, E., Po, A., Sico, M. A., Alimandi, M., Giannini, G., Maroder, M., Screpanti, I., and Gulino, A. (2006).

Numb is a suppressor of Hedgehog signalling and targets Gli1 for Itch-dependent ubiquitination. Nat Cell Biol *8*, 1415-1423.

Di Marcotullio, L., Greco, A., Mazza, D., Canettieri, G., Pietrosanti, L., Infante, P., Coni, S., Moretti, M., De Smaele, E., Ferretti, E.*, et al.* (2011). Numb activates the E3 ligase Itch to control Gli1 function through a novel degradation signal. Oncogene *30*, 65-76.

Diaz, G. A. (2005). CXCR4 mutations in WHIM syndrome: a misguided immune system? Immunological reviews *203*, 235-243.

Doranz, B. J., Orsini, M. J., Turner, J. D., Hoffman, T. L., Berson, J. F., Hoxie, J. A., Peiper, S. C., Brass, L. F., and Doms, R. W. (1999). Identification of CXCR4 domains that support coreceptor and chemokine receptor functions. Journal of virology *73*, 2752-2761.

Drake, M. T., Downs, M. A., and Traub, L. M. (2000). Epsin binds to clathrin by associating directly with the clathrin-terminal domain. Evidence for cooperative binding through two discrete sites. The Journal of biological chemistry *275*, 6479-6489.

Dunn, R., Klos, D. A., Adler, A. S., and Hicke, L. (2004). The C2 domain of the Rsp5 ubiquitin ligase binds membrane phosphoinositides and directs ubiquitination of endosomal cargo. J Cell Biol *165*, 135-144.

Dupont, S,. Mamidi, A., Cordenonsi, M., Montagner, M., Zacchigna, L., Adorno, M., Martello, G., Stinchfield, MJ., Soligo, S., Morsut, L., Inui, M., Moro, S., Modena, N., Argenton, F., Newfeld, SJ., and Piccolo, S. (2009). FAM/USP9x, a deubiquitinating enzyme essential for TGFbeta signaling, controls Smad4 monoubiquitination. Cell 136(1), 123-135

Dussart, S., Courcoul, M., Bessou, G., Douaisi, M., Duverger, Y., Vigne, R., and Decroly, E. (2004). The Vif protein of human immunodeficiency virus type 1 is posttranslationally modified by ubiquitin. Biochemical and biophysical research communications *315*, 66-72.

Dutt, P., Wang, J. F., and Groopman, J. E. (1998). Stromal cell-derived factor-1 alpha and stem cell factor/kit ligand share signaling pathways in hemopoietic

progenitors: a potential mechanism for cooperative induction of chemotaxis. J Immunol *161*, 3652-3658.

Edwin, F., Anderson, K., and Patel, T. B. (2010). HECT domain-containing E3 ubiquitin ligase Nedd4 interacts with and ubiquitinates Sprouty2. The Journal of biological chemistry *285*, 255-264.

Endo, K., Takeshita, T., Kasai, H., Sasaki, Y., Tanaka, N., Asao, H., Kikuchi, K., Yamada, M., Chenb, M., O'Shea, J. J., and Sugamura, K. (2000). STAM2, a new member of the STAM family, binding to the Janus kinases. FEBS letters *477*, 55-61.

Fan, G. H., Yang, W., Wang, X. J., Qian, Q., and Richmond, A. (2001). Identification of a motif in the carboxyl terminus of CXCR2 that is involved in adaptin 2 binding and receptor internalization. Biochemistry *40*, 791-800.

Farrens, D. L., Altenbach, C., Yang, K., Hubbell, W. L., and Khorana, H. G. (1996). Requirement of rigid-body motion of transmembrane helices for light activation of rhodopsin. Science (New York, NY *274*, 768-770.

Farzan, M., Babcock, G. J., Vasilieva, N., Wright, P. L., Kiprilov, E., Mirzabekov, T., and Choe, H. (2002). The role of post-translational modifications of the CXCR4 amino terminus in stromal-derived factor 1 alpha association and HIV-1 entry. The Journal of biological chemistry *277*, 29484-29489.

Farzan, M., Mirzabekov, T., Kolchinsky, P., Wyatt, R., Cayabyab, M., Gerard, N. P., Gerard, C., Sodroski, J., and Choe, H. (1999). Tyrosine sulfation of the amino terminus of CCR5 facilitates HIV-1 entry. Cell *96*, 667-676.

Ferguson, S. S., Downey, W. E., 3rd, Colapietro, A. M., Barak, L. S., Menard, L., and Caron, M. G. (1996). Role of beta-arrestin in mediating agonist-promoted G protein-coupled receptor internalization. Science (New York, NY *271*, 363-366.

Fong, A. M., Alam, S. M., Imai, T., Haribabu, B., and Patel, D. D. (2002a). CX3CR1 tyrosine sulfation enhances fractalkine-induced cell adhesion. The Journal of biological chemistry *277*, 19418-19423.

Fong, A. M., Premont, R. T., Richardson, R. M., Yu, Y. R., Lefkowitz, R. J., and Patel, D. D. (2002b). Defective lymphocyte chemotaxis in beta-arrestin2- and GRK6-deficient mice. Proceedings of the National Academy of Sciences of the United States of America *99*, 7478-7483.

Foord, S. M., Bonner, T. I., Neubig, R. R., Rosser, E. M., Pin, J. P., Davenport, A. P., Spedding, M., and Harmar, A. J. (2005). International Union of Pharmacology. XLVI. G protein-coupled receptor list. Pharmacol Rev *57*, 279-288.

Fredholm, B. B., Hokfelt, T., and Milligan, G. (2007). G-protein-coupled receptors: an update. Acta Physiol (Oxf) *190*, 3-7.

Fujita, H., Yamanaka, M., Imamura, K., Tanaka, Y., Nara, A., Yoshimori, T., Yokota, S., and Himeno, M. (2003). A dominant negative form of the AAA ATPase SKD1/VPS4 impairs membrane trafficking out of endosomal/lysosomal compartments: class E vps phenotype in mammalian cells. J Cell Sci *116*, 401-414.

Gabilondo, A. M., Hegler, J., Krasel, C., Boivin-Jahns, V., Hein, L., and Lohse, M. J. (1997). A dileucine motif in the C terminus of the beta2-adrenergic receptor is involved in receptor internalization. Proceedings of the National Academy of Sciences of the United States of America *94*, 12285-12290.

Gallagher, E., Gao, M., Liu, Y. C., and Karin, M. (2006). Activation of the E3 ubiquitin ligase Itch through a phosphorylation-induced conformational change. Proceedings of the National Academy of Sciences of the United States of America *103*, 1717-1722.

Ganju, R. K., Brubaker, S. A., Meyer, J., Dutt, P., Yang, Y., Qin, S., Newman, W., and Groopman, J. E. (1998). The alpha-chemokine, stromal cell-derived factor-1alpha, binds to the transmembrane G-protein-coupled CXCR-4 receptor and activates multiple signal transduction pathways. The Journal of biological chemistry *273*, 23169-23175.

Gao, M., Labuda, T., Xia, Y., Gallagher, E., Fang, D., Liu, Y. C., and Karin, M. (2004). Jun turnover is controlled through JNK-dependent phosphorylation of the E3 ligase Itch. Science (New York, NY *306*, 271-275.

Gesty-Palmer, D., Chen, M., Reiter, E., Ahn, S., Nelson, C. D., Wang, S., Eckhardt, A. E., Cowan, C. L., Spurney, R. F., Luttrell, L. M., and Lefkowitz, R. J. (2006). Distinct beta-arrestin- and G protein-dependent pathways for parathyroid hormone receptor-stimulated ERK1/2 activation. The Journal of biological chemistry *281*, 10856-10864.

Gomez-Mouton, C., Abad, J. L., Mira, E., Lacalle, R. A., Gallardo, E., Jimenez-Baranda, S., Illa, I., Bernad, A., Manes, S., and Martinez, A. C. (2001). Segregation of leading-edge and uropod components into specific lipid rafts during T cell polarization. Proceedings of the National Academy of Sciences of the United States of America *98*, 9642-9647.

Goodman, O. B., Jr., Krupnick, J. G., Santini, F., Gurevich, V. V., Penn, R. B., Gagnon, A. W., Keen, J. H., and Benovic, J. L. (1996). Beta-arrestin acts as a clathrin adaptor in endocytosis of the beta2-adrenergic receptor. Nature *383*, 447-450.

Gorlin, R. J., Gelb, B., Diaz, G. A., Lofsness, K. G., Pittelkow, M. R., and Fenyk, J. R., Jr. (2000). WHIM syndrome, an autosomal dominant disorder: clinical, hematological, and molecular studies. Am J Med Genet *91*, 368-376.

Gurevich, E. V., and Gurevich, V. V. (2006). Arrestins: ubiquitous regulators of cellular signaling pathways. Genome biology *7*, 236.

Gurevich, V. V., and Benovic, J. L. (1993). Visual arrestin interaction with rhodopsin. Sequential multisite binding ensures strict selectivity toward light-activated phosphorylated rhodopsin. The Journal of biological chemistry *268*, 11628-11638.

Hall, R. A., Premont, R. T., Chow, C. W., Blitzer, J. T., Pitcher, J. A., Claing, A., Stoffel, R. H., Barak, L. S., Shenolikar, S., Weinman, E. J., *et al.* (1998). The beta2-adrenergic receptor interacts with the Na+/H+-exchanger regulatory factor to control Na+/H+ exchange. Nature *392*, 626-630.

Han, M., Gurevich, V. V., Vishnivetskiy, S. A., Sigler, P. B., and Schubert, C. (2001). Crystal structure of beta-arrestin at 1.9 A: possible mechanism of receptor binding and membrane Translocation. Structure *9*, 869-880.

Hancock, JF., Paterson, H., and Marshall, CJ. (1990). A polybasic domain or palmitoylation is required in addition to the CAAX motif to localize p21ras to the plasma membrane. Cell 5;63(1), 133-139

Hanyaloglu, A. C., McCullagh, E., and von Zastrow, M. (2005). Essential role of Hrs in a recycling mechanism mediating functional resensitization of cell signaling. EMBO J *24*, 2265-2283.

Hardy, A. R., Conley, P. B., Luo, J., Benovic, J. L., Poole, A. W., and Mundell, S. J. (2005). P2Y1 and P2Y12 receptors for ADP desensitize by distinct kinase-dependent mechanisms. Blood *105*, 3552-3560.

Haribabu, B., Richardson, R. M., Fisher, I., Sozzani, S., Peiper, S. C., Horuk, R., Ali, H., and Snyderman, R. (1997). Regulation of human chemokine receptors CXCR4. Role of phosphorylation in desensitization and internalization. The Journal of biological chemistry *272*, 28726-28731.

Hasdemir, B., Bunnett, N. W., and Cottrell, G. S. (2007). Hepatocyte growth factor-regulated tyrosine kinase substrate (HRS) mediates post-endocytic trafficking of protease-activated receptor 2 and calcitonin receptor-like receptor. The Journal of biological chemistry *282*, 29646-29657.

Hayer, A., Stoeber, M., Bissig, C., and Helenius, A. (2010). Biogenesis of caveolae: stepwise assembly of large caveolin and cavin complexes. Traffic (Copenhagen, Denmark) *11*, 361-382.

Heeschen, C., Lehmann, R., Honold, J., Assmus, B., Aicher, A., Walter, D. H., Martin, H., Zeiher, A. M., and Dimmeler, S. (2004). Profoundly reduced neovascularization capacity of bone marrow mononuclear cells derived from patients with chronic ischemic heart disease. Circulation *109*, 1615-1622.

Helbig, G., Christopherson, K. W., 2nd, Bhat-Nakshatri, P., Kumar, S., Kishimoto, H., Miller, K. D., Broxmeyer, H. E., and Nakshatri, H. (2003). NF-kappaB promotes breast cancer cell migration and metastasis by inducing the expression of the chemokine receptor CXCR4. The Journal of biological chemistry *278*, 21631-21638.

Hernandez, P. A., Gorlin, R. J., Lukens, J. N., Taniuchi, S., Bohinjec, J., Francois, F., Klotman, M. E., and Diaz, G. A. (2003). Mutations in the chemokine receptor gene CXCR4 are associated with WHIM syndrome, a combined immunodeficiency disease. Nature genetics *34*, 70-74.

Herrador, A., Herranz, S., Lara, D., and Vincent, O. (2010). Recruitment of the ESCRT machinery to a putative seven-transmembrane-domain receptor is mediated by an arrestin-related protein. Molecular and cellular biology *30*, 897-907.

Herranz, S., Rodriguez, J. M., Bussink, H. J., Sanchez-Ferrero, J. C., Arst, H. N., Jr., Penalva, M. A., and Vincent, O. (2005). Arrestin-related proteins mediate pH signaling in fungi. Proceedings of the National Academy of Sciences of the United States of America *102*, 12141-12146.

Heuss, C., Scanziani, M., Gahwiler, B. H., and Gerber, U. (1999). G-protein-independent signaling mediated by metabotropic glutamate receptors. Nature neuroscience *2*, 1070-1077.

Hicke, L., and Riezman, H. (1996). Ubiquitination of a yeast plasma membrane receptor signals its ligand-stimulated endocytosis. Cell *84*, 277-287.

Hill, M. M., Bastiani, M., Luetterforst, R., Kirkham, M., Kirkham, A., Nixon, S. J., Walser, P., Abankwa, D., Oorschot, V. M., Martin, S., *et al.* (2008). PTRF-Cavin, a conserved cytoplasmic protein required for caveola formation and function. Cell *132*, 113-124.

Hirano, S., Kawasaki, M., Ura, H., Kato, R., Raiborg, C., Stenmark, H., and Wakatsuki, S. (2006). Double-sided ubiquitin binding of Hrs-UIM in endosomal protein sorting. Nature structural & molecular biology *13*, 272-277.

Hirsch, J. A., Schubert, C., Gurevich, V. V., and Sigler, P. B. (1999). The 2.8 A crystal structure of visual arrestin: a model for arrestin's regulation. Cell *97*, 257-269.

Hislop, J. N., and von Zastrow, M. (2011). Role of ubiquitination in endocytic trafficking of G-protein-coupled receptors. Traffic (Copenhagen, Denmark) *12*, 137-148.

Hoeller, D., Crosetto, N., Blagoev, B., Raiborg, C., Tikkanen, R., Wagner, S., Kowanetz, K., Breitling, R., Mann, M., Stenmark, H., and Dikic, I. (2006). Regulation of ubiquitin-binding proteins by monoubiquitination. Nat Cell Biol *8*, 163-169.

Imamura, T., Huang, J., Dalle, S., Ugi, S., Usui, I., Luttrell, L. M., Miller, W. E., Lefkowitz, R. J., and Olefsky, J. M. (2001). beta -Arrestin-mediated recruitment of the Src family kinase Yes mediates endothelin-1-stimulated glucose transport. The Journal of biological chemistry *276*, 43663-43667.

Ingham, R. J., Colwill, K., Howard, C., Dettwiler, S., Lim, C. S., Yu, J., Hersi, K., Raaijmakers, J., Gish, G., Mbamalu, G., *et al.* (2005). WW domains provide a platform for the assembly of multiprotein networks. Molecular and cellular biology *25*, 7092-7106.

Isakov, N. (1997). Immunoreceptor tyrosine-based activation motif (ITAM), a unique module linking antigen and Fc receptors to their signaling cascades. J Leukoc Biol *61*, 6-16.

Itoh, F., Asao, H., Sugamura, K., Heldin, C. H., ten Dijke, P., and Itoh, S. (2001). Promoting bone morphogenetic protein signaling through negative regulation of inhibitory Smads. Embo J *20*, 4132-4142.

Jacob, C., Cottrell, G. S., Gehringer, D., Schmidlin, F., Grady, E. F., and Bunnett, N. W. (2005). c-Cbl mediates ubiquitination, degradation, and down-regulation of human protease-activated receptor 2. The Journal of biological chemistry *280*, 16076-16087.

Jacoby, E., Bouhelal, R., Gerspacher, M., and Seuwen, K. (2006). The 7 TM G-protein-coupled receptor target family. ChemMedChem *1*, 761-782.

Jafri, F., El-Shewy, H. M., Lee, M. H., Kelly, M., Luttrell, D. K., and Luttrell, L. M. (2006). Constitutive ERK1/2 activation by a chimeric neurokinin 1 receptor-beta-arrestin1 fusion protein. Probing the composition and function of the G protein-coupled receptor "signalsome". The Journal of biological chemistry *281*, 19346-19357.

Janowska-Wieczorek, A., Marquez, L. A., Dobrowsky, A., Ratajczak, M. Z., and Cabuhat, M. L. (2000). Differential MMP and TIMP production by human marrow and peripheral blood CD34(+) cells in response to chemokines. Exp Hematol *28*, 1274-1285.

Janz, J. M., Sakmar, T. P., and Min, K. C. (2007). A novel interaction between atrophin-interacting protein 4 and beta-p21-activated kinase-interactive exchange factor is mediated by an SH3 domain. The Journal of biological chemistry *282*, 28893-28903.

Jimenez-Sainz, M. C., Murga, C., Kavelaars, A., Jurado-Pueyo, M., Krakstad, B. F., Heijnen, C. J., Mayor, F., Jr., and Aragay, A. M. (2006). G protein-coupled receptor kinase 2 negatively regulates chemokine signaling at a level downstream from G protein subunits. Molecular biology of the cell *17*, 25-31.

Kang, Y., Siegel, P. M., Shu, W., Drobnjak, M., Kakonen, S. M., Cordon-Cardo, C., Guise, T. A., and Massague, J. (2003). A multigenic program mediating breast cancer metastasis to bone. Cancer Cell *3*, 537-549.

Kato, M., Miyazawa, K., and Kitamura, N. (2000). A deubiquitinating enzyme UBPY interacts with the Src homology 3 domain of Hrs-binding protein via a novel binding motif PX(V/I)(D/N)RXXKP. The Journal of biological chemistry *275*, 37481-37487.

Katzmann, D. J., Babst, M., and Emr, S. D. (2001). Ubiquitin-dependent sorting into the multivesicular body pathway requires the function of a conserved endosomal protein sorting complex, ESCRT-I. Cell *106*, 145-155.

Katzmann, D. J., Stefan, C. J., Babst, M., and Emr, S. D. (2003). Vps27 recruits ESCRT machinery to endosomes during MVB sorting. J Cell Biol *162*, 413-423.

Kawai, T., and Malech, H. L. (2009). WHIM syndrome: congenital immune deficiency disease. Curr Opin Hematol *16*, 20-26.

Kern, R. C., Kang, D. S., and Benovic, J. L. (2009). Arrestin2/clathrin interaction is regulated by key N- and C-terminal regions in arrestin2. Biochemistry *48*, 7190-7200.

Kim, Y. M., and Benovic, J. L. (2002). Differential roles of arrestin-2 interaction with clathrin and adaptor protein 2 in G protein-coupled receptor trafficking. The Journal of biological chemistry *277*, 30760-30768.

Kolakowski, L. F., Jr. (1994). GCRDb: a G-protein-coupled receptor database. Receptors & channels *2*, 1-7.

Kong, M. M., Hasbi, A., Mattocks, M., Fan, T., O'Dowd, B. F., and George, S. R. (2007). Regulation of D1 dopamine receptor trafficking and signaling by caveolin-1. Molecular pharmacology *72*, 1157-1170.

Kovacs, J. J., Hara, M. R., Davenport, C. L., Kim, J., and Lefkowitz, R. J. (2009). Arrestin development: emerging roles for beta-arrestins in developmental signaling pathways. Developmental cell *17*, 443-458.

Krapp, D. (1992). [What are the patient's requirements from modern stoma care materials]. Krankenpfl J *30*, 244-247.

Krupnick, J. G., and Benovic, J. L. (1998). The role of receptor kinases and arrestins in G protein-coupled receptor regulation. Annu Rev Pharmacol Toxicol *38*, 289-319.

Krupnick, J. G., Goodman, O. B., Jr., Keen, J. H., and Benovic, J. L. (1997). Arrestin/clathrin interaction. Localization of the clathrin binding domain of nonvisual arrestins to the carboxy terminus. The Journal of biological chemistry *272*, 15011-15016.

Kumar, A., Humphreys, T. D., Kremer, K. N., Bramati, P. S., Bradfield, L., Edgar, C. E., and Hedin, K. E. (2006). CXCR4 physically associates with the T cell receptor to signal in T cells. Immunity *25*, 213-224.

Lallemand, F., Seo, S. R., Ferrand, N., Pessah, M., L'Hoste, S., Rawadi, G., Roman-Roman, S., Camonis, J., and Atfi, A. (2005). AIP4 restricts transforming growth factor-beta signaling through a ubiquitination-independent mechanism. The Journal of biological chemistry *280*, 27645-27653.

Laporte, S. A., Oakley, R. H., Zhang, J., Holt, J. A., Ferguson, S. S., Caron, M. G., and Barak, L. S. (1999). The beta2-adrenergic receptor/betaarrestin complex recruits

the clathrin adaptor AP-2 during endocytosis. Proceedings of the National Academy of Sciences of the United States of America *96*, 3712-3717.

Lataillade, J. J., Clay, D., Dupuy, C., Rigal, S., Jasmin, C., Bourin, P., and Le Bousse-Kerdiles, M. C. (2000). Chemokine SDF-1 enhances circulating CD34(+) cell proliferation in synergy with cytokines: possible role in progenitor survival. Blood *95*, 756-768.

Lazebnik, Y. A., Kaufmann, S. H., Desnoyers, S., Poirier, G. G., and Earnshaw, W. C. (1994). Cleavage of poly(ADP-ribose) polymerase by a proteinase with properties like ICE. Nature *371*, 346-347.

Le Roy, C., and Wrana, J. L. (2005). Clathrin- and non-clathrin-mediated endocytic regulation of cell signalling. Nat Rev Mol Cell Biol *6*, 112-126.

Lefkowitz, R. J., and Shenoy, S. K. (2005). Transduction of receptor signals by beta-arrestins. Science (New York, NY *308*, 512-517.

Li, B. Q., Wetzel, M. A., Mikovits, J. A., Henderson, E. E., Rogers, T. J., Gong, W., Le, Y., Ruscetti, F. W., and Wang, J. M. (2001). The synthetic peptide WKYMVm attenuates the function of the chemokine receptors CCR5 and CXCR4 through activation of formyl peptide receptor-like 1. Blood *97*, 2941-2947.

Li, J. G., Haines, D. S., and Liu-Chen, L. Y. (2008). Agonist-promoted Lys63-linked polyubiquitination of the human kappa-opioid receptor is involved in receptor down-regulation. Molecular pharmacology *73*, 1319-1330.

Li, S., Couet, J., and Lisanti, M. P. (1996). Src tyrosine kinases, Galpha subunits, and H-Ras share a common membrane-anchored scaffolding protein, caveolin. Caveolin binding negatively regulates the auto-activation of Src tyrosine kinases. The Journal of biological chemistry *271*, 29182-29190.

Li, S. S. (2005). Specificity and versatility of SH3 and other proline-recognition domains: structural basis and implications for cellular signal transduction. The Biochemical journal *390*, 641-653.

Li, Y. M., Pan, Y., Wei, Y., Cheng, X., Zhou, B. P., Tan, M., Zhou, X., Xia, W., Hortobagyi, G. N., Yu, D., and Hung, M. C. (2004). Upregulation of CXCR4 is essential for HER2-mediated tumor metastasis. Cancer Cell *6*, 459-469.

Liang, Z., Wu, T., Lou, H., Yu, X., Taichman, R. S., Lau, S. K., Nie, S., Umbreit, J., and Shim, H. (2004). Inhibition of breast cancer metastasis by selective synthetic polypeptide against CXCR4. Cancer Res *64*, 4302-4308.

Lin, C. H., MacGurn, J. A., Chu, T., Stefan, C. J., and Emr, S. D. (2008). Arrestin-related ubiquitin-ligase adaptors regulate endocytosis and protein turnover at the cell surface. Cell *135*, 714-725.

Lohse, M. J., Benovic, J. L., Codina, J., Caron, M. G., and Lefkowitz, R. J. (1990). beta-Arrestin: a protein that regulates beta-adrenergic receptor function. Science (New York, NY *248*, 1547-1550.

Lu, Z., Xu, S., Joazeiro, C., Cobb, M. H., and Hunter, T. (2002). The PHD domain of MEKK1 acts as an E3 ubiquitin ligase and mediates ubiquitination and degradation of ERK1/2. Mol Cell *9*, 945-956.

Luo, L., and Li, T. (2008). Idiopathic CD4 lymphocytopenia and opportunistic infection--an update. FEMS immunology and medical microbiology *54*, 283-289.

Luttrell, L. M., Ferguson, S. S., Daaka, Y., Miller, W. E., Maudsley, S., Della Rocca, G. J., Lin, F., Kawakatsu, H., Owada, K., Luttrell, D. K., *et al.* (1999). Beta-arrestin-dependent formation of beta2 adrenergic receptor-Src protein kinase complexes. Science (New York, NY *283*, 655-661.

Luttrell, L. M., and Lefkowitz, R. J. (2002). The role of beta-arrestins in the termination and transduction of G-protein-coupled receptor signals. J Cell Sci *115*, 455-465.

Luttrell, L. M., Roudabush, F. L., Choy, E. W., Miller, W. E., Field, M. E., Pierce, K. L., and Lefkowitz, R. J. (2001). Activation and targeting of extracellular signal-regulated kinases by beta-arrestin scaffolds. Proceedings of the National Academy of Sciences of the United States of America *98*, 2449-2454.

Ma, Y. C., Huang, J., Ali, S., Lowry, W., and Huang, X. Y. (2000). Src tyrosine kinase is a novel direct effector of G proteins. Cell *102*, 635-646.

Macias, M. J., Hyvonen, M., Baraldi, E., Schultz, J., Sudol, M., Saraste, M., and Oschkinat, H. (1996). Structure of the WW domain of a kinase-associated protein complexed with a proline-rich peptide. Nature *382*, 646-649.

Macias, M. J., Wiesner, S., and Sudol, M. (2002). WW and SH3 domains, two different scaffolds to recognize proline-rich ligands. FEBS letters *513*, 30-37.

Malik, R., and Marchese, A. (2010). Arrestin-2 interacts with the endosomal sorting complex required for transport machinery to modulate endosomal sorting of CXCR4. Molecular biology of the cell *21*, 2529-2541.

Manes, S., del Real, G., Lacalle, R. A., Lucas, P., Gomez-Mouton, C., Sanchez-Palomino, S., Delgado, R., Alcami, J., Mira, E., and Martinez, A. C. (2000). Membrane raft microdomains mediate lateral assemblies required for HIV-1 infection. EMBO Rep *1*, 190-196.

Marchese, A., and Benovic, J. L. (2001). Agonist-promoted ubiquitination of the G protein-coupled receptor CXCR4 mediates lysosomal sorting. The Journal of biological chemistry *276*, 45509-45512.

Marchese, A., Paing, M. M., Temple, B. R., and Trejo, J. (2008). G protein-coupled receptor sorting to endosomes and lysosomes. Annu Rev Pharmacol Toxicol *48*, 601-629.

Marchese, A., Raiborg, C., Santini, F., Keen, J. H., Stenmark, H., and Benovic, J. L. (2003). The E3 ubiquitin ligase AIP4 mediates ubiquitination and sorting of the G protein-coupled receptor CXCR4. Developmental cell *5*, 709-722.

Martin, N. P., Lefkowitz, R. J., and Shenoy, S. K. (2003). Regulation of V2 vasopressin receptor degradation by agonist-promoted ubiquitination. The Journal of biological chemistry *278*, 45954-45959.

Mathiesen, J. M., and Ramirez, M. T. (2006). The metabotropic glutamate receptor 4 is internalized and desensitized upon protein kinase C activation. Br J Pharmacol *148*, 279-290.

McCullough, J., Clague, M. J., and Urbe, S. (2004). AMSH is an endosome-associated ubiquitin isopeptidase. J Cell Biol *166*, 487-492.

McCullough, J., Row, P. E., Lorenzo, O., Doherty, M., Beynon, R., Clague, M. J., and Urbe, S. (2006). Activation of the endosome-associated ubiquitin isopeptidase AMSH by STAM, a component of the multivesicular body-sorting machinery. Curr Biol *16*, 160-165.

Miller, W. E., Maudsley, S., Ahn, S., Khan, K. D., Luttrell, L. M., and Lefkowitz, R. J. (2000). beta-arrestin1 interacts with the catalytic domain of the tyrosine kinase c-SRC. Role of beta-arrestin1-dependent targeting of c-SRC in receptor endocytosis. The Journal of biological chemistry *275*, 11312-11319.

Miller, W. E., McDonald, P. H., Cai, S. F., Field, M. E., Davis, R. J., and Lefkowitz, R. J. (2001). Identification of a motif in the carboxyl terminus of beta -arrestin2 responsible for activation of JNK3. The Journal of biological chemistry *276*, 27770-27777.

Milne, J. L., and Devreotes, P. N. (1993). The surface cyclic AMP receptors, cAR1, cAR2, and cAR3, promote Ca2+ influx in Dictyostelium discoideum by a G alpha 2-independent mechanism. Molecular biology of the cell *4*, 283-292.

Mines, M. A., Goodwin, J. S., Limbird, L. E., Cui, F. F., and Fan, G. H. (2009). Deubiquitination of CXCR4 by USP14 is critical for both CXCL12-induced CXCR4 degradation and chemotaxis but not ERK ativation. The Journal of biological chemistry *284*, 5742-5752.

Moore, C. A., Milano, S. K., and Benovic, J. L. (2007). Regulation of receptor trafficking by GRKs and arrestins. Annu Rev Physiol *69*, 451-482.

Moriuchi, M., Moriuchi, H., Turner, W., and Fauci, A. S. (1997). Cloning and analysis of the promoter region of CXCR4, a coreceptor for HIV-1 entry. J Immunol *159*, 4322-4329.

Morris, S. A., Schroder, S., Plessmann, U., Weber, K., and Ungewickell, E. (1993). Clathrin assembly protein AP180: primary structure, domain organization and identification of a clathrin binding site. Embo J *12*, 667-675.

Muller, A., Homey, B., Soto, H., Ge, N., Catron, D., Buchanan, M. E., McClanahan, T., Murphy, E., Yuan, W., Wagner, S. N., *et al.* (2001). Involvement of chemokine receptors in breast cancer metastasis. Nature *410*, 50-56.

Mund, T., and Pelham, H. R. (2009). Control of the activity of WW-HECT domain E3 ubiquitin ligases by NDFIP proteins. EMBO Rep *10*, 501-507.

Mundell, S. J., Matharu, A. L., Kelly, E., and Benovic, J. L. (2000). Arrestin isoforms dictate differential kinetics of A2B adenosine receptor trafficking. Biochemistry *39*, 12828-12836.

Nabhan, J. F., Pan, H., and Lu, Q. (2010). Arrestin domain-containing protein 3 recruits the NEDD4 E3 ligase to mediate ubiquitination of the beta2-adrenergic receptor. EMBO Rep *11*, 605-611.

Nagasawa, T., Hirota, S., Tachibana, K., Takakura, N., Nishikawa, S., Kitamura, Y., Yoshida, N., Kikutani, H., and Kishimoto, T. (1996). Defects of B-cell lymphopoiesis and bone-marrow myelopoiesis in mice lacking the CXC chemokine PBSF/SDF-1. Nature *382*, 635-638.

Namkung, Y., and Sibley, D. R. (2004). Protein kinase C mediates phosphorylation, desensitization, and trafficking of the D2 dopamine receptor. The Journal of biological chemistry *279*, 49533-49541.

Naumann, U., Cameroni, E., Pruenster, M., Mahabaleshwar, H., Raz, E., Zerwes, H. G., Rot, A., and Thelen, M. (2010). CXCR7 functions as a scavenger for CXCL12 and CXCL11. PloS one *5*, e9175.

Nguyen, D. H., and Taub, D. (2002). CXCR4 function requires membrane cholesterol: implications for HIV infection. J Immunol *168*, 4121-4126.

Oakley, R. H., Laporte, S. A., Holt, J. A., Barak, L. S., and Caron, M. G. (1999). Association of beta-arrestin with G protein-coupled receptors during clathrin-

mediated endocytosis dictates the profile of receptor resensitization. The Journal of biological chemistry *274*, 32248-32257.

Oakley, R. H., Laporte, S. A., Holt, J. A., Barak, L. S., and Caron, M. G. (2001). Molecular determinants underlying the formation of stable intracellular G protein-coupled receptor-beta-arrestin complexes after receptor endocytosis*. The Journal of biological chemistry *276*, 19452-19460.

Oakley, R. H., Laporte, S. A., Holt, J. A., Caron, M. G., and Barak, L. S. (2000). Differential affinities of visual arrestin, beta arrestin1, and beta arrestin2 for G protein-coupled receptors delineate two major classes of receptors. The Journal of biological chemistry *275*, 17201-17210.

Orsini, M. J., Parent, J. L., Mundell, S. J., Marchese, A., and Benovic, J. L. (2000). Trafficking of the HIV coreceptor CXCR4: role of arrestins and identification of residues in the C-terminal tail that mediate receptor internalization. The Journal of biological chemistry *275*, 25876.

Overington, J. P., Al-Lazikani, B., and Hopkins, A. L. (2006). How many drug targets are there? Nature reviews *5*, 993-996.

Ozawa, K., Whalen, E. J., Nelson, C. D., Mu, Y., Hess, D. T., Lefkowitz, R. J., and Stamler, J. S. (2008). S-nitrosylation of beta-arrestin regulates beta-adrenergic receptor trafficking. Mol Cell *31*, 395-405.

Paing, M. M., Johnston, C. A., Siderovski, D. P., and Trejo, J. (2006). Clathrin adaptor AP2 regulates thrombin receptor constitutive internalization and endothelial cell resensitization. Molecular and cellular biology *26*, 3231-3242.

Palamidessi, A., Frittoli, E., Garré, M., Faretta, M., Mione, M., Testa, I., Diaspro, A., Lanzetti, L., Scita, G., Di Fiore, PP. (2008). Endocytic trafficking of Rac is required for the spatial restriction of signaling in cell migration. Cell 134(1), 135-147.

Pandey, A., Fernandez, M. M., Steen, H., Blagoev, B., Nielsen, M. M., Roche, S., Mann, M., and Lodish, H. F. (2000). Identification of a novel immunoreceptor

tyrosine-based activation motif-containing molecule, STAM2, by mass spectrometry and its involvement in growth factor and cytokine receptor signaling pathways. The Journal of biological chemistry *275*, 38633-38639.

Parton, R. G., and Richards, A. A. (2003). Lipid rafts and caveolae as portals for endocytosis: new insights and common mechanisms. Traffic (Copenhagen, Denmark) *4*, 724-738.

Patel, H. H., Murray, F., and Insel, P. A. (2008). Caveolae as organizers of pharmacologically relevant signal transduction molecules. Annu Rev Pharmacol Toxicol *48*, 359-391.

Peacock, J. W., and Jirik, F. R. (1999). TCR activation inhibits chemotaxis toward stromal cell-derived factor-1: evidence for reciprocal regulation between CXCR4 and the TCR. J Immunol *162*, 215-223.

Pickart, C. M. (2001). Mechanisms underlying ubiquitination. Annu Rev Biochem *70*, 503-533.

Pierce, K. L., Premont, R. T., and Lefkowitz, R. J. (2002). Seven-transmembrane receptors. Nat Rev Mol Cell Biol *3*, 639-650.

Pitcher, J. A., Freedman, N. J., and Lefkowitz, R. J. (1998). G protein-coupled receptor kinases. Annu Rev Biochem *67*, 653-692.

Plant, P. J., Yeger, H., Staub, O., Howard, P., and Rotin, D. (1997). The C2 domain of the ubiquitin protein ligase Nedd4 mediates Ca2+-dependent plasma membrane localization. The Journal of biological chemistry *272*, 32329-32336.

Pornillos, O., Alam, S. L., Davis, D. R., and Sundquist, W. I. (2002). Structure of the Tsg101 UEV domain in complex with the PTAP motif of the HIV-1 p6 protein. Nat Struct Biol *9*, 812-817.

Prag, G., Watson, H., Kim, Y. C., Beach, B. M., Ghirlando, R., Hummer, G., Bonifacino, J. S., and Hurley, J. H. (2007). The Vps27/Hse1 complex is a GAT domain-based scaffold for ubiquitin-dependent sorting. Developmental cell *12*, 973-986.

Preobrazhensky, A. A., Dragan, S., Kawano, T., Gavrilin, M. A., Gulina, I. V., Chakravarty, L., and Kolattukudy, P. E. (2000). Monocyte chemotactic protein-1 receptor CCR2B is a glycoprotein that has tyrosine sulfation in a conserved extracellular N-terminal region. J Immunol *165*, 5295-5303.

Prior, I. A., Harding, A., Yan, J., Sluimer, J., Parton, R. G., and Hancock, J. F. (2001). GTP-dependent segregation of H-ras from lipid rafts is required for biological activity. Nat Cell Biol *3*, 368-375.

Probst, W. C., Snyder, L. A., Schuster, D. I., Brosius, J., and Sealfon, S. C. (1992). Sequence alignment of the G-protein coupled receptor superfamily. DNA and cell biology *11*, 1-20.

Puertollano, R., Aguilar, R. C., Gorshkova, I., Crouch, R. J., and Bonifacino, J. S. (2001). Sorting of mannose 6-phosphate receptors mediated by the GGAs. Science (New York, NY *292*, 1712-1716.

Pyo, R. T., Sui, J., Dhume, A., Palomeque, J., Blaxall, B. C., Diaz, G., Tunstead, J., Logothetis, D. E., Hajjar, R. J., and Schecter, A. D. (2006). CXCR4 modulates contractility in adult cardiac myocytes. Journal of molecular and cellular cardiology *41*, 834-844.

Qiu, L., Joazeiro, C., Fang, N., Wang, H. Y., Elly, C., Altman, Y., Fang, D., Hunter, T., and Liu, Y. C. (2000). Recognition and ubiquitination of Notch by Itch, a hect-type E3 ubiquitin ligase. The Journal of biological chemistry *275*, 35734-35737.

Ramjaun, A. R., Micheva, K. D., Bouchelet, I., and McPherson, P. S. (1997). Identification and characterization of a nerve terminal-enriched amphiphysin isoform. The Journal of biological chemistry *272*, 16700-16706.

Ren, X., and Hurley, J. H. (2011). Structural basis for endosomal recruitment of ESCRT-I by ESCRT-0 in yeast. EMBO J.

Ren, X., Kloer, D. P., Kim, Y. C., Ghirlando, R., Saidi, L. F., Hummer, G., and Hurley, J. H. (2009). Hybrid structural model of the complete human ESCRT-0 complex. Structure *17*, 406-416.

Resh, M. D. (1999). Fatty acylation of proteins: new insights into membrane targeting of myristoylated and palmitoylated proteins. Biochim Biophys Acta *1451*, 1-16.

Rietveld, A., Neutz, S., Simons, K., and Eaton, S. (1999). Association of sterol- and glycosylphosphatidylinositol-linked proteins with Drosophila raft lipid microdomains. The Journal of biological chemistry *274*, 12049-12054.

Rismanchi, N., Puertollano, R., and Blackstone, C. (2009). STAM Adaptor Proteins Interact with COPII Complexes and Function in ER-to-Golgi Trafficking Traffic *10(2)*: 201–217.

Rodriguez-Frade, J. M., del Real, G., Serrano, A., Hernanz-Falcon, P., Soriano, S. F., Vila-Coro, A. J., de Ana, A. M., Lucas, P., Prieto, I., Martinez, A. C., and Mellado, M. (2004). Blocking HIV-1 infection via CCR5 and CXCR4 receptors by acting in trans on the CCR2 chemokine receptor. Embo J *23*, 66-76.

Rolland, J. F., Henquin, J. C., and Gilon, P. (2002). G protein-independent activation of an inward Na(+) current by muscarinic receptors in mouse pancreatic beta-cells. The Journal of biological chemistry *277*, 38373-38380.

Ross, E. M., and Wilkie, T. M. (2000). GTPase-activating proteins for heterotrimeric G proteins: regulators of G protein signaling (RGS) and RGS-like proteins. Annu Rev Biochem *69*, 795-827.

Rossi, M., De Laurenzi, V., Munarriz, E., Green, D. R., Liu, Y. C., Vousden, K. H., Cesareni, G., and Melino, G. (2005). The ubiquitin-protein ligase Itch regulates p73 stability. Embo J *24*, 836-848.

Rossi, M., De Simone, M., Pollice, A., Santoro, R., La Mantia, G., Guerrini, L., and Calabro, V. (2006). Itch/AIP4 associates with and promotes p63 protein degradation. Cell cycle (Georgetown, Tex *5*, 1816-1822.

Roth, A. F., and Davis, N. G. (2000). Ubiquitination of the PEST-like endocytosis signal of the yeast a-factor receptor. The Journal of biological chemistry *275*, 8143-8153.

Rotin, D., and Kumar, S. (2009). Physiological functions of the HECT family of ubiquitin ligases. Nat Rev Mol Cell Biol *10*, 398-409.

Row, P. E., Prior, I. A., McCullough, J., Clague, M. J., and Urbe, S. (2006). The ubiquitin isopeptidase UBPY regulates endosomal ubiquitin dynamics and is essential for receptor down-regulation. The Journal of biological chemistry *281*, 12618-12624.

Rue, S. M., Mattei, S., Saksena, S., and Emr, S. D. (2008). Novel Ist1-Did2 complex functions at a late step in multivesicular body sorting. Molecular biology of the cell *19*, 475-484.

Sachse, M., Strous, G. J., and Klumperman, J. (2004). ATPase-deficient hVPS4 impairs formation of internal endosomal vesicles and stabilizes bilayered clathrin coats on endosomal vacuoles. J Cell Sci *117*, 1699-1708.

Saini, V., Marchese, A., and Majetschak, M. (2010). CXC chemokine receptor 4 is a cell surface receptor for extracellular ubiquitin. The Journal of biological chemistry *285*, 15566-15576.

Samara, G. J., Lawrence, D. M., Chiarelli, C. J., Valentino, M. D., Lyubsky, S., Zucker, S., and Vaday, G. G. (2004). CXCR4-mediated adhesion and MMP-9 secretion in head and neck squamous cell carcinoma. Cancer Lett *214*, 231-241.

Satoh, M. S., and Lindahl, T. (1992). Role of poly(ADP-ribose) formation in DNA repair. Nature *356*, 356-358.

Scheerer, P., Park, J. H., Hildebrand, P. W., Kim, Y. J., Krauss, N., Choe, H. W., Hofmann, K. P., and Ernst, O. P. (2008). Crystal structure of opsin in its G-protein-interacting conformation. Nature *455*, 497-502.

Scheffner, M., Nuber, U., and Huibregtse, J. M. (1995). Protein ubiquitination involving an E1-E2-E3 enzyme ubiquitin thioester cascade. Nature *373*, 81-83.

Schioppa, T., Uranchimeg, B., Saccani, A., Biswas, S. K., Doni, A., Rapisarda, A., Bernasconi, S., Saccani, S., Nebuloni, M., Vago, L., *et al.* (2003). Regulation of the chemokine receptor CXCR4 by hypoxia. J Exp Med *198*, 1391-1402.

Schmid, C. L., and Bohn, L. M. (2010). Serotonin, but not N-methyltryptamines, activates the serotonin 2A receptor via a ss-arrestin2/Src/Akt signaling complex in vivo. J Neurosci *30*, 13513-13524.

Scott, A., Chung, H. Y., Gonciarz-Swiatek, M., Hill, G. C., Whitby, F. G., Gaspar, J., Holton, J. M., Viswanathan, R., Ghaffarian, S., Hill, C. P., and Sundquist, W. I. (2005). Structural and mechanistic studies of VPS4 proteins. Embo J *24*, 3658-3669.

Scott-Algara, D., Balabanian, K., Chakrabarti, L. A., Mouthon, L., Dromer, F., Didier, C., Arenzana-Seisdedos, F., and Lortholary, O. (2009). Idiopathic CD4+ T-cell lymphocytopenia is associated with impaired membrane expression of the chemokine receptor CXCR4. Blood *115*, 3708-3717.

Seta, K., Nanamori, M., Modrall, J. G., Neubig, R. R., and Sadoshima, J. (2002). AT1 receptor mutant lacking heterotrimeric G protein coupling activates the Src-Ras-ERK pathway without nuclear translocation of ERKs. The Journal of biological chemistry *277*, 9268-9277.

Shearwin-Whyatt, L., Dalton, H. E., Foot, N., and Kumar, S. (2006). Regulation of functional diversity within the Nedd4 family by accessory and adaptor proteins. Bioessays *28*, 617-628.

Shen, X., Artinyan, A., Jackson, D., Thomas, R. M., Lowy, A. M., and Kim, J. (2010). Chemokine receptor CXCR4 enhances proliferation in pancreatic cancer cells through AKT and ERK dependent pathways. Pancreas *39*, 81-87.

Shenoy, S. K., Barak, L. S., Xiao, K., Ahn, S., Berthouze, M., Shukla, A. K., Luttrell, L. M., and Lefkowitz, R. J. (2007). Ubiquitination of beta-arrestin links seven-transmembrane receptor endocytosis and ERK activation. The Journal of biological chemistry *282*, 29549-29562.

Shenoy, S. K., and Lefkowitz, R. J. (2003). Trafficking patterns of beta-arrestin and G protein-coupled receptors determined by the kinetics of beta-arrestin deubiquitination. The Journal of biological chemistry *278*, 14498-14506.

Shenoy, S. K., McDonald, P. H., Kohout, T. A., and Lefkowitz, R. J. (2001). Regulation of receptor fate by ubiquitination of activated beta 2-adrenergic receptor and beta-arrestin. Science (New York, NY *294*, 1307-1313.

Shenoy, S. K., Xiao, K., Venkataramanan, V., Snyder, P. M., Freedman, N. J., and Weissman, A. M. (2008). Nedd4 mediates agonist-dependent ubiquitination, lysosomal targeting, and degradation of the beta2-adrenergic receptor. The Journal of biological chemistry *283*, 22166-22176.

Shih, S. C., Katzmann, D. J., Schnell, J. D., Sutanto, M., Emr, S. D., and Hicke, L. (2002). Epsins and Vps27p/Hrs contain ubiquitin-binding domains that function in receptor endocytosis. Nat Cell Biol *4*, 389-393.

Shih, W., Gallusser, A., and Kirchhausen, T. (1995). A clathrin-binding site in the hinge of the beta 2 chain of mammalian AP-2 complexes. The Journal of biological chemistry *270*, 31083-31090.

Signoret, N., Oldridge, J., Pelchen-Matthews, A., Klasse, P. J., Tran, T., Brass, L. F., Rosenkilde, M. M., Schwartz, T. W., Holmes, W., Dallas, W*., et al.* (1997). Phorbol esters and SDF-1 induce rapid endocytosis and down modulation of the chemokine receptor CXCR4. J Cell Biol *139*, 651-664.

Simaan, M., Bedard-Goulet, S., Fessart, D., Gratton, J. P., and Laporte, S. A. (2005). Dissociation of beta-arrestin from internalized bradykinin B2 receptor is necessary for receptor recycling and resensitization. Cellular signalling *17*, 1074-1083.

Simons, K., and Ikonen, E. (1997). Functional rafts in cell membranes. Nature *387*, 569-572.

Slagsvold, T., Aasland, R., Hirano, S., Bache, K. G., Raiborg, C., Trambaiolo, D., Wakatsuki, S., and Stenmark, H. (2005). Eap45 in mammalian ESCRT-II binds ubiquitin via a phosphoinositide-interacting GLUE domain. The Journal of biological chemistry *280*, 19600-19606.

Sohy, D., Parmentier, M., and Springael, J. Y. (2007). Allosteric transinhibition by specific antagonists in CCR2/CXCR4 heterodimers. The Journal of biological chemistry *282*, 30062-30069.

Sohy, D., Yano, H., de Nadai, P., Urizar, E., Guillabert, A., Javitch, J. A., Parmentier, M., and Springael, J. Y. (2009). Hetero-oligomerization of CCR2, CCR5, and CXCR4 and the protean effects of "selective" antagonists. The Journal of biological chemistry *284*, 31270-31279.

Song, K. S., Li, S., Okamoto, T., Quilliam, L. A., Sargiacomo, M., and Lisanti, M. P. (1996). Co-purification and direct interaction of Ras with caveolin, an integral membrane protein of caveolae microdomains. Detergent-free purification of caveolae microdomains. The Journal of biological chemistry *271*, 9690-9697.

Song, X., Coffa, S., Fu, H., and Gurevich, V. V. (2009). How does arrestin assemble MAPKs into a signaling complex? The Journal of biological chemistry *284*, 685-695.

Staller, P., Sulitkova, J., Lisztwan, J., Moch, H., Oakeley, E. J., and Krek, W. (2003). Chemokine receptor CXCR4 downregulated by von Hippel-Lindau tumour suppressor pVHL. Nature *425*, 307-311.

Stringer, D. K., and Piper, R. C. (2011). A single ubiquitin is sufficient for cargo protein entry into MVBs in the absence of ESCRT ubiquitination. J Cell Biol *192*, 229-242.

Sun, Y., Cheng, Z., Ma, L., and Pei, G. (2002). Beta-arrestin2 is critically involved in CXCR4-mediated chemotaxis, and this is mediated by its enhancement of p38 MAPK activation. The Journal of biological chemistry *277*, 49212-49219.

Sun, Y., Huang, J., Xiang, Y., Bastepe, M., Juppner, H., Kobilka, B. K., Zhang, J. J., and Huang, X. Y. (2007). Dosage-dependent switch from G protein-coupled to G protein-independent signaling by a GPCR. Embo J *26*, 53-64.

Sundquist, W. I., Schubert, H. L., Kelly, B. N., Hill, G. C., Holton, J. M., and Hill, C. P. (2004). Ubiquitin recognition by the human TSG101 protein. Mol Cell *13*, 783-789.

Suratt, B. T., Petty, J. M., Young, S. K., Malcolm, K. C., Lieber, J. G., Nick, J. A., Gonzalo, J. A., Henson, P. M., and Worthen, G. S. (2004). Role of the CXCR4/SDF-1 chemokine axis in circulating neutrophil homeostasis. Blood *104*, 565-571.

Tachibana, K., Hirota, S., Iizasa, H., Yoshida, H., Kawabata, K., Kataoka, Y., Kitamura, Y., Matsushima, K., Yoshida, N., Nishikawa, S.*, et al.* (1998). The chemokine receptor CXCR4 is essential for vascularization of the gastrointestinal tract. Nature *393*, 591-594.

Takeshita, T., Arita, T., Asao, H., Tanaka, N., Higuchi, M., Kuroda, H., Kaneko, K., Munakata, H., Endo, Y., Fujita, T., and Sugamura, K. (1996). Cloning of a novel signal-transducing adaptor molecule containing an SH3 domain and ITAM. Biochemical and biophysical research communications *225*, 1035-1039.

Takeshita, T., Arita, T., Higuchi, M., Asao, H., Endo, K., Kuroda, H., Tanaka, N., Murata, K., Ishii, N., and Sugamura, K. (1997). STAM, signal transducing adaptor molecule, is associated with Janus kinases and involved in signaling for cell growth and c-myc induction. Immunity *6*, 449-457.

Tan, W., Martin, D., and Gutkind, J. S. (2006). The Galpha13-Rho signaling axis is required for SDF-1-induced migration through CXCR4. The Journal of biological chemistry *281*, 39542-39549.

Tanaka, N., Kaneko, K., Asao, H., Kasai, H., Endo, Y., Fujita, T., Takeshita, T., and Sugamura, K. (1999). Possible involvement of a novel STAM-associated molecule "AMSH" in intracellular signal transduction mediated by cytokines. The Journal of biological chemistry *274*, 19129-19135.

Tang, Y., Zeng, X., He, F., Liao, Y., Qian, N., and Toi, M. (2011). Caveolin-1 is related to invasion, survival, and poor prognosis in hepatocellular cancer. Medical oncology (Northwood, London, England).

Tang, Z., Scherer, P. E., Okamoto, T., Song, K., Chu, C., Kohtz, D. S., Nishimoto, I., Lodish, H. F., and Lisanti, M. P. (1996). Molecular cloning of caveolin-3, a novel member of the caveolin gene family expressed predominantly in muscle. The Journal of biological chemistry *271*, 2255-2261.

Tanowitz, M., and Von Zastrow, M. (2002). Ubiquitination-independent trafficking of G protein-coupled receptors to lysosomes. The Journal of biological chemistry *277*, 50219-50222.

Teo, H., Perisic, O., Gonzalez, B., and Williams, R. L. (2004). ESCRT-II, an endosome-associated complex required for protein sorting: crystal structure and interactions with ESCRT-III and membranes. Developmental cell *7*, 559-569.

Thelen, M. (2001). Dancing to the tune of chemokines. Nat Immunol *2*, 129-134.

Toth, P. T., Ren, D., and Miller, R. J. (2004). Regulation of CXCR4 receptor dimerization by the chemokine SDF-1alpha and the HIV-1 coat protein gp120: a fluorescence resonance energy transfer (FRET) study. The Journal of pharmacology and experimental therapeutics *310*, 8-17.

Valenzuela-Fernandez, A., Planchenault, T., Baleux, F., Staropoli, I., Le-Barillec, K., Leduc, D., Delaunay, T., Lazarini, F., Virelizier, J. L., Chignard, M., *et al.* (2002). Leukocyte elastase negatively regulates Stromal cell-derived factor-1 (SDF-1)/CXCR4 binding and functions by amino-terminal processing of SDF-1 and CXCR4. The Journal of biological chemistry *277*, 15677-15689.

Veldkamp, C. T., Seibert, C., Peterson, F. C., Sakmar, T. P., and Volkman, B. F. (2006). Recognition of a CXCR4 sulfotyrosine by the chemokine stromal cell-derived factor-1alpha (SDF-1alpha/CXCL12). J Mol Biol *359*, 1400-1409.

Verdecia, M. A., Bowman, M. E., Lu, K. P., Hunter, T., and Noel, J. P. (2000). Structural basis for phosphoserine-proline recognition by group IV WW domains. Nat Struct Biol *7*, 639-643.

Vila-Coro, A. J., Rodriguez-Frade, J. M., Martin De Ana, A., Moreno-Ortiz, M. C., Martinez, A. C., and Mellado, M. (1999). The chemokine SDF-1alpha triggers CXCR4 receptor dimerization and activates the JAK/STAT pathway. FASEB J *13*, 1699-1710.

Vines, C. M., Revankar, C. M., Maestas, D. C., LaRusch, L. L., Cimino, D. F., Kohout, T. A., Lefkowitz, R. J., and Prossnitz, E. R. (2003). N-formyl peptide receptors internalize but do not recycle in the absence of arrestins. The Journal of biological chemistry *278*, 41581-41584.

Vishnivetskiy, S. A., Schubert, C., Climaco, G. C., Gurevich, Y. V., Velez, M. G., and Gurevich, V. V. (2000). An additional phosphate-binding element in arrestin

molecule. Implications for the mechanism of arrestin activation. The Journal of biological chemistry *275*, 41049-41057.

Vroon, A., Heijnen, C. J., Raatgever, R., Touw, I. P., Ploemacher, R. E., Premont, R. T., and Kavelaars, A. (2004). GRK6 deficiency is associated with enhanced CXCR4-mediated neutrophil chemotaxis in vitro and impaired responsiveness to G-CSF in vivo. J Leukoc Biol *75*, 698-704.

Wang, J. F., Park, I. W., and Groopman, J. E. (2000). Stromal cell-derived factor-1alpha stimulates tyrosine phosphorylation of multiple focal adhesion proteins and induces migration of hematopoietic progenitor cells: roles of phosphoinositide-3 kinase and protein kinase C. Blood *95*, 2505-2513.

Watson, J. V., Chambers, S. H., and Smith, P. J. (1987). A pragmatic approach to the analysis of DNA histograms with a definable G1 peak. Cytometry *8*, 1-8.

Wegner, S. A., Ehrenberg, P. K., Chang, G., Dayhoff, D. E., Sleeker, A. L., and Michael, N. L. (1998). Genomic organization and functional characterization of the chemokine receptor CXCR4, a major entry co-receptor for human immunodeficiency virus type 1. The Journal of biological chemistry *273*, 4754-4760.

Wettschureck, N., and Offermanns, S. (2005). Mammalian G proteins and their cell type specific functions. Physiol Rev *85*, 1159-1204.

Wiesner, S., Ogunjimi, A. A., Wang, H. R., Rotin, D., Sicheri, F., Wrana, J. L., and Forman-Kay, J. D. (2007). Autoinhibition of the HECT-type ubiquitin ligase Smurf2 through its C2 domain. Cell *130*, 651-662.

Wilden, U., Hall, S. W., and Kuhn, H. (1986). Phosphodiesterase activation by photoexcited rhodopsin is quenched when rhodopsin is phosphorylated and binds the intrinsic 48-kDa protein of rod outer segments. Proceedings of the National Academy of Sciences of the United States of America *83*, 1174-1178.

Williams, R. L., and Urbe, S. (2007). The emerging shape of the ESCRT machinery. Nat Rev Mol Cell Biol *8*, 355-368.

Wolfe, B. L., Marchese, A., and Trejo, J. (2007). Ubiquitination differentially regulates clathrin-dependent internalization of protease-activated receptor-1. J Cell Biol *177*, 905-916.

Wu, B., Chien, E. Y., Mol, C. D., Fenalti, G., Liu, W., Katritch, V., Abagyan, R., Brooun, A., Wells, P., Bi, F. C.*, et al.* (2010). Structures of the CXCR4 chemokine GPCR with small-molecule and cyclic peptide antagonists. Science (New York, NY *330*, 1066-1071.

Wyatt, D., Malik, R., Vesecky, A. C., and Marchese, A. (2011). Small ubiquitin-like modifier modification of arrestin-3 regulates receptor trafficking. The Journal of biological chemistry *286*, 3884-3893.

Xu, W., Smith, F. J., Jr., Subaran, R., and Mitchell, A. P. (2004). Multivesicular body-ESCRT components function in pH response regulation in Saccharomyces cerevisiae and Candida albicans. Molecular biology of the cell *15*, 5528-5537.

Yamada, M., Ishii, N., Asao, H., Murata, K., Kanazawa, C., Sasaki, H., and Sugamura, K. (2002). Signal-transducing adaptor molecules STAM1 and STAM2 are required for T-cell development and survival. Molecular and cellular biology *22*, 8648-8658.

Yamada, M., Takeshita, T., Miura, S., Murata, K., Kimura, Y., Ishii, N., Nose, M., Sakagami, H., Kondo, H., Tashiro, F.*, et al.* (2001). Loss of hippocampal CA3 pyramidal neurons in mice lacking STAM1. Molecular and cellular biology *21*, 3807-3819.

Yang, C., Zhou, W., Jeon, M. S., Demydenko, D., Harada, Y., Zhou, H., and Liu, Y. C. (2006). Negative regulation of the E3 ubiquitin ligase itch via Fyn-mediated tyrosine phosphorylation. Mol Cell *21*, 135-141.

Yang, L., Jackson, E., Woerner, B. M., Perry, A., Piwnica-Worms, D., and Rubin, J. B. (2007). Blocking CXCR4-mediated cyclic AMP suppression inhibits brain tumor growth in vivo. Cancer Res *67*, 651-658.

Yao, X., Parnot, C., Deupi, X., Ratnala, V. R., Swaminath, G., Farrens, D., and Kobilka, B. (2006). Coupling ligand structure to specific conformational switches in the beta2-adrenoceptor. Nat Chem Biol *2*, 417-422.

Ye, Y., and Rape, M. (2009). Building ubiquitin chains: E2 enzymes at work. Nat Rev Mol Cell Biol *10*, 755-764.

Yu, T., Wu, Y., Helman, J. I., Wen, Y., Wang, C., and Li, L. (2011). CXCR4 promotes oral squamous cell carcinoma migration and invasion through inducing expression of MMP-9 and MMP-13 via the ERK signaling pathway. Mol Cancer Res *9*, 161-172.

Zhai, P., Yamamoto, M., Galeotti, J., Liu, J., Masurekar, M., Thaisz, J., Irie, K., Holle, E., Yu, X., Kupershmidt, S., *et al.* (2005). Cardiac-specific overexpression of AT1 receptor mutant lacking G alpha q/G alpha i coupling causes hypertrophy and bradycardia in transgenic mice. J Clin Invest *115*, 3045-3056.

Zhang, D., Fan, G. C., Zhou, X., Zhao, T., Pasha, Z., Xu, M., Zhu, Y., Ashraf, M., and Wang, Y. (2008). Over-expression of CXCR4 on mesenchymal stem cells augments myoangiogenesis in the infarcted myocardium. Journal of molecular and cellular cardiology *44*, 281-292.

Zlotnik, A., and Yoshie, O. (2000). Chemokines: a new classification system and their role in immunity. Immunity *12*, 121-127.

Zlotnik, A., Yoshie, O., and Nomiyama, H. (2006). The chemokine and chemokine receptor superfamilies and their molecular evolution. Genome biology *7*, 243.

VITA

The author, Rohit Malik, was born on July 6th, 1982 in Jodhpur, India to Pitam Singh and Rita Malik. Rohit has an elder brother, Sandeep Malik.

After completing high school in 1999, Rohit enrolled in a combined bachelors and masters program in Microbiology at Panjab University Chandigarh, India. During his Masters at Panjab University, he completed a dissertation project in the laboratory of Dr. Sanjay Chhibber studying the role of bacteriophage Kφ1 in protection against fatal *Klebsiella pneumoniae*-induced burn wound infections in mice. Following graduation in July 2005, Rohit joined DNA finger printing division of Central Forensic Science Laboratory where he worked as a DNA analyst.

Rohit enrolled in the Molecular Biology Ph.D. program at Loyola University Chicago in 2006. In the fall of 2007, Rohit joined the laboratory of Dr. Adriano Marchese in the Department of Molecular Pharmacology, where he studied the molecular mechanisms that regulate the signaling of chemokine receptor CXCR4. In 2007, Rohit was awarded the American Heart Association pre-doctoral fellowship to complete his doctoral research.

While studying at Panjab University, Rohit met Bhavna, whom he married in June 2007 and together they had a baby boy Armaan in July 2011.
Upon the successful completion of his doctoral thesis, Rohit will be pursuing a Howard Hughes Medical Institute postdoctoral position in the laboratory of Dr. Arul

Chinnaiyan at the Michigan Institute of translational pathology (MCTP), University of Michigan, Ann Arbor, where he will be studying the genetic causes of solid tumors.